

Sustainable Aviation

T. Hikmet Karakoc · Öznur Usanmaz ·  
Ravi Rajamani · Hakan Oktal ·  
Alper Dalkiran · Ali Haydar Ercan *Editors*

# Advances in Electric Aviation


Proceedings of the International  
Symposium on Electric Aircraft and  
Autonomous Systems 2021

 **SARES**  
INTERNATIONAL SUSTAINABLE AVIATION  
AND ENERGY RESEARCH SOCIETY


 Springer


# Sustainable Aviation

## Series Editors

T. Hikmet Karakoc , Faculty of Aeronautics and Astronautics  
Eskisehir Technical University  
Eskisehir, Türkiye

Information Technology Research and Application Centre  
Istanbul Ticaret University  
Istanbul, Türkiye

C. Ozgur Colpan , Department of Mechanical Engineering  
Dokuz Eylül University  
Buca, Izmir, Türkiye

Alper Dalkiran , School of Aviation  
Süleyman Demirel University  
Isparta, Türkiye

The Sustainable Aviation book series focuses on sustainability in aviation, considering all aspects of the field. The books are developed in partnership with the International Sustainable Aviation Research Society (SARES). They include contributed volumes comprising select contributions to international symposiums and conferences, monographs, and professional books focused on all aspects of sustainable aviation. The series aims at publishing state-of-the-art research and development in areas including, but not limited to:

- Green and renewable energy resources and aviation technologies
- Aircraft engine, control systems, production, storage, efficiency, and planning
- Exploring the potential of integrating renewables within airports
- Sustainable infrastructure development under a changing climate
- Training and awareness facilities with aviation sector and social levels
- Teaching and professional development in renewable energy technologies and sustainability

T. Hikmet Karakoc • Öznur Usanmaz  
Ravi Rajamani • Hakan Oktal  
Alper Dalkiran • Ali Haydar Ercan  
Editors


# Advances in Electric Aviation

Proceedings of the International Symposium  
on Electric Aircraft and Autonomous  
Systems 2021

 Springer





### *Editors*


T. Hikmet Karakoc   
Faculty of Aeronautics and Astronautics  
Eskisehir Technical University  
Eskisehir, Türkiye


Information Technology Research  
and Application Centre  
Istanbul Ticaret University  
Istanbul, Türkiye

Ravi Rajamani  
drR2 Consulting  
West Hartford, CT, USA

Alper Dalkiran   
School of Aviation  
Süleyman Demirel University  
Keciborlu, Isparta, Türkiye

Öznur Usanmaz   
Faculty of Aeronautics and Astronautics  
Eskisehir Technical University  
Eskisehir, Türkiye

Hakan Oktal   
Faculty of Aeronautics and Astronautics  
Eskisehir Technical University  
Eskisehir, Türkiye

Ali Haydar Ercan   
Porsuk Vocational School  
Eskisehir Technical University  
Eskisehir, Türkiye

ISSN 2730-7778

Sustainable Aviation

ISBN 978-3-031-32638-7

<https://doi.org/10.1007/978-3-031-32639-4>

ISSN 2730-7786 (electronic)

ISBN 978-3-031-32639-4 (eBook)

© The Editor(s) (if applicable) and The Author(s), under exclusive license to Springer Nature Switzerland AG 2023

This work is subject to copyright. All rights are solely and exclusively licensed by the Publisher, whether the whole or part of the material is concerned, specifically the rights of translation, reprinting, reuse of illustrations, recitation, broadcasting, reproduction on microfilms or in any other physical way, and transmission or information storage and retrieval, electronic adaptation, computer software, or by similar or dissimilar methodology now known or hereafter developed.

The use of general descriptive names, registered names, trademarks, service marks, etc. in this publication does not imply, even in the absence of a specific statement, that such names are exempt from the relevant protective laws and regulations and therefore free for general use.

The publisher, the authors, and the editors are safe to assume that the advice and information in this book are believed to be true and accurate at the date of publication. Neither the publisher nor the authors or the editors give a warranty, expressed or implied, with respect to the material contained herein or for any errors or omissions that may have been made. The publisher remains neutral with regard to jurisdictional claims in published maps and institutional affiliations.

This Springer imprint is published by the registered company Springer Nature Switzerland AG  
The registered company address is: Gewerbestrasse 11, 6330 Cham, Switzerland

Paper in this product is recyclable

# Preface

Electric aircraft have a brighter future than their conventional counterparts thanks to a road map that illuminates the answer to the problems of energy storage, propulsion, and airworthiness. The availability of runway space or “vertiports” will also likely become a significant issue for air travel. The electric aircraft still confronts challenges, despite an improved understanding of its measurements, success factors, risks, and environmental consequences. It is also taken into account that recent technological and structural developments have made it possible to electrify aircraft fully.

What may be anticipated from an electric airplane and what is at stake should be examined balanced and impartially. One of the primary aims of this symposium and this proceedings book is to discuss the future and limitations of design, the duration of development, how long it will take to achieve satisfactory performance and maturity, and the obstacles in the way of further advancement.

In order to achieve successful results, each party should involve cooperative actions; factories that make the airplanes to the companies that provide the parts for them (engines and systems), including schools, labs, airlines, and regulators. This task is accomplished, and now professionals from the aviation sector may discuss their divergent perspectives on electric aircraft. Ideas about the future will not lose their “grounded” status by deviating too far from how things are. Since so many initiatives exist, especially in the urban transportation industry, there is no way to escape a “make or break” moment. These investments are promising because the aviation industry is very risk-averse. New technology is only “certified” for flight once proven to significantly lower hazards, leaving no opportunity for error.

This proceedings book would not have been available without the researchers’ participation in the sessions and the presentation of their research that provides alternative visions of the electric airplane. Expert knowledge in straightforward technical language is now available to all readers thanks to the audience’s participation, questions, and special sessions, all of which deserve praise.

International Symposium on Electric Aviation and Autonomous Systems (ISEAS ’21), an international and multi-disciplinary symposium, was held online between December 16 and 18, 2021, to address current issues in the field of electric aviation,

including such topics as Electric General Aviation, More Electric Aircraft, Electric Aircraft Systems, Safe and Reliable Electric Power, Electric Energy Storage, Electric in Airport Operation, Hydrogen Fuel Cells for Aviation, and Electrical Machines for Aircraft Propulsion. We kindly invite academics, scientists, engineers, practitioners, policymakers, and students to attend ISEAS symposiums to share knowledge, demonstrate new technologies and breakthroughs, and debate the future direction, strategies, and goals in aviation sustainability. This conference featured keynote presentations by invited speakers and general papers in oral and poster sessions.

We would like to thank Springer's editorial team for their support towards the preparation of this book and the chapter authors and reviewers for their outstanding efforts.

We would also like to give special thanks to the SARES Editorial office members for gathering these chapters, who are the heroes behind the veil of the stage. Dilara Kılıç and Kemal Keles played a significant role in sharing the load and managing the chapters with Betül Özcan, Betül Kacar, and Sinem Kılıç. Their efforts in the long run for a symposium author communication, following the standards, are necessary to creating a proceedings book.

Eskisehir, Türkiye  
Eskisehir, Türkiye  
West Hartford, CT, USA  
Eskisehir, Türkiye  
Keciborlu, Isparta, Türkiye  
Eskisehir, Türkiye

T. Hikmet Karakoc  
Öznur Usanmaz  
Ravi Rajamani  
Hakan Oktal  
Alper Dalkiran  
Ali Haydar Ercan

# Contents

<b>1</b>	<b>A Short Review on Electric Aircraft Development and Futures, Barriers to Reduce Emissions in Aviation . . . . .</b>	<b>1</b>
	Selcuk Ekici, Alper Dalkiran, and T. Hikmet Karakoc	
<b>2</b>	<b>Design Considerations for Hybrid-Electric Propulsion Systems for FW-VTOL Aircraft . . . . .</b>	<b>9</b>
	Daniele Obertino, Phillip Sharikov, Jay Matlock, and Afzal Suleman	
<b>3</b>	<b>Influence of Battery Aging on Energy Management Strategy . . . . .</b>	<b>17</b>
	Teresa Donateo, Ludovica Spada Chiodo, and Antonio Ficarella	
<b>4</b>	<b>Sustainable Aviation of the Leather Industry: Life Cycle Assessment of Raw Materials, Energy Consumption and Discharge of Pollutants, and Recovery of Some Economical Merit Substances. . . . .</b>	<b>25</b>
	Delia Teresa Sponza and Nefise Erdinçmer	
<b>5</b>	<b>Resampling Based Particle Filter Estimation of a Quadrotor . . . . .</b>	<b>35</b>
	Aziz Kaba and Ahmet Ermeydan	
<b>6</b>	<b>Electric Aircraft: Motivations and Barriers to Fly . . . . .</b>	<b>41</b>
	Paul Parker and Chelsea-Anne Edwards	
<b>7</b>	<b>Determination of Environmental Impact Assessment Criteria in the Life Cycle of Transport Facilities. . . . .</b>	<b>49</b>
	Victoriia Khrutba, Inessa Rutkovska, Tatiana Morozova, Lesia Kriukovska, and Natasha Kharitonova	
<b>8</b>	<b>Two-Phase Heat Exchangers for Thermal Control of Electric Aircraft Equipment . . . . .</b>	<b>63</b>
	Leonard Vasiliev and Alexander Zhuravlyov	

<b>9</b>	<b>Subjective Decision-Making of Aviation Operators (Pilots, ATCOs)</b> . . . . .	<b>69</b>
	Utku Kale, Omar Alharasees, Jozsef Rohács, and Dániel Rohács	
<b>10</b>	<b>Acoustic Operational Monitoring of Unmanned Aerial Vehicles Near Vertiports</b> . . . . .	<b>77</b>
	Vitalii Makarenko and Vadim Tokarev	
<b>11</b>	<b>Peculiarities of Pre-processing of ADS-B Data for Aircraft Noise Modeling and Measurement During Specific Stages of LTO Cycle</b> . . . . .	<b>83</b>
	Kateryna Kazhan, Oleksandr Zaporozhets, and Sergii Karpenko	
<b>12</b>	<b>Test Bench for Electric Propellers and Distributed Propulsion</b> . . . . .	<b>91</b>
	Castroviejo Daniel and Patrick Hendrick	
<b>13</b>	<b>Aircraft Accidents and Their Causes</b> . . . . .	<b>97</b>
	Samer Al-Rabeei, Simona Pjurová, and Utku Kale	
<b>14</b>	<b>Possibilities of Using Fuel Cells in Transport Aircraft</b> . . . . .	<b>103</b>
	Marian Hocko, Samer Al-Rabeei, and Utku Kale	
<b>15</b>	<b>An Examination of the Usage Areas of Big Data Technology in Civil Aviation</b> . . . . .	<b>109</b>
	Betul Kacar and Emre Nalcacigil	
<b>16</b>	<b>Solar-Electric Long Endurance Reflector Craft for Meteorology and Climate Simulation</b> . . . . .	<b>117</b>
	Narayanan M. Komerath, Ravi Deepak, and Adarsh Deepak	
<b>17</b>	<b>Examination Of Different Systems Used For UAV Detection And Tracking</b> . . . . .	<b>125</b>
	Alpaslan Durmuş and Erol Duymaz	
<b>18</b>	<b>Misunderstandings in Aviation Communication</b> . . . . .	<b>131</b>
	Omar Alharasees, Abeer Jazzar, and Utku Kale	
<b>19</b>	<b>Modeling of Exhaust Gases Jet from Aircraft Engine for Different Operational Conditions</b> . . . . .	<b>139</b>
	Kateryna Synylo	
<b>20</b>	<b>Automation Level Impact on the Operators' (Pilot, Air Traffic Controller) Role and Total Loads</b> . . . . .	<b>149</b>
	Abeer Jazzar, Omar Alharasees, and Utku Kale	
<b>21</b>	<b>Aircraft Noise Measurements in Ukrainian Airports</b> . . . . .	<b>157</b>
	Oleksander Zaporozhets, Vadym Gulevets, Sergii Karpenko, Kateryna Kazhan, Olena Konovalova, and Vjacheslav Paraschanov	

<b>22</b>	<b>PIV Experimental Setup Integrated Wind Tunnel Initial Design: Size and Power Requirement Calculation</b> . . . . .	169
	Murat Ayar and Tahir Hikmet Karakoc	
<b>23</b>	<b>Particle Image Velocimetry Measurement with Scaled-Down Aircraft Models: A Review of the Experiments and Applications</b> . . . . .	173
	Murat Ayar, Ali Haydar Ercan, and Tahir Hikmet Karakoc	
<b>24</b>	<b>A Conceptual Use Case Evaluation of Unmanned Aerial Vehicles in the Structural Inspection of Greenhouses</b> . . . . .	179
	Elif Koruyucu, Emre Özbek, Selcuk Ekici, and T. Hikmet Karakoc	
<b>25</b>	<b>Applications of Drone Control &amp; Management in Urban Planning</b> . . . . .	187
	Dinh-Dung Nguyen, Utku Kale, Muhammed Safa Baş, Munevver Ugur, and T. Hikmet Karakoc	
<b>26</b>	<b>Imaging Techniques based on Unmanned Aerial Vehicles</b> . . . . .	195
	Alpaslan Durmuş and Erol Duymaz	
<b>27</b>	<b>Polarization Effect Between Entropy and Sustainability of Cruise Altitude for Jet-Prop Engine Performance</b> . . . . .	201
	M. Ziya Sogut	
<b>28</b>	<b>Latest Developments on Electrical Air Vehicles Powered by Electric and Hybrid Propulsion Systems</b> . . . . .	213
	Ozgun Balli, Alper Dalkiran, and T. Hikmet Karakoc	
<b>29</b>	<b>Conceptual Application of Hybrid-Electric Propulsion System Configurations on Cessna 172S</b> . . . . .	221
	Burak Akgul and Ismail Ata	
<b>30</b>	<b>The Effects of Total Initial Concentration in a Vanadium Redox Flow Battery</b> . . . . .	229
	Ilker Kayali	
<b>31</b>	<b>Effect of Phase Change Material on Thermal Behavior of a Lithium-Ion Battery</b> . . . . .	237
	Uğur Morali	
<b>32</b>	<b>Global, Regional, and Local Decision Levels to Aircraft Noise Management in Airports</b> . . . . .	243
	Oleksandr Zaporozhets	
<b>33</b>	<b>Increase of Engine Characteristics Using Alcohol Conversion</b> . . . . .	263
	Sviatoslav Kryshchtopa, Liudmyla Kryshchtopa, Ruslans Šmigins, Volodymyr Korohodskyi, Myroslav Panchuk, and Igor Prunko	

<b>34</b>	<b>Modern Tendencies in the Improvement of Technologies for Utilization of Fulfilled Tires</b> .....	271
	Anna Yakovlieva, Sergii Boichenko, Iryna Shkilniuk, and Igor Kubersky	
<b>35</b>	<b>On the Peculiarities of Alkaline-Catalyzed Route of Synthesis of Fatty Acid Monoalkyl Esters</b> .....	275
	Serhii Konovalov, Stepan Zubenko, Lyubov Patrylak, Anjela Yakovenko, Volodymyr Povazhnyi, and Kateryna Burlachenko	
<b>36</b>	<b>Use of Polyfunctional Additives As a Part of Motor Fuels and Lubricants</b> .....	283
	Andrii Grigorov and Alexander Trotsenko	
	<b>Index</b> .....	291

# Chapter 1

## A Short Review on Electric Aircraft Development and Futures, Barriers to Reduce Emissions in Aviation



Selcuk Ekici, Alper Dalkiran , and T. Hikmet Karakoc 

### 1.1 Introduction

The yearly quantity of carbon dioxide emitted into the atmosphere by aircraft stationed in the middle of aviation is estimated to be half a billion tons (Reuters 2019). To assume that a factor of this size would have no impact on climate change (Gössling and Upham 2009) and global warming (Johnson et al. 1992) is irrational. The potential threat of running out of fossil fuels is made clearer by such a large number, which also reveals fresh insights into the connection between resource usage efficiency and consumption volume (Bringezu and Bleischwitz 2017). The threat of depletion of fossil resources and the degradation of the environment have led scientists and researchers to explore environmentally friendly technologies that are also very effective (Dincer 2000). The aviation sector is attempting to shoulder the weight of scientists and researchers in the hunt for green and efficient technology, given its continuously expanding and highly favored qualities among the transportation sectors due to its many benefits (Hasan et al. 2021; Lee and Mo 2011). Electric aircraft concepts, put forward by researchers and scientists in search of minimizing the effects of the aviation industry, attracted the attention of the public and quickly became popular in the press (Brelje and Martins 2019).

---

S. Ekici  
Department of Aviation, Iğdır University, Iğdır, Turkey

A. Dalkiran (✉)  
School of Aviation, Suleyman Demirel University, Kecioboru, Turkey  
e-mail: [alperdalkiran@sdu.edu.tr](mailto:alperdalkiran@sdu.edu.tr)

T. H. Karakoc  
Faculty of Aeronautics and Astronautics, Eskişehir Technical University, Eskişehir, Turkey  
Information Technology Research and Application Center, Istanbul Ticaret University,  
Istanbul, Turkey  
e-mail: [hkarakoc@eskisehir.edu.tr](mailto:hkarakoc@eskisehir.edu.tr)



## 1.2 Electric Aircraft Development Futures

To address some of the most pressing issues of our time—including pollution, climate change, and global warming—the aviation industry is actively exploring new technological frontiers (Fuad et al. 2021). There is a position in the literature for electric aviation, which is regarded as a ground-breaking innovation with a variety of different multidisciplinary study themes (Karakoc et al. 2022). Electric aircraft are being proposed as a solution to the challenges that humans are aware of, which include climate change and global warming (Pinto Leite and Voskuijl 2020). In the content of the solution proposal, one of the outstanding issues is that it does not produce greenhouse gas emissions (Adu-Gyamfi and Good 2022), which are harmful to both humans and the environment, arising from flight operations in terms of the atmosphere. As a result, it does not create a pollution load on the biota and ecosystem (Seeley et al. 2020). The most environmentally friendly kind of aviation, therefore, is electric flight, which has emerged as the result of recent technological developments (Naayagi 2013). It is anticipated that in the not-too-distant future, electric aircraft, which is now the focus of study in the field of technology, will quickly infuse the market with new competitors (Adu-Gyamfi and Good 2022). Particularly, the realized form of electric aircraft designs is planned to fulfill its mission in the sky in a very short period of time (Prapotnik Brdnik et al. 2019). Of course, electric aircraft designs with new technological breakthroughs are getting ready to enter our lives in light of international regulations (Adu-Gyamfi and Good 2022).

Electric aviation is anticipated to not only minimize the aviation industry's environmental impact but also bring financial advantages to enterprises that choose electric transportation (Erzen et al. 2018). In the literature, financial benefits are classified into two groups and summarized as follows (Brelje and Martins 2019):

- (i) Reduction in operating and maintenance costs incurred during flight operations with conventional aircraft propulsion systems.
- (ii) and profitable investments that can contribute to the advantages of electric transportation, which has emerged as a new market area.

The first issue, which is one that is anticipated to result in a reduction in the overall expenses of running a flight operation, relates to the fuel costs that are brought about as a direct consequence of the switch from kerosene, which is the fuel used in aircraft, to electrical system architecture (Dahal et al. 2021). It is reported that the unit cost of electricity is less than that of kerosene per liter (Brelje and Martins 2019). Additionally, a brand-new market is opening up for companies that can provide practical and effective solutions in the field of electric aviation technology, as well as those that can transform their fleet of current fossil-fuel-powered aircraft into high-end electric aircraft (Schäfer et al. 2019).

Electric aircraft are operated with propulsion systems of various topologies (Rohacs and Rohacs 2020). The main goal is to reduce or minimize the need for kerosene without reducing the required thrust of a fossil fuel-powered turbojet,

turboprop, turbofan, and turboshaft engine. Electric aircraft concepts provide a reduction or complete absence in the amount of fossil fuel needed in aircraft propulsion systems by hybridizing. Adu-Gyamfi and Good present the hybridization anatomy of the electric aircraft propulsion system in their research as follows (Adu-Gyamfi and Good 2022):

- (i) The architectural structure that does not require batteries and is powered by an electric generator powered by a gas turbine engine: Turbo-electric (Barzkar and Ghassemi 2020; Epstein and O’Flarity 2019; Rendón et al. 2021; Schäfer et al. 2019; Welstead and Felder 2016).
- (ii) Architectural structure in which the thrust needed in flight operation is provided by both gas turbine engine and batteries: Hybrid electric (Bravo et al. 2021; Cameretti et al. 2018; Economou et al. 2019; Gesell et al. 2019; Glasscock et al. 2017; Hiserote and Harmon 2010; Voskuijl et al. 2018).
- (iii) Architectural structure in which the thrust is provided only by the batteries: All electric (Borghei and Ghassemi 2021; Cronin 1990; Epstein and O’Flarity 2019; Schäfer et al. 2019; Schefer et al. 2020; Viswanathan and Knapp 2019; Wheeler 2016).

Figure 1.1 describes the electric aircraft development and barriers to resolving the emission problem. The electric aviation sector, where expectations are high, is confronting many hurdles in transitioning from existing propulsion systems to next-generation propulsion systems. Particularly, the weight of the batteries in the hybridization architecture, which can correspond to the required thrust, is about 30 times the weight of the currently needed kerosene (Larsson et al. 2019). Unfortunately, one of the barriers to electric aircraft is the unappealing look of the weight that comes with the batteries since an increase in weight in aviation equals an increase in fuel consumption (Finger et al. 2019). A further barrier is the financial strain that businesses will incur when they replace conventional aircraft fleets with electric aircraft. As an alternative to hybrid systems, propulsion systems that can directly use hydrogen as a fuel are another possibility (Khandelwal et al. 2013; Petrescu et al. 2020). In contrast to the propulsion systems in which batteries are included in the architecture, hydrogen-powered propulsion systems will not be included in the range limitations. The generation of hydrogen without the use of fossil fuels is presented as a requirement to be ecologically beneficial for systems that utilize hydrogen as a fuel (Midilli and Dincer 2007). In the use of hydrogen as a direct fuel in aircraft, the water vapor discharged from the exhaust may present another danger over time (Yılmaz et al. 2012), while at the same time, hydrogen production facilities and an airport’s internal or external hydrogen distribution system are needed to provide the amount of fuel needed by a completely renewed fleet using hydrogen as fuel (Jones et al. 1983; Thalin 2019).

There has been a recent increase in the number of projects started to build urban air mobility. A number of modifications have been required for an electric aircraft to fly with electric energy to support aircraft systems. These systems must be powered autonomously by a flying aircraft. When engines convert fuel to electricity, more thrust is required. Most improvements in this field aim for a middle-city diameter,

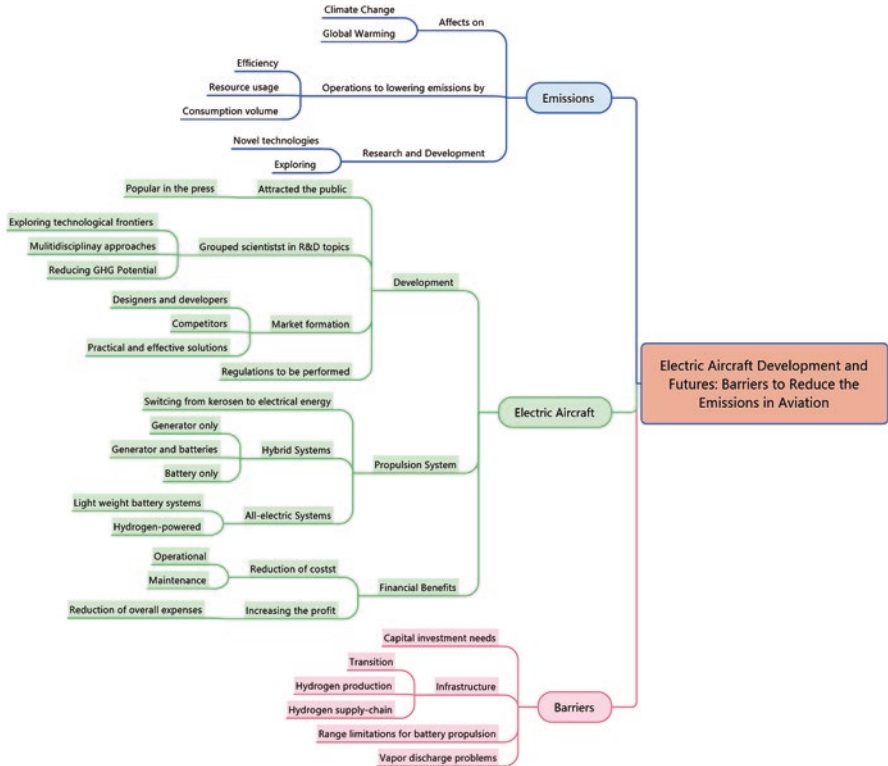


Fig. 1.1 Development and futures for electric aircraft barriers to reduce the emissions

the ability to takeoff and land vertically, and electric propulsion to cut down on noise pollution and get rid of pollutants (Thapa et al. 2021). Expanded efforts should define improved measuring methods/procedures to support noise legislation and community noise effect and collaborate with electric aircraft manufacturers on low-noise approaches and takeoff procedures for human and unmanned operations. Predicting and monitoring the fleet noise consequences of electric aircraft and evaluating additional parameters for audibility and annoyance will let the public adapt (Rizzi 2014).

### 1.3 Conclusion

The radical transformation and adoption of the above-mentioned breakthrough technologies by businesses will not happen in the near future. Currently, it is thought to be very challenging for numerous multinational businesses to go through a world-wide change with great collaboration. Reducing emissions (noise and gas) originating from flight operations is among the emergency action plans of international

organizations. Therefore, besides the conceptual discussion of the term electric aviation, it is desirable to determine the advantages and disadvantages of electric aviation in a remarkable way to reveal acceptable advantages over other technologies (alternative and renewable fuels — hydrogen, biofuels, and so on) and to take action globally to reduce the environmental impact of aviation. As a result of advancements in battery technology, specifically specific energy, more electric general aviation aircraft will fly at the turn of the decade. It might take another decade or two to develop mature and power-dense electrical solutions for larger aircraft for short- and long-distance flights. Even so, these aircraft may be exclusively hybrid-electric.

## References

- B.A. Adu-Gyamfi, C. Good, Electric aviation: a review of concepts and enabling technologies. *Transp. Eng.* **9**(4), 100134 (2022). <https://doi.org/10.1016/j.treng.2022.100134>
- A. Barzkar, M. Ghassemi, Electric power systems in more and all electric aircraft: a review. *IEEE Access* **8**, 169314–169332 (2020). <https://doi.org/10.1109/ACCESS.2020.3024168>
- M. Borghei, M. Ghassemi, Insulation materials and systems for more- and all-electric aircraft: a review identifying challenges and future research needs. *IEEE Trans. Transp. Electrification*. **7**(3), 1930–1953 (2021). <https://doi.org/10.1109/TTE.2021.3050269>
- G.M. Bravo, N. Praliyev, Á. Veress, Performance analysis of hybrid electric and distributed propulsion system applied on a light aircraft. *Energy* **214**(1268), 118823 (2021). <https://doi.org/10.1016/j.energy.2020.118823>
- B.J. Brelje, J.R.R.A. Martins, Electric, hybrid, and turboelectric fixed-wing aircraft: a review of concepts, models, and design approaches. *Prog. Aerosp. Sci.* **104**(5), 1–19 (2019). <https://doi.org/10.1016/j.paerosci.2018.06.004>
- S. Bringezu, R. Bleischwitz, *Sustainable Resource Management: Global Trends, Visions and Policies* (Taylor and Francis, London, 2017)
- M. Cameretti, A. Del Pizzo, L. Di Noia, M. Ferrara, C. Pascarella, Modeling and investigation of a turboprop hybrid electric propulsion system. *Aerospace* **5**(4), 123 (2018). <https://doi.org/10.3390/aerospace5040123>
- M.J.J. Cronin, The all-electric aircraft. *IEE Rev.* **36**(8), 309 (1990). <https://doi.org/10.1049/ir:19900132>
- K. Dahal, S. Brynolf, C. Xisto, J. Hansson, M. Grahn, T. Grönstedt, et al., Techno-economic review of alternative fuels and propulsion systems for the aviation sector. *Renew. Sust. Energ. Rev.* **151**(22), 111564 (2021). <https://doi.org/10.1016/j.rser.2021.111564>
- I. Dincer, Renewable energy and sustainable development: a crucial review. *Renew. Sust. Energ. Rev.* **4**(2), 157–175 (2000). [https://doi.org/10.1016/S1364-0321\(99\)00011-8](https://doi.org/10.1016/S1364-0321(99)00011-8)
- J.T. Economou, A. Tsourdos, S. Wang, Design of a distributed hybrid electric propulsion system for a light aircraft based on genetic algorithm, in *AIAA Propulsion and Energy 2019 Forum: Indianapolis, IN*, (American Institute of Aeronautics and Astronautics, Reston, 2019)
- A.H. Epstein, S.M. O’Flarity, Considerations for reducing aviation’s CO<sub>2</sub> with aircraft electric propulsion. *J. Propuls. Power* **35**(3), 572–582 (2019). <https://doi.org/10.2514/1.B37015>
- D. Erzen, M. Andrejasic, T. Kosel, An optimal propeller design for in-flight power recuperation on an electric aircraft, in *Aviation Technology, Integration, and Operations Conference: Atlanta, Georgia*, (American Institute of Aeronautics and Astronautics, Reston, 2018), p. 06252018
- D.F. Finger, C. Braun, C. Bil, Impact of electric propulsion technology and mission requirements on the performance of VTOL UAVs. *CEAS Aeronaut. J.* **10**(3), 827–843 (2019). <https://doi.org/10.1007/s13272-018-0352-x>

- A. Fuad, M. Al-Hashimi, A. Hamdan, The impact of innovative technology on the aviation industry and on customers preference, in *The Fourth Industrial Revolution: Implementation of Artificial Intelligence for Growing Business Success*, ed. by A. Hamdan, A.E. Hassanien, A. Razzaque, B. Alareeni, (Springer, Cham, 2021), pp. 57–69
- H. Gesell, F. Wolters, M. Plohr, System analysis of turbo-electric and hybrid-electric propulsion systems on a regional aircraft. *Aeronaut. J.* **123**(1268), 1602–1617 (2019). <https://doi.org/10.1017/aer.2019.61>
- R. Glasscock, M. Galea, W. Williams, T. Glesk, Hybrid electric aircraft propulsion case study for skydiving mission. *Aerospace* **4**(3), 45 (2017). <https://doi.org/10.3390/aerospace4030045>
- S. Gössling, P. Upham. *Climate Change and Aviation: Issues, Challenges and Solutions*, ed. by S. Gössling, P. Upham (Earthscan, London, 2009)
- M.A. Hasan, A.A. Mamun, S.M. Rahman, K. Malik, M.I.U. Al Amran, A.N. Khondaker, et al., Climate change mitigation pathways for the aviation sector. *Sustainability* **13**(7), 3656 (2021). <https://doi.org/10.3390/su13073656>
- R. Hiserote, F. Harmon, Analysis of hybrid-electric propulsion system designs for small unmanned aircraft systems, in *8th Annual International Energy Conversion Engineering Conference: Nashville, TN*, (Reston, American Institute of Aeronautics and Astronautics, 2010)
- C. Johnson, J. Henshaw, G. McInnes, Impact of aircraft and surface emissions of nitrogen oxides on tropospheric ozone and global warming. *Nature* **355**(6355), 69–71 (1992). <https://doi.org/10.1038/355069a0>
- L. Jones, C. Wuschke, T. Fahidy, Model of a cryogenic liquid-hydrogen pipeline for an airport ground distribution system. *Int. J. Hydrog. Energy* **8**(8), 623–630 (1983). [https://doi.org/10.1016/0360-3199\(83\)90231-8](https://doi.org/10.1016/0360-3199(83)90231-8)
- T.H. Karakoc, C.O. Colpan, A. Dalkiran (eds.), *New Frontiers in Sustainable Aviation*, 1st edn. (Springer, Cham, 2022)
- B. Khandelwal, A. Karakurt, P.R. Sekaran, V. Sethi, R. Singh, Hydrogen powered aircraft The future of air transport. *Prog. Aerosp. Sci.* **60**(4), 45–59 (2013). <https://doi.org/10.1016/j.paerosci.2012.12.002>
- J. Larsson, A. Elofsson, T. Sterner, J. Åkerman, International and national climate policies for aviation: a review. *Clim. Pol.* **19**(6), 787–799 (2019). <https://doi.org/10.1080/14693062.2018.1562871>
- J. Lee, J. Mo, Analysis of technological innovation and environmental performance improvement in aviation sector. *Int. J. Environ. Res. Public Health* **8**(9), 3777–3795 (2011). <https://doi.org/10.3390/ijerph8093777>
- A. Midilli, I. Dincer, Key strategies of hydrogen energy systems for sustainability. *Int. J. Hydrog. Energy* **32**(5), 511–524 (2007). <https://doi.org/10.1016/j.ijhydene.2006.06.050>
- R.T. Naayagi, A review of more electric aircraft technology, in *2013 International Conference on Energy Efficient Technologies for Sustainability; 10 April 2013 to 12 April 2013*, (IEEE, Nagercoil, 2013)
- R.V.V. Petrescu, A. Machín, K. Fontánez, J.C. Arango, F.M. Márquez, F.I.T. Petrescu, Hydrogen for aircraft power and propulsion. *Int. J. Hydrog. Energy* **45**(41), 20740–20764 (2020). <https://doi.org/10.1016/j.ijhydene.2020.05.253>
- J.P.S. Pinto Leite, M. Voskuilj, Optimal energy management for hybrid-electric aircraft. *AEAT* **92**(6), 851–861 (2020). <https://doi.org/10.1108/AEAT-03-2019-0046>
- A. Prapotnik Brdnic, R. Kamnik, M. Marksel, S. Božičnik, Market and technological perspectives for the new generation of regional passenger aircraft. *Energies* **12**(10), 1864 (2019). <https://doi.org/10.3390/en12101864>
- M.A. Rendón, R. Sánchez, M.J. Gallo, A.H. Anzai, Aircraft hybrid-electric propulsion: development trends, challenges and opportunities. *J. Control Autom. Electr. Syst.* **32**(5), 1244–1268 (2021). <https://doi.org/10.1007/s40313-021-00740-x>
- Reuters. Fly electric: the aircraft of the future takes flight (2019). <https://www.theatlantic.com/sponsored/thomson-reuters-why-2025-matters/electric-flight/208/>. Accessed 23 Oct 2022

- S.A. Rizzi. Tools for assessing community noise of dep vehicles, enabling new flight concepts through novel propulsion and energy architectures, Arlington, VA, USA, 26–27 August 2014 (2014)
- J. Rohacs, D. Rohacs, Energy coefficients for comparison of aircraft supported by different propulsion systems. *Energy* **191**(3), 116391 (2020). <https://doi.org/10.1016/j.energy.2019.116391>
- A.W. Schäfer, S.R.H. Barrett, K. Doyme, L.M. Dray, A.R. Gnad, R. Self, et al., Technological, economic and environmental prospects of all-electric aircraft. *Nat. Energy* **4**(2), 160–166 (2019). <https://doi.org/10.1038/s41560-018-0294-x>
- H. Schefer, L. Fauth, T.H. Kopp, R. Mallwitz, J. Friebe, M. Kurrat, Discussion on electric power supply systems for all electric aircraft. *IEEE Access* **8**, 84188–84216 (2020). <https://doi.org/10.1109/ACCESS.2020.2991804>
- B.A. Seeley, D. Seeley, J. Rakas, *A Report on the Future of Electric Aviation* (University of California, Berkeley, Berkeley, 2020)
- P. Thalin, Electrification of aircraft systems – Part I, Power generation and distribution, electrical networks and architectures, in *Fundamentals of Electric Aircraft*, ed. by P. Thalin, (SAE, Warrendale, 2019)
- N. Thapa, S. Ram, S. Kumar, J. Mehta, All electric aircraft: A reality on its way. *Mater. Today Proc.* **43**, 175–182 (2021)
- V. Viswanathan, B.M. Knapp, Potential for electric aircraft. *Nat. Sustain.* **2**(2), 88–89 (2019). <https://doi.org/10.1038/s41893-019-0233-2>
- M. Voskuijl, J. van Bogaert, A.G. Rao, Analysis and design of hybrid electric regional turboprop aircraft. *CEAS Aeronaut. J.* **9**(1), 15–25 (2018). <https://doi.org/10.1007/s13272-017-0272-1>
- J. Welstead, J.L. Felder, Conceptual design of a single-aisle turboelectric commercial transport with fuselage boundary layer ingestion, in *54th AIAA Aerospace Sciences Meeting: San Diego, California, USA*, (American Institute of Aeronautics and Astronautics; 01042016, Reston, Virginia, 2016)
- P. Wheeler, Technology for the more and all electric aircraft of the future, in *2016 IEEE International Conference on Automatica (ICA-ACCA); 19 October 2016 to 21 October 2016*, (IEEE, Curicó, 2016)
- İ. Yılmaz, M. İlbaş, M. Taştan, C. Tarhan, Investigation of hydrogen usage in aviation industry. *Energy Convers. Manag.* **63**(4–5), 63–69 (2012). <https://doi.org/10.1016/j.enconman.2011.12.032>

# Chapter 2

## Design Considerations for Hybrid-Electric Propulsion Systems for FW-VTOL Aircraft



Daniele Obertino, Phillip Sharikov, Jay Matlock, and Afzal Suleman

### 2.1 Introduction

In recent years, the development of UAVs combined with Hybrid-Electric Propulsion Systems (HEPS) has emerged as a promising area of research for greening aviation. The use of HEPS is particularly relevant to VTOL aircraft with distributed propulsion, leading to a variety of operating modes, more versatility and redundancy.

Together with the well-known series and parallel HEPS, which are classically composed of conventional engines, electric motors and batteries, novel intriguing opportunities towards a completely electric-powered aircraft can come from the usage of fuel cells. The high specific energy of hydrogen makes it an attractive option for long-range more-electric aircraft, as proven by the several UAVs and manned aircraft flown purely under fuel cell power (Baroutaji et al. 2019).

The modelling of HEPS for UAV has proven to be a helpful tool for studying powertrain performance (Xie et al. 2021). In the past years, many researchers tried to build tools capable of simulating multiple aircraft architectures and propulsion systems along different mission profiles to size and optimize new or existing configurations, with a special focus on the extra degrees of freedom coming from HEPS concepts. In the wake of that, a simulation platform capable of evaluating aircraft performance independently from the propulsion system was created by Matlock et al. (2018) in the MathWorks MATLAB environment. Recently new features and models have been implemented. The main novelty of the tool is the capability to simulate, besides the classic takeoff, cruise, and landing segments for fixed-wing

---

D. Obertino (✉)  
Instituto Superior Tecnico, Lisbon, Portugal  
e-mail: [daniele.obertino@tecnico.ulisboa.pt](mailto:daniele.obertino@tecnico.ulisboa.pt)

P. Sharikov · J. Matlock · A. Suleman  
Department of Mechanical Engineering, University of Victoria, Victoria, BC, Canada  
e-mail: [suleman@uvic.ca](mailto:suleman@uvic.ca)



(FW) aircraft, also mission phases typical of VTOL architectures, performing hover and transition segments. These configurations are usually characterized by distributed propulsion systems and thus the framework has been extended from the single propeller concept to allow the control and simulation of more power outputs and their respective powertrains at the same time. Finally, the model for the internal combustion engine has been updated to ease its scalability and a mathematical model of the fuel cell has been created.

## 2.2 Methodology

The design framework aims to evaluate the performance of hybrid electric propulsion systems with application to UAVs. It allows to run comparison analysis against conventional electric and gasoline propulsion systems sharing a common mission profile, as well as to optimize an existing system by sweeping mission parameters, internal components and testing different control logics that, especially for small hybrid UAVs implementing this new combined type of propulsion, are strongly linked to the overall efficiency of the power-train and must be incorporated in the optimization study to achieve the best working synergy between the components. In fact, the strength of the tool lies in its modularity, since each component is modelled separately and single parts can easily be exchanged to meet the top-level requirements in the most effective way.

The framework is based on an iterative backward-looking system architecture. The aircraft aerodynamic model parameters are defined and allow to determine the thrust required at the propellers and then, according to the propulsion type selected, the single models are activated to match the requirements, giving as output the component status in terms of throttle, power and consumption for that time step. Each powertrain component is modelled with numerical and surrogate modelling techniques, therefore, the models can be simply adapted and updated to quickly evaluate the performance of different propulsion systems, independently from the aircraft dynamics. The accuracy of these models has been increased based on experimental data recorded during test bench demonstrations and flight test campaigns.

The battery modelling is based on the Simulink model developed by MathWorks for the charging and discharging characteristics of Li-Po batteries (Tremblay and Dessaint 2009). The model allows to select the size of the battery in terms of number of cells, operating voltage and capacity. As common practice, the brushless and brushed DC motors are modelled with a simple equivalent circuit, as explained by Lundström et al. (2010). Blade element and momentum theory combined with propeller databases have been used to predict lift, drag and the propeller coefficients, which are then used to compute thrust, torque and power at the shaft (MacNeill and Verstraete 2017). The internal combustion modelling is based on both manufacture and experimental engine maps. Engine maps including fuel consumption, power output, RPM and torque were collected for a range of two-stroke combustion engines. This database was used as reference for the Willans line formulation



(Rizzoni et al. 1999), which has been recently applied also in the aviation field to build elastic scaling of the models, allowing the selection of the optimal component by sweeping the engine displacement and piston stroke.

The mathematical model for Proton-Exchange Membrane Fuel Cells (PEMFC) receives the aircraft power request, its initial temperature, the type of cooling performed, the pressures of the fuel and the oxidizer streams. Moreover, the fuel cell configuration is defined by its five most relevant parameters such as the number of stacks, the number of cells in each stack, the stack weight, volume, and heat capacity. Temperature-invariant parameters responsible for reaction kinetics, as well as structural limitations such as fuel utilization rate, are considered constant. Fuel is assumed to be hydrogen and oxidizer is assumed to be ambient air. Other components, such as clutch, Electronic Speed Controller (ESC), and generator for the case of the hybrid configurations have been modelled with efficiency coefficients taken from the literature or manufacture data.

### 2.2.1 Test Bench Setup

To validate the theoretical models and scaling efforts, an experimental test bench has been created. This test bench allows for component and system level characterization of several different hybrid architectures. With its modular design, new components of various sizes or fuel sources can easily be implemented to evaluate performance as illustrated in Fig. 2.1. Current efforts towards the conversion to a series configuration and the integration of a BZ-130 fuel cell in the test bench, as shown in Fig. 2.2 are ongoing.

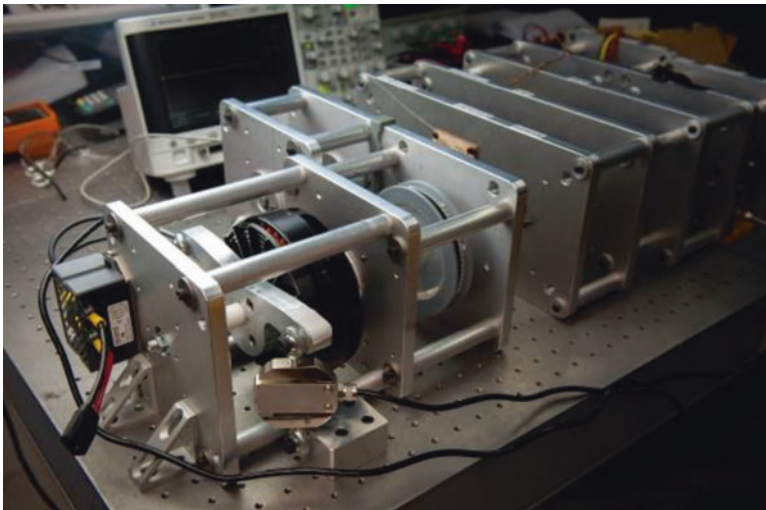


**Fig. 2.1** Parallel hybrid-electric test bench



Fig. 2.2 BZ-130 fuel cell stand

## 2.3 Simulation Results

The proposed investigation aims to evaluate and compare the performance of a series and parallel HEPS designed for a VTOL UAV configuration (Fig. 2.3) and other two fuel cell/battery and fuel cell/gasoline hybrid schemes developed for a conventional FW UAV, shown in Fig. 2.5, against conventional battery-electric and gasoline aircraft systems.

### 2.3.1 Thrust-Vectoring Configuration

The Eusphyra model is a VTOL tilt-rotor canard-wing architecture designed to perform Magnetic Anomaly Detection (MAD) along the Canadian coast (Fig. 2.3). The tilting rear rotor mechanism was selected to reduce the power installed on board, to optimize the usage of the components and thus reduce the overall weight. The main driving parameter is the maximum takeoff mass (MTOM) set to 25 kg, due to current Canadian legislation on non-recreational UAV system operations. A baseline mission was built according to defined requirements, including a vertical takeoff, forward transition, dash until the area of interest, cruise over that region, dash back, transition and landing.

The endurance analysis (Fig. 2.4) shows the intersection point at which one configuration becomes more desirable compared to another. The electric configuration results infeasible after only 30 min of cruise time, since the mass of the battery linearly reaches values that are not acceptable for the defined MTOM. The parallel and series have roughly the same dry mass, due to the balance between extra

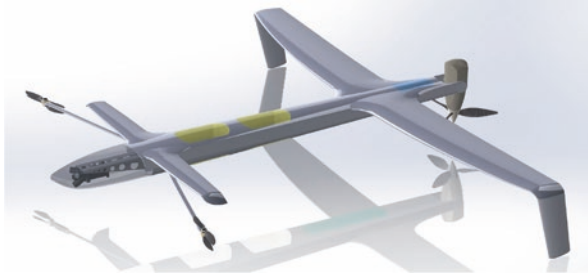


Fig. 2.3 Eusphyra VTOL CAD model

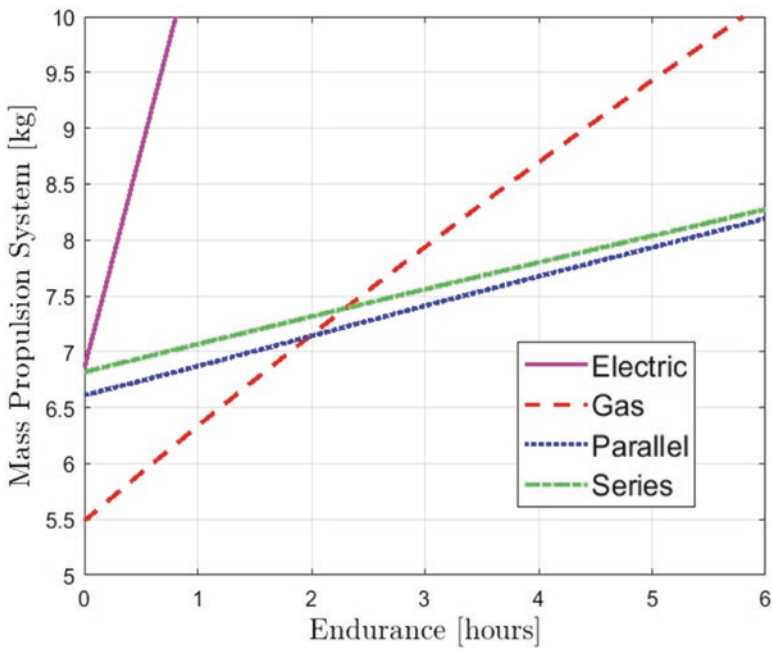


Fig. 2.4 Propulsion mass sweep for VTOL

components and connections complexity, while the gasoline is slightly lighter. However, since the ICE has been selected for maximum power request for the VTOL segment, it is oversized for cruise and thus far away from its optimal operating point (OOP). This leads to higher fuel consumption, causing a rapid increase of the overall weight and making it an unsuitable solution for a longer cruise phase. On the other hand, the hybrid configurations lead to savings in terms of fuel burnt due to the downsizing of the engine and the possibility to operate it in its OOP for cruise, and hence, they become a more and more advantageous solution with time.



**Fig. 2.5** QT-1 FW CAD model

### 2.3.2 Conventional Configuration

The hybridization process for the QT-1 FW model has previously been studied by Matlock (2016), but without considering the implementation of fuel cell technologies on board (Fig. 2.5).

The new design includes a fuel cell/battery hybrid architecture, which uses a fuel cell electrically coupled with a battery in parallel to drive an electric motor for propulsion, and a fuel cell/gasoline hybrid architecture, which mechanically couples an electric motor powered by a fuel cell to an internal combustion engine. For the fuel cell/gasoline hybrid, the internal combustion engine is the main power source and therefore hydrocarbon fuel is prioritized; instead, the other fuel cell/battery aircraft prioritizes hydrogen over the batteries. A generic mission designed to maximize the UAV's loiter time was used to compare the propulsion systems.

The propulsion systems were evaluated in a takeoff mass (TOM) range of 25–33 kg (Fig. 2.6). The fuel cell/gasoline hybrid concept can be seen to suffer from the structural weight added by the fuel cell; configurations with TOM below 27 kg were impossible to implement within the propulsion system constraints. However, fuel cell and gasoline-powered aircraft were noted to be evenly matched throughout the explored range, with gasoline aircraft having higher endurance below TOM of approximately 30 kg, and fuel cell-powered aircraft having higher endurance above this weight.

## 2.4 Concluding Remarks

Two architectures were hybridized, a VTOL and a FW configurations. For the first case, it was shown that significant savings of energy and cost are achievable for both series and parallel. In fact, especially for aircraft that require high excess power for short periods, like during the vertical takeoff, HEPS are a viable solution. Generally, the parallel configuration is preferred to the series due to its higher efficiency and lower weight thanks to the absence of the generator. However, in this case, considerations regarding the complexity, efficiency, weight of the tilting mechanism, ease

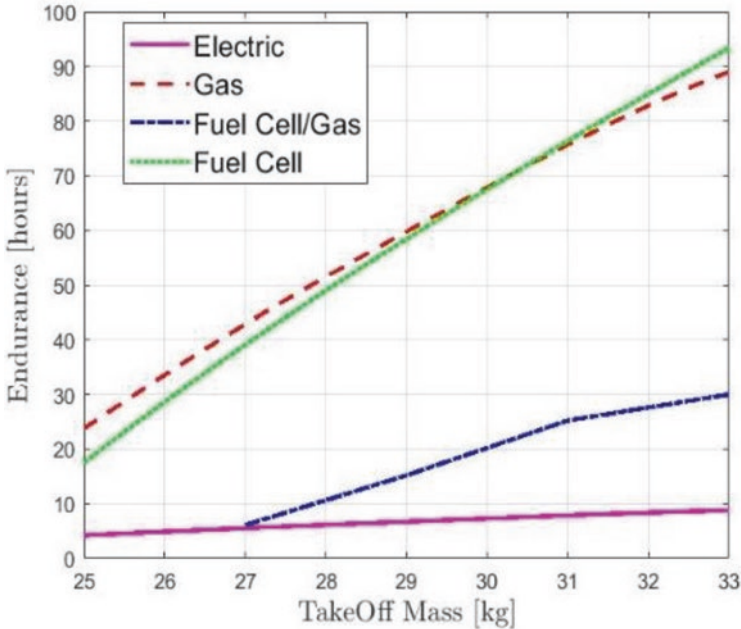


Fig. 2.6 Takeoff mass sweep for fixed-wing aircraft

of control, and rapid-response during vertical operations led to the architecture in series to be chosen for the propulsive system, since it is simpler and is easier to implement in small aircraft even at a cost of a slightly higher mass. In fact, for distributed propulsion configurations, this initial downside can be compensated by integration and aerodynamic benefits. For the second case, it was shown that for higher MTOM, the fuel cell technology is a solid possibility that warrants further research to reduce or completely eliminate the dependence on fossil fuels and thus reach a greener aviation.

UVIC CFAR has long term plans to continue to research and develop HEP technologies for use in a variety of UAV applications. Future studies must aim to optimize the configurations by developing more information on modelling and increasing the confidence in the design by testing them, and finally to assess the risks and benefits coming from the integration of these systems on board.

## References

A. Baroutaji, T. Wilberforce, M. Ramadan, A.G. Olabi, Comprehensive investigation on hydrogen and fuel cell technology in the aviation and aerospace sectors. *Renew. Sust. Energ. Rev.* **106**(February), 31–40 (2019). <https://doi.org/10.1016/j.rser.2019.02.022>

- D. Lundström, K. Amadori, P. Krus. Validation of models for small scale electric propulsion systems. 48th AIAA aerospace sciences meeting including the new horizons forum and aerospace exposition, 1–18 January (2010). <https://doi.org/10.2514/6.2010-483>
- R. MacNeill, D. Verstraete, Blade element momentum theory extended to model low Reynolds number propeller performance. *Aeronaut. J.* **121**(1240), 835–857 (2017). <https://doi.org/10.1017/aer.2017.32>
- J. Matlock. Evaluation of hybrid-electric propulsion systems for unmanned aerial vehicles. Master's thesis, University of Victoria (2016)
- J. Matlock, P. Sharikov, S. Warwick, J. Richards, A. Suleman. Evaluation of energy efficient propulsion technologies for unmanned aerial vehicles. May (2018). <https://doi.org/10.25071/10315/35397>
- G. Rizzoni, L. Guzzella, B.M. Baumann, Unified modeling of hybrid electric vehicle drivetrains. *IEEE/ASME Trans. Mechatron.* **4**(3), 246–257 (1999). <https://doi.org/10.1109/3516.789683>
- O. Tremblay, L. A. Dessaint. Experimental validation of a battery dynamic model for EV applications. 24th international battery, hybrid and fuel cell electric vehicle symposium and exhibition 2009, EVS 24, 2, 930–939 (2009). <https://doi.org/10.3390/wevj3020289>
- Y. Xie, A. Savvarisal, A. Tsourdos, D. Zhang, J. Gu, Review of hybrid electric powered aircraft, its conceptual design and energy management methodologies. *Chin. J. Aeronaut.* **34**(4), 432–450 (2021). <https://doi.org/10.1016/j.cja.2020.07.017>

# Chapter 3

## Influence of Battery Aging on Energy Management Strategy



Teresa Donateo, Ludovica Spada Chiodo, and Antonio Ficarella

### Nomenclature

$C$	Capacity
DPM	Dynamic Programming Method
HEPS	Hybrid Electric Propulsion System
$k$	Hybridization Degree
$n$	Peukert Coefficient
PLA	Power Lever Angle
$R$	Resistance
RSoC	Reference State of Charge
SoC	State of Charge
SoH	State of Health

### 3.1 Introduction

Although today, batteries performance in terms of specific power and energy density represents the major obstacle for the diffusion of electric propulsion for commercial aircrafts, their capability of enabling electrification of small aviation and urban air mobility vehicles has been proven in literature (Airbus 2021).

The present study focuses on the performance of a parallel HEPS running the same mission with two different energy management strategies. In fact, once the propulsive system has been properly sized, one of the main issues to be deal with is the implementation of a suitable strategy which is necessary to achieve the primary objective of fuel economy, together with allowing the battery to sustain the mission in electric mode in case of engine failure occurrence (Donateo et al. 2021a).

---

T. Donateo (✉) · L. Spada Chiodo · A. Ficarella  
Department of Engineering for Innovation, University of Salento, Lecce, Italy  
e-mail: [teresa.donateo@unisalento.it](mailto:teresa.donateo@unisalento.it); [ludovica.spadachiodo@unisalento.it](mailto:ludovica.spadachiodo@unisalento.it);  
[antonio.ficarella@unisalento.it](mailto:antonio.ficarella@unisalento.it)

Numerous literature sources address the investigation of energy management strategies with both heuristic and optimization approaches (Guzzella and Sciarretta 2007). This paper applies a previously developed fuzzy logic strategy with membership functions optimized through a genetic algorithm. Moreover, the optimal battery discharge curve has been previously obtained through an off-line optimization algorithm (DPM) and will serve as reference for the implementation of the fuzzy rules. For details of the development of the energetic strategy, see Donateo et al. (2021a, b).

The present study aims to evaluate how a health-conscious strategy (that considers battery aging by varying its optimal discharge curve) will influence the global behavior of the hybrid system along a typical mission, particularly in terms of fuel consumption and battery SoC.

### 3.1.1 The UAM Vehicle

A coaxial rotor air-taxi with a parallel HEPS is considered. The HEPS consists of a two-spool turboshaft and two identical electric motors driven by a Li-ion battery of 130 Ah nominal capacity and maximum life of 436 cycles.

### 3.1.2 Battery Aging

Battery specification and model parameters are not constant, since they change during battery life due to several phenomena such as capacity fade, thermal influence, etc. Time, temperature, depth of discharge and discharge rate are among the most influential factors affecting capacity loss (Wang et al. 2011).

The main specifications of the battery can be expressed as a function of the battery cycle number,  $N$ , which is defined as the number of complete discharging-charging cycles. A battery is conventionally said to have reached its end of life when the capacity reaches 80% of the nominal value. This usually happens, for a Li-ion battery, after  $N=300-500$ .

The reduction of nominal capacity together with an increase of the Peukert coefficient causes energy retention, while the power retention is associated mainly to the increase of the internal resistance. The open circuit voltage is also affected by the battery cycle number.

For each parameter  $P$  of the battery (namely nominal capacity  $C$ , Peukert coefficient  $n$  and internal resistance  $R$ ), a correction factor related to battery age  $N$  can be defined as follows:

$$CF = \frac{P(N)}{P^0} \quad (3.1)$$

where the superscript 0 denotes the initial condition.



The dependence of the correction factors on battery cycle number  $N$  is expressed as a double exponential:

$$CF = a \cdot \exp(b \cdot N) + c \cdot \exp(d \cdot N) \quad (3.2)$$

where the coefficients have been found interpolating experimental data from Dubarry and Liaw (2009). Their trends with respect to battery age are depicted in Fig. 3.1.

More details about battery model and aging can be found in Donateo and Ficarella (2020).

## 3.2 Methods

The system is supposed to run a typical mission with a duration of 2080s which goes in input to the model (Simulink model validated with Gas Turbine Simulation Program) in the form of PLA command, altitude, and airspeed. The simulation is repeated for different ages of the battery, ranging from new (1 cycle) to 401 cycles. The energy management strategy is set by a supervisory controller based on fuzzy rules which consider power request, battery SoH and deviation of actual SoC from a reference SoC (ideal battery discharge obtained with the application of a DPM which guarantees minimum fuel usage and electric backup availability during the entire mission). At this point, a dual strategy has been tested: in one case, the RSoC is considered that of a new battery; in the second case, the RSoC is interpolated with battery age to consider the effects of battery performance decay. In fact, the RSoC curve was been previously obtained by running the mission in electric mode with both new and aged battery and resulted in a minimum allowed SoC of 60% for the new battery and 70% for incipient end of life battery to complete the mission safely. The typical RSoC curves are depicted in Fig. 3.2.

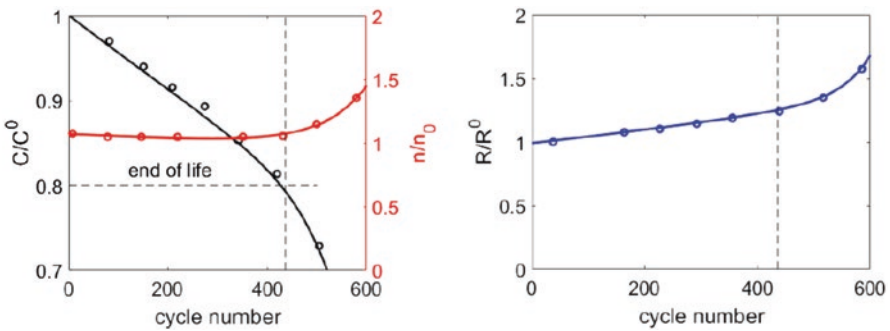


Fig. 3.1 Capacity, Peukert coefficient and internal resistance variation with battery age

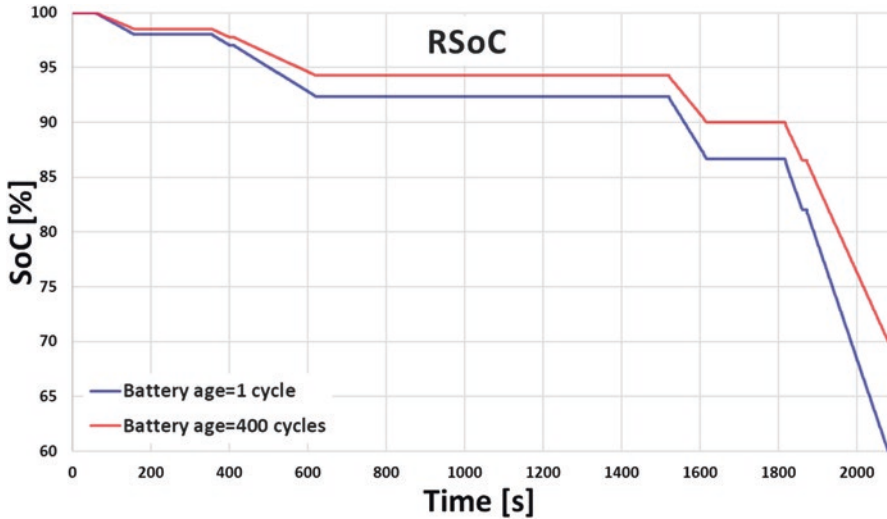


Fig. 3.2 Reference state of charge of new and aged battery

### 3.3 Results and Discussion

The torque ratio of electric to total request (named  $k$ ), resulting as output from the supervisory controller with both RSoC curves (either interpolated with battery age or typical of new battery), is depicted in Fig. 3.3.

Obviously, the electric torque request is always lower when battery age is considered. Moreover,  $k$  gradually decreases with battery age for both strategies, since fuzzy logic rules built in the supervisory controller take as input battery SoH, too. The latter is strongly affected by internal resistance increase, declining from more than 90% at the beginning to 75% at the end of life. Note that, in the last 100 cycles of battery life, recourse to electric power source is zero and all the power request is loaded onto the turboshaft engine.

The amount of fuel required to run the mission is shown in Fig. 3.4.

As it can be seen, the worsening of battery SoH has a huge negative influence on fuel consumption. The slight difference in  $k$  due to dependence of RSoC from cycle number results in a weak increase of fuel consumption for the age-dependent strategy. Such increase is quite negligible during battery early life, becoming more evident with cycle number increase, as long as the turboshaft power request becomes higher (the maximum difference between the two strategies is noticeable at 250 cycles, when the age-dependent strategy consumption is higher by an amount of 1.7% with respect to age-independent strategy at the same cycle number). However, fuel consumption at battery end of life can be considered as a benchmark, representing the amount of fuel that would be required by a only-thermal propulsive system, so that an estimate of fuel savings due to the hybridization of the system can

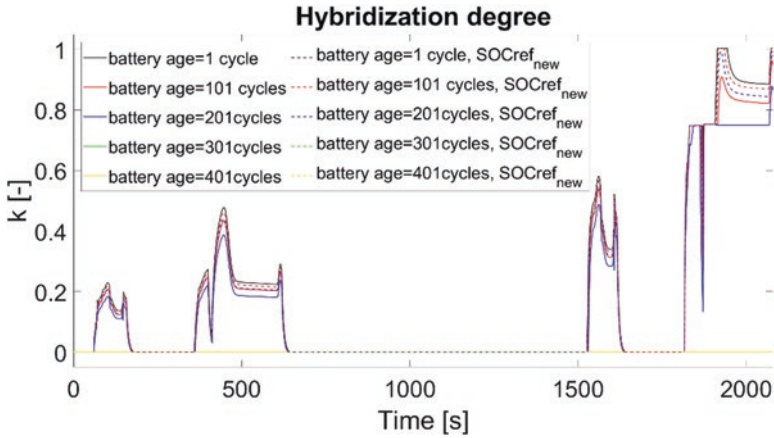


Fig. 3.3 Hybridization degree along the mission

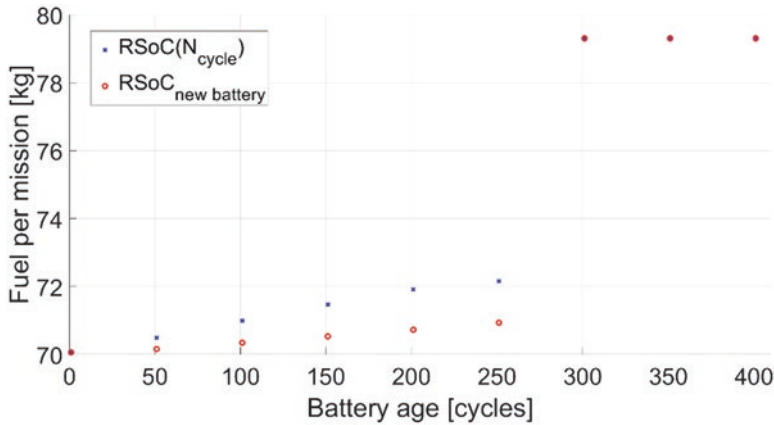


Fig. 3.4 Total fuel consumption

be made: a percentage as high as 11.7% could be saved thanks to system electrification (in the best case, that is with new battery).

Finally, the battery SoC at the end of mission is given in Fig. 3.5.

The battery is exploited almost until SoC threshold value (60%) when battery aging is neglected, except for the last 100 cycles when the too low SoH determines  $k$  to go to 0, so that SoC remains unaltered at its initial value. However, discharging the battery up to 60% independently of its age is against safety because the battery will not be able to perform an electric back-up operation in case of engine failure.

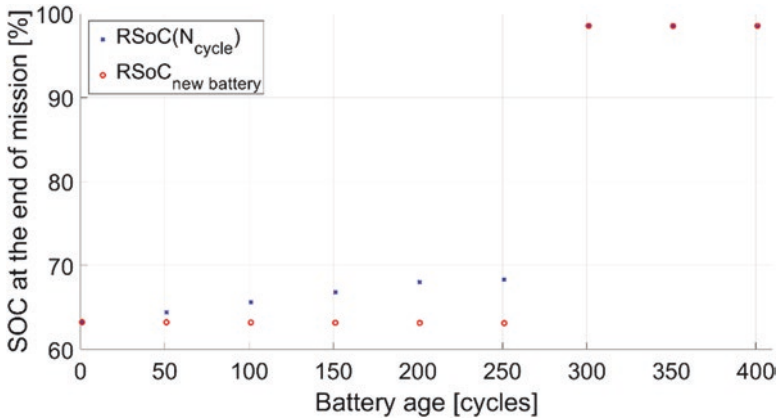


Fig. 3.5 Battery state of charge at the end of mission

### 3.4 Conclusion

In the present study, authors intended to evaluate the impact of battery aging on fuel consumption and battery discharge of a parallel HEPS whose energy management strategy for a given mission is determined by a unique set of fuzzy rules implemented into the supervisory controller.

Particularly, it has been evaluated how raising SoC threshold to compensate for battery aging effects, and thus ensure electric operation in case of engine failure even with aged battery, affects overall fuel consumption and battery discharge.

As expected, since age-dependent strategy reduces recourse to electric motor torque with increasing cycle number, this results in slightly higher consumption when such strategy is adopted; although it must be said that this increase is quite negligible, especially considering that minimum SoC level necessary to have electric backup available could be violated by the other management.

Both strategies revert to only-thermal mode when the battery becomes too aged, because of prevailing SoH decay.

### References

- Airbus. Micro-hybridisation: the next frontier to electrify flight? (2021). [Online] Available at: <https://www.airbus.com/en/newsroom/news/2021-09-micro-hybridisation-the-next-frontier-to-electrify-flight>
- T. Donateo, A. Ficarella, A modeling approach for the effect of battery aging on the performance of a hybrid electric rotorcraft for urban air-mobility. *Aerospace* **7**(5), 56 (2020)
- T. Donateo, C. De Pascalis, L. Strafella, A. Ficarella, Off-line and on-line optimization of the energy management strategy in a hybrid electric helicopter for urban air-mobility. *Aerosp. Sci. Technol.* **113**, 106677 (2021a)

- T. Donato, A. Terragno, A. Ficarella. An optimized fuzzy logic for the energy management of a hybrid electric air-taxi. Rome, 76th ATI National Congress (2021b)
- M. Dubarry, B. Liaw, Identify capacity fading mechanism in a commercial LiFePO<sub>4</sub> cell. J. Power Sources **194**, 541–549 (2009)
- L. Guzzella, A. Sciarretta, *Vehicle propulsion systems: introduction to modeling and optimization* (Springer, Berlin, 2007)
- J. Wang et al., Cycle-life model for graphite-LiFePO<sub>4</sub> cells. J. Power Sources **196**(8), 3942–3948 (2011)

# Chapter 4

## Sustainable Aviation of the Leather Industry: Life Cycle Assessment of Raw Materials, Energy Consumption and Discharge of Pollutants, and Recovery of Some Economical Merit Substances



Delia Teresa Sponza and Nefise Erdinçmer

### 4.1 Introduction

Nowadays, the main pollutants in the leather industry wastes are liquid wastewaters, particulate wastes, sludge generation, and gases emitted to the atmosphere (Zhao and Chen 2019). These pollutants mainly include organics, toxic heavy metals such as chromium, sodium ammonium salts, chlorides, and sulphonated inorganics (Kanchinadham and Kalyanaraman 2017). The recent studies showed that the composition of wastewaters emitted to the receiving media varies between 140 and 160 million tons per year (Tasca and Puccini 2019). Meanwhile, 800–900 kg of solid effluents and 60–70 tons of outputs originated from different types of organic and inorganic chemicals produce 1.9 ton of raw effluents into leather effluents. This corresponds to a huge pollutant load, and it should be treated. Therefore, the solid and liquid emissions of the leather industry should be treated effectively by considering the innovative treatment processes. However, first the wastewater characterization and the pollutant yields should be calculated, and the pollution level of the wastewater should be performed (Cabeza et al. 1998). At the beginning, the leather production process should be environmentally friendly and sustainable, and the output pollutants should be minimized by eco-friendly treatment processes. A sustainable mass and balance inventory should be performed. In this work, a life cycle assessment was performed for the leather industry by considering the raw materials, discharging of pollutants, energy consumption, and recoveries of gelatine, collagen, and chromium from a reverse osmosis (RO) plant.

---

D. T. Sponza (✉) · N. Erdinçmer  
Faculty of Engineering, Department of Environmental Engineering, Dokuz Eylül University,  
İzmir, Turkey  
e-mail: [delya.sponza@deu.edu.tr](mailto:delya.sponza@deu.edu.tr)

## 4.2 Method

Based on ISO 14040 environmental management system, to investigate the life cycle assessment of 1 kg of chrome tanned leather, the case studies were conducted in four steps namely life cycle inventory analysis, life cycle impact assessment, results, and interpretation of the results (Proske and Finkbeiner 2019). In this study, tanned leather industry was chosen since it has a big emission originated from the chromium. Footprint software (USA 2018) was utilized for the modelling process. For the modelling of this matrix, suitable data were collected, a database matrix was designed, a life cycle assessment model was generated (SimaPro LCA, 2023). The analysis results obtained from the laboratory scale analysis and the removal yield distribution data were placed to the studied method program. In the first step, environmental impact from raw materials to finished leather was determined using chrome tanning technology. Then, the major contributing factors were identified. In this model, the data taken by the beamhouse, tanning, and finishing steps were evaluated. The beamhouse process includes e.g., soaking, liming, delimiting, bating, several mechanical operations and pickling. Tanning can be defined as the process of treating skins and hides of animals. Animal skins are processed in a place called tannery. During tanning, an acidic chemical called tannin penetrate the leather, the protein structure of the skin is permanently altered, becoming durable and less susceptible to decomposition, and provide colour. Prior to tanning, the skins are dehaired, desalted, degreased, and soaked into water from 6 h to 2 days. In finishing, appearance of the leather is improved. It includes mechanical processes that give shape and smoothness to the leather, and chemical treatments that provide colour, lubrication, softening and application of surface finish to the leather (Roy Choudhury 2017).

## 4.3 Results and Discussion

The pollutant parameters considered in the life cycle assessments of the leather industry studied is shown in Table 4.1.

### 4.3.1 Impacts to the Model Used

Life cycle impact assessment method includes all the numerical data and characteristic properties of the leather emissions to the environment known as environmental impact of all input and output in the chromium leather industry. To determine the environmental impact inventory, four impacts were embedded to our targeted model in suspension. These items were: main energy requirement (PED, MJ), effect of temperature increase on the CO<sub>2</sub> production potential (GWP, kg CO<sub>2</sub> eq), water

**Table 4.1** The characterization of pollutants in the studied leather industry for evaluation of life cycle assessment

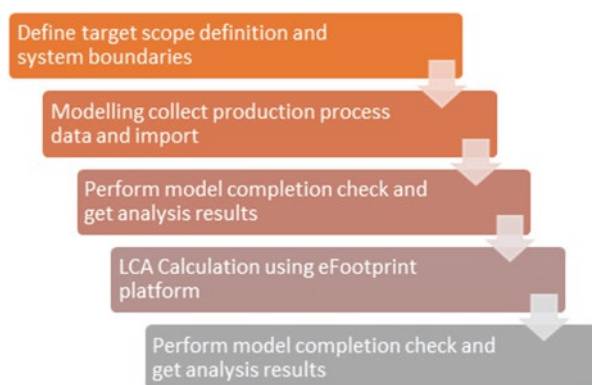
Process flow	Raw materials	Dosage (%)
Pre-soaking	Water	400.0
	Soaking bactericide KF	0.8
	Wetting agent WT-H	0.5
Soaking	Water	400.0
	Bactericide KL	0.4
	Degreasing agent DFH	0.4
	Wetting agent WT-H	0.5
	Sodium carbonate	0.3
	Sodium sulfide	0.4
Liming and unhairing	Water	380.0
	Degreasing agent DN	0.4
	Wetting agent WT-H	0.5
	Liming additives	1.9
	Lime	5.3
	Sodium sulfide	2.95
	Liming additives SP	2.0
Pre-delimiting	Water	180.0
	Ammonium sulfate	2.0
Delimiting	Water	130.0
	Ammonium sulfate	4.0
Bating	Water	120.0
	Bating enzyme U2	2.0
Pickling	Water	90.0
	Salt	7.0
	Formic acid	0.9
	Sulfuric acid	0.9
Chrome tanning	Cationic oil	2.0
	Chrome tanning agent (Cr <sub>2</sub> O <sub>3</sub> 29%, basicity 38%)	10.0
	Sodium formate	1.8
	Sodium bicarbonate	1.9
	Water	200.0
Retanning	Water	190.0
	Formic acid (85%)	0.9
	Glutaraldehyde (30%)	3.0
	Acrylic retanning agent	3.0
	Chromium powder (Cr <sub>2</sub> O <sub>3</sub> 29%, basicity 38%)	6.0
	Sodium bicarbonate	0.9

(continued)



**Table 4.1** (continued)

Process flow	Raw materials	Dosage (%)
Neutralizing	Water	160.0
	PAK-N	1.6
	Sodium acetate	1.8
	Sodium bicarbonate	0.9
Filling	Water	180.0
	Tanning extract	9.0
	Protein filling agent	4.0
	Formic acid (80%)	2.0
Fatliquoring and dyeing	Water	150.0
	Dyestuff	2.0
	Fatliquoring agents	9.0
	Formic acid (85%)	2.0
Base coating	Water	320.0
	Pigment paste 3	12.0
	Filler resin	2.9
Model leather top coating	Water	780.0
	Pigment paste 3.	0 11
	Casein solution	1.9
	Urethane resin	4.9
	Filling agent	0.9

**Fig. 4.1** Steps used in the modelling of tanned cowhide leather containing chromium

volume consumed (WU, kg), and acid production data from the leather industry process (AP, kg SO<sub>2</sub> eq). Figure 4.1 showed the steps designed during the modelling intervals.

In the first step, the toxic and no-toxic organic, inorganic, and emergency materials released during the main and co-product productions. Meanwhile, the recovery of energy used during energy losses and utilization of the recycled compounds

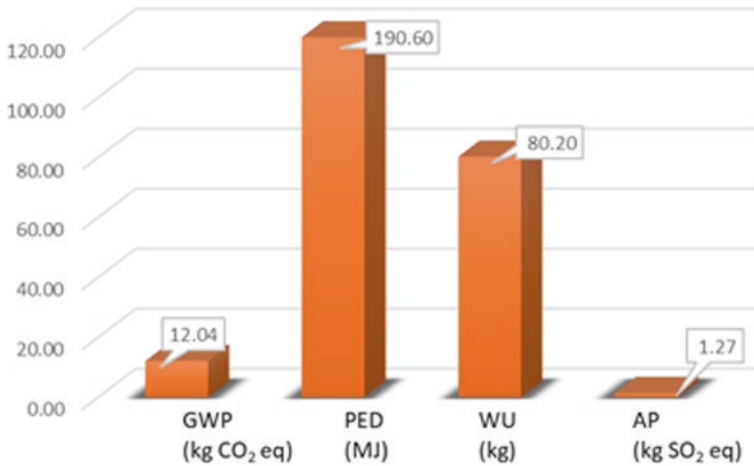


**Fig. 4.2** Variation of temperature increase, energy, water, and acid production values during production of 1 kg of cowhide leather via chrome-based tanning

during wastewater treatment were not considered. The limit for the utilization of the raw compounds should be lower than the 1% of the produced leather masses. This assumption was incorporated to the life cycle assessment process in the studied model.

As shown in Fig. 4.2, the effect of temperature increase (GWP), energy requirement (PED), consumed water (WU), and acid production rate (AP) of 1 kg of cow-mass leather produced during tanning process with chromium were 12.040 kg CO<sub>2</sub> eq, 190.60 MJ, 80.20 kg and 1.27 kg SO<sub>2</sub> eq, respectively. Generally, the acid production and increase of weather temperature limited the life cycle assessment process, whereas energy requirement and water consumption significantly affected the life cycle assessment process. Water was extremely used in the beamhouse and tanning processes. Under these conditions a big value of water was consumed during this step.

### 4.3.2 Energy Utilization

In the tanning step of leather, a huge amount of power was used as high as 90% of the total power used in the leather industry (Fig. 4.3). Majority of the machines utilized high power and electricity and a high energy consumption occurred during this leather processing step. To minimize the energy utilization, some green ultrasound and low frequency microwave devices should be utilized. This will shorten the tanning duration, and will improve the exhaustion of some toxic, refractory chemicals during tanning process. In the absence of chromium, a green leather processing will be safe to the environment during tanning process. This should also minimize the chemical cost.

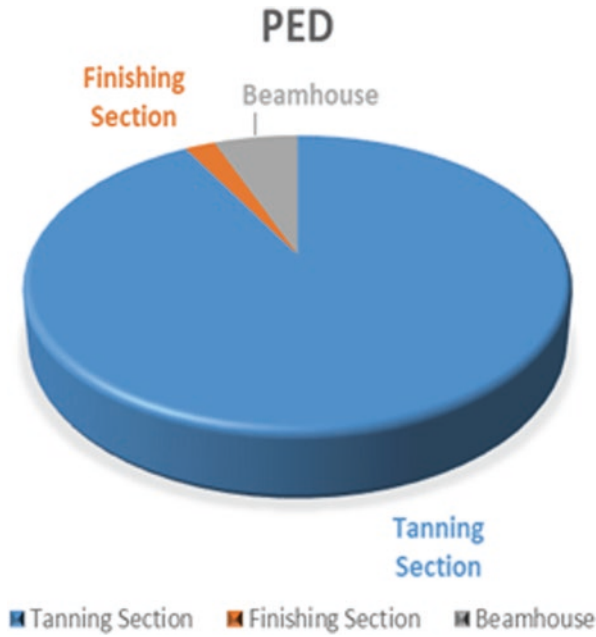


Fig. 4.3 Variation of energy requirements in the tanning section of the leather industry

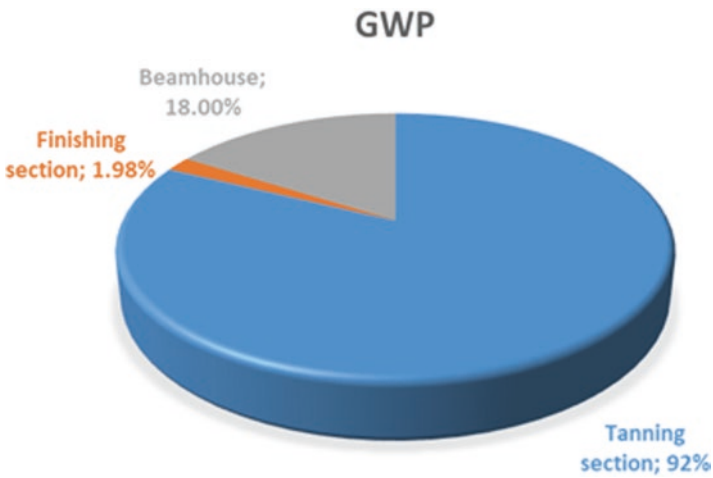


Fig. 4.4 Variables in the global warming versus increase of temperature in the tanning leather industry

### 4.3.3 $CO_2$ Production

As shown in Fig. 4.4, the  $CO_2$  emissions were 92% in the tanning section, whereas the beamhouse and finishing sections emitted low  $CO_2$  percentages such as 18% and 1.98%, respectively. During the tanning and retanning processes, chromium powder was extremely used. The amount of the chromium powder utilized in these two processes were approximately 49% of the total global warming effect mentioned in full leather process. Some other green chemicals instead of chromium powder should be utilized to minimize the carbon dioxide emissions releasing to the atmosphere during leather processing. By decreasing the amounts of sodium sulphide and lime utilized during the unhairing and liming steps, the carbon dioxide emissions to the atmosphere should be decreased. By the utilization of enzymes during unhairing process and collagen fiber instead of lime should be utilized. Recovery of floating tanning materials reduces the utilization of toxic sodium sulphide. Re-used tanning compounds will decrease the lime and chromium percentages during the end of leather tanning and un-hairing steps.

### 4.3.4 Consumed Water

In the beamhouse process, it was used a hug amount of water. In this process, the consumed water percentage was 78% of total water utilized during total leather production. The water percentage used during tanning process was 26.4% of the total water consumption. Figure 4.5 illustrated the water consumption during washing and beamhouse processes. In the beamhouse step the utilized water ratio was 16% of the total water consumption of the whole leather processing. To minimize

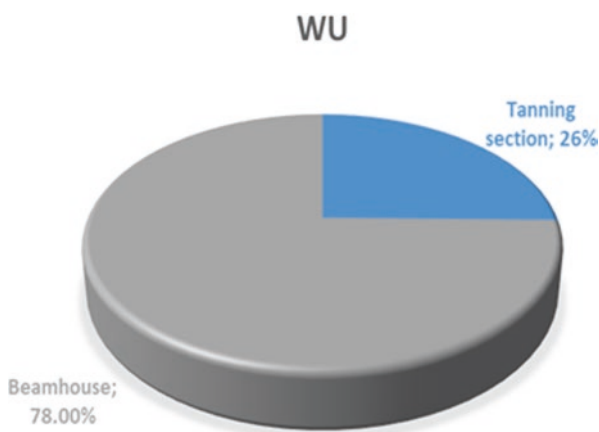
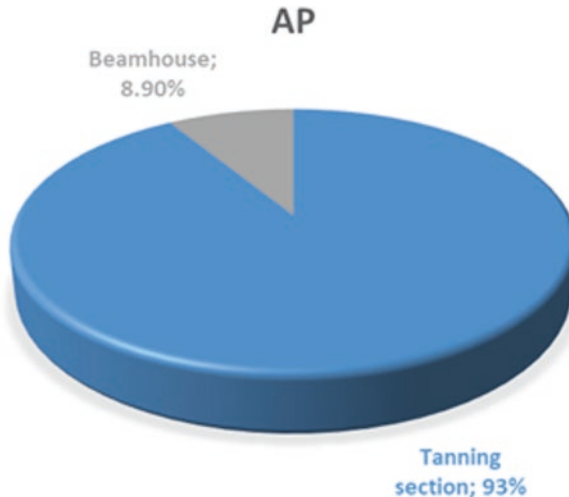


Fig. 4.5 Variation of water consumption in the entire tanning process

the water used in this process the washing devices could be improved and the excess dirty, polluted wastewater should be treated and re-used. In other words, the treated water should be re-used after the tanning process and should be used again in the next processes such tanning and pickling processes. This should reduce the cost of water utilized in the leather processes.

### 4.3.5 Acid Production

During tanning processing, the acid production percentage was 93% of the total acid formation during leather processing. The produced acid percentage from the beamhouse step was only 8.9% of the total acid production from whole leather process (Fig. 4.6). Furthermore, acid production was detected during delimiting and retanning steps. The utilization of chromium during tanning of the leathers and the sulphide productions in delimiting processes decrease the pH of the liquids to 2.0. Furthermore, acidification occurred during dissolving of chromium powder. This phenomenon affects the environment negatively. Instead of chromium powder and sulphides, some enzymes should be used. Enzymes can be used effectively during the unhairing process. This should decrease the sodium sulphide amount utilized during process and should decrease the hydrogen sulphide emissions resulting with very low pH levels in the delimiting process. Some new green chemicals without ammonia and chromium should decrease the pH lowering via the acidification (Cabeza et al. 1998; Zhang and Chen 2019).



**Fig. 4.6** Variation of acid production variables in the tanning leather industry

### 4.3.6 Recovery of the Leather Industry Compounds

Chrome recoveries from the RO retentates are chemically studied and it is found to complex with collagen. Hydrolysis of this waste involves the breakdown of bonds responsible for its stability. The bonds are responsible for collagen stability as the collagen-chromium bond. Other covalent bonds have linkage between the complex chromium ion and the ionized carboxyl groups on collagen. The concentrate of the RO was subjected with an alkali for denaturation and degrading the protein fraction. These studies were performed at 70 °C temperature and at a pH of 10 according to procedure by Sponza (2021). The alkaline condition was achieved by the utilization of sodium carbonate. The collagen was broken down to large molecular weight peptides into aqueous solution while the chromium was converted to an insoluble condition under alkaline conditions. The chemical characteristics of the hydrolysate was as follows: The peptides passed into the aqueous solution as collagen hydrolysates whose concentration is expressed as % total nitrogen. The hydrolysis yield was 87% for total nitrogen. The production of low molecular weight degradation products showed the reduction in the dry matter content of the collagen hydrolysate. The composition of hydrolysate was inorganic ash (2%), TKN (49%), chromium (28%), collagen (28%), and gelatine (19%) according to a dried compound.

## 4.4 Conclusion

As a result of tanning process, when chromium was used, 1 kg of chrome tanned cow hide leather waste affect the aquatic and soil ecosystem negatively. On the other hand, utilization of chromium powder in tanning and retanning process; sodium sulphide and lime in the liming and unhairing processes affect the environment negatively resulting in toxicities and non-biodegradable accumulations in the environment. Toxic discharges containing beamhouse, tanning, and retanning wastes should be detoxified. By the utilization of some non-toxic, non-refractory, non-accumulative, and bio-compounds, the sustainability of the leather industry wastes should be maintained with processes revealing low acid production and low CO<sub>2</sub> emissions in this industry, and by recovering and reusing the water and the energy.

## References

- L.F. Cabeza, M.M. Taylor, G.L. Dimaio, E.M. Brown, W.N. Marmer, R. Carrió, P.J. Celma, J. Cot, Processing of leather waste: pilot scale studies on chrome shavings. Isolation of potentially valuable protein products and chromium. *Waste Manage* **18**(3), 211–218 (1998)
- S.B.K. Kanchinadham, C. Kalyanaraman, Carbon trading opportunities from tannery solid waste: a case study. *Clean Tech Environ* **19**(4), 1247–1253 (2017)

- M. Proske, M. Finkbeiner, Obsolescence in LCA—methodological challenges and solution approaches. *Int. J. Life Cycle Assess.* **25**(3), 495–507 (2019)
- A.K. Roy Choudhury, Sustainable chemical technologies for textile production, in *Sustainable Fibres and Textiles*, The textile institute book series, (Elsevier, Amsterdam, 2017), pp. 267–322
- SimaPro Software for LCA calculations <https://simapro.com/business/life-cycle-assessments/>  
11.05.2023
- D.T. Sponza, Treatment of leather industry wastewater with sequential forward osmosis (FO) and reverse osmosis (RO) hybrid processes and recoveries of economical merit materials. *J. Nanosci. Nanomed. Nanobiol.* **4**(1), 1–8 (2021)
- A.L. Tasca, M. Puccini, Leather tanning: life cycle assessment of retanning, fatliquoring and dyeing. *J. Clean Prod.* **226**, 720–729 (2019)
- J.W. Zhang, W.Y. Chen, A rapid and cleaner chrome tanning technology based on ultrasound and microwave. *J. Clean Prod.* **247**, 119452 (2019)
- C. Zhao, W. Chen, A review for tannery wastewater treatment: some thoughts under stricter discharge requirements. *Environ. Sci. Pollut. Res. Int.* **26**(25), 26102–26111 (2019)

# Chapter 5

## Resampling Based Particle Filter

### Estimation of a Quadrotor



Aziz Kaba and Ahmet Ermeydan

#### Nomenclature

$\delta(\cdot)$	Delta Dirac function
$\theta$	Pitch angle
$\psi$	Yaw angle
$\phi$	Roll angle
$P$	Roll rate
$p(\cdot)$	Probability density function
$Q$	Pitch rate
$R$	Yaw rate
UAV	Unmanned aerial vehicle
$w_k$	Particle weight
$x_k$	Random particles

#### 5.1 Introduction

Nowadays, there are many application fields for Unmanned Aerial Vehicles (UAVs) and drones such as surveillance, emergency operations, military applications, and package transportation (Metin and Aygün 2019). Especially quadrotor becomes popular among researchers due to its hovering capacity and high maneuverability. Quadrotor is a multicopter which consists of four motors and propellers. The two opposite propeller turn in the same direction and the other two turn in the opposite direction. The speeds of the rotors are equal in a balanced flight (Kose and Oktay 2019).

Quadrotor is a highly nonlinear system and hard to control with linear control methods which operate around an equilibrium point. Although linear control techniques such as Proportional Derivative (PD) (Kıyak 2016), Proportional Integral

---

A. Kaba (✉) · A. Ermeydan  
Faculty of Aeronautics and Astronautics, Eskişehir Technical University, Eskişehir, Turkey  
e-mail: [azizkaba@eskisehir.edu.tr](mailto:azizkaba@eskisehir.edu.tr); [aermeydan@eskisehir.edu.tr](mailto:aermeydan@eskisehir.edu.tr)



Derivative (PID) (Ermeýdan and Kiyak 2017), Linear Quadratic Regulator (LQR) (Khatoon et al. 2014) and H infinity ( $H\infty$ ) (Araar and Aouf 2014) are applied to the quadrotor successfully, these control approaches experience a performance drop when deviating from the equilibrium point (Kendoul 2012). Quadrotors mostly suffer from dynamic nonlinearities, state couplings, model uncertainties, and external disturbances. To overcome these issues, numerous controllers are studied in the literature. However, control of a quadrotor is not sufficient enough without an estimator to eliminate the noise from low-cost sensors.

Particle filter is a recursive approximate solution to the Bayesian estimator based on the Monte Carlo method. In Xia and Weitnauer (2019), particle filter is combined with interacting multiple models for time difference of arrival-based localization problem. Posterior Cramer-Rao lower bounds are derived to demonstrate the effectiveness of the proposed model. According to the simulation results, the proposed algorithm outperforms the others with an improvement in time. An unscented Kalman filter, extended Kalman filter, and particle filter-based methods are implemented in Ullah et al. (2019) for localization problem. Implemented methods are compared with each other and according to the results, methods can be used for tracking and localization problems. Dual particle filter-based estimation methodology for nonlinear stochastic systems is proposed in Daroogheh et al. (2018). Both state and parameters are estimated using the proposed scheme. Fault detection is achieved by dual particle filter and superiority of the scheme is showed with extensive simulation results.

In this work, particle filter-based attitude estimator is proposed and utilized as a hybrid scheme for nonlinear quadrotor dynamics. But, since recursive Bayesian estimation steps may rise degeneracy issues, the proposed scheme is improved with used resampling algorithm. Robustness of the proposed schemes is tested under different particle sizes. According to the statistical analysis, the proposed estimator is capable of reducing sensor noise under different particle sizes.

## 5.2 Quadrotor Model

There are different methods for expressing a vector in one axis set in another axis set. Euler transformation is one of these methods. In this transformation, one set of axes is rotated three times to overlap the other. Here, the order of rotation of the axis assembly is important, since the rotation order changes, it leads to a different result (Pamadi 2015).

Inertial reference system is  $I = (x_i, y_i, z_i)$  and body reference system is  $B = (x_b, y_b, z_b)$ . So the following is obtained if  $I$  reference system is rotated around  $B$  reference system with angles  $\psi, \theta, \phi$  sequentially as shown in Fig. 5.1.

$$R_3(\psi) = \begin{bmatrix} \cos\psi; \sin\psi; 0 \\ -\sin\psi; \cos\psi; 0 \\ 0; 0; 1 \end{bmatrix} \quad (5.1)$$

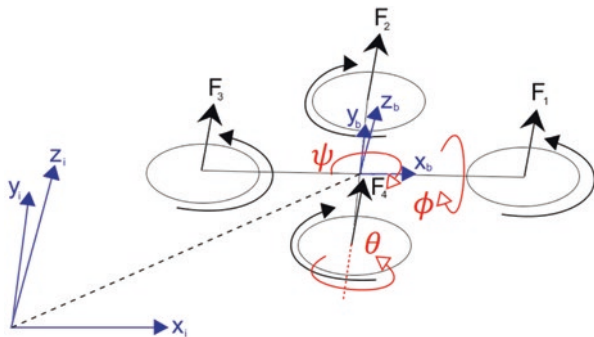


Fig. 5.1 Quadrotor frames

$$R_2(\theta) = \begin{bmatrix} \cos \theta & 0 & -\sin \theta \\ 0 & 1 & 0 \\ \sin \theta & 0 & \cos \theta \end{bmatrix} \quad (5.2)$$

$$R_1(\phi) = \begin{bmatrix} 1 & 0 & 0 \\ 0 & \cos \phi & \sin \phi \\ 0 & -\sin \phi & \cos \phi \end{bmatrix} \quad (5.3)$$

There are four control inputs of a quadrotor which has six degrees of freedom.

$$u_z = F_1 + F_2 + F_3 + F_4 \quad (5.4)$$

$$u_\phi = l(F_4 - F_2) \quad (5.5)$$

$$u_\theta = l(F_3 - F_1) \quad (5.6)$$

$$u_\psi = d(F_1 - F_2 + F_3 - F_4) \quad (5.7)$$

A summary of the equations of motion of the quadrotor is given below.

$$\dot{P} = \frac{1}{I_x} \left[ (I_y - I_z) QR + u_\phi - k_r P \right] \quad (5.8)$$

$$\dot{Q} = \frac{1}{I_y} \left[ (I_z - I_x) RP + u_\theta - k_r Q \right] \quad (5.9)$$

$$\dot{R} = \frac{1}{I_z} \left[ (I_x - I_y) PQ + u_\psi - k_r R \right] \quad (5.10)$$

### 5.3 Particle Filter

Particle filter is a Monte Carlo method that is based on the sequential importance sampling algorithm. Particle filter is used to find a suboptimal approximate solution to the recursive Bayesian estimation method. When the number of particles in the sample set becomes large enough, then particle filter is said to be a near-optimal solution of the recursive Bayesian estimation. Let  $\chi$  be the random measure of the form

$$X_k = \{x_k^{(n)}, w_k^{(n)}\}, n = 1, 2, \dots, N \quad (5.11)$$

Weights are normalized according to Eq. 5.12.

$$\sum_{n=1}^N w_k^{(n)} = 1 \quad (5.12)$$

Posterior probability density function is obtained as Eq. 5.13.

$$p(x_k | z_{1:k}) \approx \sum_{n=1}^N w_k(n) \delta(x_k - x_k(n)) \quad (5.13)$$

### 5.4 Results and Discussion

Resampling based particle filter estimator for the quadrotor is implemented in MATLAB. Performance of the proposed estimator under three different particle size is evaluated which are 100, 1000, and 10,000 particles. So, the proposed estimator is simulated with different conditions to cover the real quadrotor environment and challenges as much as possible.

The effects of the particle size into the estimation performance is tested under various particle sizes. For the given uncertainty level; performance of the resampling algorithm for 100, 1000, and 10,000 particle sizes is given in Fig. 5.2.

### 5.5 Conclusion

In this work, particle filter-based attitude estimation scheme for nonlinear quadrotor dynamics is proposed. Particle filter estimator is improved with resampling algorithms to address the particle degeneracy issue. The performance of the estimator with 1000 and 10,000 particles has better estimation performance in comparison to the estimator with 100 particles. So, according to the aforementioned remarks, it is concluded that the proposed scheme is capable of estimating the attitude angles of the quadrotor efficiently.

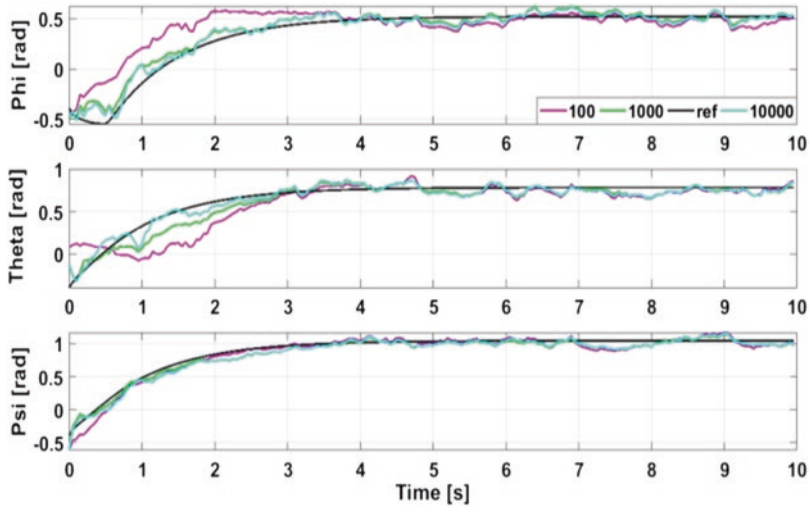


Fig. 5.2 Comparison of particle sizes

## References

- O. Araar, N. Aouf, *Full Linear Control of a Quadrotor UAV, LQ vs  $H^\infty$*  (IEEE, Loughborough, 2014)
- N. Daroogheh, N. Meskin, K. Khorasani, A dual particle filter-based fault diagnosis scheme for nonlinear systems. *IEEE Trans. Control Syst. Technol.* **26**(4), 1317–1334 (2018)
- A. Ermeydan, E. Kiyak, Fault tolerant control against actuator faults based on enhanced PID controller for a quadrotor. *Aircr. Eng. Aerosp. Technol.* **89**(3), 468–476 (2017)
- F. Kendoul, Survey of advances in guidance, navigation, and control of unmanned rotorcraft systems. *J. Field Rob.* **29**(2), 315–378 (2012)
- S. Khatoun, D. Gupta, L.K. Das, *PID & LQR Control for a Quadrotor: Modeling and Simulation* (IEEE, New Delhi, 2014)
- E. Kiyak, Tuning of controller for an aircraft flight control system based on particle swarm optimization. *Aircr. Eng. Aerosp. Eng.* **88**(6), 799–809 (2016)
- O. Kose, T. Oktay, Dynamic modeling and simulation of quadrotor for different flight. *Eur. J. Sci. Technol.* **15**, 132–142 (2019)
- E.Y. Metin, H. Aygün, Energy and power aspects of an experimental target drone engine at nonlinear controller loads. *Energy* **185**, 981–993 (2019)
- B.N. Pamadi, *Performance, Stability, Dynamics and Control of Airplanes*, AIAA education series (AIAA, Reston, 2015)
- I. Ullah et al., A localization based on unscented Kalman filter and particle filter localization algorithms. *IEEE Access* **8**, 2233–2246 (2019)
- N. Xia, M.A. Weitnauer, TDOA-based mobile localization using particle TDOA-based mobile localization using particle. *IEEE Access* **7**, 21057–21066 (2019)

# Chapter 6

## Electric Aircraft: Motivations and Barriers to Fly



Paul Parker and Chelsea-Anne Edwards

### 6.1 Introduction

Electric planes became a certified aviation option in 2020 when the European Aviation Safety Agency, EASA, certified an electric two-seat aeroplane designed primarily for flight training. The new technology offers several potential benefits that motivate adoption, including reduced greenhouse gas (GHG) emissions, reduced lead emissions, reduced noise and reduced operating costs. However, barriers such as uncertainty or lack of trust in the technology, limited battery capacity, limited battery life and costs associated with battery replacement may limit its appeal. The rate of adoption of this new technology will depend on perceptions regarding how important these benefits and barriers are among key stakeholders. This study provides insights from surveys of four groups: student pilots, instructors, managers/owners and others. The results will identify similarities and differences in the perceptions of these stakeholders influencing e-plane adoption at flight schools.

Flight schools are identified as an important first market for e-planes because their high usage rate (annual hours flown per aeroplane) and they are an important source of skills to enable change in the aviation industry. The introduction of new technology early in training will give students the skills in managing electric battery systems as a foundation for them to take to the aviation industry. E-planes may also reduce the cost of training thus reducing the financial barrier to entry into the pilot profession. This paper will set the context by starting with the global challenge to reduce GHG emissions from aviation and the entry of electric technology as a viable flight propulsion system. The literature on the expected benefits and barriers is reviewed and then the methods and research questions presented.

---

P. Parker (✉) · C.-A. Edwards  
Faculty of Environment, University of Waterloo, Waterloo, ON, Canada  
e-mail: [pparker@uwaterloo.ca](mailto:pparker@uwaterloo.ca); [ce2edwards@uwaterloo.ca](mailto:ce2edwards@uwaterloo.ca)

### 6.1.1 *Context and Literature*

The impacts of climate change and the urgent need for action to reduce GHG emissions is well documented (IPCC 2021). The use of electric aircraft (e-planes) in place of conventional fossil-fuel powered aircraft allows for the elimination of in-flight emissions, providing deep reductions in GHGs (Borer et al. 2016; Moua et al. 2020; Thapa et al. 2021). Although this technology is not at the commercial airliner scale, integrating e-planes into small scale operations such as flight schools provides an opportunity for the technology to be tested, proven and further developed. An example is the Pipistrel Velis Electro, a two-seat electric aircraft, officially certified by EASA in 2020 (Pipistrel 2020). This certification made the Velis Electro the first fully electric aircraft in the world to be type certified (EASA 2020). In addition to the deep emissions savings from using electric aircraft such as the Velis Electro for flight training, costs to student pilots can also be dramatically cut (Moua et al. 2020). However, before assuming the success of electric aircraft in flight training, it is important to understand the perceptions of key stakeholders.

A global study completed by Ansys (2020) of 16,037 participants from 10 different countries (U.K, U.S, Austria, Germany, Switzerland, France, Sweden, Japan, Chile, India) found that 63% of those surveyed, think about the emissions they create from personal or work air travel. The findings from the Ansys global study also showed that 89% of participants reported a willingness to pay for greener air travel, with 60% of participants considering e-planes because of the benefits to the environment. In terms of what would prevent the participants from wanting to travel on an electric aircraft, the most popular reason, at 49% of respondents, was that the technology is not yet proven. The other top reasons included the plane running out of battery, the battery technology failing or exploding, and expensive ticket prices. Pilot training was also addressed, with 17% concerned about additional pilot training needed (Ansys 2020). Only 14% of participants reported that they have no concerns.

In Canada, half of the population agrees that now is the best time for Canada to be ambitious in addressing climate change (Nanos Research 2021). In terms of aviation emissions, Canada successfully set a world record in 2019 by operating the world's first fully electric commercial aircraft (Guardian News and Media 2019). Harbour Air completed this flight in a retrofitted 1950's DHC de Havilland Beaver seaplane and has announced ambitions to retrofit all of their aircraft to become fully electric and free of in-flight emissions. Canadian flight schools also have aging fleets with 60% of the single engine flight training fleet built before 1980. If these aircraft were replaced by e-planes, flight training emissions would be sharply reduced.

## 6.2 Method

Given that no e-planes are currently certified or used for training in Canada, this study examines self-reported perceptions to gauge the importance of motivations and barriers to stakeholder groups (student pilots, instructors, flight school managers). We particularly wanted to answer the following questions:

1. How much do respondents know about e-planes?
2. What factors motivate respondents to want to fly e-planes?
3. What factors or barriers reduce respondent's desire to fly e-planes?

To answer these questions, the authors sent email invitations to 10 flight school managers in Canada and one in India (who had recently moved from Canada) to inform them about the study. When they agreed to participate, they were provided with an electronic survey link to forward to the students, instructors and staff at their flight school. In total, 186 responses were collected: 117 student pilots, 35 flight instructors, 15 managers/owners, and 19 others. Participation by gender was 28 females (15%), 155 males (83%), and 3 who preferred to not indicate gender (2%). Distribution by country: 158 Canada (85%), 24 India (13%), 4 other countries (2%).

The research instrument was created using Qualtrics and approved by the Office of Research Ethics (ORE# 43089). Information and recruitment letters preceded the 34-item survey. Most questions were answered on graphic scale: 0 represents "not an important reason to me" and 10 represents an "extremely important reason to me". A limitation was that the scale was automatically set at 0, so for questions where 0 was likely (low average), more respondents did not interact with the scale.

## 6.3 Results and Discussion

### 6.3.1 Knowledge and Desire to Fly an E-plane

Knowledge about a new technology is essential to support its adoption. Participants were asked about their knowledge of e-planes. Generally, knowledge was limited (mean value of 3.7 on a 10-point scale). Students reported the lowest level of knowledge (3.3), then instructors (4.0), and then managers (4.7). Finally, the group who classified themselves as "other" reported the highest level of knowledge, although it was still limited (5.0). This may indicate a higher level of knowledge and higher interest in e-planes and thus their willingness to participate in the survey (Table 6.1).

The second knowledge question asked participants to rate their knowledge of e-planes for flight training. As expected, the knowledge about this specialized type of e-plane (3.1) was lower than that for e-planes in general (3.7). All four cohorts followed this trend of less knowledge about e-planes for training. Again, students indicated the lowest level of knowledge (2.7) while managers reported the highest (4.1).

**Table 6.1** How much do you know about e-planes?, mean value by cohort (0 = none at all, 10 = complete knowledge)

	All	Student	Instructor	Manager	Other
E-planes – mean	3.7	3.3	4.0	4.7	5.0
<i>n</i> =	179	112	34	14	19
E-planes for training – mean	3.1	2.7	3.6	4.1	3.7
<i>n</i> =	117	67	27	12	11

**Table 6.2** Would you like to learn to fly an e-plane? (0 = not at all, 10 = definitely)

	All	Student	Instructor	Manager	Other
Type certified – mean	8.9	9.0	8.7	9.5	8.7
<i>n</i> =	180	113	34	15	18
Experimental – mean	8.0	8.3	7.5	7.7	7.9
<i>n</i> =	177	113	33	15	16

When asked if they would like to learn to fly an e-plane, all cohorts gave their most positive responses out of all the questions in the survey. When asked if they would like to learn to fly an e-plane that had been officially certified, all four stakeholder groups gave extremely strong positive responses. The average response from students was 9 out of 10. Managers provided an even higher average rating of 9.5. The instructors and other cohort gave a slightly lower average rating (8.7). Even learning to fly an experimental e-plane was rated very highly with students giving the highest rating (8.3) and instructors the lowest (7.5) (Table 6.2).

### 6.3.2 Motivations and Barriers

Questions regarding the importance of reasons to want to fly an e-plane identified different priorities among the stakeholder cohorts. The strongest reason among any cohort was manager's rating of the potential to cut costs (mean = 8.5). The managers rated the potential for quieter flights as their second reason (7.9), cutting emissions was third (7.5) and increased safety fourth (7.4). Instructors followed the managers' pattern of rating cost reduction the highest (8.0), but their second strongest reason was that e-planes were a technology of the future (7.7). Student motivation was different with cutting emissions rated most important (8.2). The next reasons for students were cutting costs (7.3) and flying a technology of the future (7.3) (Table 6.3).

The barriers or reasons for not wanting to fly an e-plane saw much stronger consistency across cohorts. Students, instructors, and managers each rated limited battery endurance as their strongest reason to not fly an e-plane. Students and managers both rated the likelihood that oil-based technologies would continue to dominate the



**Table 6.3** Reasons to fly an e-plane, (0 = not important, 10 = extremely important)

	All	Student	Instructor	Manager	Other
Cut emissions	7.9	8.2	7.2	7.5	7.1
Reduce cost	7.5	7.3	8.0	8.5	6.9
Future tech	7.3	7.3	7.7	7.0	6.9
Quieter	6.9	6.8	6.7	7.9	6.9
Safer	6.0	5.8	6.0	7.4	6.1
Growing share	5.6	5.7	5.7	5.6	4.5

**Table 6.4** Reasons not to fly an e-plane, (0 = not important, 10 = extremely important)

	All	Student	Instructor	Manager	Other
Battery endurance	5.8	5.6	6.7	6.3	5.1
Oil tech continues	5.5	5.6	4.9	6.2	5.1
Battery safety	4.8	4.5	5.3	4.8	5.6
Increase cost	4.6	4.7	3.5	4.9	4.9
Increase accident risk	4.2	4.2	4.1	3.7	4.5
Not trust electric tech	3.7	3.4	4.1	4.3	4.5
Increase training time	3.6	3.4	3.2	4.0	4.9

industry for their career as the second strongest reason and a possible increase in costs as the third. In contrast, instructors rated battery safety as their second strongest reason and the continued dominance of oil-based technologies as third. The concern about battery safety was rated as the strongest reason to not fly e-planes by the “other” cohort. The clear conclusion is that this study supports findings of earlier studies (Han et al. 2019) that batteries are the biggest perceived barrier and that students, instructors and flight school managers share this assessment (Table 6.4).

Having identified the top motivations and barriers to the adoption of e-planes, their relative strength can be considered. The top motivation among all participants was cutting emissions rated an importance of 7.9 while the strongest barrier was battery endurance rated at 5.8. This indicates a much stronger perception of the top motivation than the top barrier. This overall result is strongly influenced by the student perceptions because of the large number of student respondents. An examination of each stakeholder cohort reaches the same conclusion. The student rating of cutting emissions (8.2) is much higher than their rating of battery endurance and the continued use of oil-based technologies (5.6). Similarly, the instructor and manager ratings of reducing costs (8.0 and 8.5, respectively) is much higher than battery endurance (6.7 and 6.3, respectively). The other cohort repeated the pattern with cutting emissions (7.1) rated more highly than battery safety (5.6).

## 6.4 Recommendations and Conclusions

The survey findings lead to the following recommendations:

- Address limited e-plane knowledge with knowledge dissemination
  - Media, social media, demonstrations, air shows, etc.
- Reinforce motivations with information
  - Share cost information
    - Top priority for manager/owner, instructor cohorts
    - Important for other cohorts
  - Share emission performance information
    - Top priority for student pilots
    - Important for other cohorts
- Address barriers with research and knowledge dissemination
  - Document and share improved battery performance
  - Make direct comparisons in the flight school environment

Overall, participants in the survey demonstrated that different stakeholder cohorts place different levels of importance on reasons to fly an e-plane. The most important reason among student pilots was to reduce emissions while the most important reason among instructors and managers was to reduce costs. These differences should be recognized when prioritizing information to be shared with each cohort. Secondary reasons were also rated as important so information on noise reduction, improved safety and developing skills for technologies of the future should also be developed. The perceptions of barriers or reasons not to want to fly e-planes were consistent across cohorts with the limited endurance of batteries being the most important. Improvements in battery performance need to be shared.

Providing performance results across multiple sustainability criteria (emissions, cost, noise, appeal to diverse cohorts, safety, endurance, etc.) will help overcome the limited knowledge currently available regarding electric aviation. Improved knowledge dissemination will help create a market for the new technology and attract a new generation of talent to the industry.

## References

- Ansys, *Electrification Aero Global: Survey Infographics. Eyes on Greener Skies* (Ansys, Canonsburg, 2020)
- N.K. Borer, C.L. Nickol, F. Jones, R. Yasky, K. Woodham, J. Fell, A. Samuel, Overcoming the adoption barrier to electric flight. 54th AIAA aerospace sciences meeting (2016). <https://doi.org/10.2514/6.2016-1022>

- European Union Aviation Safety Agency (EASA), *EASA certifies electric aircraft, first type certification for fully electric plane world-wide* (EASA, Cologne, 2020)
- H. Han, J. Yu, W. Kim, An electric airplane: assessing the effect of travelers' perceived risk, attitude, and new product knowledge. *J. Air Transp. Manag.* **78**, 33–42 (2019). <https://doi.org/10.1016/j.jairtraman.2019.04.004>
- Guardian News and Media. World's first fully electric commercial aircraft takes flight in Canada. *The Guardian*. 11 Dec. (2019). <https://www.theguardian.com/world/2019/dec/11/worlds-first-fully-electric-commercial-aircraft-takes-flight-in-canada>
- Intergovernmental Panel on Climate Change (IPCC), AR6 climate change 2021: the physical science basis (2021). <https://www.ipcc.ch/report/ar6/wg1/>
- L. Moua, J. Roa, Y. Xie, D. Maxwell, 'Critical review of advancements and challenges of all-electric aviation'. International Conference on Transportation and Development (2020). <https://doi.org/10.1061/9780784483138.005>
- Nanos Research. Climate ambition steady: Urgency to act now trending up (2021). <https://nanos.co/wpcontent/uploads/2021/04/2021-1809-Positive-Energy-Feb-Populated-report-Updated-with-Tabs.pdf>
- Pipistrel, Velis electro: arriving from the future, EASA type-certified now (2020). <https://www.pipistrel-aircraft.com/aircraft/electric-flight/velis-electro-easa-tc>
- N. Thapa, S. Ram, S. Kumar, J. Mehta, All electric aircraft: A reality on its way. *Mater. Today Proc.* (2021). <https://doi.org/10.1016/j.matpr.2020.11.611>

# Chapter 7

## Determination of Environmental Impact Assessment Criteria in the Life Cycle of Transport Facilities



Victoriia Khrutba, Inessa Rutkovska, Tatiana Morozova, Lesia Kriukovska, and Natasha Kharitonova

### Nomenclature

EIA	Environmental Impact Assessment
RC	Road Constructions
RS	Rolling Stock
TF	Transport Facility

### 7.1 Introduction

The vast majority of ecosystems in Ukraine are characterized by uneven spatial pollution. Under such conditions, the impact on humans, populations or ecosystems is assessed as a spatially distributed source, where complex biogeochemical transformations occur with continuous redistribution of man-made compounds as a result of transformation and migration. Usually, the limits of environmental change significantly exceed the area of land allotment (watering can of depression at a point source – a well with an area of several tens of km<sup>2</sup>). Several zones of man-made impact are formed around each source of pollution, the size and configuration of which depend on the type and nature of the impact, geographical location, and natural conditions of the territory.

Ensuring the optimal level of environmental safety and prevention of the cumulative effect of the accumulation of regular disturbances is possible with the help of ecosystem development criteria (Yakovlieva et al. 2021). The key concepts for the development of criteria are the stability of biosphere elements and allowable loads.

---

V. Khrutba (✉) · I. Rutkovska · T. Morozova · L. Kriukovska · N. Kharitonova  
National Transport University, Kyiv, Ukraine

State Enterprise “M.P. Shulgin State Road Research Institute” (“DerzhdorNDI” SE),  
Kyiv, Ukraine

Environmental impact assessment of transport facilities and roads at all stages of their life cycle embodies a new approach to the problem of safety of territories based on ecological paradigm, characterizes the protection of natural and social environment, ensures the sustainability of ecosystems and environmental safety (Yakovlieva et al. 2019). For the development and implementation of large infrastructure projects for the construction and reconstruction of roads, during which there is a significant impact on the atmosphere, hydrosphere, lithosphere, and biodiversity, especially relevant is the implementation of environmental impact assessment, which minimizes environmental impacts at the design stage.

This approach requires a new organizational structure and information model of environmental control by involving specially formed new indicators of the state of the environment – criteria and quality indices (Klymenko 2010).

Researches of the territory ecological safety indicators were conducted by Anikiev and Zakharova (2002), Bykova et al. (2006), and others, the issue of environmental impact assessment in their research papers considered Sydor (2018), Sharavara et al. (2019), however, the choice of criteria for environmental safety of roads remains poorly studied.

The complex idea of environmental impact assessment and economic value of the life cycle of the road surface based on the life cycle assessment system, which is equivalent to the method of environmental impact assessment taking into account economic costs was considered by Jiawen Liu, Hui Li, Yu Wang, and Nailong Ge in *Transportation Systems Analysis and Assessment* (2019).

Peculiarities of environmental impact assessment and pollution potential of projects implemented in Brazil are given in (Tagliani et al. 2020).

Sardinia's case study on the collection and analysis of information related to regional environmental impact assessment procedures in Italy is done in Cannao and Onni (2019).

The study (Ashofteh et al. 2017) assesses the impact on the environment of the Shahriar dam irrigation project in Iran.

The studies of the specifics of environmental impact assessment procedures in Lao PDR examine practical experience and research EIA legislation, administrative procedures, recommendations and relevant documents, models, and criteria (Wayakone and Makoto 2012).

The comprehensive approach to the quantitative assessment of criteria and indicators of environmental impact with an improved Leopold matrix using multicriteria optimization methods and the Harrington function is presented in Rudenko et al. (2013) and Olekh (2015).

Some criteria for environmental impact assessment for projects of planned construction/reconstruction/operation of transport facilities that have a primary (or direct) impact on the environment are proposed in Nevedrov (2020).

In the work (Khrutba et al. 2021a), the algorithm for conducting stages of environmental impact assessment in Ukraine was developed.

At the same time, the lack of quantitative assessment of environmental impact in the project documentation for the construction of roads complicates the development and examination of relevant project documentation. Existing methods and

techniques for forecasting environmental impact assessments of public roads are not adapted to the input design parameters or are not correct at all. Furthermore, the introduction of new methods of forecasting the impact of the road on the environment and improving existing ones requires verification and testing in road design organizations in the development of the EIA section of project documentation for construction, reconstruction, overhaul of engineering and transport infrastructure. The difficulty of choosing and justifying the criteria for assessing the environmental safety of transport facilities is the diversity and variety of indicators, which makes it virtually impossible to form a single quantitative assessment. The system of indicators/criteria at different stages of the life cycle may change and expand, depending on the characteristics of the region.

Therefore, there is an urgent problem of choosing criteria for assessing the level of environmental safety of the road. It is important to form a system of criteria/indicators and methods of their calculation and comparison. It is most expedient to use three groups of indicators of sustainable development, among which the most important in the formation of a balanced assessment of the territory and the least studied and scientifically sound are the indicators/criteria of the ecological group.

The objective of the work is the establishment of quantitative indices of the environmental impact of the transportation facilities' projected construction, exploitation, maintenance, and reconstruction activities assessment.

## 7.2 Features of Environmental Impact Assessment Criteria in the Life Cycle of Transport Facilities

The criterion/indicator is both a pointer and a symbol, which is given the value of a measure of magnitude, property, process (Klymenko 2010). The mathematical essence of the ecological criterion/indicator: it can be a scalar, a vector and a more complex quantity that can be given in the form of a matrix.

Criteria for environmental safety of roads are aimed at minimizing the negative impact on ecosystems; ensuring safety, convenience, and comfort; relate to technologies and materials of construction, reconstruction, operation, and repair; constructions of engineering constructions of highways, objects of road service; consumption of natural resources in the construction and operation of roads, considering their regeneration/restoration. For example, in the area of implementation of the planned activities, it is advisable to use the criteria that can be represented by the following sequence:

$$Kr = (k_1, k_2, k_3, k_4, k_5, k_6, k_7) \quad (7.1)$$

where  $k_1$  – sensitivity;  $k_2$  – resistance to change;  $k_3$  – possibility of adaptation;  $k_4$  – uniqueness;  $k_5$  – complexity/variety of connections;  $k_6$  – value, compared to other objects/resources;  $k_7$  – vulnerability, etc.

In addition, it is necessary to assess the scale of the impact, while using different parameters, including spatial boundaries, duration, and intensity.

Environmental impact assessment requires a probabilistic forecast of changes in the most vulnerable natural components that are directly affected. Qualitative and quantitative criteria/indicators characterize intensity (pollution per unit time), specific power (pollution per unit area), periodicity (discrete, continuous, one-time impact), duration, spatial boundaries (depth, size, and shape of the impact zone).

To select the criteria for assessing the project's impact on the environment, the principles and procedures presented in ISO 21929-1 (2011), ISO 15392 (2019), DSTU ISO 14040 (2013), DSTU ISO 14020 (2003), DSTU ISO 14021 (2016), DSTU ISO 14024 (2018), and DSTU ISO 14025 (2008) are used. Also, if appropriate, the principles set out in ISO 26000 (2010) should be considered.

Criteria and indicators of TF impact on the environment are systematized according to the following aspects: object of assessment (by location; by construction (operation, repair); by process); TF life cycle stage (typical for new TF; characterize TF life cycle stage; typical for existing TF); the type of information being evaluated (criteria based on planned or calculated indicators; criteria based on measured or other factual data); impact characteristics (direct or indirect); complexity (criteria represented by one parameter, criteria described by many parameters); the nature of the evaluation process (quantitative, descriptive, qualitative); system of spatial constraints (global, regional, local); system of time constraints (recorded impact over the next 100 years, short-term impact) (Fig. 7.1).

Requirements for the criteria of TF environmental impact: informativeness and significance; clear attitude to one or more zones of influence; based on data that is available and easily accessible; the need for coordination with stakeholders.

The system of criteria and indicators of TF impact on the environment should include indicators that are representative of the aspects of TF that affect one or more aspects of the environment (Khrutba et al. 2021a).

Considering the typical problems of the transport complex, their environmental safety can be assessed from the analysis of the dynamics of changes in basic indicators, which are grouped into the next hierarchical link – aggregate indicators (criteria). The main aspects of TF environmental impact belong to the following categories: impact on the quality of the surface layer of atmospheric air, the consumption of non-renewable resources, the impact on the quality of the aquatic environment, the efficiency of waste management; impact on the quality of land resources, impact on the quality of the geological environment; physical factors of impact on the environment, impact on flora and fauna, protected areas; the impact of TF on the social environment; the impact of TF on the man-made environment.

Table 7.1 presents the basic criteria, indicators, and main impacts of TF on the environment. The set of indicators may change according to the natural conditions and requirements of the project.

Criteria and indicators of the impact of TF on the environment are determined throughout the life cycle of TF in compliance with the basic principles set out in DSTU ISO 14040, namely, at the stage of design; construction/reconstruction; operation and completion of the life cycle.

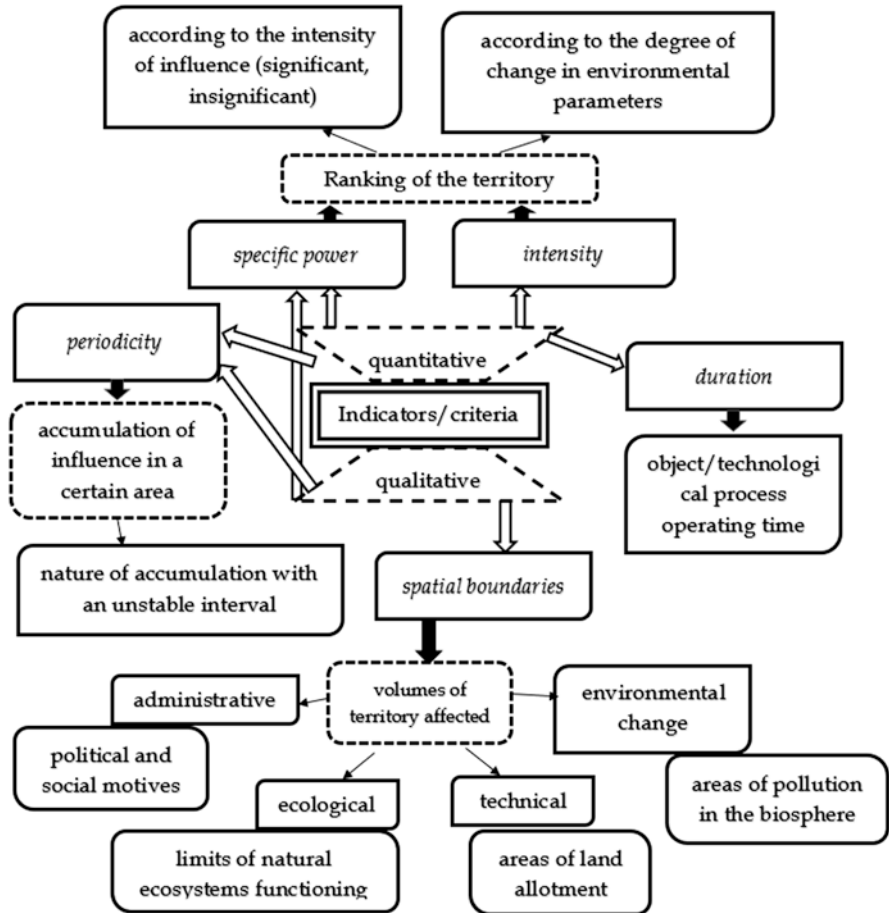


Fig. 7.1 Types of criteria

### 7.3 Method for Calculating Criteria

Theoretical and empirical methods were used for the research, the main ones being the system approach, methods of analysis and synthesis (comparison, analogy, abstraction, formalization, classification). Other complementary methods can be used to conduct EIA: the method of combined map analysis; flow chart system method; simulation method; method of expert groups, etc.

To determine the quantitative assessment of the intensity of impact (amplitude) and the importance of changes in the ecosystem (importance) for each  $K_{rez}$  criterion, the expert assessment is conducted, which is calculated according to the formula:

$$K_{rez} = Risk + Low + Soc + M + Fin + Tex + Time \cdot Y \tag{7.2}$$



**Table 7.1** Basic criteria, indicators, and main impacts of TF on the environment

Criterion	Indicator	RS	RC
Impact on atmospheric air	Mass concentration of pollutant in the surface layer of air	XX	XX
	The content of ozone-depleting substances	X	–
	Mass concentration of greenhouse gases in the air	XX	X
	Mass concentration of solid particles (dust)	XX	XX
Resource and energy saving	Use of industrial waste for construction of TF	X	XX
	Use of plastic or rubber materials for construction of TF	X	X X
	The level of use of natural resources	XX	XX
	The level of environmental friendliness of vehicles	XX	X
	Use of alternative energy sources	XX	X
	Use of environmentally certified products	XX	XX
The level of water pollution	Concentration of pollutants in water bodies	X	X
	Biochemical or chemical level of oxygen consumption	–	X
	Ecological condition of surface waters	X	X
Waste management	The amount (volume) of waste generation	XX	XX
	Waste recycling level	XX	XX
Quality of land resources	Mass concentration of pollutants in soils	X	XX
	The level of fragmentation of territories	X	XX
	Increasing the area of green areas	X	XX
The quality of the geological environment	Level of influence on geological processes	–	X
	Level of influence on hydrological processes	–	X
Criteria for physical impact on the environment	The level of noise pollution	XX	X
	Level of vibration pollution	XX	X
	The level of light pollution	–	X
	The level of electromagnetic pollution	XX	X
	The level of thermal pollution	X	–
	The level of radiation pollution	–	X
Biodiversity conservation	Impact on flora	XX	XX
	Impact on the animal world	X	XX
	Impact on nature reserves	X	X
Level of social security	Transport accessibility to life support facilities	XX	XX
	Proximity of TF to public transport	XX	XX
	The level of comfort of the territory	XX	XX
	Influence on the cultural and historical value of the territory	X	XX
	Living conditions of the population	X	XX
The level of man-made safety	Natural hazards	XX	XX
	Man-made hazards	XX	XX

“XX” indicates a primary (or direct) impact; “X” indicates a secondary (or indirect) impact, “–” indicates a potential impact is insignificant or absent

where Risk – impact risk assessment; Low – assessment of compliance with legal and regulatory requirements; Soc – assessment of public opinion; M – assessment of the scale of impact; Fin – assessment of financial costs to overcome the effects of the impact; Tex – use of new innovative technologies; Time – time or duration of impact; Y – assessment of the ability to manage.

Indicators of criteria evaluation parameters are set by assigning points from 0 to 3 for each. To establish the score of the criterion ( $K_{ASS}$ ), for each individual EIA criterion calculation tables are formed (Khrutba et al. 2021b). The typical example of table design is shown in Table 7.2.

Estimation of the intensity of impact (amplitude) and/or significance of changes in the ecosystem (importance) for each criterion of the processes of construction, operation, repair, reconstruction of TF  $\omega_i$ , which have an impact on the environment, is determined by the Table 7.3.

Below please see the example of defining certain criteria for environmental impact in road construction and reconstruction projects.

#### 1. The quality of the surface layer of atmospheric air.

This criterion assesses the impact on the quality of the surface layer of atmospheric air during the construction or operation of TF.

$$K_1 = (K_{1.1}, K_{1.2}) \quad (7.3)$$

The criterion includes the following indicators:

$K_{1.1}$  – mass concentration of the pollutant in the surface layer of atmospheric air for a certain period in the area of influence of TF;

$K_{1.2}$  – mass concentration of solid pollutants (dust).

##### 1.1 Mass concentration of the pollutant in the surface layer of atmospheric air for a certain period in the area of influence of TF.

This criterion determines the mass concentrations of pollutants in the surface layer of atmospheric air for a certain period in a certain area of TF location. Emissions of pollutants may be the result of exposure to processes during construction or operation of TF.

$$K_{1.1} = (K_{1.1.1}, K_{1.1.2}) \quad (7.4)$$

Emissions of pollutants include:

$K_{1.1.1}$  – emissions of vapor and gaseous inorganic compounds;

$K_{1.1.2}$  – emissions of pollutants classified as organic compounds.

To estimate the mass concentration of pollutants in the surface layer of atmospheric air for a certain period in a certain area of influence of TF from the technical documentation determine the mass concentration of pollutants, such as: Sulfur (IV) oxide, Carbon (II) oxide, Nitrogen oxides, etc., we choose the receptor points at

**Table 7.2** The typical calculation table for scoring a specific criterion ( $K_{ass}$ ). Name of TF EIA criterion: Use of slag materials for general construction works

Application	Material from natural raw materials	Substitute	Content of substitute in the composition of the material, %	Environmental impact from the use of slag materials (blast furnace, steelmaking, ash carriers) as a pavement material									
				Danger of impact	Law, regulations	Public opinion	Scale	Financial expenses	New technology	Time or duration of impact	Ability to manage	Score of criterion	Intensity of impact
				Risk	Low	Soc	M	Fin	Tex	Time	Y	Krez	$\omega_i$

**Table 7.3** Determination of impact intensity

Final evaluation of the criterion	Degree/intensity of impact	
KASS, scores	The value of impact, $\omega_i$	Category of impact:
3–13	0	Missing
14–24	1	Weak
25–35	2	Average
36–46	3	Strong
47–57	4	Very strong
58–63	5	Critical

which to determine the effect of the pollutant. The evaluation results are entered in Table 7.4.

### 1.2 Mass concentration of solid pollutants (dust).

This criterion evaluates the emissions of solid pollutants into the environment (dust), and determines the content of solid particles (SP10, SP2,5) and/or the total content of suspended particles, emissions of suspended solid particles (microparticles and fibers); emissions of suspended solids pollutants defined as carcinogenic and emissions of suspended solid pollutants undifferentiated by composition. To estimate the concentrations of solid particles ( $PM_{10}$  i  $PM_{2,5}$ ) in the surface layer of atmospheric air for a certain period in a certain area of influence of TF from the technical documentation the concentrations of solid particles ( $PM_{10}$  i  $PM_{2,5}$ ) of individual pollutants are determined, we choose the receptor points at which to determine the effect of the pollutant. The result of the calculation is entered in Table 7.5.

## 7.4 Results and Discussion

The proposed criteria and method of their calculation were used to assess the environmental impact of the project “Construction of the state road H-31 Dnipro – Tsarychanka – Kobeliaky – Reshetylivka from the village Loboykivka to the border of Dnipropetrovsk region I-b technical category with 4 lanes bypassing settlements Loboykivka, Petrykivka, Mohyliv, Kitaygorod, Tsarychanka, Lyashkivka” (Report 2018).

During preparation of the environmental impact report, the main production processes and their impact on the environment were identified. For each identified process, the emissions of pollutants in the lower atmosphere are determined (oxides of sulfur and nitrogen, oxides of carbon (II), benzo(a)pyrene, etc.) from emissions of construction machinery engines (jib cranes, excavators, etc.), emissions of pollutants during transportation of materials, equipment, and workers. A fragment of the results of the calculation of the impact on air quality of individual production processes are given in Table 7.6.

The analysis of the results allowed to assess the level of negative impacts on individual components of the environment of all production processes of this

**Table 7.4** Determination of environmental impact from emissions of pollutants in the surface in the layer of atmospheric air in the impact zone of TF

Pollutant	CAS registration number <sup>a</sup>	Receptor point	Environmental impact from emissions of pollutants in the surface in the layer of atmospheric air in the impact zone of TF									
			Danger of impact	Law, regulations	Public opinion	Scale	Financial expenses	New technology	Time or duration of impact	Ability to manage	Score of criterion	Intensity of impact
			Risk	Low	Soc	M	Fin	Tex	Time	Y	Krez	$\omega_j$

<sup>a</sup>CAS registration number is determined from the Environmental Quality Standards for priority substances and some other pollutants, Directive 2013/39/EU of the European Parliament and the Council of 12 August 2013

**Table 7.5** Determination of environmental impact from solid pollutants in the surface layer of atmospheric air

Pollutant	CAS registration number <sup>a</sup>	Receptor point	Environmental impact from solid pollutants in the surface layer of atmospheric air					Time or duration of impact	Ability to manage	Score of criterion	Intensity of impact	
			Danger of impact	Law, regulations	Public opinion	Scale	Financial expenses					New technology
PM2,5	PM10		Risk	Low	Soc	M	Fin	Tex	Time	Y	Krez	$\omega_i$

<sup>a</sup>CAS registration number is determined from the Environmental Quality Standards for priority substances and some other pollutants, Directive 2013/39/EU of the European Parliament and the Council of 12 August 2013

**Table 7.6** Calculation of environmental impact criteria of the Liashkivka localities project fragment

		Risk	Low	Soc	M	Fin	Tex	Time	Y	Krez	$\omega_i$
Influence on the quality of the surface layer of atmospheric air											
Mass concentration of pollutant in the surface layer of atmospheric air											
<i>Sulfur oxide. On the axis of the road</i>											
Road formation	Arrangement of the ground	2	2	2	2	2	2	2	2	28	2
	Removal of topsoil	2	3	2	2	2	2	2	2	30	2
Road dressing	Left-hand drive	3	2	3	3	2	2	3	2	36	3
	Right-hand drive	2	2	2	2	1	2	2	3	39	3
<i>Nitrogen oxide. On the axis of the road</i>											
Road formation	Arrangement of the ground	2	2	2	2	2	3	2	2	30	2
	Removal of topsoil	2	2	3	2	3	2	3	2	34	2
Road dressing	Left-hand drive	3	2	3	3	2	2	3	2	36	3
	Right-hand drive	3	3	3	3	3	3	3	3	42	3
Strengthening of roadside. Arrangement of road dressing to strengthen the roadside		2	2	3	2	2	2	3	2	32	2
<i>Carbon monoxide. On the axis of the road</i>											
Road formation	Arrangement of the ground	1	2	2	2	1	1	2	2	22	1
	Removal of topsoil	1	1	1	1	1	1	2	2	16	1
Road dressing	Left-hand drive	2	2	2	3	2	2	3	2	32	2
	Right-hand drive	3	2	3	2	2	2	1	2	30	2
Strengthening of roadside. Arrangement of road dressing to strengthen the roadside		2	1	1	2	1	2	2	2	22	1
<i>Benzo(a)pyrene. On the axis of the road</i>											
Road formation	Arrangement of the ground	1	1	1	1	1	1	1	1	7	0
	Removal of topsoil	2	1	1	2	1	2	2	1	11	0
Road dressing	Left-hand drive	3	2	3	3	3	2	3	2	38	3
	Right-hand drive	3	2	3	3	2	3	2	2	36	3
Strengthening of roadside. Arrangement of road dressing to strengthen the roadside		3	1	1	1	2	3	2	2	26	2
<i>Mass concentration of solid pollutants (dust). PM<sub>2,5</sub> on the axis of the road</i>											
Road formation	Arrangement of the ground	2	2	2	2	2	2	2	2	28	2
	Removal of topsoil	2	3	2	3	2	2	2	2	32	2
Road dressing	Left-hand drive	3	2	3	2	3	2	3	2	36	3
	Right-hand drive	3	2	3	3	3	2	3	2	38	3

project, to identify the processes that most affect the environment and environmental components that are most affected during the planned activities of construction, operation, repair, and reconstruction of TF.

## 7.5 Conclusion

Based on the analysis of literature sources, the list of criteria for environmental impact assessment in construction and reconstruction projects of transport facilities is proposed. The list of criteria includes: impact on the quality of the surface layer of atmospheric air; volume of consumption of non-renewable resources; impact on the quality of the aquatic environment; waste management efficiency indicator; impact on the quality of land resources; impact on the quality of the geological environment; physical factors influencing the environment; impact on flora and fauna, protected objects; impact of TF on the social environment; impact of the transport structure on the man-made environment. Each of the criteria is a set of local indicators.

The method of quantitative assessment of environmental impact assessment criteria has been developed, which provides for expert assessment of each criterion according to the proposed scale and determination of the level of impact of this indicator on the environment.

The method was implemented during the environmental impact assessment of the project “Construction of the state road H-31 Dnipro – Tsarychanka – Kobeliaky – Reshetylivka from the village of Loboykivka to the border of Dnipropetrovsk region I-b technical category with 4 lanes bypassing Loboykivka, Petrykivka, Mohyliv, Kitaygorod, Tsarychanka, Lyashkivka.” The analysis of the results allowed to assess the level of negative impacts on individual components of the environment of all production processes of this project, to identify the processes that most affect the environment and environmental components that are most affected during the planned activities of construction, operation, repair, and reconstruction of transport facilities.

## References

- V.V. Anikiev, P.V. Zakharova, Integral criterion of environmental safety. *Geoinformatics* **1**, 8–16 (2002)
- P.S. Ashofteh, O. Bozorg-Haddad, H.A. Loáiciga, Multi-criteria environmental impact assessment of alternative irrigation networks with an adopted matrix-based method. *Water Resour. Manag.* **31**, 903–928 (2017)
- E.V. Bykova, M.K. Tsaranu, T.I. Kirillova, Approaches to the formation of a system of environmental indicators as a component of the system of energy security indicators. *Problemele Energeticii Regionale* **1**, 38–47 (2006)
- C. Cannao, G.A. Onni, Methodological approach on the procedural effectiveness of EIA: the case of Sardinia. *City Territ. Arch.* **6**, 1 (2019)



- DSTU ISO 14020:2003, Eco-labels and declarations. General principles
- DSTU ISO 14021:2016, Eco-labels and declarations. Environmental self-declarations (environmental labeling type II) (ISO 14021:2016, IDT)
- DSTU ISO 14024:2018, Eco-labels and declarations. Environmental labeling type I. Principles and procedures (ISO 14024:2018, IDT)
- DSTU ISO 14025:2008, Eco-labels and declarations. Environmental declarations type III. Principles and procedures (ISO 14025:2006, IDT)
- DSTU ISO 14040:2013, Environmental management. Life cycle assessment. Principles and structure (ISO 14040:2006, IDT)
- ISO 15392:2019, Sustainability in buildings and civil engineering works – general principles
- ISO 21929-1:2011, Sustainability in building construction—sustainability indicators—Part 1: framework for the development of indicators and a core set of indicators for buildings. <https://www.iso.org/obp/ui/#iso:std:iso:21929:-1:ed-1:v1:en>
- V. Khrutba, Y. Anpilova, V. Lukianova, I. Kotsiuba, L. Kriukovska, O. Spasichenko, Evaluation of the impact on the environmental building and reconstruction of motorways using the system analysis method environmental research. *Eng. Manag.* **77**(1), 85–95 (2021a)
- V. Khrutba, L. Globa, V. Lukianova, Y. Anpilova, Application of a multi-criteria optimisation method for road reconstruction projects to assess the environmental impact. *CEUR Workshop Proc.* **3021**, 87–104 (2021b)
- L.P. Klymenko, N.O. Voskoboinikova, The Choice of Indicators of Changes in the Level of Environmental Safety of the Region during Introduction of Alternative Heat and Cold Supply Systems. *Environmental Safety*, **2**, 16–19 (2010)
- D.S. Nevedrov, Methods and models of environmental impact assessment in projects of construction and reconstruction of critical infrastructure. Thesis for a candidate degree in technical sciences on a specialty 13 May 22 – projects and programs management. National Transport University, Ministry of Education and Science of Ukraine, Kyiv (2020), p. 208
- T.M. Olekh, Development of goal-setting models and decision-making methods in projects based on multidimensional assessments. Thesis for a candidate degree in technical sciences. Odesa National Polytechnic University, Odesa (2015), p. 174
- Report, Environmental impact assessment of the construction of the highway of state importance H-31 Dnipro – Tsarychanka – Kobeliaky – Reshetylivka from the village of Lobyokivka to the border of Dnipropetrovsk region I-b technical category with 4 lanes (2 lanes in each direction) in bypassing the settlements of Lobyokivka, Petrykivka, Mohylyv, Kytayhorod, Tsarychanka, Lyashkivka. *Dnipro* (2018), p. 459
- Rudenko, S., Olekh, T., Gogunsky, D., 2013. Model of generalized environmental impact assessment in projects. *Manag. Complex Syst. Dev.* **15**, p. 53–60
- V.V. Sharavara, O.O. Bondarenko, O.G. Tarasova, R.B. Gavrilyuk, D.V. Gulevets, S.A. Savchenko, *Introduction of Environment Impact Assessment in Ukraine: Risks and Prospects Analysis (Public Vision)* (Kyiv, NECU, 2019), p. 29
- International Standard ISO 26000:2010. Guidelines on social responsibility [https://iso26000.info/wp-content/uploads/2017/06/ISO-26000\\_2010\\_E\\_OBPPages.pdf](https://iso26000.info/wp-content/uploads/2017/06/ISO-26000_2010_E_OBPPages.pdf)
- V. Sydor, Environmental impact assessment: the law works, the problems remain. *Entrepreneurship Econ Law* **6**, C.142–C.145 (2018) URL: <http://pgp-journal.kiev.ua/archive/2018/6/25.pdf>
- Paulo Roberto A. Tagliani, Pohlen Roberta, Luis Fernando Carvalho Perello. Brazilian environmental-impact assessment system: a critical analysis. *WIT Transactions on Ecology and the Environment*. WIT Press Southampton, 2020, p. 245
- Transportation Systems Analysis and Assessment. Integrated life cycle economic and environmental impact assessment for transportation infrastructure: a review by Jiawen Liu, Hui Li, Yu Wang and Nailing Ge (2019). <https://www.intechopen.com/chapters/67636>
- S. Wayakone, I. Makoto, Evaluation of the environmental impacts assessment (EIA) system in lao PDR. *J. Environ. Prot.* **3**(12), 1655–1670 (2012). <https://doi.org/10.4236/jep.2012.312182>
- A.V. Yakovlieva, S.V. Boichenko, J. Zarembo, Improvement of air transport environmental safety by implementing alternative jet fuels. MOSATT 2019 – modern safety technologies in transportation international scientific conference, proceedings (2019), pp. 146–151, 894412
- A. Yakovlieva, S. Boichenko, U. Kale, A. Nagy, Holistic approaches and advanced technologies in aviation product recycling. *Aircr. Eng. Aerosp. Technol.* **93**(8), 1302–1131 (2021)

# Chapter 8

## Two-Phase Heat Exchangers for Thermal Control of Electric Aircraft Equipment

Leonard Vasiliev and Alexander Zhuravlyov

### Nomenclature

HP Heat pipe  
TS Thermosyphon

### 8.1 Introduction

In connection with the growing requirements for improving the environment, nowadays the world attaches great importance to the creation and improvement of hybrid and electric vehicles. The development of electric aircraft is a logical and inevitable step for commercial aviation, which offers great opportunities for reducing carbon emissions. The carbon footprint is one of the biggest challenges facing air travel this century. Even the most efficient aircraft engines today burn significant amounts of fossil hydrocarbon fuels. For example, in the United States, aviation is responsible for 12% of all carbon emissions.

Electric transport means are in great need of cooling as the majority of their components pass current and are heated up (cooling of the power drive, navigation electronic devices, storage battery, heating of intake air in air conditioners, etc.). The control system of the traction electric drive of the aircraft includes relay-contact converters, amplifiers, elements of digital and analog computers, microprocessors and other equipment, the operation of which is accompanied by heat release. The inverter transforming a high-voltage direct current from a battery into an alternating one supplied to electric motors is a high-power source of heat release along with the electric motor. The released heat must be dissipated to ensure optimal thermal conditions for the operation of the aircraft equipment. Typical of the modern electronic apparatuses used in the electrical vehicle are the high density of removed heat flows,

---

L. Vasiliev (✉) · A. Zhuravlyov  
Luikov Heat and Mass Transfer Institute, Minsk, Republic of Belarus  
e-mail: [zhuravl@hmti.ac.by](mailto:zhuravl@hmti.ac.by)

large distance between the sources and sinks of heat, high compactness of the power electronics components.

## 8.2 Two-Phase Heat Conductors for Thermal Management

The problem of removal of excess heat from a heat-generating electronic facility can be solved successfully with the aid of two-phase heat-transmitting devices such as heat pipes (HP) and thermosyphons (TS). These devices are autonomous, noiseless, their operation does not consume energy, which is very important for wireless electric transport. They can perceive heat from a cooled object, remove it beyond the limits of the volume filled with the equipment and then transmit it to the cooling liquid or air. Such a system is efficient, reliable, and convenient in service. Two-phase loop thermosyphons constitute rather simple, reliable, and, at the same time, efficient heat transmitting devices capable of operating in a wide range of parameters and angles of inclination to the horizontal. A peculiar form of thermosyphon is a vapor-dynamic thermosyphon, Fig. 8.1 (Vasiliev et al. 2015). The moving vapor and two-phase flow of the working fluid are separated in space (a double-pipe heat exchanger), which makes it possible to avoid the negative interaction between the oppositely directed vapor and liquid flows, typical of convective thermosyphons. The condensing liquid is pushed from the condenser to the evaporator by the vapor – hence the fundamental difference of the vapor-dynamic thermosyphons from other thermosyphons and heat pipes. Vapor-dynamic thermosyphons have a high heat transmitting ability (tens of kW), allow various designs, including bent, flexible or assembled elements. Using the principle of heat transfer employed in vapor-dynamic thermosyphons, it is possible to create equipment for cooling and heating the components of electric and hybrid transport. Figure 8.2 presents the scheme of a radiator with air cooling constructed based on a loop thermosyphon with a plane evaporator. The radiator is intended for the system of cooling unit (inverter/IGBT) of the

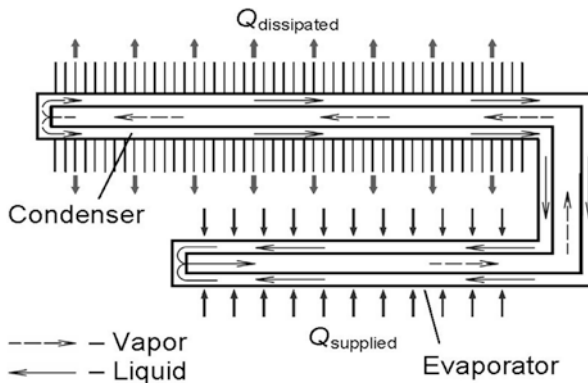
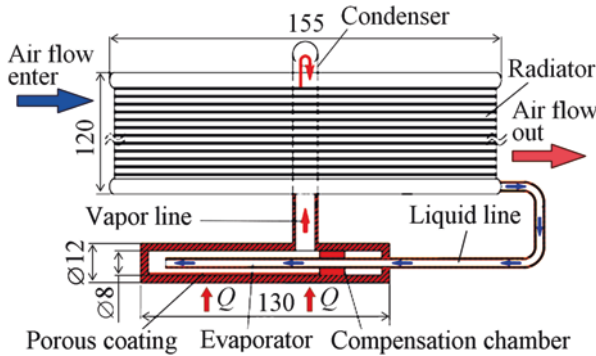
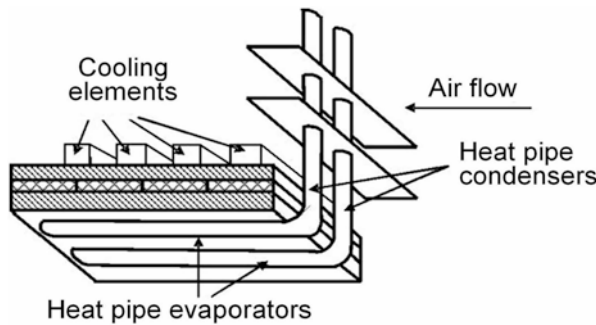


Fig. 8.1 Selecting the citation from Google Scholar



**Fig. 8.2** Loop thermosyphon with a plane horizontal evaporator and a porous wick inside for cooling the power electronics of the electric vehicles



**Fig. 8.3** The system based on the use of special L-type heat pipes for cooling the power electronics of the electric vehicles

electric vehicle with heat loading from 0.5 to 1 kW. The system of cooling the power electronics of the vehicles can also be based on the use of special L-type heat pipes, in which the evaporator is located horizontally and the condenser vertically. The cylindrical evaporator has a good thermal contact with the copper plate on which the semiconducting components of the power electronics are located (Fig. 8.3).

Lithium-ionic batteries are used widely in electric vehicles due to the high energy density and long service life. Since the characteristics and service life of these batteries are sensitive to temperature, it is very important that the needed temperature range of their operation be constantly sustained. One of the methods of leveling out the temperature of the battery is the transfer of heat from its modules to the systems of liquid cooling by means of heat pipes and loop thermosyphons.

An alternative of the metal heat pipe and thermosyphon is the horizontal thermosyphon made from polymer nanocomposites – polyamide with micro- and nanodiamond particles introduced into it and reinforced by carbon fibers (Vasiliev et al.

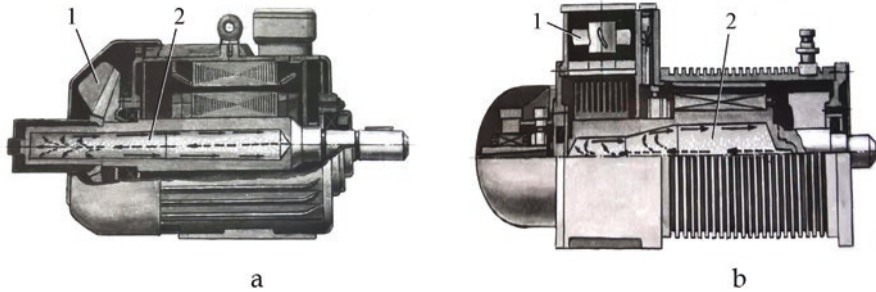


**Fig. 8.4** Electric motor with an inserted centrifugal heat pipe whose condenser is cooled by air flow by self-ventilation (a) and by a fan with an independent drive (b): (1) fan; (2) centrifugal heat pipe

2018). Loop thermosyphons with plane evaporators and condensers are well suited as liquid cooling systems.

The rotor of the electric engine may be cooled with the aid of centrifugal heat pipes inserted inside the rotor, Fig. 8.4. Large heat losses in the rotor occur in engines with increased slipping and frequency regulation (electric vehicles, electric loaders). The efficiency of application of heat pipes for cooling the electric motor increases considerably if the motor is not blown externally by air, which is typical of engines with thorough regulation of relation frequency.

To intensify heat transfer inside the electric motor rotor it is worthwhile to apply the unique construction of the heat pipe devised at the A.V. Luikov Heat and Mass Transfer Institute of the National Academy of Sciences of Belarus and made in the form of a cylindrical vapor chamber. The construction of the cooler proposed in the present work for the rotor is compatible with various coolants (liquid, gas, two-phase flow, spray cooling). The external envelope of the vapor chamber evaporator serves as the cooler, the condenser is the internal pipe through which a flow of a cooling substance passes (liquid, two-phase flow, sputtered oil microdrops, etc.). Particularly, this facility is a symbiosis of the centrifugal vapor chamber located on the internal pipe cooled by the agent moving inside it (cylindrical vapor chamber) and a cylindrical heat pipe.

### 8.3 Conclusion

The system of cooling with heat pipes ensures a high capacity, reliable and safe operation, temperature uniformity. It is an attractive alternative technology because of the absence of moving parts.

The system of cooling of electrical or hybrid air transport with the use of heat pipes and thermosyphons is preferential in comparison with the traditional single phase cooling with the aid of a mechanical pump.

## References

- L. Vasiliev, L. Vassiliev, A. Zhuravlyov, A. Shapovalov, A. Rodin, Vapordynamic thermosyphon – heat transfer two-phase device for wide application. *Arch. Thermodyn.* **36**(4), 65–76 (2015)
- L. Vasiliev, A. Zhuravlyov, L. Grakovich, M. Rabetsky, L. Vassiliev, Flat polymer loop thermosyphons. *Arch. Thermodyn.* **39**(1), 75–90 (2018)

# Chapter 9

## Subjective Decision-Making of Aviation Operators (Pilots, ATCOs)



Utku Kale, Omar Alharasees, Jozsef Rohács, and Dániel Rohács

### Nomenclature

ATCOs    Air Traffic Controllers  
ATM      Air Traffic Management  
ICAO     International Civil Aviation Organization

### 9.1 Introduction

Operators “subjective decision-making” is considered as an important part in managing and controlling today’s aviation sector. This means that they use the subjective situation awareness, situation analysis, and decision-making processes in aircraft controls (FAA, 1991). Operators must first characterize the scenarios issue, then choose a solution from a set of resources and make a subjective judgements followed by decisions in the event of an unanticipated and unforeseeable situations. As shown in Fig. 9.1, the resources are divided into two categories: (i) “active resources” such as physical, intellectual, and psycho-physiological behaviors, and (ii) “passive resources” such as knowledge, materials, and finance – the physical form of the aircraft control system.

There are numerous references and criteria for considering the subjective aspects of operators decision-making techniques. For example, Previous research analyzed the operator’s workload subjectively and objectively. The aircraft control system is subjective, endogenous, stochastic, and dynamic due to the idea of human-operators (pilot or ATCO) loop, who are dynamically controlling information flow based on the flight circumstances using decision-making process (Papanikou et al., 2021). The system is endogenous because the control first initiates within the system while

---

U. Kale (✉) · O. Alharasees · J. Rohács · D. Rohács  
Faculty of Transportation Engineering and Vehicle Engineering, Department of Aeronautics and Naval Architecture, Budapest University of Technology and Economics, Budapest, Hungary  
e-mail: [KALE.UTKU@kjk.bme.hu](mailto:KALE.UTKU@kjk.bme.hu); [oalharasees@edu.bme.hu](mailto:oalharasees@edu.bme.hu); [drohacs@vrht.bme.hu](mailto:drohacs@vrht.bme.hu)

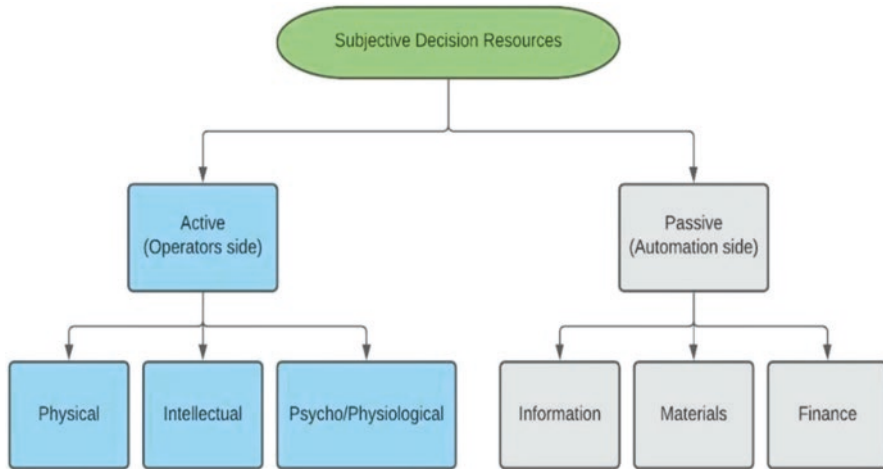


**Fig. 9.1** Subjective decision resources

being observed by the operator. The executed decision is based on the operator's current mental state, physical condition, situation awareness, knowledge, experience, and skill. The aforementioned explanation is known as the “subjective decision mechanism.” (Wise et al., 2016).

Air transport capacity is expected to have a significant growth within the coming decades (Rohacs et al., 2016), prompting the funding of multiple international programs. With an increase in air transport traffic and the available networks, “subjective decision-making” has a greater influence on global aircraft safety. The current major ATM projects are mainly concentrating on (i) improving safety, (ii) decreasing ATM costs, and (iii) enhancing the environmental aspects. The first two aspects are connected to the operator's decision-making. Operators' decisions are influenced by their skills, abilities, practice, knowledge, and situation awareness. The management system of the aircraft is a dynamic, subjective, stochastic, and nerve (endogenous) system.

The “passive resources” are the resources of the aircraft, while the “active resources” are related to the operator itself. The active resources are defined by the operator decisions, which also determine how passive resources will be used. In this process, the remaining time, until the last moment, while the decision must be applied plays the most crucial role.

## 9.2 Method

The operator's subjective decision should always be comprehensively evaluated and maintained in the new networks at the beginning, establishing investigational procedures and represent subjective decision-making processes. The improved techniques



might be used in a wide range of disciplines, including unmanned aero-nautical vehicle distance control.

As seen from the model in Fig. 9.2, the operator gathers the data about the situation of the “technical system,”  $S_i$ , that changes depending on the system performance and characteristics, environmental conditions, effects of other interacting systems, and realized control (management).

The first step done by the operator is to recognize and realize the current scenario, then evaluate the existing situation, and choose an appropriate decision while choosing the best action from a set of options using decision-making, and finally execution process. In the decision-making process, the operator selects the choice from the set of the “possible actions,”  $S_p$ , including all the accessible or achievable devices, methods, and factors. The operator must then identify “disposable actions,”  $R_{disp}$ , that might be applied in a given situation for controlling the system. Finally, the operator should choose the “required actions,”  $R_{Req}$ , that moves the system to the proposed state. As a result, this process realizes and depends on the operator behaviors. In a more general approach, the operator has to initiate passive resources and then apply physical mechanisms and active resources (Simongáti, 2010).

The estimated subjective decision time explained in Fig. 9.3 could be calculated by considering the core features which contain “situation awareness,” “decision-making,” and “performance actions,” although some external aspects could affect the decision time in a vital way such as the experience level of the operators and the human error factor.

It is important and crucial to understand that all the factors are interdependent with each other, which make calculating the exact required time a complex issue,

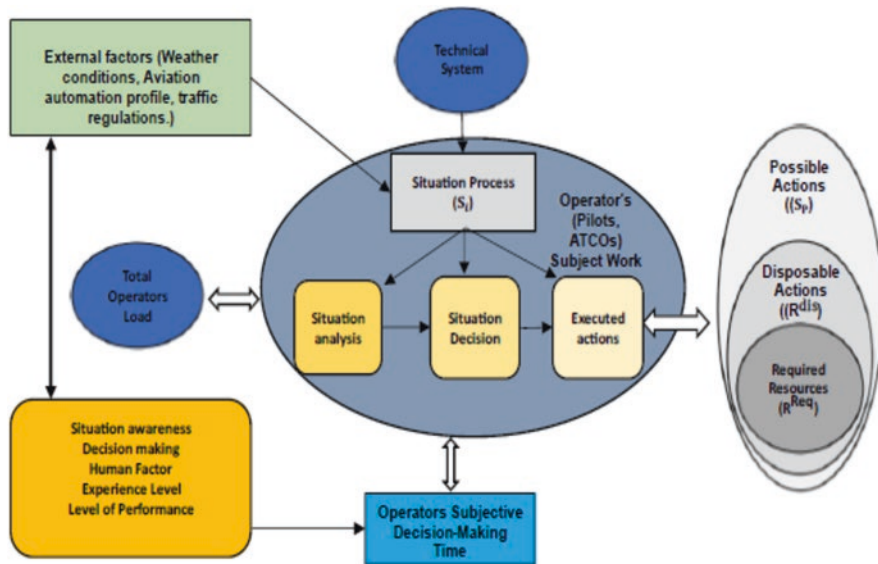


Fig. 9.2 Subjective decision-making model



**Fig. 9.3** The estimated subjective decision time

yet an approximation is highlighted in the proposed equations. The successful decision can be made if the remaining time would be greater than the required time.

The quality of the operators’ work might be described as with active resources ( $R_{\text{req}}$ ) that defines how passive resources ( $R_{\text{preq}}$ ) are used. Other analogical possible characterization might be given by the velocity of utilization of the active resources.

The operator must have time ( $t_{\text{req}}$ ) to understand and evaluate the given  $\sigma_k$  situation  $t_{\text{uereq}}(\sigma_k)$ , making-decision  $t_{\text{decreq}}(S_a)$  that intends to transit the situation from  $S_k$  state into the  $S_a$  state and the required time to perform the action  $t_{\text{reactreq}}(\sigma_k, S_a)$ :

$$t^{\text{req}} = t_w^{\text{req}}(\sigma^k) + t_{\text{dec}}^{\text{req}}(\delta^a) + T_{\text{react}}^{\text{req}}(\sigma_k, \delta_a) \tag{9.1}$$

There is not enough information on the physical, systematic, intellectual, and psychophysiology characteristics of the subjective analysis, on the way of thinking and making a decision of subjects-operators. Only limited information is available on the time effects, possible damping the non-linear oscillations, and long-term memory (Kasyanov, 2007). Figure 9.4 describes the simplified decision-making process at the final phase of the aircraft approach, the set of alternative situations were given by  $t_0, x_0, S_a: (\sigma_1, \sigma_2)$  with the distribution of preferences  $p(\sigma_k)$ , where  $\sigma_1, \sigma_2$  identifies the landing and the go-around, respectively.

The preferences are oscillating, because of the exogenous fluctuation (while decision altitude is getting closer) and the endogenous processes (depending on the uncertainties in the situation awareness and operators-pilot incapacity to make decisions). If pilots are able to overcome their entropy barrier up to command for go-around (reaching the decision minimum altitude),  $t^*, x^*$ , then they perform the proposed decision.

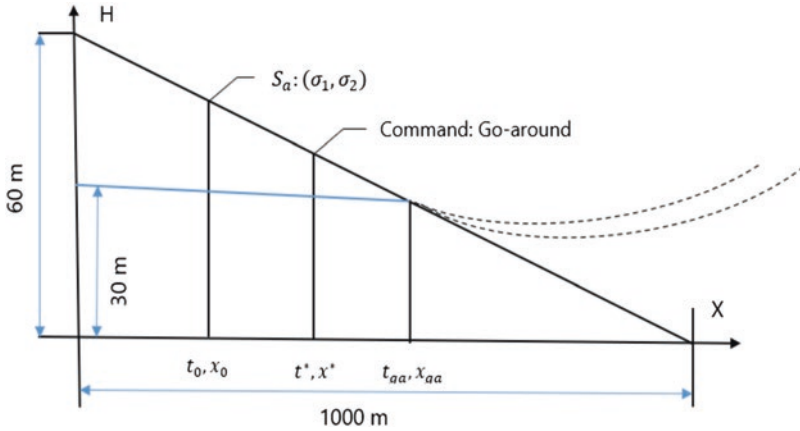


Fig. 9.4 Aircraft final phase (landing, go-around)

### 9.3 Results and Discussion

The illustrated model utilized and examined the EU FP7 PPlane (Rohacs, 2010, 2012; PPLANE, 2011) to define the constraints of safe landings associated with private airplane pilots, named as less-skilled pilots in the current research. In a previous research (Kasyanov, 2007), the following values are recommended for a medium sized aircraft (weight of aircraft  $W = 106 \text{ N}$ ; wing area,  $S = 100 \text{ m}^2$ ; wing aspect ratio  $A = 7$ ; thrust  $T = 9.4 \times 10^4 \text{ N}$ ; and velocity  $V = 70 \text{ m/s}$ ):  $A = 8$ ;  $B = 8$ ;  $C = 20$ ;  $D = 43$ ;  $F = 0.8$ ;  $H = 0.065$ ;  $M = 0.065$ ;  $N = 0.065$ . Using these parameters, the subjective probabilities might be chosen as  $(\sigma_1) = 0.53$ ,  $P(\sigma_2) = 0.6$  and  $\epsilon_1 = 5.5 + 0.01t$ ,  $\epsilon_2 = 5.4 + 0.04t$  take into account the decreasing difference in the required and the available time for the decision.

In this research, a simulation model was created, by the current researcher, using the modified Lorenz attractor on MATLAB for the subjective decision-making of the pilots in different level of pilot expertise, namely (i) Cadet, (ii) less-skilled, (iii) skilled. and (iv) expert.

Chaotic Lorenz’s model was introduced to describe the way of thinking of pilots during the final approach. The simulated parameters and model were utilized based on the real measured characteristics of pilots (Table 9.1). This model was used for investigating go-around and landing situations during final approach.

The results of using the described model for four different levels of pilots are shown in Figs. 9.5 and 9.6. The results demonstrate the chaotic character of the decision-making process for go-around and landing, which can vary depending on the level of experience of pilots.

According to these results, the cadet and less-skilled pilots are not able to make their final decisions easily in which situations create chaotic orbits seen in Fig. 9.5. The final decision time of the pilots can be calculated from these results by checking when s/he will not have any hesitancy between landing and go-around. The final

**Table 9.1** Aircraft parameters for four groups of pilots

Cadet pilot	Less-skilled pilot	Skilled pilot	Expert pilot
A: 6	A: 8	A: 10	A: 12
B: 6	B: 8	B: 10	B: 12
C: 10	C: 20	C: 35	C: 45
D: 0	D: 0.43	D: 1	D: 1.2
F: 1.3	F: 0.8	F: 0	F: 0
H: 0.065	H: 0.065	H: 0.065	H: 0.065
M: 0.065	M: 0.065	M: 0.065	M: 0.065
N: 0.065	N: 0.065	N: 0.065	N: 0.065
$P(\sigma_1)$ : 0.53	$P(\sigma_1)$ : 0.53	$P(\sigma_1)$ : 0.53	$P(\sigma_1)$ : 0.53
$P(\sigma_2)$ : 0.6	$P(\sigma_2)$ : 0.6	$P(\sigma_2)$ : 0.6	$P(\sigma_2)$ : 0.6

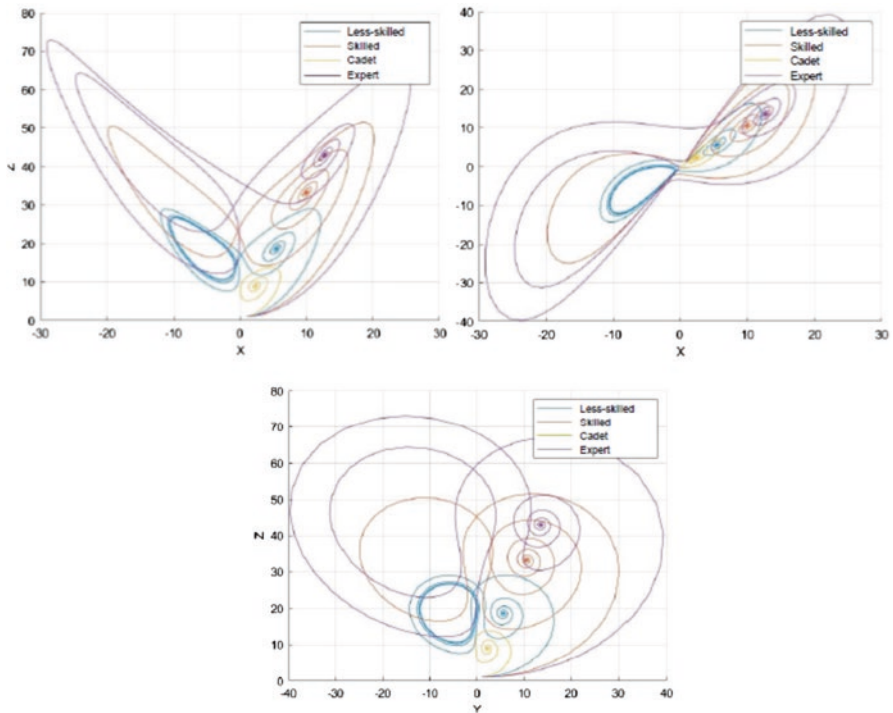


**Fig. 9.5** Pilots way of thinking and decision-making process for four different levels of pilots (yellow: cadet, blue: less-skilled, orange: skilled and purple: expert pilot)

decision is made when the probability of a specific situation (landing or go-around) gets stable as shown in Fig. 9.6.

The results could be summarized as follow:

- Cadet pilot entropy would quickly decrease, the hesitation is very high, and the final decision was taken in about 10 s.

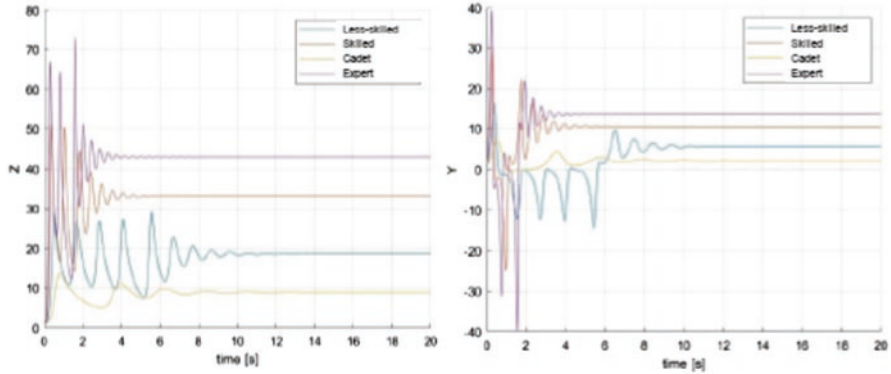


Fig. 9.6 Results of using the developed model to landing by four different levels of pilots

- The less-skilled pilot entropy would decrease, the hesitation is still very high, and the final decision was taken in about 8 s.
- The skilled pilot entropy would be decreased, the hesitation is reasonable, and the final decision was taken in about 4 s.
- Expert pilot entropy would quickly be decreased, the hesitation is optimum, and the final decision was taken in about 2 s.

### 9.4 Conclusion

Due to the increasing number of mishaps in comparable flight scenarios, the research underlined the urgent need to recognize and acquaint aviation operators with subjective Aeronautical Decision-Making in the final approach phase.

The modified Lorenz attractor was used in MATLAB to simulate the subjective decision-making process of four groups of pilots with different levels of expertise in the aircraft final phase (landing and go-around) by measuring “hesitation frequency” and “decision-making time.”

The outcomes show that the time needed for less-skilled pilot is 4 times more to make a decision between landing and go-around compared to the expert pilots. This model is well usable for the investigation of the endogenous dynamics of the pilot decision-making from different skills and experience. The result of the research suggested that this method improves pilot training and helps instructors to specify the pilots’ weak points as well. These results demonstrate that the model is suitable to investigate the different levels of pilots expertise while checking their way of thinking and decision-making process.

## References

- Federal Aviation Administration (FAA), *Aeronautical Decision-Making* (FAA, Washington, DC, 1991)
- V. Kasyanov, *Subjective Analysis* (National Aviation University of Kyiv, Kyiv, 2007)
- M. Papanikou, U. Kale, A. Nagy, K. Stamoulis, Understanding aviation operators' variability in advanced systems. *Aircr. Eng. Aerosp. Technol.*, ahead-of-print (2021). <https://doi.org/10.1108/AEAT-03-2021-0065>
- PPLANE, PPLANE-The personal plane project, EU FP7 (2011)
- J. Rohacs, Subjective aspects of the less-skilled pilots, performance, safety and well-being in aviation, in *Proceedings of the 29th conference of the European association for aviation psychology*, 2010, pp. 153–159
- J. Rohacs, Subjective factors in flight safety, in *Recent Advances in Aircraft Technology*, (2012). <https://doi.org/10.5772/37823>
- J. Rohacs, D. Rohacs, I. Jankovics, Conceptual development of an advanced air traffic controller workstation based on objective workload monitoring and augmented reality. *Proc. Inst. Mech. Eng. Part G J. Aerosp. Eng.* **230**(9), 1747 (2016)
- G. Simongáti, Multi-criteria decision making support tool for freight integrators: Selecting the most sustainable alternative. *Transport* **25**(1), 89 (2010)
- J. Wise, V. Hopkin, D. Garland, *Handbook of Aviation Human Factors* (Routledge, London, 2016)

# Chapter 10

## Acoustic Operational Monitoring of Unmanned Aerial Vehicles Near Vertiports



Vitalii Makarenko and Vadim Tokarev

### Nomenclature

DATEMM	Disambiguation of TDOA estimates in multi-path multi-source environments
FFT	Fast Fourier transform
ICA-SCT	Independent component analysis with state coherence transform
SPrL	Sound pressure level
SPwL	Sound power level
SRP-PHAT	Steered-response power phase transform
TDOA	Time difference of arrival
UAM	Urban air mobility
UAS	Unmanned aerial systems
UTM	Unmanned aircraft system traffic management

### 10.1 Introduction

It is expected that UAS will be able to operate safely soon within both controlled and uncontrolled airspace with no human intervention. UAS operations in urban environment significantly increase collision risks and corresponding damage, because operations will occur near people, infrastructure and other urban air mobility (UAM) participants. The future technologies, such as advanced detect and avoid systems, will allow UAS operations in congested areas over densely populated communities. In-flight separation services will be provided by automation systems, and contingency procedures used to handle both small- and large-scale off-nominal events. In this paper, acoustic localization system is used as a part of the collision

---

V. Makarenko (✉) · V. Tokarev  
National Aviation University, Kyiv, Ukraine  
e-mail: [vitmakarenko@nau.edu.ua](mailto:vitmakarenko@nau.edu.ua); [tokarev@nau.edu.ua](mailto:tokarev@nau.edu.ua)

avoidance support decision system for UAS Traffic Management (UTM). This section is aimed on provision of the means to support the management of UAS operations in uncontrolled airspace, reduce risk collision with static ground objects and sounding dynamic objects in populated zones. Within the UTM concept UAS coordinates are also required to provide services such as corridors, dynamic geo-fencing, severe weather and wind avoidance, congestion management, terrain avoidance, route planning, re-routing, separation management, sequencing, spacing, and contingency management.

## 10.2 Proposed Algorithm

Figure 10.1 shows the proposed algorithm of UAS localization in line of sight. This algorithm is invariant with respect to UAS speed and number of sound wave reflections.

The method of determining the UAS coordinates by acoustic parameters is based on the use of algorithms for statistical processing of noise, which engine, screw and UAS elements generate. The signals from array of microphones are amplified by low-noise broadband amplifiers and fed to the input of analog-to-digital converter. The digital signals are transmitted to computer, which digitally processes the measured acoustic signals and calculates UAS location in 3D space.

As a method of UAS localization, a method based on the calculation of coordinates directly from the delays between acoustic signals is chosen, similar to the DATEMM algorithm in Zannini et al. (2010) and Scheuing and Yang (2008). Space scanning, which is characteristic for SRP-PHAT and ICA-SCT localization algorithms, results in higher computer memory costs to achieve the required accuracy, and most importantly, longer calculations (Loesch et al. n.d.).

The Doppler effect, which distorts the shape of the signals, is taken into account when detecting signals from moving objects. To eliminate the consequences of this effect, changes in the time scale of the signals are applied, and before the calculation of the correlation function, the time scale of the signals is changed. For this purpose, a resampling algorithm is used to change the time between discrete signal values. Resampling is used to change the sampling rate of a signal. This allows us

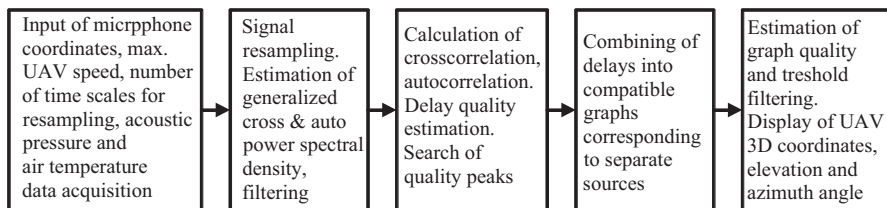


Fig. 10.1 Scheme of UAS localization algorithm



constructing a signal detection procedure independent of the possible speed of the sound source.

To separate the UAS signal from the mixture of sounds coming into the microphone, bandpass filtering is performed using Fast Fourier Transform (FFT). For frequency bands, at which SPRL of UAS computed at a distance of 1 m are less than background SPRL, the generalized cross and auto-power spectral density values are replaced with zero. Since the FFT operation is used to calculate the correlation function by the spectral method, this filtering technique does not lead to additional computational costs.

Our approach for selecting the positions of noise sources among the erroneous positions generated by the combination of delays is to set a threshold for the value of the graph quality  $V$ :

$$V = \frac{1}{\sum_{\{i,j\} \in P} F_{ij}^2} \sum_{\{i,j,k\} \in C} (r_{ij} + r_{jk} + r_{ik}) \Gamma_{\Sigma}(\Delta_{ij} + \Delta_{jk} + \Delta_{ki}) \Gamma_{\Pi}(\beta_{ij} \beta_{jk} - \beta_{ik}), \quad (10.1)$$

where the set  $C$  consist of all microphone triples  $\{i, j, k\}$  included in compatible graph, and the set  $P$  consist of all microphone pairs  $\{i, j\}$  included in compatible graph,  $\Delta_{ij}$  is the delay of sound propagation between microphone  $i$  and  $j$  in samples.  $\beta_{ij}$  is factor of  $i$ -th signal relative to  $j$ -th signal time scaling, which was determined during resampling for each pair of signals. The function indicates how good sound source coordinates  $(x_s, y_s, z_s)$  correspond to delay  $\tau_{ij}$  found from crosscorrelation  $r_{ij}$ .  $F_{ij}$  is given by equation.

$$F_{ij} = \sqrt{(x_s - x_i)^2 + (y_s - y_i)^2 + (z_s - z_i)^2} - \sqrt{(x_s - x_j)^2 + (y_s - y_j)^2 + (z_s - z_j)^2} - c\tau_{ij} \quad (10.2)$$

where  $\tau_{ij}$  is the time delay of the arrival of acoustic waves from the microphone  $i$  to the microphone  $j$ ,  $c$  is the sound speed.

The function  $\Gamma_{\Sigma}$  in Eq. (10.1) is designed to ensure the operation of the localization system in conditions of inaccuracies in cyclic sums. The function  $\Gamma_{\Pi}$  is used because of inaccuracies in cyclic products, which arise due to finite discretization of sound source speeds.

To determine the coordinates of the noise source, a geometric method is used: the intersections of the hyperboloids obtained as a result of the construction of surfaces for  $(i, j)$  pairs of microphones are found. In case of exact intersections,  $F_{ij} = 0$  for all possible pairs of microphones. However, due to errors in determination of microphone coordinates, discrete sampling and finite size of sound source exact intersections never appear in practice. Sound source coordinates  $(x_s, y_s, z_s)$  are defined as the result of solving an optimization task:

$$\min_{x_S, y_S, z_S} F_{ij} = 0 \quad (10.3)$$

To speed up solution, especially at assumption of sound source location in far field, hyperboloids are replaced with cones. This leads to transformation from non-linear optimization problem to the problem of solving of overdetermined system of linear algebraic equations.

### 10.3 Selection of Optimal Antenna Structure for Sound Source Localization

To select an optimal microphone location let us consider error caused by inaccuracy of microphone positioning. Assume that the error of microphone location has normal distribution with standard deviation of 0.01 m. Good localization accuracy can be achieved with several microphone arrays distributed in urban terrain. Figure 10.2 shows localization error for microphone arrays located near vertiport landing pad and on top of nearby tall building. Both microphone arrays acquire data for single localization system, although only TDOA between microphones within each array are used. These arrays consist of five microphones located in vertices of square pyramid with 10 m edge length.

### 10.4 Experimental Verification of Localization Algorithm for UAS

Field tests of the UAS localization system were performed for the syma 8 M quadcopter for the stationary UAS position (Fig. 10.3). The location of microphones and stationary UAS in the experiment is shown in Table 10.1.

Figure 10.3 shows the coordinates of the multicopter at the stationary position of UAS syma 8 M in the microphone coordinate system. The microphone coordinate system is constructed in such a way that the points at which the microphones 1, 2, and 3 are placed define the plane  $Oxy$ . The beginning of the coordinate system is in the position of the first microphone. The  $Ox$  axis is directed to the second microphone.

### 10.5 Conclusion and Further Research

This investigation presents approaches to modelling of sUAS noise emission at takeoff and landing modes. Presented UAS localization procedure will be used for providing safe UAS operations in urban environment. If the aircraft detection method in Chervoniak et al. (2017a, b) has demonstrated merely the main principle and efficiency of the proposed approach, currently, the method is of practical use for

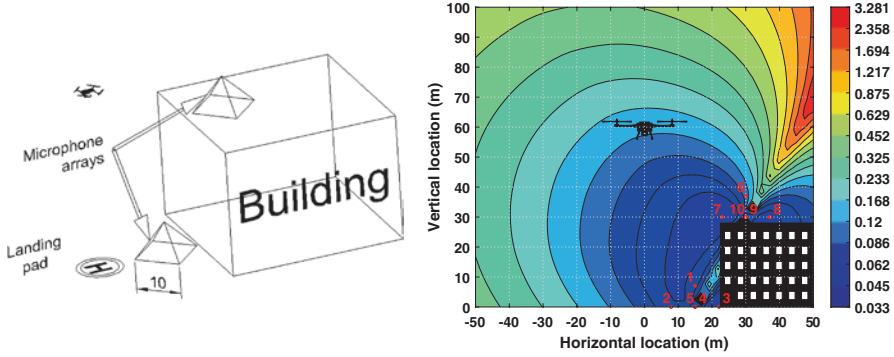
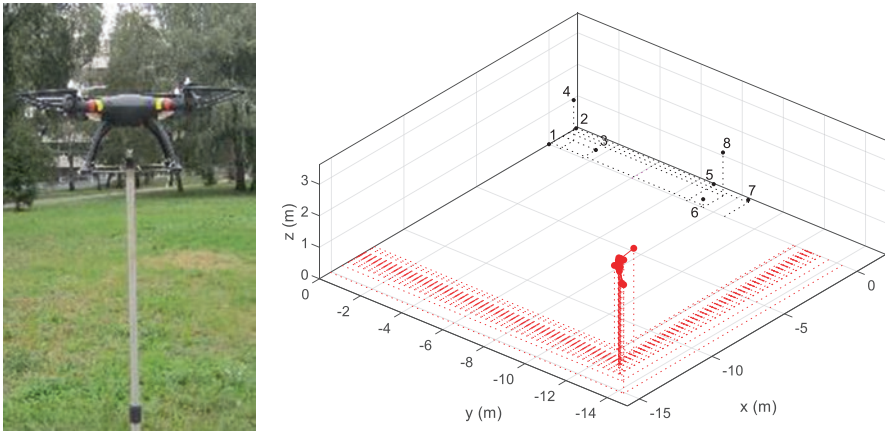


**Fig. 10.2** Localization error in  $yz$  plane,  $x = 0$ , for microphone arrays placed on ground and on top of the 30 m height building. (a) Scheme of microphone array location; (b) UAS localization error above landing pad



(a)Photo of fixed syma 8M (b) Syma 8M microphone and its estimated location in 3D space

**Fig. 10.3** Experimental verification of algorithm for the stationary position of UAS. (a) Photo of fixed syma 8 M; (b) Syma 8 M microphone and its estimated location in 3D space

**Table 10.1** Location of microphones and sound source in meters

Microphones	$xm$	$ym$	$zm$
1	0	0	0
2	1.87	0	0
3	0.935	-1.619	0
4	0.948	-0.532	1.287
5	1.893	-6.679	0.019
6	0.169	-7.382	0.196
7	1.647	-8.53	0.083
8	1.385	-7.488	1.379
Syma 8M	12.721	12.114	3.346

localization, flight and velocity tracking. The usage of measured SPwL for signal filtering allowed removing UAS unrelated noise influence on accuracy of 3D coordinates estimation. This study also shows how the usage of small acoustic antenna can lead to fast location estimation for moving UAS. Conducted experimental researches show potential for application of passive acoustic localization system for UTM services more specifically and for urban noise monitoring in general (Bukala et al. 2019).

Further investigation required to test the efficiency of sound localization system as part of UAS on-board equipment. In the future, it is planned to use the results of these studies in the following areas:

- considering the impact of complex urban topologies, dangerous and unpredictable atmospheric hazards, such as unsteady wind-fields;
- reducing the risk of UASs operation taking into account ground static objects (power lines, towers, structures, overpasses) and other aircraft (manned and unmanned); and
- separation assurance and collision avoidance between air vehicles in a mixed-use airspace.

## References

- M. Bukala, O. Zaporozhets, V. Isaienko, A. Chyla, Noise monitoring for improvement of operational performances of the aircraft in vicinity of airports, Ch. 3.5, in *Selected Aspects of Providing the Chemmotological Reliability of the Engineering*, (National Aviation University, Kyiv, 2019), pp. 271–279
- Y. Chervoniak et al., *Algorithm of Passive Acoustic Locator Data Processing for Flying Vehicle Detection and Tracking* (Kiev, IEEE, 2017a), pp. 43–48
- Y. Chervoniak et al., *Signal Processing in Passive Acoustic Location for Aircraft Detection* (IEEE, Jachranka, 2017b), pp. 1–5
- B. Loesch, P. Ebrahim, B. Yang, Comparison of different algorithms for acoustic source localization (n.d.). [Online] Available at: [https://www.iss.uni-stuttgart.de/forschung/publikationen/loesch\\_itg2010.pdf](https://www.iss.uni-stuttgart.de/forschung/publikationen/loesch_itg2010.pdf). Accessed 1 Dec 2022
- J. Scheuing, B. Yang, Correlation-based TDOA-estimation for multiple sources in reverberant environments, in *Speech and Audio Processing in Adverse Environments*, ed. by E. Hänsler, G. Schmidt, (Springer, Berlin/Heidelberg, 2008), pp. 381–416
- C.M. Zannini, A. Cirillo, R. Parisi, A. Uncini, *Improved TDOA Disambiguation Techniques for Sound Source Localization in Reverberant Environments* (IEEE, Paris, 2010), pp. 2666–2669

# Chapter 11

## Peculiarities of Pre-processing of ADS-B Data for Aircraft Noise Modeling and Measurement During Specific Stages of LTO Cycle



Kateryna Kazhan, Oleksandr Zaporozhets, and Sergii Karpenko

### Nomenclature

ADS-B	Automatic Dependent Surveillance-Broadcast
AIP	Aeronautical Information Performance
GPS	Global Positioning System
ICAO	International Civil Aviation Organization
LTO	Landing and Taking-Off
MP	Measurement Point
SEL	Sound Exposure Level

### 11.1 Introduction

Measuring aircraft noise and noise monitoring in the vicinity of an airport to achieve the main goal – reducing the population affected by noise and improving the quality of life – requires a relevant organization of field acoustic research. According to ISO 20906 for successful processing of monitoring data, in addition to long-term measurements, the selection of the sound event associated with aircraft is necessary, as well as its classification and identification (ISO/CD 20906, 2009).

Under the Directive 49/2002 (Directive 2002/49), the task of noise zoning should be fulfilled based on noise index – Lden. This criterion belongs to the group of the equivalent sound levels that could be applied for zoning purposes; however, there are some countries in the European region where maximum noise level is defined by legislative limits (for example, Ukraine has both types of limits – equivalent (LAeq) and maximum (L<sub>Amax</sub>) sound levels). In the current circumstances, noise contours L<sub>Amax</sub> occupy a larger area than noise contours LAeq (Table 11.1), and thus,

---

K. Kazhan (✉) · O. Zaporozhets · S. Karpenko  
National Aviation University, Kyiv, Ukraine

**Table 11.1** Ranges of boundaries of noise restricted zones on the basis of criteria:  $L_{AmaxN} = 70$  dBA and  $L_{AeqN} = 50$  dBA

Airport	$L_{AmaxN} = 70$ dBA $km^2$	$L_{AeqN} = 50$ dBA, $km^2$
Boryspil' (UKBB)	326.1	94.1
Dnipro (UKDD)	59.3	14.8
Antonov-2 (UKKM)	450.4	37.8
Mylolaiv (UKON)	120.1	11.1
Odesa (UKOO)	71.2	15.1
L'viv (UKLL)	63.3	11.9

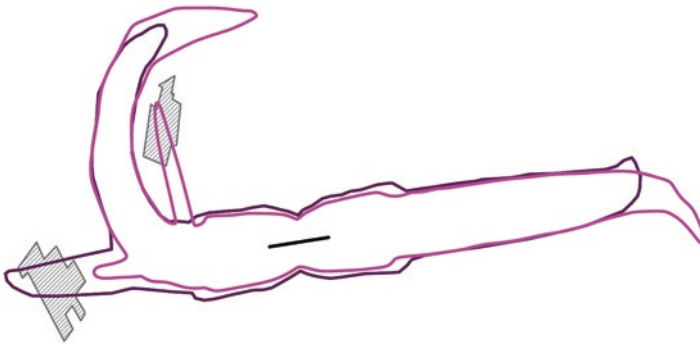


**Fig. 11.1** Two approaches to noise zoning on the basis of  $L_{Amax}$ : purple – AIP as a sources of track information; magenta – averaged ADS-B tracks and flight data; grey – residential areas

defines boundaries of noise restricted zones. The form and size of noise protection zones (defined on the maximum sound level  $L_{Amax}$ ) are very sensitive to real track dispersion, flight altitude, and total assessment of the operation scenarios (Fig. 11.1).

To clarify the results of aviation noise modeling at the airport and to explain the possible gaps between measured and modeled results, open track data based on the results of ADS-B surveillance were analyzed (particularly, the results are presented on the FlightRadar24 and OpenSky websites).

According to ADS-B surveillance technology, aircraft determines its position using satellite, inertial, and radio navigation systems, and transmits it (approximately 1 sample per 1 second) periodically with other relevant parameters to ground stations and other equipped aircraft. The signals are transmitted at a frequency of 1090 MHz. The receiver's ADS-B antenna is capable of receiving messages from aircraft up to 400 km away. However, for aircraft at lower altitudes, the range may be significantly limited, especially for aircraft that are on the ground, or in the stages immediately before landing or in the initial stages of takeoff (Schultz et al. 2020).

The possibility of using pre-processed FlightRadar24 data, particularly for the purpose of modeling aviation noise generated at different stages of LTO cycle was analyzed for test case at different airports in Ukraine: ground stage (UKBB, UKKK), departure (UKKM), and arrival (UKKM, UKKK).

## 11.2 Analysis of Track Data in Terms of Noise Event Reconstruction

The importance of taxiing noise modeling, as indicated in many studies (Page et al. 2009, 2013; Zaporozhets and Levchenko 2021) is not always the same. For some of airports because of the specific aerodrome layout, infrastructure, and much quieter aircraft in operation due to the ICAO Balanced Approach influence on acoustic performances of new aircraft designs taxiing of the aircraft may contribute essentially on noise footprints (Zaporozhets and Levchenko 2021). The usage of aircraft real trajectories along the apron and taxiways before and after takeoff/landing, engine mounting height, and engine operating mode should be considered during noise modeling and measuring for airports such as Kyiv/Juliany Airport (UKKK), Kharkiv Airport (UKHH), and Zaporizhzhia Airport (UKDE) located near residential areas, or in the center of city directly and on closer distances from the apron and taxiways to multi-storey buildings from the runway (UKKK).

Paths tracked by individual receivers or generated by aggregators (FR24) receiving information from many receivers all at the same time, require pre-processing of data to avoid the false data. The study of such erroneous data can be useful in improving the monitoring system or correcting the location of receivers.

### 11.2.1 Taxiing

Information on the movement of aircraft on the ground is the easiest to process, as it is transmitted in the form of individual messages MSG 2 and they are easy to separate from the general flow of flight data. At the preliminary stage, it is necessary to exclude trajectories from the general stream with (Schultz et al. 2020): messages formed in the absence of GPS data; insufficient number of signals, which leads to missed points and false trajectories, which is most evident in the ground stages due to mismatch with the geometric dimensions of the runway, taxiways, and platforms (Fig. 11.2).

Such changes in tracks based on the ADS-B data are usually connected (Page et al. 2009) with a lack of reception in the signal, for example, breaks in continuously transmission of a signal due radio interruptions. The location of the receivers is the other important factor. Aprons often are not in the zone or the reception. For example, according to the FR24 data for the UKKK aerodrome, there are a number of receivers operated in a stable mode (more than 97% of total working time). However, mutual influence of factors such as location of receiver, relief features, and large distance from the runway to aprons (over 1 km) leads to the low data quality during taxiing (Fig. 11.2).

Three possible locations of receivers were analyzed in the current research (Fig. 11.3). The best efficiency in terms of assessment of environmental factors (noise, air pollution) for ground stages of aircraft movement was defined at the



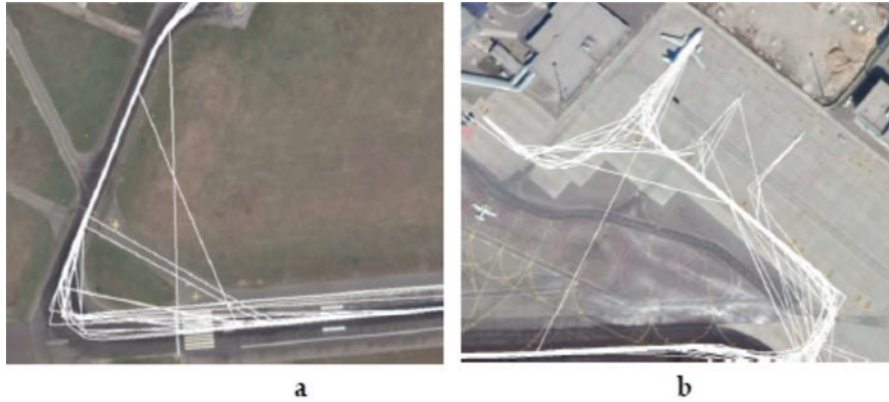


**Fig. 11.2** Examples of distortion of the aircraft trajectory during ground operation: aircraft taxiing from the runway (a); movement on the apron (b); UKKK, October–November 2021



**Fig. 11.3** Location of additional receivers A1-A3 (a) and track (yellow) correspondence to runway and taxiways geometry (A2) (b)

airfield or very close to the outer perimeter of the aerodrome (Fig. 11.3a) – for example, point A2. The main recommendation for selection of final location of the receiver for tracking of ground operation is providing line of sight with moving aircraft from the moment of start of runway operation to final location at apron.

### 11.2.2 Arrival Tracks

Measured arrival altitudes tend to be close to the modeled altitudes at the shorter track distances, higher than the modeled altitudes at the middle distances, and lower than modeled at the furthest track distances (Page et al. 2009). For the descent and approach stages, the track dispersion is significantly lower: the deviation does not exceed 200 m at a distance of 6 km (Fig. 11.4) for the same flight (October–November 2021).





**Fig. 11.4** Track dispersion (white lines) during descent and arrival procedures, typical for city airport; 70–85 dBA are L<sub>Amax</sub> noise levels

Very different picture can be observed for manufacturing airport UKMM: test flight data compared with AIP recommendation are significantly different. Such differences, considering the very rare flight events, lead to the significant gap in modeled and measured results only because of dispersion of ground track trajectories.

Additionally, the altitude dispersion should be included into noise calculations.

### 11.2.3 *Departure Tracks*

The horizontal dispersion of takeoff tracks for the same flight performed on A320 aircraft during October 2021 for the runway end 26 is shown in Fig. 11.5. As shown, such a dispersion of tracks can affect the acoustic situation in the vicinity of aerodrome, changing the shape of the contours of equal noise, determining the boundaries of the noise restricted zones for the residential development.

Thus, an important task for the takeoff phase is to consider the actual flight trajectories when modeling noise contours and substantiating the boundaries of residential restriction zones, as well as comparing the L<sub>Amax</sub> sound levels obtained as a result of modeling and measurements.

## 11.3 Results and Discussion

The complex measurements of aircraft noise in addition to ADS-B data recording were performed in the vicinity of airports (UKMM, UKKK). The results have shown that calculated altitude of flight is higher than standard altitude at noise models (INM, AEDT) because of shifted moment of runway touching in comparison with AIP data about displaced thresholds. This causes the changes in NDP-dependencies. The results of the altitude and thrust correction are presented in Table 11.2.



**Fig. 11.5** Dispersion of takeoff tracks for the same flight and its impact on the form of noise contours  $L_{Amax} = 70 \dots 85$  dBA; A320, October 2021

**Table 11.2** Comparison of measured and modeled data on example of A321

Point	Model led data	Measured data	Difference	Correction	Difference (corr)
<i>L<sub>Amax</sub>, dBA</i>					
MP2	89.4	95.2	-5.8	91.8	-3.4
MP3	84.2	88.01	-3.81	85.6	-2.41
<i>SEL, dBA</i>					
MP2	94.4	96.7	-2.3	95.1	-1.6
MP3	91.1	90.91	0.19	90.9	-0.01

## 11.4 Conclusion

Noise contours simulating along nominal routes and standard takeoff/landing profiles embedded in modern noise modeling systems (AEDT, INM, IsoBella), in comparison with noise contours along the trajectories of aircraft traffic, obtained from the results of ADS-B observations can significantly differ in area and shape: both close to the aerodrome (for levels  $L_{Amax} = 85$  dBA), and for large distances from the ends of the runway (for levels  $L_{Amax} = 60-65$  dBA).

## References

Directive 2002/49/EC of the European Parliament and of the Council of 25 June 2002 relating to the assessment and management of environmental noise

- ISO/CD 20906, *Acoustics—Unattended Monitoring of Aircraft Sound in the Vicinity of Airports* (ISO Central Secretariat, Vernier, Geneva, 2009)
- J. Page, K. Bassarab, C. Hobbs, D. Robinson, T. Schultz, B. Sharp, S. Usdrowski, P. Lucic, *Enhanced Modeling of Aircraft Taxiway Noise, Volume 1: Scoping*, No. ACRP Project 02-27 (National Academies, Washington, DC, 2009)
- J. Page, C. Hobbs, P. Gliebe, *Enhanced Modeling of Aircraft Taxiway Noise, Volume 2: Aircraft Taxi Noise Database and Development Process*, No. ACRP Project 02-27 (National Academies, Washington, DC, 2013)
- M. Schultz, X. Olive, J. Rosenow, H. Fricke, S. Alam, Analysis of airport ground operations based on ADS-B data. International conference on artificial intelligence and data analytics for air transportation, Singapore, Singapore (2020), pp. 1–9
- O. Zaporozhets, L. Levchenko, Accuracy of noise-power-distance definition on results of single aircraft noise event calculation. *Aerospace* **8**(5), 121 (2021)

# Chapter 12

## Test Bench for Electric Propellers and Distributed Propulsion



Castroviejo Daniel and Patrick Hendrick

### Nomenclature

EDF    Electric Ducted Fan  
DP    Distributed Propulsion  
ESC    Electronic Speed Controller

### 12.1 Introduction

In today's world, the drone industry is quickly expanding, their role is becoming more vital, and an increasing number of drones are conceived to effectively conduct military, humanitarian and rescue missions among others. However, one of their major limitations is their endurance (or range), which limits their application purposes. Many existing technologies are being upgraded and new ones are being developed to further push these limits. Fundamentally, there are two main ways to increase the endurance of a drone (without modifying its geometry), and this is done either by having a higher power density of the power source (more energy for the same weight) or having a more efficient propulsion system, the latter will be done here. This paper is focused on exploring an existing but rather unpopular technology, known as electric ducted fans and to quantify the effect of the duct.

It is important to have a clear definition of what distributed propulsion (DP) really is. It is defined as the spanwise distribution of the propulsive thrust stream such that overall, the vehicle benefits in terms of structural, aerodynamic, propulsive, and/or other efficiencies (Kim 2010). On the other hand, electric ducted fans are electric powered propellers equipped with a duct. To conduct this study rightfully, it was essential to have a test bench on which electric ducted fans (EDFs) and propellers could be tested.

---

C. Daniel (✉) · P. Hendrick  
ULB, Brussels, Belgium  
e-mail: [daniel.castroviejo@ulb.be](mailto:daniel.castroviejo@ulb.be)

However, although the final aim is to fully explore the benefits of DP, this paper focuses on the effect of the presence of the duct around the propeller for electric drone motors (the results can be scaled up using non-dimensional numbers theory)

## 12.2 State of the Art

The actual number of projects exploring the advantages of electric DP are limited. It was decided here to show a promising ongoing concept plane that the French society Office National d'Etudes et de Recherches Aérospatiales (ONERA) has been developing. This plane, which uses DP is known as the AMPERE (from French "Avion à Motorisation réPartie Electrique de Recherche Expérimentale", which basically means it is a DP research plane). It uses a distributed electric propulsion with an electric ducted fans system and should be capable of transporting up to 6 persons within a 500 km range in 2 h (2017). One of their aims is to achieve optimal propulsion while keeping the drag on the plane as low as possible. To do so, their project aims to use EDFs. Indeed, the concept plane is built such that 32 independent motors are installed on its wings. These electric motors are supposed to be driven by 8 hydrogen fuel cells. Onera has planned for different configurations of the plane, one with a top mounted wing with leading edge EDFs (Fig. 12.1), while the other is a low mounted wing with canard configuration with EDFs mounted on the trailing edge. No published results have been found concerning the aerodynamic performance of the AMPERE (Dillinger et al. 2018) but a wind tunnel testing on a one-fifth scaled model has already been shown in a Paris (Sigler 2017) conference with some interesting results regarding the boundary layer attachment on the airfoil allowing for greater performance.



Fig. 12.1 Ampere DP concept plane

### 12.3 Method

To study the effect of the duct on the propulsive force and the consumed power, it is mandatory to have a fully functional and reliable test bench. Thus, a test bench was built to measure different physical variables of the tested motors.

The test bench (Fig. 12.2) was built and equipped with throttle, torque, thrust, rpm, current, voltage, temperature, static, and dynamic pressure sensors. All of the data is then collected and processed by an Arduino Mega board and sent to a Raspberry Pi from which it is transferred to MATLAB where it is analyzed and treated. Before exploiting the results of the test bench, it is important to validate the measurements taken by the data acquisition system. For the following parameters (rotational speed, voltage, current, and thus power), the measurements have been compared to those of the Scorpion Tribunus I. Indeed, this high-quality electronic speed controller (ESC) is equipped with various internal sensors allowing for the latter parameters to be recorded and thus compared to those of the test bench. The comparison, although chosen not to be shown here, shows a good working condition of the test bench. With an increasing sampling frequency, the difference between both acquisition system seems to reduce.

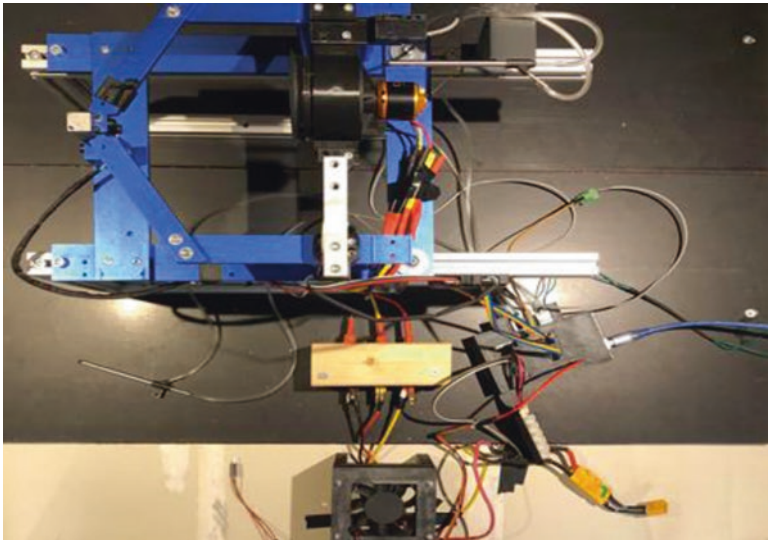


Fig. 12.2 EDF test bench. (View from the top)

### 12.3.1 Calculation

For what regards the validation of the thrust measurement, the theoretical versus experimental values have been confronted. However, to do so, a good estimate of the thrust has to be computed. Thrust is computed using the thrust formula (<https://www.grc.nasa.gov/www/k-12/airplane/turbth.html>. Accessed 10 Nov 2020) of a turbojet:

$$\dot{F} = \dot{m}(v_j - va) \quad (3.1)$$

As we are in static conditions with no air current, the aircraft velocity ( $va$ ) is considered to be null. To compute the exhaust flow velocity ( $v_j$ ), a pitot tube sensor has been used. Indeed, from the dynamic pressure the air velocity can be computed as follows:

$$v = v_j = \sqrt{\frac{2P_{\text{dyn,out}}}{\rho}} \quad (3.2)$$

Where the air density ( $\rho$ ) is computed with the temperature and pressure sensors (through means of a BME280 that is a reliable sensor from which we can assume the data is adequate and precise enough) using the perfect gas law. Additionally, the mass flow is needed. It was initially computed with the following equation (Kubica 2017):

$$\dot{m} = \rho v A \quad (3.3)$$

Where  $A$  is the swept section of the propeller blades. This method gave poor results, the reason being that the exhaust velocity was computed as being constant (pitot tube measurement in a fixed position). To correct this mistake, the boundary layer must be considered. By precisely positioning the pitot tube at different locations along a constant radial position and assuming no flow conditions on the walls, a real exhaust velocity profile has been made. By later interpolating the data points and then by integrating in function of the radius distance to the shaft, a more accurate mass flow and thus thrust have been computed. This finally gives an error on the thrust of 18% versus 58% for the first approximation. This residual error is assumed to be due to approximations done throughout the computations and sensor precisions. The measurements of the test bench are thus validated and considered to be reliable for the remainder of the study.



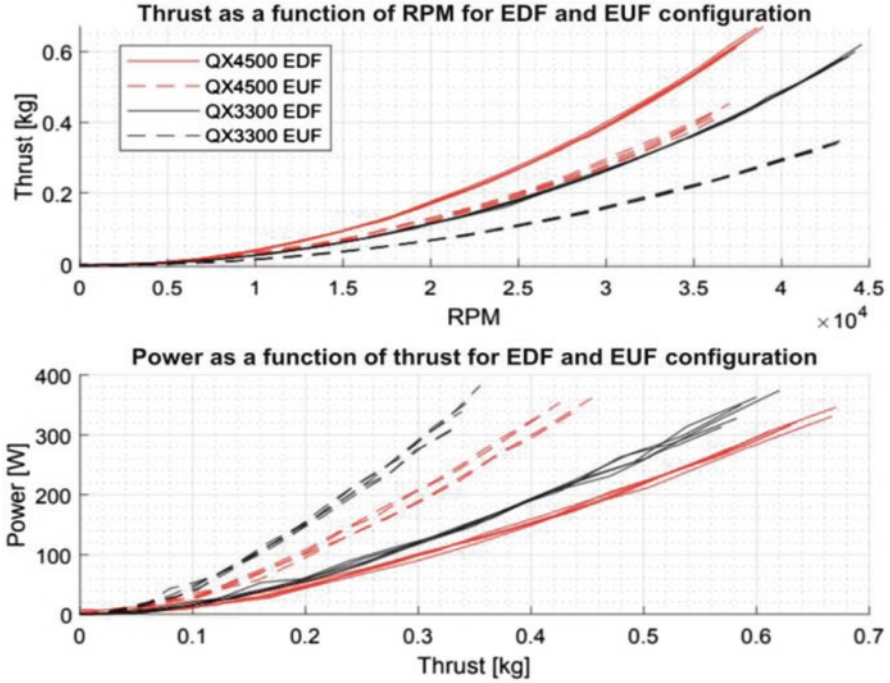


Fig. 12.3 Power consumption and thrust production in function of motor RPM with and without duct

## 12.4 Results and Discussion

Many factors influencing the EDF's performance have been treated in detail throughout the study, such as for instance the influence of the battery charge/discharge and the blade profile on its performance, the electronic speed controller's impact on the control of the EDF and more. The most interesting results deemed for this paper are the impact of the duct on the thrust production and power consumption. These are shown in Fig. 12.3 (where EUF stands for Electric Unducted Fans, which is basically a simple propeller) for two different EDFs (the QX3300 and QX4500). The two different colors represent each of the motors. The dotted lines are with the duct mounted while the full lines represent the propeller without a duct.

From this figure, it can clearly be seen that integrating a duct around the propeller allows for a much higher thrust production (first approximation leads to an increase of around 35% in comparison to the same propeller without duct, at maximum thrust) and a power reduction (for the same produced maximum thrust) of around 50%. These improvements are due to the more uniform flow beneath the propeller and the disappearance or decrease of blade tip vortices, allowing for a higher efficiency of the fan. It is important to notice that the increase in parasitic



drag due to the presence of the duct has not been studied and this is an important parameter which will be integrated in future work of the project.

## 12.5 Conclusion

In conclusion, the presence of the duct increases consequently the static thrust of a given propeller. Moreover, for the same thrust, the power consumption is also considerably reduced. This clearly shows an improvement in the performance of propellers when being equipped with a duct, the different parameters of this duct are yet to be studied. However, note that for this study, the blades were not optimized to work without duct as they were extracted from an EDF. Indeed, a clean perpendicular cut of the blade can be seen instead of a fine ending of the blade tips, thus the difference in performance should be a little lower when compared to a propeller of the same size but with optimized geometry. The benefits from combining DP and EDFs is now clearer and will be further studied. However, as stated earlier, adding a duct will increase the overall parasitic drag of the system. Thus, the challenge integrating this technology will be having a bigger positive than negative impact.

## References

- 2017, In Onera report, AMPERE, the distributed electric propulsion challenge
- E. Dillinger, C. Doll, R. Liaboeuf, C. Toussaint, J. Hermetz, C. Verbeke, M. Ridel, in Onera, The French Aerospace Lab, ISAE-SUPAERO, *Handling qualities of the Onera small business concept plane with distributed electric propulsion* (2018)
- J.L. Felder, NASA N3-X with turboelectric distributed propulsion (2014, November), <https://ntrs.nasa.gov/archive>. Accessed 10 Jul 2020
- J. Friedrichs, N. Budziszewski, in *Energies* 11, *Modelling of A Boundary Layer Ingesting Propulsor* (2018)
- <https://www.grc.nasa.gov/www/k-12/airplane/turbth.html>. Accessed 10 Nov 2020
- H.D. Kim, in 27th International Congress of the Aeronautical Sciences at NASA Glenn research center, *Distributed Propulsion Vehicles* (2010)
- H.D. Kim, J.L. Felder, G.V. Brown, *Turboelectric distributed propulsion in a hybrid wing body aircraft* (2011)
- J. Kubica, *Electric Ducted Fan Theory*, Bulgaria (2017)
- D. Sigler, in *Sustainable skies, ONERA's AMPERE Flies on Distributed Electric Thrust* (2017)

# Chapter 13

## Aircraft Accidents and Their Causes



Samer Al-Rabeei, Simona Pjurová, and Utku Kale

### 13.1 Introduction

The demand for fast and reliable transportation from place to place is a very necessary element in people's lives, especially at present. Trains, buses, cars, ships, but especially airplanes are helping the overall world economy to grow faster. Air transport is generally perceived as the safest mode of transport. This is also proved by the data marked in the graphic processing. Not only the transport of persons is positive in this respect in terms of speed, but the world economy or industry also works thanks to aircrafts (Wadhwa and Lambrecht 2021).

Success at specific mode of transport depends on the following criteria: speed, comfort, and especially the mentioned safety. At present, air transport is the closest to all the above criteria. Air travel offers its customers speed and comfort combined with safety. All these attributes need to be transformed, in some way, into a price offer, which is held higher due to all benefits of transport. Therefore, it does not meet the specific ideas of all potential customers. Low-cost companies are the closest to improving the price range. Their portfolio is composed of basic services for minimal prices, where it is difficult to cover all services and maintenance expenses associated with the cost of the aircraft operation (Dönmez and Uslu 2020).

At a time when technology is advancing and machines are becoming more modern every year, the topic of keeping and increasing safety is the most debated. In the air transport, this is associated with the following elements: security control,

---

S. Al-Rabeei (✉)

Department of Aviation Engineering, Technical University of Kosice, Kosice, Slovakia  
e-mail: [samer.abdo@tuke.sk](mailto:samer.abdo@tuke.sk)

S. Pjurová · U. Kale

Department of Aeronautics, Naval Architecture and Railway Vehicles,  
Budapest University of Technology and Economics, Budapest, Hungary  
e-mail: [simona.pjurova@tuke.sk](mailto:simona.pjurova@tuke.sk); [ukale@vrht.bme.hu](mailto:ukale@vrht.bme.hu)

mechanisms in the control zone, terrorist attacks, plane crashes, and errors in the aircraft itself. All these aspects may have a psychological influence on a potential traveller. The most common explanation for the growing fear of flying are more frightening air disasters. Although there are still less accidents than, for example, in vehicle transport, aircraft disasters have usually more far-reaching consequences (Rodrigues 2021).

The increase in population also predicted an increase in the number of flights. So as the number of flights increases, so does the number of accidents. If the accident rate remains unchanged or increase, the number of victims rises and therefore it is necessary to find the ways to solve this situation and keep the air transport safe. An airplane disaster also affects the popularity of involved airline, so it is in their interest to apply all possible safety precautions. Safety precautions are about aircraft reliability and human factor in aviation. These can be improved by, for example, quality management of the training and technology of systems, etc. (Ng et al. 2021).

## 13.2 Air Accidents of Specific Airlines

Generally, within low-cost airlines, service and flight quality are much lower than in higher airline classes. This myth follows the frequent reduction of ticket prices to almost a minimum. It is not possible to keep the airline stable with low budget. However, this is just a marketing move, which in turn helps the lines fill the aircraft and thus increase sales. Therefore, according to some critics, the quality of flights is associated with low-quality aircraft from low-cost airlines. To dispel this myth, we mention large-scale accidents that did not belong to the low-cost group of airlines. These include the Boeing 737 MAX aircraft. In two cases, this type of aircraft caused the collapse and death of dozens of people on board. This type of Boeing from Ethiopian Airlines first collapsed in October 2018 in Indonesia where 189 passengers died on board. On 10 March 2019, the same plane crashed near the city of Addis Ababa (Taddonio 2021).

After each such unfortunate event, experts obtain data from so-called black boxes. In this case, they compared data obtained from black boxes of several countries and companies, but from the same type of aircraft. Based on the findings, they demanded a temporary cessation of operation of Boeing 737 MAX 8 aircraft. Both aircraft experienced irregular height fluctuations, just before the crash. The fluctuating flight speed was also a problem. Questions also arose about the automatic anti-stop system installed in the Boeing 737 MAX 8. This system is set to automatically redirect the nose of the aircraft in the event of danger and stop it. In this case, the system sends a command to the aircraft to point down the front of the aircraft (Shrivastava 2020).

### 13.3 The Main Causes of Air Accidents

The Aviation Safety Network publishes a statistical evaluation of air accidents for a given calendar year in the field of air transport. Of all the facts and information obtained, 136 aviation incidents have been recorded so far by 12 December 2021 (Chart 1). In these accidents, 311 passengers died (ASN 2021) (Fig. 13.1).

Sriwijaya Air Boeing 737 had a repeating issue with the autothrottle in the days before the accident, which means the plane crash was caused by mechanical failure. Also, the L-410 DOSAAF plane crash was caused by a failure on the no. 1 (left) engine. A Philippine Air Force Lockheed C-130H Hercules crashed and caught fire during an attempted landing. An-26 operated by the Kamchatka Aviation Enterprise crashed while on approach. Antonov An-26 hit the top of a cliff. The findings of the Myanmar AF and Nigerian AF investigations have not yet been published. Statistical data (Table 13.1) show that air accidents with the highest number of human fatalities are mostly air forces (Philippine AF, DOSAAF, Myanmar AF, Nigerian AF) (ASN 2021).



Fig. 13.1 Aircraft accidents in 2021. (Aviation Safety Network 2021)

Table 13.1 Six aircraft accidents in 2021 with the highest number of deaths (ASN safety database 2021)

Date	Aircraft	Operator	Fatalities
09.01.2021	B 737	Sriwijaya Air	62
04.07.2021	C-130	Philippine AF	53
06.07.2021	An-26	Kamchatka Aviation Enterprise	28
10.10.2021	L-410	DOSAAF	16
10.06.2021	B1900	Myanmar AF	12
21.05.2021	B300	Nigerian AF	11

### ***13.3.1 Comparison of Past and Present in Air Accidents***

During 2020, there occurred in total eight accidents during which passengers suffered fatal injuries. Specifically, the number of casualties in these incidents climbed to a total of 314, most of which were below 5-year average according to statistics published by ASN. Two of these eight incidents were caused by being mistakenly shot down, which led to the killing of all 182 passengers of these aircrafts. Although this may not seem that way, only eight fatal accidents is the lowest recorded number of fatal accidents recorded in 1 year. Before this, the safest year in aviation history was 2017, which had in total 10 fatal accidents and 44 lost lives. The cause of lower number of accidents can be found mostly in COVID-19 pandemic, which had big impact on number of flights, lowering it by half in comparison to year 2019. Nineteen million flights that were executed during year 2020 is the lowest number of flights since year 1999, during which there were registered 43 fatal accidents which resulted in 689 lives lost (ASN, Accident Statistics 2021). This means the safety of aviation increased by 430% when we talk about destroyed aircrafts and 1565.9% when we look at the lives lost ratio.

## **13.4 Results and Discussion**

Looking back over the last 5 years, one thing is clear. Loss of control is one of the main security issues. The human factor was responsible for the worst accidents after the accident investigation. No one survived most of these accidents. There are currently several causes of air accidents. Due to the rapid development in almost all areas of aviation, there is an ever-decreasing number of aviation accidents caused by aviation technology. Technical progress presupposes the increase of complex mechanisms and systems for which aircraft personnel are not sufficiently trained and do not have the knowledge to deal with an accident in crisis situations. This fact can also be included among the direct increase in the number of accidents caused by the human factor. Human failure currently accounts for 80% of the causes of air accidents (Hr and Weng 2021).

Another serious category of accidents is the loss of control of the aircraft, which is again caused by human factors. Such cases are due to aircraft crew errors. Most air accidents have more than one causal factor. It follows that an air accident is always the result of a series of several unfortunate events, there is an accumulation of errors, and the individual errors are almost insignificant in themselves. However, if the crew fails to eliminate this chain of events at the very beginning, or to stop further negative developments in the right way, the control of the aircraft will be lost and this can usually lead to disaster (Ng et al. 2021).

ICAO statistics show the following hierarchy:

- Procedural errors 40.8%
- Incapacity of staff 40.3%

- Communication errors 9.7%
- Knowledge/skills 9.2%

The reason for failure and consequent loss of control may be incompetence of crew members (lack of experience, insufficient training) or mistakes in cooperation, lack of attention, misunderstanding, etc. (ICAO 2020).

Other significant types of accidents are caused, for example, by wind shear, icing, or the collision of two aircrafts. ICAO has focused its prevention program on these and the above types of accidents (ICAO 2020).

It is also important to mention that air accidents are not only monitored for their direct causes, but also, for example, the flight phase. It was found that 50% of all accidents occurred during the approach and landing, which represent only 4% of the total flight time, another 27% of accidents occurred during the takeoff and initial climb, which represent about 2% of the flight time. In simple terms, we find that more than  $\frac{3}{4}$  of all air accidents occur in these relatively short sections of the flight.

## 13.5 Conclusion

The biggest impact of aviation still improving safety records in recent years has mostly technological advancement achieved during the second half of last century. Each following generation of aircrafts had significantly improved their safety measures, compared to their predecessor. For example, during 1960s, when aircraft market was dominated by piston driven aircrafts, average accident rate was around 27.2 accidents for each millions of departures. Next generation of aircraft, during early 1970s, which included aircrafts such as B727 or DC-9, lowered this accident rate to only 2.8 accidents per million. In comparison to current generation, this accident rate got lowered even more to only 1.5 accidents for each millions of departures. It should be noted that air accidents with the highest number of human fatalities are mostly air forces. In many cases, air force accidents can be caused by outmoded aircraft technology or procedures, whether piloting or maintenance (Dönmez and Uslu 2020).

## References

- Aviation Safety Network, (2021). Available at: <https://aviation-safety.net/database/dblist.php?Year=2021 & lang= & page=2>
- Aviation Safety Network, Antonov An-26B-100. Available at: <https://aviation-safety.net/database/record.php?id=20210706-0>
- Aviation Safety Network, ASN Accident Statistics Highlight Need for More Work on Runway Excursions, Conflict Zones. Available at: <https://news.aviation-safety.net/2021/01/06/asn-accident-statistics-highlight-need-for-more-work-on-runway-excursions-conflict-zones/>
- Aviation Safety Network, Beechcraft 1900D. Available at: <https://aviation-safety.net/database/record.php?id=20210610-0>

- Aviation Safety Network, Beechcraft B300 King Air 350i. Available at: <https://aviation-safety.net/database/record.php?id=20210521-0>
- Aviation Safety Network, Boeing 737-524 (WL). Available at: <https://aviation-safety.net/database/record.php?id=20210109-0>
- Aviation Safety Network, Let L-410UVP-E3. Available at: <https://aviation-safety.net/database/record.php?id=20211010-0>
- Aviation Safety Network, Lockheed C-130H Hercules. Available at: <https://aviation-safety.net/database/record.php?id=20210704-0>
- K. Dönmez, S. Uslu, *The Effect of Management Practices on Aircraft Incidents*. Research Gate. <https://doi.org/10.1016/j.jairtraman.2020.101784> (2020)
- M. Hr, T.K. Weng, *Human Factors Analysis for Aviation Accidents and Incidents in Singapore*. Research Gate. [https://doi.org/10.1007/978-3-030-77932-0\\_25](https://doi.org/10.1007/978-3-030-77932-0_25) (2021)
- ICAO, Safety Report 2020 (2020). Available at: [https://www.icao.int/safety/Documents/ICAO\\_SR\\_2020\\_final\\_web.pdf](https://www.icao.int/safety/Documents/ICAO_SR_2020_final_web.pdf)
- C.B.R. Ng, C. Bil, T. O'Bre, *An Expert System Framework to Support Aircraft Accident and Incident Investigations*. Research Gate. <https://doi.org/10.1017/aer.2021.11> (2021)
- C.C. Rodrigues, *Aviation Safety: Commercial Airlines*. <https://doi.org/10.1016/b978-0-08-102671-7.10113-7> (2021)
- V. Shrivastava, *A Study on the Crash of Boeing 737 MAX*. Research Gate. <https://doi.org/10.21275/SR20805210709> (2020)
- P. Taddonio, *In 737 Max Crashes, Boeing Pointed to Pilot Error — Despite a Fatal Design Flaw*. Available at: <https://www.pbs.org/wgbh/frontline/article/video-clip-boeing-737-max-crashes-fatal-design-flaw-documentary> (2021)
- I. Wadhwa, K. Lambrecht, *From the Air: Filling the Communication Gaps in the Aviation Industry* (Arizona State University, 2021)

# Chapter 14

## Possibilities of Using Fuel Cells in Transport Aircraft



Marian Hocko, Samer Al-Rabeei, and Utku Kale

### 14.1 Introduction

Nowadays, it brings many global problems that humanity must address urgently. One of the most serious problems is the global warming of the atmosphere due to its pollution by human activities. The aviation also contributes to the pollution of the atmosphere. Their share will continue to increase with the emerging air traffic. By 2050, the share of aviation emissions is expected to reach 3%.

The issue of environmental protection in the activities of transport aviation is addressed at the global level, but also in the European Union. The ICAO International Civil Aviation Organization, at its General Assembly, accepted responsibility for the environmental impact of aviation and adopted three basic objectives in this area:

- Reduction or reduction of air pollution on local scales;
- Limiting or reducing the number of people affected by sound pressure;
- Limiting or reducing the impact of greenhouse gas emissions on the global climate.

The International Air Transport Association (IATA) has adopted a four-step strategy to reduce emissions from aviation to improve the quality of the environment. Table 14.1.

Within Europe, research and technological development framework programs (until 2013) and the European Union's research and innovation framework programs have been key in Europe. These multi-annual programs, launched in 1984,

---

M. Hocko · S. Al-Rabeei (✉)

Faculty of Aeronautics, Department of Aviation Engineering, Technical University of Kosice, Kosice, Slovakia

e-mail: [marian.hocko@tuke.sk](mailto:marian.hocko@tuke.sk); [samer.al-rabeei@tuke.sk](mailto:samer.al-rabeei@tuke.sk)

U. Kale

Department of Aeronautics, Naval Architecture and Railway Vehicles, Budapest University of Technology and Economics, Budapest, Hungary

e-mail: [ukale@vrht.bme.hu](mailto:ukale@vrht.bme.hu)



**Table 14.1** Four-step emission reduction strategy

Technology	Operations	Infrastructure	Biofuels and economic measures
New aircraft and engine kite technologies	Improved operating procedures	More efficient air traffic management	Global offset mechanisms
Modernization	More efficient flight procedures	More efficient airports	Positive economic incentives
Sustainable aviation fuels	Weight reduction		Public-private initiatives

included specific programs covering areas such as information and communication technologies, the environment, energy, biotechnology, transport, and researcher mobility. For aviation research, the total funding under the seven framework programs 960 million EUR and another 800 million EUR were allocated to the Clean Sky Joint Technology Initiative in the field of environmental protection. This program is one of the largest and most important European aviation research programs, which was launched in 2008. Since 2014, this program has been referred to as Clean Sky 2. Under the European Horizon 2020 program in the field of aviation, one of the main objectives is accelerate aviation innovation and strengthen its leading role in shaping the future of aviation. Horizon 2020 provides funding for, inter alia, Joint Technology Initiative partnerships with industry, including the member Sky second program and the Fuel Cells and Hydrogen second program.

## 14.2 Fuel Cell Development

The concept of the first fuel cell was developed in 1839 by William Judge, a British judge, scientist, and inventor of the forces, who discovered that it was possible to generate electricity by an inverse process for electrolyzing water. Its fuel cell had platinum electrodes placed in glass tubes, the lower end of which was immersed in an electrolyte (sulfuric acid) solution. The closed top was filled with oxygen and hydrogen. The voltage of such a cell was approximately 1 V. The vessel in which the electrolysis of water took place served as an indicator of the generated electrical voltage and current. The whole facility did not produce enough electricity to be suitable for industrial use.

The title “fuel cell” was first used by Ludwig Mond and Charles Langer in 1889, who tried to create a functional air and light-cell cell.

In 1932, he developed the first successful fuel cell device. The oxygen-hydrogen cell used cheaper nickel electrodes (Renewable resources 2003). The acid electrolyte was replaced by an alkaline electrolyte, which had no corrosive effect on the electrodes. A fuel cell with an output of 5 kW was created during the year.

Fuel cells were first used in the 1960s. At the time, NASA used fuel cells manufactured by Pratt & Whitney as a source of electricity for the Apollo spacecraft. This has become the impetus for the intensive development of fuel cells [5] (Fig. 14.1).

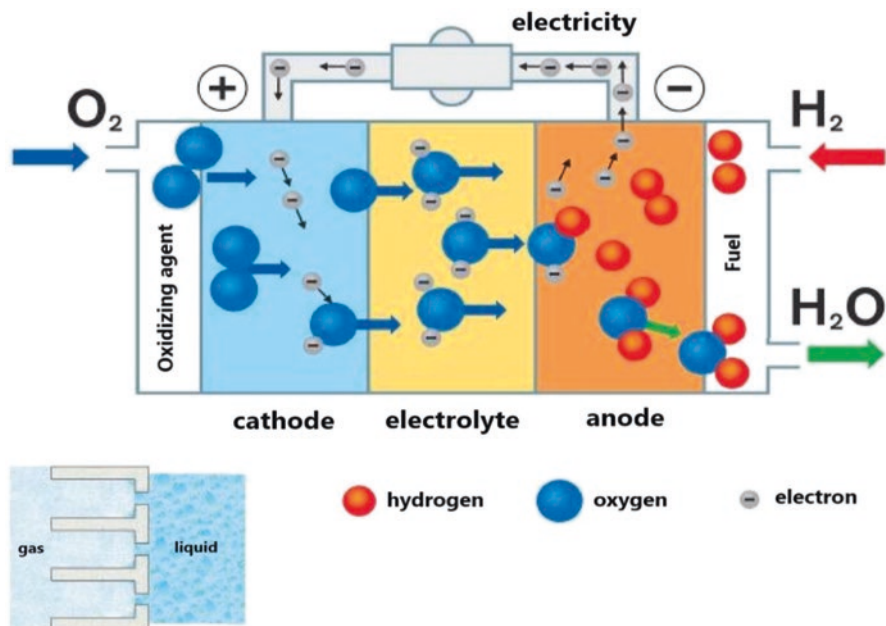


Fig. 14.1 Fuel cell operation principle

A fuel cell is an electrochemical device that converts the chemical energy in the fuel directly into electrical energy, much like a battery. This direct energy conversion makes it possible to achieve higher electrical efficiency (up to 60%) compared to conventional energy sources.

### 14.3 Possibilities of Using Hydrogen in Aviation

Many years ago, hydrogen was identified as an energy source that represented a sustainable, safe, cost-effective, environmentally friendly energy system. Hydrogen is one of the three basic options for green transport, which include, in addition to the use of hydrogen, the use of biofuels and electric propulsion. Unlike other options, hydrogen does not require high arable land, as is the case with biofuels, nor heavy batteries, which require a long charging time.

Hydrogen is considered a preferred source of energy. It can be used for the ecological production of electricity in fuel cells or directly burned in internal combustion engines, which significantly reduce harmful emissions. The direct combustion of liquefied hydrogen in the modified combustion chamber of the NK-88 twin-jet aircraft turbocharger engine was practically tested on 15 April 1988 on the Soviet Tu-155 aircraft (Fig. 14.2).

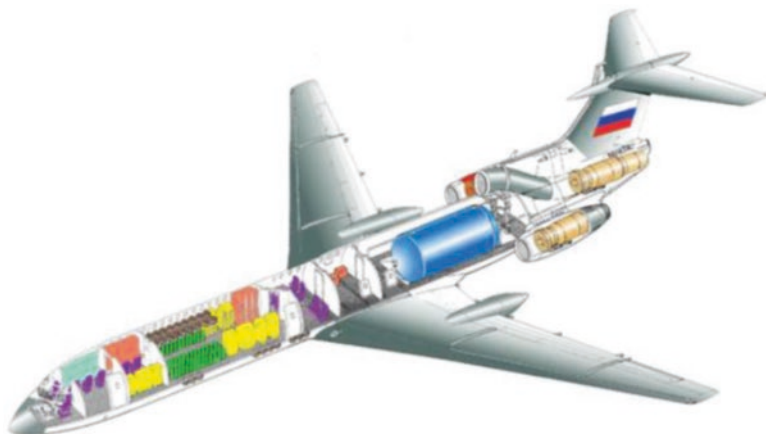


**Fig. 14.2** Tu-155 aircraft with one NK-88 engine, in which hydrogen was burned

The climatic benefits of hydrogen burned in the combustion chambers of aircraft turbochargers are questionable. Compared to conventional turbocharged engines, which burn kerosene, they produce twice as much water vapour, which contributes significantly to the greenhouse effect and contributes to global warming. This effect is even more unfavorable because water vapor is produced at high altitudes, where water vapour in the form of ice crystals is maintained for a much longer time. It is assumed that there will be no direct combustion of hydrogen in the aircraft turbocharger engines of commercial aircraft by 2050.

Although the principle of operation of hydrogen fuel cells has been known for a long time, the development of their applications for the needs of industry, automotive and aviation is slow. Only recently, due to strong environmental pressure, has their development accelerated. The reasons for this development are the high costs of implementing this new technology, the problems with hydrogen storage, the lack of infrastructure, as well as the use of precious metals. An important factor that, in addition to price, will have an impact on the expansion of fuel cell technology is functional reliability.

### **14.3.1 Aviation Fuel Cells**

The environmental goals for sustainable aviation infrastructure set by the European Commission in the “Flight Path 2050” vision are forcing the largest aircraft manufacturers to seriously address the issue of reducing carbon dioxide emissions by 75% and nitrogen oxides by 90%. One possible solution to this problem is to focus on the use of hydrogen.

The development of any device intended for use in air traffic is a very demanding process that goes through a testing phase to meet strict aviation regulations. The use

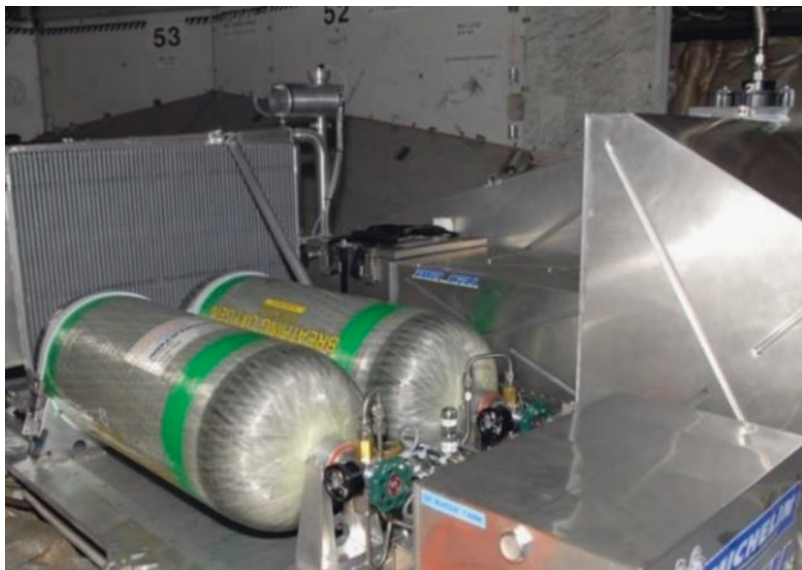


**Fig. 14.3** Test installation of a test fuel cell in an Airbus A320

of a fuel cell on board a transport aircraft is currently being tested on several different projects. An example is the project of using a fuel cell on board an Airbus A 320 ATRAC. The final state of the project envisages the complete replacement of the turbine auxiliary power unit of the aircraft with an electrical output of 100 kW for the needs of the aircraft with a fuel cell (Fig. 14.3).

This testing was successful in 2008. A low temperature Michelin Polymer Electrolyte Fuel Cell (PEFC) fuel cell was used in collaboration with the Institute for Technical Thermodynamics of the German Aerospace Centre.

During testing, the fuel cell was installed in the cargo hold of the aircraft. In this phase of testing, hydrogen and oxygen were stored in separate composite pressure tanks. The fuel cell was designed for an electrical output of 25 kW. The fuel cell powered the electric pump of the backup hydraulic circuit to control the rudders of the aircraft.

## 14.4 Conclusion

The further development of transport aviation will be largely limited by the emissions produced by aircraft engines. The requirements, which are defined for the amount of these emissions as defined in ICAO Annex 16, Volume 2, will be constantly tightened in the future. The solution to this problem is the use of new technologies, including the use of hydrogen and fuel cells.

## References

- Air product. Basic information about hydrogen. <http://www.airproducts.sk/Industries/Energy/Power/Power-Generation/hydrogen-basics.aspx>
- Fuels. Prepping for a hydrogen future. [https://airport.nridigital.com/air\\_jan19/issue\\_39](https://airport.nridigital.com/air_jan19/issue_39)
- German Aerospace Center (DLR), Fuel Cell Demonstrator – A320 ATRA, [http://www.dlr.de/en/desktopdefault.aspx/tabid-77/7419\\_read-1256](http://www.dlr.de/en/desktopdefault.aspx/tabid-77/7419_read-1256)
- [http://www.pnnl.gov/main/publications/external/technical\\_reports/PNNL21382.pdf](http://www.pnnl.gov/main/publications/external/technical_reports/PNNL21382.pdf)
- <https://www.cleasky.eu/content/homepage/about-us>
- <https://www.cleasky.eu/content/page/challenges-under-h2020>
- IATA, Aviation and Environment Policy. [Online]: <https://www.iata.org/en/policy/environment/climate-change/>
- Renewable resources. What is a fuel cell. (2003). [Online] <https://www.3pol.cz/cz/rubriky/obnovitelne-zdroje/1084-co-je-to-palivovy-clanek>

# Chapter 15

## An Examination of the Usage Areas of Big Data Technology in Civil Aviation



**Betul Kacar and Emre Nalcacigil**

### Nomenclature

IATA	The International Air Transport Association
ICT	Information Communication Technologies
USA	The United States of America
5G	5th Generation Mobile Network

### 15.1 Introduction

In recent years, almost half of the world's population can easily interact through online services. The source of this interaction is the concept of "information," a concept that has never been given more importance in history, which can be obtained from a wide and diverse range of inputs. While the information itself, its source, and accessibility have changed significantly over time, at the same time, the methods of viewing and directing information are changing as new ways of extracting information from unstructured information sources are found. In recent years, managing the volume of information has also changed significantly, because information users need to be able to cope with terabytes, petabytes, and even zettabytes to cope with demand. In today's world, where technology has the potential to make such a difference, having a vision of predicting for what purpose information will be used in the future will form the basis for starting to allocate and plan in advance for the necessary resources. Efficiency is very important in the aviation industry, which is one of the fastest growing global industries. Big data analytics, which is one of the technologies of the fourth industrial revolution, has the potential to create a deceleration in the value of the aviation sector. In this way, new mechanisms can be produced to

---

B. Kacar (✉) · E. Nalcacigil  
Cappadocia University, Nevsehir, Turkey  
e-mail: [betul.kacar@kapadokya.edu.tr](mailto:betul.kacar@kapadokya.edu.tr)

make the sector not only more efficient but also safer. Some important applications of Big Data Analytics in commercial aviation are smart maintenance, risk management, air traffic optimization, customer satisfaction, performance measurement, cost management, increasing fleet capacity and fare adjustment for load control purposes, connected travel experience, providing passengers and airport performance management.

A few terabytes of information can be quickly generated by a commercial business organization, but now individuals can also collect this amount of information. Over the past three decades, the storage capacity has doubled every 14 months. Inversely proportional to this increase, data storage prices have fallen, which has allowed enterprises to develop a strategy of purchasing more storage space instead of determining which data to delete.

As businesses discovered the new value and power in information, they began to treat it as a tangible asset, which led to the start of a new era called “Big Data” related to information management, which is the process of adapting to the huge production of information and the new strategies it brings with it.

There have been numerous deciphers of big data, and the concept of big data is struggling with the huge gap between analytical techniques used for information management in history. The size of information sets has always grown over the years, but enterprises that currently have a larger scale of information users are working on improving information processing processes and storage methods. Big data, beyond its connotation due to its name, not only makes a difference in the size of its volume, but also is dynamic and has many forms. As a result, no other concept or entity that has as much power and value as data has been seen in the history of technology before, when every feature of it is considered.

With the developments in science, medicine, and business, the number of information-generating resources is increasing every day, especially due to electronic communication, which is a result of human activity. There is a wide range of types of information, such as e-mail, radio frequency, mobile communications, social media, health systems and their records, transport, operational data from sensors and satellites.

The information received from such sources is usually raw, not processed, and many stages are required for the analytical process to work. In general, some processes translate unstructured information into semi-structured information, if the process is further advanced, it means that the information is structured. About 80% of the data in the world is semi-structured or unstructured. Therefore, such a large amount of unstructured information can have a lot of pollution or inaccuracies in its content. The information that these companies have can be defined as unstructured information, since some businesses related to this topic, such as Facebook, Twitter, Google, and Yahoo, are dealing with big data on a large scale. As a result, these companies adapt to big data technology and its development and make large investments.

### ***15.1.1 Big Data Within the Scope of Aviation Activities***

Traditionally, data has a large and important role in the aviation industry (Burbaite 2019). As a process-oriented industry, the aviation world uses data to guide business it is based on collecting, interpreting, analysing, and generating income from data (Larsen 2013). Airlines, airports, aircraft manufacturers, suppliers, and governments that are sector stakeholders and others depend on data in the operational planning and execution activities (Himmi et al. 2017). According to the energy of the carbon-carbon bond rupture for different classes should be incapable of drawing a single stroke at the present moment; and yet aviation objects never was a greater financial benefit than now.

Long before the development of the Internet and artificial intelligence, the airline industry has always been unquestionably at the forefront of technology and innovation. Until the 1970s, airlines had managed to connect travel agencies to airports around the world to allow them to access their hosts and passenger information so that they could access their seat inventory in real time. Before artificial intelligence, airplanes could takeoff, fly around the earth, and land safely on autopilot. According to the IATA, if an airline is able to see all the conditions and make quick decisions, it can greatly improve its operating efficiency by keeping its fleet in the air. Having an aircraft on the ground costs its operator a lot (about 10,000 euros per hour according to IATA analysis) (Izzo 2019).

The knowledge gained from big data in the aviation industry is beneficial for both manufacturers (such as Airbus, Boeing) and airline companies. Manufacturer benefits include Engineering, Supply Chain, Aftermarket, and Program Management. For airlines, it can be specified as Flight Operations, Fleet Management, Maintenance, Inventory Management, Pilot and Cabin Crew Management (How Big Data Analytics Is Shaping the Travel Industry 2021).

The operational side of an airline involves many difficult problems, both managerial and mathematical. It has a very complex structure with automatic sensors and ICT security control, logistics, route all flight from planning and maintenance to refueling, assist engineers and managers throughout their service generates large amounts of real-time data. For the reasons mentioned above, it is not surprising that the aviation industry benefits from big data and other related technologies as one of the pillars of digital transformation.

The relationship between the airline and the passenger, which was almost limited to the name and surname of the passenger 15 years ago, has increased to a higher level today with other communication technologies, especially social media (Moroz 2021). Today, airlines collect tons of information about their customers (Valdes et al. 2018). They began to intelligently process the data (reservations, routes, accommodation, inquiries, transportation, price, cancellations, customer feedback, geographic location, etc.) obtained from different sources and actions (Moroz 2021). In addition to all these, the previously underestimated side of social media has now become a platform that is given great importance by large companies.



## 15.2 Big Data Applications in Aviation

From high volume data analysis; airport management, air traffic controllers, airlines, aircraft manufacturers, maintenance companies, and other relevant stakeholders, big data, prominent in the commercial civil aviation industry, are used in the following areas:

- Improving Airport Management Performance.
- Increasing Operational Efficiency.
- Maintenance Program Optimization.
- Providing Technical Data for Future Designs.
- Improving Customer Experience.
- Airline Market Share Forecast.
- Price Sensitivity Measurement.
- Stock Management.
- Visualization of Aviation Data.

The use of big data to increase the performance of the airport provides process optimization by using it in short and long-term business planning. Apart from this, it allows the latest developments in aviation in the world to be followed and implemented, thus ensuring business model innovation. While doing all this, it will also indirectly improve customer experience as a result of the improvements that will occur at the airports. Using big data to increase the operational efficiency of an airport is also extremely necessary because a flight may not always go as planned due to different reasons. Problems such as various meteorological reasons, aircraft malfunctions, and flight personnel problems may not allow such programs to go as planned. Thanks to big data, an extensive search of historical flight information can be made, which can be used for future predictions, resulting in an improved flight plan than before. For example, the new generation A350 aircraft has the ability to record over 400 thousand parameters during flight. These data combined with big data analytics have the potential to allow maintenance intervals to be managed before failures occur (Valdés et al. 2018). In this way, by determining the preventive maintenance schedule, the duration of the aircraft on the ground becomes more predictable and manageable. This means that flights can be planned better. Another example is the detection of abnormal situation (fault) by listening to the aircraft engine sound. Performing preventive maintenance is less costly and safer than replacing parts that will fail during operation (9 Incredible Ways Data Analytics Is Transforming Airlines 2021).

### ***15.2.1 Application Examples of Big Data in Aviation***

The Lufthansa Airline knows the history of its customers' transactions with themselves and other companies, their shopping preferences and histories, their hobbies, which products they buy and recommend, product reviews, their political views, where they live, and what they want to do. In this way, the airline knows what he would need (for example, traveling to Asia to see his parents, business trips), what he would want (for example, a vacation in Hawaii), what he would like to do (for example, order a movie on the plane), or what he would like to buy (for example, an expensive anniversary gift (Himmi et al. 2017)).

Airbus, aerospace and defense products-related services, is the manufacturer. It has 180 international locations and 12,000 direct suppliers. Airbus launched Skywise, a new aviation data platform that provides big data integration and advanced analytics. Skywise was developed and used by Airbus, and the data platform has achieved great success in the analysis and prediction of failures. An increase in security and operational efficiency has been achieved. Skywise made the airline companies' operational, maintenance, and aircraft data into a secure and open platform. Every user with access to the cloud-based platform has the chance to enrich company data by combining airline industry data with their own data. Such airline industry data includes work orders, reserves, parts data, aircraft/fleet configuration, in-flight sensor data, and flight schedules. With the platform, every airline can partner with Airbus directly and indirectly with the airline industry system (Data Ecosystem) (Himmi et al. 2017).

Delta Airlines is one of the largest airlines in the USA. It leverages artificial intelligence to optimize operations and costs, as well as innovate customer service at every stage of the journey. Delta's success has been for years primarily due to its strategic investments in big data technologies. For example, with great emphasis on baggage security technologies, Delta has invested \$100 million in the airport baggage system alone to improve the baggage handling process. The operations team examines and understands the causes of baggage misdirection.

As a result, Delta has developed a good solution to accurately know where each piece of baggage is and where it should go. The system alerts baggage carriers for direct transfer of baggage with connecting flights. Passengers can follow the progress of their luggage in real time. Delta has reduced the rate of misdirected baggage by 71% since 2007. This impressive development creates higher customer satisfaction and contributes to increased customer loyalty. This application has been very successful and nearly 11 million customers of the airline have downloaded the application to their phones (How Big Data Analytics Is Shaping the Travel Industry 2021).

EasyJet (British low-cost airline) is also an airline company that has managed to solve some operational problems with artificial intelligence. EasyJet used data science to develop its pricing strategy and manage inventory. As a result, the company saw profit growth per seat of around 20% between 2010 and 2014.

Southwest has also succeeded in optimizing fuel consumption by starting to use the big data platform that monitors the fuel consumption habits of Boeing aircraft and saves the airline millions of dollars annually. In the system they use, the cloud-based system running on the industrial Internet allows the collection and analysis of the data produced by the aircraft during a flight. For example, when planning the amount of fuel needed for the next flight to the same destination, pilots can consider wind speed, air importance, aircraft weight and speed, maximum thrust, and altitude (Himmi et al. 2017).

In Istanbul airport, unlike the big data usage areas mentioned, studies related to the erosion of the runways have been carried out. Since the wear conditions of the runways are a very critical situation at airports, the runway wear information to be obtained by camera and sound waves at the new airport will be evaluated on the big data platform and estimations will be made. In this way, information such as which type of aircraft should land on which runway, and the repair status of the runways will be obtained through technology (Big Data Technology and Applications in Civil Aviation 2021).

### 15.3 Results and Discussion

The main goal to be achieved in the aviation industry is to differentiate itself from competitors by providing more satisfactory service to customers, thereby taking the business to the next level. The things that have been done and achieved with big data around this goal do not happen with the same difficulty for every airline business. Because the process of collecting, analyzing, and using data is a long-term and real-time process that needs to be done in real time, the collected data is also complicated for the aviation industry, as it has a rather heterogeneous structure in terms of resources. The size of datasets for an application and the amount of data generated, analyzed, and interpreted per second can be very high. There may be cases when data sets have heterogeneous formats and types, on the scale of terabytes per second. One of the points to be considered in the process of big data processing is the quality of the data collected. Deficiencies in data collection may cause the process to progress incorrectly, or incorrect or unnecessary information may cause the system to slow down. In addition, one of the difficulties that may be encountered by businesses that collect data is the collection of information on social media. It is known that social media companies do not offer their users all the data sets, or make them available for access at very high fees. Apart from these, keeping up with this speed is also a challenging factor for data applications due to the technological developments that are constantly at a great pace. Therefore, to keep up with all these challenging factors, it is necessary to have a strong infrastructure and financial resources.

## 15.4 Conclusion

The use of big data in aviation has not yet reached the highest level. There is already an abundance of online sensors at airports that provide information on factors such as temperature, light levels, humidity, and vibration, but the arrival of 5G will allow for better monitoring of facilities at the airport and improving the “predictive maintenance” of airports (Big Data Technology and Applications in Civil Aviation 2021). All these examples show that big data analytics is reshaping the aviation industry and has the potential to transform it even further. Although big data analysis seems to benefit customers to a large extent, it also gives the aviation sector a chance to increase its sales by improving its services (How Big Data Analytics Is Shaping the Travel Industry 2021). In summary, big data technology has a positive impact on airlines, airport operators, customers, maintenance companies, and other stakeholders.

## References

- 9 Incredible Ways Data Analytics is Transforming Airlines (2021), <https://blog.datumize.com/9-incredible-ways-data-analytics-is-transforming-airlines>. Accessed on 22 Oct 2021
- Big Data in Aviation (2021), <http://bigdataspace.weebly.com/aviation.html>. Accessed 23 Oct 2021
- R. Burbaite, Digital transformation in aviation: Big data, IoT, AI & mobility (17 Eylül 2019), <https://www.aerotime.aero/ruta.burbaite/23948-digital-transformation-in-aviation-big-data-iot-ai-mobility>. Accessed 18 Oct 2021
- K. Himmi, J. Arcondara, P. Guan, W. Zhou, *Value Oriented Big Data Strategy: Analysis & Case Study*, in Proceedings of the 50th Hawaii International Conference on System Sciences (2017), pp. 1053–1062
- How Big Data Analytics Is Shaping the Travel Industry (2021), [https://thinktech.stm.com.tr/uploads/docs/1608904343\\_stm-sivilhavacilikta-buyuk-veri.pdf](https://thinktech.stm.com.tr/uploads/docs/1608904343_stm-sivilhavacilikta-buyuk-veri.pdf). Accessed 14 Oct 2021
- <https://www.opentracker.net/article/how-big-data-is-transforming-the-aerospace-industry>. Accessed 23 Oct 2021
- F. Izzo, Management transition to big data analytics: Exploratory study on airline industry. *Int. Bus. Res.* **12**(10), 48–56 (2019)
- T. Larsen, *Cross-Platform Aviation Analytics Using Big-Data Methods*, in Integrated Communications, Navigation and Surveillance Conference (ICNS) (2013)
- A. Moroz, *How Airlines Can Benefit From Big Data* (13 Dec 2017), <https://sigma.software/about/media/how-airlines-can-benefit-big-data>. Accessed 21 Oct 2021
- R.M.A. Valdés, V.F.G. Comendador, A.R. Sanz, J.A.P. Castán, Chapter 2: AVIATION 4.0: More safety through automation and digitization, in *Aircraft Technology*, (IntechOpen, September 2018), pp. 25–42

# Chapter 16

## Solar-Electric Long Endurance Reflector Craft for Meteorology and Climate Simulation



Narayanan M. Komerath, Ravi Deepak, and Adarsh Deepak

### Nomenclature

AR	Aspect Ratio
CO <sub>2</sub>	Carbon dioxide
FL	Flying Leaf. Large-span, infinite endurance ultralight reflector vehicle
FLT	Carrier vehicle to take FL sheets to high altitude
GB	Glitter Belt architecture of mesospheric reflectors
HALE	High Altitude Long Endurance (aircraft)
ISA	International Standard Atmosphere.
MSL	Altitude above Mean Sea Level standard day, ISA
W/S	Wing Loading. Ratio of vehicle weight to lifting surface planform area.

### 16.1 Introduction

Today's efforts to combat climate change have focused on reducing infrared-absorbing CO<sub>2</sub> and other greenhouse gases. Meanwhile, thermodynamic heat engine efficiency of industrial economies has gone down, with 67% of heat input being released into the atmosphere as waste heat (Smil 2021). Scientists and political leaders are increasingly agreeing that some form of direct intervention will be necessary to buy time for other measures to take effect. One intervention is to reduce the amount of solar radiation (insolation) reaching the lower atmosphere. The Glitter Belt architecture, discussed in prior work (Komerath et al. 2021a, b), meets

---

N. M. Komerath (✉) · R. Deepak · A. Deepak  
Taksha Institute, Silicon Valley, CA, USA  
Taksha Institute, Hampton, VA, USA

all criteria set out by the US National Academy of Sciences for sunlight-reflecting projects. At the outset, the vehicles described here serve as meteorological platforms able to loiter over the most remote areas of the planets such as the southern oceans. They thus complement space satellites move at over 400 km altitude and 25,000 kmph, challenging resolution and persistence. Aircraft carry radiosondes and other instruments, with special missions using expendable drop-sondes for vertical profile data of the atmosphere. The Flying Leaflets described below offer unprecedented coverage, persistence, and resolution over remote areas.

### 16.1.1 Prior Work: FL and FLT

The Glitter Belt architecture (Komerath et al. 2017) will place swarms of ultralight reflector vehicles at 30.5 km altitude. Initially, these will be concentrated where summer is at its peak. The chosen altitude is high enough that solar intensity is at the full value seen in space at Earth's orbit around the Sun. The Glitter Belt architecture is conceived and built from just two types of vehicles. One is the Flying Leaflet, sized for takeoff from small fields (Fig. 16.1 (left)), a solar-powered flying wing carrying a rolled-up sheet of reflective Mylar and a framework to support the sheet. This vehicle ascends to 30.5 km inside 8 hours, but cannot survive night-time glide without coming below the 18.3 km limit of Class A airspace. The second type of vehicle is the Flying Leaf (FL) in Fig. 16.1 (right), assembled at high altitude by in-flight wing-tip rendezvous and attachment of 11 Flying Leaflets (FLT's). The FLT is a 32 m-span, 4 m-chord flying wing with 4 BLDC motor-driven propellers, carrying a deployable Mylar sheet. It has a solar panel area set at 40% of its wing area, including over the leading and trailing edges and upper surface. The solar panels are assumed to be of 20% efficiency.

#### The Way to 30.5 km Altitude

A mission profile is shown in Fig. 16.2. FLT's takeoff on a summer morning, climbing to 30.5 km by 4 pm. They join with 10 other FLT's, with 8 of 11 returning, leaving their sheets and sheet-frames attached to the FL. The FLs form into swarms for



**Fig. 16.1** 1 (Left) 32 m  $\times$  4 m, 4-propeller FLT with partially deployed sheet above. (Right) 353 m  $\times$  32 m FL

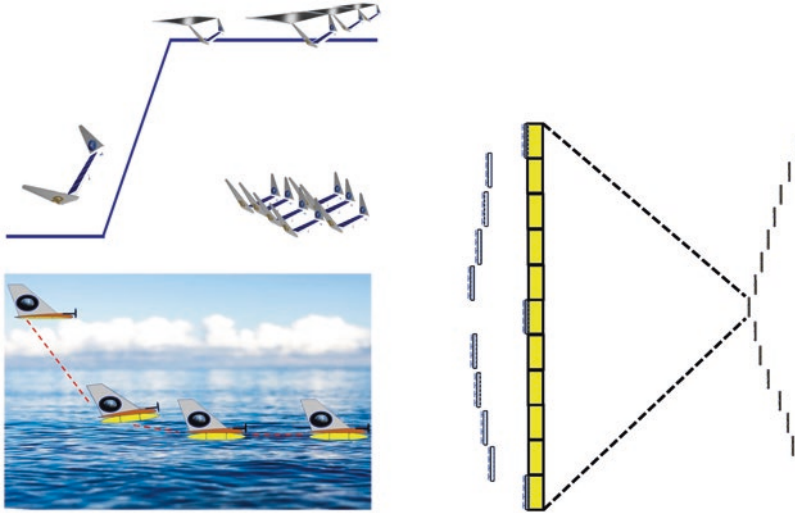


Fig. 16.2 FLT mission profile. (With permission)



Fig. 16.3 Prior HALE vehicles: The NASA Pathfinder, Helios 1, and Helios 3. From Ravikovich et al. (2021) and Wikipedia

easier control and for distributed antenna functions. Solar power rises with altitude, from about  $1.0$  to  $1.367 \text{ kW/m}^2$ . Temperature varies from  $85 \text{ }^\circ\text{C}$  when exposed to the sun, to below  $-57 \text{ }^\circ\text{C}$  at night in the stratosphere. Strongest winds are in the lower stratosphere during initial climb; while dynamic pressure is highest close to sea level. Motor cooling in solar-heated, near-vacuum, rendezvous and swarm operation for high-precision distributed antenna applications pose challenges.

## 16.2 Conceptual Design

Figure 16.3 shows three successful HALE concepts: The NASA Pathfinder, Helios-1, and Helios-2 used to benchmark the FLT and FL concepts. Relevant parameters are shown in Table 16.1. Our FLT and FL aspire to far lower wing loading (W/S) than prior concepts. This is because much of the lift is carried by the large area of ultrathin reflective sheets, supported by a carbon fiber truss and grid.

**Table 16.1** Benchmarking

	Pathfinder	Pathfinder +	Centurion	Helios HP01	Helios HP03	FLT 32 m	FL 32 × 11	FL64 × 11
Length	3.6	3.6	3.6	3.6	5	6	6	6
MAC	2.4	2.4	2.4	2.4	2.4	4	32	64
Span m	29.5	36.3	61.8	75.3	75.3	32	352	704
W/S N/m <sup>2</sup>	34.9	35.4	57.0	50.4	57.0	10.4	1.2	1.2
AR	12.3	15.1	25.8	31.4	31.4	8.0	11.0	11.0
MTOW, kg	252	315	862	929	1052	135	1379	5517
Payload, kg	45	67.5	270	329		50	150	300
Hmax. Fl, m	21,802	24,445		29,523	19,812	35,661	35,661	35,661
Motor: BLDC1.5 kW	1.50	1.50	1.50	1.50	1.50	1.5	1.5	1.5
# of motors	6	8	14	14	10	4	12	12
Nsum, KW	12	16	28	28	20	6	18	18
Max power SC, kW	8	13	31	35	18.5			
Add'l battery	NiCd		NiCd	LiPO	LiPO, airH2	LiPo	LiPo	LiPo

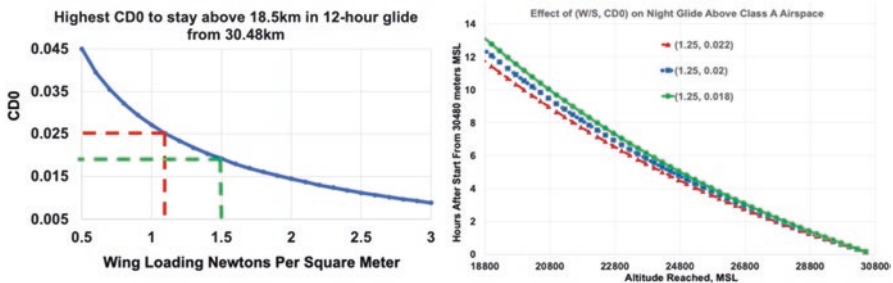


**Fig. 16.4** (Left) Highest value of profile drag coefficient at each wing loading, to stay up above 18.3 km in 12-h glide. (Right) Effect of profile drag coefficient on glide timeline, at W/S of 1.25 Pascals. From Komerath et al. (2021b), with permission

Figure 16.4 (left) shows necessary performance parameters to stay above Class A airspace. The zone between red and green vertical dashed lines is feasible, with CD0 below 0.025, and wing loading below 1.5 Pascals. Figure 16.4 (right) shows how descent profile varies with profile drag coefficients. The notion of joining wings at the tip to increase aspect ratio, decrease induced drag coefficient, and increase range, has been discussed in Quinlan (2019). Wu et al. (2021) have explored joining 2–6 single-propeller wing-tail UAVs at the wingtips. We note in passing that with sufficient control to perform rendezvous, it is also possible to form swarms of sufficient precision to act as synthetic aperture antennae.

Very large antennae can be formed with FLs, a topic for future discussion. In the FL, the main power source is solar panels (assumed 20% efficient) (Ackermann



et al. 2021; Kleemann et al. 2020) covering 40–85% of the FLT wings including around the leading edge to capture low-horizon sunlight, and some on the bottom surface to pick up diffused cloud reflections. A small battery (100 Wh) is provided to operate instruments and communications. A generator charges the batteries. Propeller windmilling can recover some power, keeping the battery charged, and enabling a burst flare maneuver for landing at night. The lift and drag coefficient data for a thin cambered flat plate were used to model the lifting sheet (Gilbert 2020). Maximum lift coefficient is 1.2. We restrict operations to CL of 1.0. Structural weight was modelled assuming the technology of the benchmark vehicles of Fig. 16.3 to estimate the total weight of the FLT's and known strength/weight profile of carbon fiber beams supporting the thin ( $0.05 \text{ kg/m}^2$ ) aluminized Mylar sheets. Figure 16.5 shows that FLT models smaller than 30 m span may not be able to stay above 18.3 km through the night.

Space limitations prevent detailing other aspects such as power system (Fazelpour et al. 2013; Isaienko et al. 2020; Dantsker et al. 2020), motors and propellers (Anon EPI 2020; Serrano et al. 2021), and the use of propellers instead of deflectable control surfaces for attitude control, winds, radiation, and other constraints. The risk-reduction process has gone from conceptual design to wind tunnel (gauging wing/sheet positioning and measuring aerodynamic coefficients), ground and low-altitude glide, and powered tests for strength, stability of Mylar sheets and flying wings, and robustness to gusts and sunlight/weather exposure. Flight simulation with present vehicle designs is being used to demonstrate performance and identify

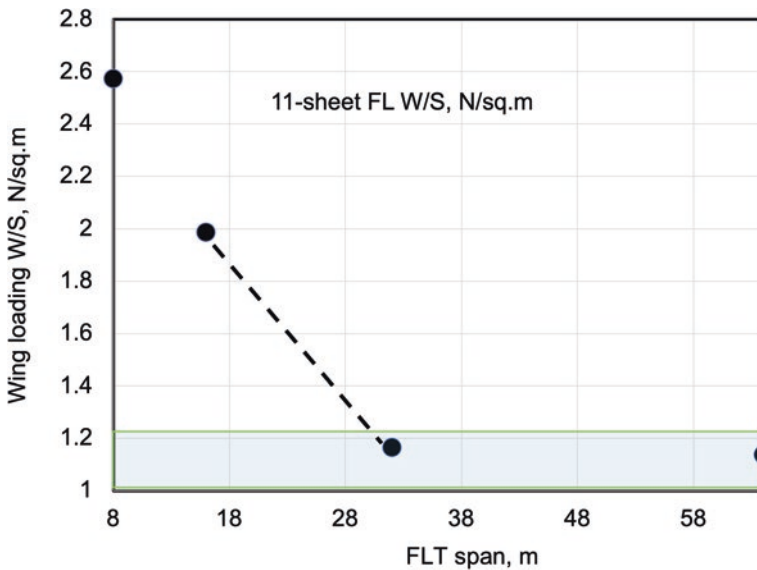


**Fig. 16.5** A diagram showing why sheet spans of over 30 m are needed to achieve 12-h glide above 18.3 km

problems. Thermal and aeroelastic verification (Voß et al. 2020) and control strategies remain to be done.

## 16.3 Conclusions

Electric-aircraft aspects of Flying Leaflet (FLT) and Flying Leaf (FL) vehicles that comprise the initial Glitter Belt system are summarized in this short paper. The 30.5 km altitude and slow glide requirements provide unique challenges. Conceptual design, small scale design-build-fly tests, and dynamic flight simulation are used to remove uncertainties and derive properties of this system. The FLT, a 32 m-span, 4 m-chord, 4-propeller flying wing, carries a variably-deployed Mylar sheet to 30.5 km, and joins with 10 other similar craft to form an FL with 12 BLDC motors driving low-inertia propellers. The rise of solar power with altitude is a unique feature. Motor cooling in near-vacuum, rendezvous and swarm operation for high-precision distributed antenna applications pose unique challenges. Rendezvous and swarm operation for high-precision distributed antenna applications pose unique challenges and opportunities.

**Acknowledgements** This work was partially supported by the Taksha Institute.

## References

- D. Ackermann, A. Bierig, N. Reininghaus, *Modeling Spectrum Dependent Characteristics of Triple Junction Solar Cells for Solar-Powered Aircraft*, in 2021 Annual Modeling and Simulation Conference (ANNSIM) (IEEE, 2021, July), pp. 1–12
- Anon EPI, Propeller Performance Factors. An Introduction to Propeller Technology. EPI Inc. Based on Aircraft Propeller Design, F. E. Weick, 1930 (2020, January 1), 452 p. Viewed 14/11/2021. [http://www.epi-eng.com/propeller\\_technology/selecting\\_a\\_propeller.htm](http://www.epi-eng.com/propeller_technology/selecting_a_propeller.htm)
- O. Dantsker, M. Caccamo, S. Imtiaz, *Propulsion System Design, Optimization, Simulation, and Testing for a Long-Endurance Solar-Powered Unmanned Aircraft*, in AIAA Propulsion and Energy 2020 Forum (2020), p. 3966
- F. Fazelpour, M. Vafaeipour, O. Rahbari, R. Shirmohammadi, Considerable parameters of using PV cells for solar-powered aircrafts. *Renew. Sust. Energ. Rev.* **22**(2013), 81–91 (2013)
- L. Gilbert, Sail section lift, in *Technical & Theoretical Aspects of RC yacht racing. Lester Gilbert's Radio Sailing*. November 2020. <http://www.onemetre.net/design/sailsect/sailsect.htm>
- V. Isaienko, V. Kharchenko, M. Matiychyk, I. Lukmanova, *Analysis of Layout and Justification of Design Parameters of a Demonstration Aircraft Based on Solar Cells*, in E3S Web of Conferences, vol. 164 (EDP Sciences, 2020), p. 13007
- N. Kleemann, S. Karpuk, A. Elham, *Conceptual Design and Optimization of a Solar-Electric Blended Wing Body Aircraft for General Aviation*, in AIAA Scitech 2020 Forum (2020), p. 0008
- N. Komerath, S. Hariharan, D. Shukla, S. Patel, V. Rajendran, E. Hale, *The Flying Carpet: Aerodynamic High-Altitude Solar Reflector Design Study (No. 2017-01-2026)*. SAE Technical Paper (2017)

- N. Komerath, A. Sharma, R. Deepak, A. Deepak, *Glitter Belt Global Measurement System: Indian Ocean Component Preparation*, in Proceedings of the IEEE ICECCME 2021, Mauritius (October 2021a)
- N. Komerath, R. Deekak, A. Deepak, *Flight Testing and Simulation of High Altitude Reflector Components*, in Proceedings of ISSA2021, Bangkok, Thailand (November 2021b)
- J.R. Quinlan, *System and Method for Modular Unmanned Aerial System*. US Patent 10,196,143 B2 (5 Feb 2019)
- Y. Ravikovich, L. Ponyaev, M. Kuprikov, R. Domjan, *Innovation Design Analysis of the Optimal Aerodynamic Adaptive Smart Structures for Disk-Body Solar Hybrid Electric Aircraft and Airship Concepts*, in IOP Conference Series: Materials Science and Engineering, vol. 1024, no. 1 (IOP Publishing, 2021), p. 012078
- J.R. Serrano, A.O. Tiseira, L.M. García-Cuevas, P. Varela, Computational study of the propeller position effects in wing-mounted, distributed electric propulsion with boundary layer ingestion in a 25 kg remotely piloted aircraft. *Drones* **5**(3), 56 (2021)
- V. Smil, *Energy Conversion Efficiency is Falling*. IEEE Spectrum February, 18–19. PDF (2021)
- A. Voß, V. Handojo, C. Weiser, S. Niemann, Preparation of Loads and Aeroelastic Analyses of a High Altitude, Long Endurance, Solar Electric Aircraft (2020)
- M. Wu, Z. Shi, T. Xiao, H. Ang, Effect of wingtip connection on the energy and flight endurance performance of solar aircraft. *Aerosp. Sci. Technol.* **108**, 106404 (2021)

# Chapter 17

## Examination of Different Systems Used for UAV Detection and Tracking



Alpaslan Durmuş  and Erol Duymaz 

### 17.1 Introduction

UAV systems are spreading rapidly nowadays. The main reasons for the rapid growth of the UAV industry are: it can transfer low-cost video and images and be used for logistics purposes in different areas. At the same time, UAV systems can be designed in different body structures. This situation increases the demand for UAV systems. It is stated that more than 10,000 UAVs will be operational for commercial use in 5 years (Chan et al. 2018). UAV systems offer more cost-effective solutions than other aircraft (Erdelj et al. 2017). The use of UAV systems is not limited to commercial or hobby use.

Together with technological developments and their integration into UAV systems, these systems are used in many different fields for the benefit of humanity. Some of these areas are:

- Reconnaissance and surveillance by security forces.
- Gathering information about the victims by search and rescue teams by search and rescue teams such as AFAD (Disaster and Emergency Department) in case of accident or natural disaster.
- Transportation of commercial materials for logistics purposes.
- Receiving video or images in the field of advertising or publishing.

They can be listed as the use of different camera technologies (multispectral) to be used in integration with UAV systems in the field of agriculture, to monitor product developments, or to carry out agricultural activities such as product spraying (Yaacoub et al. 2020).

---

A. Durmuş (✉) E. Duymaz  
Ostim Technical University, Ankara, Türkiye  
e-mail: [alpaslan.durmus@ostimteknik.edu.tr](mailto:alpaslan.durmus@ostimteknik.edu.tr)

Today, especially for hobby purposes, UAV systems with a takeoff weight of less than 500 g are seen more intensely around us. UAV systems with a takeoff weight of less than 500 g are excluded from classification according to SHGM (General Directorate of Civil Aviation) regulations. These UAV systems deployed under 500 g have the potential to pose a security threat (Öz and Sert 2019). These systems can easily be used for illegal purposes such as terrorist attacks, illegal surveillance and reconnaissance, smuggling, and electronic surveillance, and also pose a potential collision risk in aircraft flying legally (Sommer et al. 2017).

According to the United States (US) Federal Aviation Administration (FAA), more than 3 million UAV systems are registered in the United States. The number of UAVs is expected to reach 7 million by 2020. In addition, it is estimated that the technological and economic growth of e-commerce will bring about the more widespread use of UAV systems and the change of regulations. It is seen that the widespread use of unmanned aerial vehicles will increase security threats. In this context, there are UAV identification, tracking and blocking systems with different features to prevent security threats that may arise from UAV systems.

In this study, different techniques used for identification, classification, monitoring, and blocking of UAV systems were examined.

## **17.2 Investigation of UAV Detection and Monitoring Systems**

Different technologies and systems are used to detect UAV systems. In this context, there are four most used systems. These are: radar, acoustic detection, radio frequency system, and electro-optical detection systems. These systems are explained below according to their basic features.

### **17.2.1 Radar**

Radar systems are ineffective against small UAVs as they are developed to detect large air platforms moving at high speeds. Since UAV systems fly at similar speeds and altitudes to birds, they cannot detect the difference between two objects (Coluccia et al. 2020).

### **17.2.2 Acoustic Detection**

Acoustic sensors work by identifying the distinctive noise made by the UAV's engines. They work by utilizing a database of acoustic signatures of commonly used UAV engines. The most important advantage of acoustic sensing is its low cost even when used as a network of sensing devices placed around the protected area (Yang

et al. 2019). However, acoustic detection cannot detect gliders or fixed-wing UAVs. Advanced operators can change a UAV's sound signature by purchasing different propellers or making other modifications. The effective working range is 500 m. It is unlikely to provide reliable detection at greater distances and is ineffective in urban areas with a lot of ambient noise.

Advantages:

- It has a lower cost compared to RF-based systems.
- It can be produced in smaller sizes in terms of volume.
- It can operate with high performance in areas with high magnetic frequency pollution.
- Due to its low cost, it can be used in integration with other systems.
- It is very suitable for machine learning algorithms in obtaining information such as drone type, brand, flight characteristics.

Disadvantages:

- It can work effectively at a distance of about 500 m. Since the cost is low, it is possible to create a network structure with more than one and increase the distance.
- Its performance decreases in areas with sound and noise pollution.
- It cannot make environmental perception.

### ***17.2.3 Radio Frequency (RF) Emission Detection***

To control the UAV systems, communication is provided between the transmitter and the receiver on the UAV using the RF band. Using antennas or a network of synchronized ground stations, such RF transmissions can be detected and located. For the system to be economical and to offer fast detection, the system must have data recorded in the database about the propagation frequencies and bandwidths arranged for commercial UAVs (Guvenc et al. 2018).

The ILTER system developed in Turkey works on an RF basis. It captures and automatically blocks communication signals between ground control stations and controls of rotary or fixed-wing mini/micro-UAVs with its RF sensors. ILTER RF Drone Detection and Interception System, which is widely used in Turkey, has a fully automatic detection, jamming, and deception feature against drones/UAVs. The features of the ILTER system developed in this context are given below.

- Detects rotary-wing and fixed-wing low-altitude UAVs.
- Detects the wireless communication between the drone and its remote control.
- Detects frequency bands in the UHF, S and C range.

Advantages:

- It has a wider coverage area compared to acoustic systems in terms of operating range.

- It can detect 360 degrees peripherally.

Disadvantages:

- It has a higher cost compared to acoustic systems.
- Working performance decreases in areas with high magnetic pollution such as airports.
- It has a jamming feature, but today's drone systems can understand the jamming and put itself in autonomous mode and complete the flight route.
- It is difficult to obtain information such as drone type, brand, flight characteristics.

### 17.2.4 Electro-Optical (EO) Detection

Electro optical sensors in the form of optical and thermal cameras are very effective in detecting UAVs. However, optical cameras have problems in distinguishing small objects from UAVs. With the use of computer algorithms, a bird can be distinguished from a UAV.

## 17.3 Conclusion

Below is a comparison of different systems used for UAV detection. These systems have different advantages and disadvantages. Table 17.1 shows the advantages and disadvantages of these systems. The use of different techniques under appropriate conditions will give the most appropriate result.

**Table 17.1** Comparison of advantages/disadvantages of different drone detection and tracking techniques (Guvenc et al. 2018)

Detection technique	Advantages	Disadvantages
Ambient RF signals	Low-cost RF sensors (e.g., SDRs), works in NLOS, long detection range. May allow deauthentication attacks for taking control of drone by mimicking a remote controller or spoofing GPS signal	Need prior training to identify/classify different drones. Fails for fully/partially autonomous drone flights due to no/limited signal radiation from a drone/controller
Radar	Low-cost FMCW radars, does not get affected by fog/clouds/dust as opposed to vision-based techniques, can work in NLOS (more sophisticated). Higher (mmWave) frequencies allow capturing micro-Doppler/range accurately at the cost of higher path loss. Does not require active transmission from the drone	Small RCS of drone makes identification/classification difficult. Further research needed for accurate drone detection/classification and machine learning techniques, considering different radar/drone geometries and different drone types which all affect micro-Doppler signatures. Higher path loss at mmWave bands limits drone detection range

(continued)

**Table 17.1** (continued)

Detection technique	Advantages	Disadvantages
Acoustic signals	Low cost for simple microphones (cost depends on the quality of microphones). Can work in NLOS as long as the drone is audible	Need to develop database of acoustic signature for different drones. Knowledge of current wind conditions and background noise is needed. May operate poorly under high ambient noise such as in urban environments
Computer vision	Low cost for basic optical sensors. Pervasive availability of cameras even at most commercial drones that can be used as sensors	Higher cost for thermal, laser-based, and wide FOV cameras. Requires LOS. Level of visibility impacted by fog, clouds, and dust
Sensor fusion	Can combine advantages of multiple different techniques for wider application scenario, high detection accuracy, and long-distance operation	Higher cost and processing complexity. Need effective sensor fusion algorithms

## References

- K.W. Chan, U. Nirmal, W.G. Cheaw, *Progress on Drone Technology and Their Applications: A Comprehensive Review*, in AIP Conference Proceedings, vol. 2030, no. 1 (AIP Publishing, 2018), p. 020308
- A. Coluccia, G. Parisi, A. Fascista, Detection and classification of multirotor drones in radar sensor networks: A review. *Sensors* **20**(15), 4172 (2020)
- M. Erdelj, E. Natalizio, K.R. Chowdhury, I.F. Akyildiz, Help from the sky: Leveraging UAVs for disaster management. *IEEE Pervasive Comput.* **16**(1), 24–32 (2017)
- I. Guvenc, F. Koohifar, S. Singh, M.L. Sichitiu, D. Matolak, Detection, tracking, and interdiction for amateur drones. *IEEE Commun. Mag.* **56**(4), 75–81 (2018)
- T. Öz, S. Sert, The present role of anti-drone technologies in modern warfare and projected developments. *Güvenlik Stratejileri Dergisi* **15**(32), 691–711 (2019)
- L. Sommer, A. Schumann, T. Müller, T. Schuchert, J. Beyerer, *Flying Object Detection for Automatic UAV Recognition*, in 2017 14th IEEE International Conference on Advanced Video and Signal Based Surveillance (AVSS) (IEEE, 2017, August), pp. 1–6
- J.P. Yaacoub, H. Noura, O. Salman, A. Chehab, Security analysis of drones systems: Attacks, limitations, and recommendations. *IoT* **11**, 100218 (2020)
- B. Yang, E.T. Matson, A.H. Smith, J.E. Dietz, J.C. Gallagher, *UAV Detection System with Multiple Acoustic Nodes Using Machine Learning Models*, in 2019 Third IEEE International Conference on Robotic Computing (IRC) (IEEE, 2019, February), pp. 493–498



# Chapter 18

## Misunderstandings in Aviation Communication



Omar Alharasees, Abeer Jazzar, and Utku Kale

### Abbreviation

ATCOs    Air Traffic Controllers  
ICAO     International Civil Aviation Organisation  
IATA     International Air Transport Association

## 18.1 Introduction

The aviation business is rapidly growing; the International Air Transport Association (IATA) estimates that global traffic will double in the next two decades. In fact, it is predicted that by 2050, nearly 10 billion passengers will travel by air annually (ATAG 2021). The burden on radio communication will naturally increase as global air traffic grows, and operators' total load (work, task, information, communication, and mental) will be unbalanced by excess or underload. If nothing is done, this growth will raise the rate of operator errors and misunderstandings (Kale et al. 2021), resulting in an increase in the number of people killed in communication-related plane crashes around the world. To deal with this expansion, it is critical to provide the greatest degree of communication safety and security.

Misunderstandings and miscommunication between pilots and ATCOs are a common cause of aviation accidents and mishaps (Prinzo and Britton 1993). The rate of errors in radio communications is influenced by a variety of factors (Ragan 2002). According to the European Organisation for the Safety of Air Navigation (Aviation and Agency 2020), technical issues include blocked transmission, frequency congestion, radio equipment malfunction – air/ground, radio interference,

---

O. Alharasees (✉) · A. Jazzar · U. Kale  
Department of Aeronautics and Naval Architecture, Faculty of Transportation Engineering and Vehicle Engineering, Budapest University of Technology and Economics,  
Budapest, Hungary  
e-mail: [oalharasees@edu.bme.hu](mailto:oalharasees@edu.bme.hu); [abeer.jazzar@edu.bme.hu](mailto:abeer.jazzar@edu.bme.hu); [utku@kjk.bme.hu](mailto:utku@kjk.bme.hu)

and sleeping VHF receivers. In addition to human characteristics and skills, tacit knowledge, such as language level, speech rates, and ambiguous or non-standard phraseology (Papanikou et al. 2021), may play a vital role in aviation communication.

A considerable number of aviation operators, according to Alderson (2009) in a prior study, are not native English speakers, which is the language of international aviation communication. Another key element stated by Parasuraman et al. (2000) is the influence of the conflict between the high automation level and the operators during the flight, particularly when receiving or passing crucial information.

Operators must understand the functionality of flying the aircraft, adhere with standards, rules, and regulations, and manage continual situational awareness and decision-making processes to safely control an aircraft. However, one of the most difficult challenges for operators is maintaining a high level of situational awareness in the changing environment of flight (Kale and Tekbas 2017). There has been a lot of research on operator workload in recent years. Because of the rapid speed of technology change in aviation, operators now get far more, and sometimes contradictory, information from a variety of sources than they did in the early days of the industry.

The current authors define communication load burden as the level of comprehension between operators, which is strongly dependent on language, cultural norms, and social ties, among other factors. Because of the constant evolution of communication technologies, the technological backdrop of the operator's communication requirements should also be enveloped.

Based on a survey issued to operators in various places across the world, this study assesses the communication load of operators in highly automated systems. This research is based on 110 operator replies, 88 pilots (75%), and 17 ATCOs (15%) from multiple nations. In addition, there is a tiny group of five operators that have both an ATCO and a pilot license (4.8%).

## 18.2 Method

By performing a survey on the descriptive characteristics of the operators from various angles, the research focused on the essential factors in operators' communication load. The purpose of the questionnaire is to quantify the most important issues as seen through the eyes of the operators, based on their experience and knowledge.

The questionnaire was created based on aviation operators (pilots, ATCOs). There were 88 pilots (25 female), 22 of them were native English speakers and five ATCOs. There were 22 ATCOs in total, six of whom were female. The participants' average age was 30 years for females and 34 years for males. Figure 18.1 depicts the gender-based variation in participant age and count.

The experience levels of the participants are shown in Fig. 18.2 for pilots in hours flown and ATCOs in years.

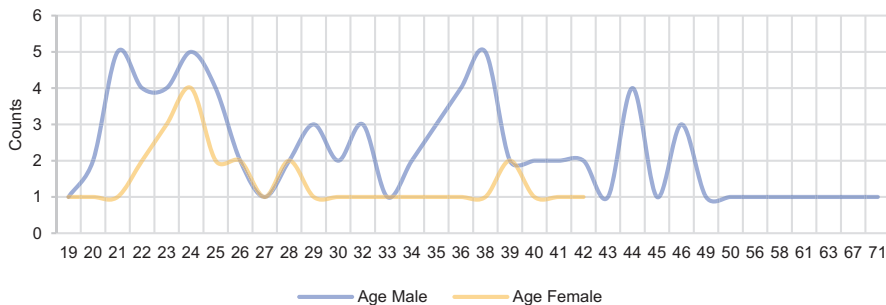


Fig. 18.1 Participants' age and gender variation

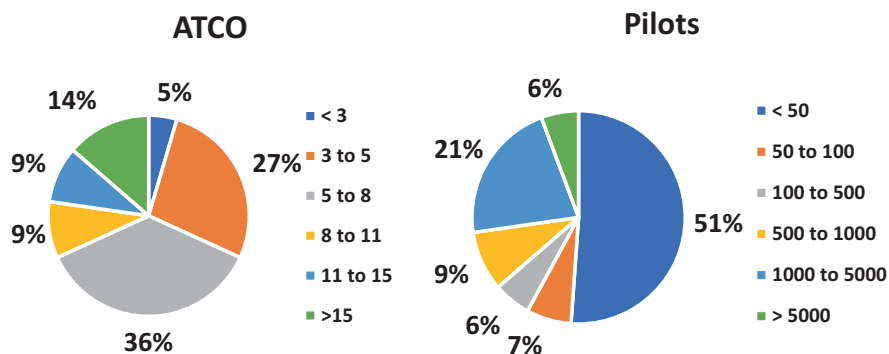


Fig. 18.2 Experience levels for pilot (right) & ATCOs (left)

### 18.3 Results and Discussion

There was a section at the beginning part of the questionnaire asking the operators to mention the problematic nation in communicating, which is related to both the operators' origin and cultural norms, shown in Fig. 18.3.

Because the majority of airline operators are non-native English speakers, studying their original tongue would have a significant impact on the language barrier (see Fig. 18.4).

The second section of the survey raised several concerns about aviation language competency hurdles between operators, such as cultural influences on language and native language effects. The findings revealed that non-native English speakers of operators have difficulty understanding native English speakers. Two more issues emerge from the findings: the cultural background plays a big impact on misunderstandings in communication, which can lead to accidents; and the responses demonstrated how effective communication affects the burden of the ICAO phraseology as a cornerstone in the communication between operators (see Fig. 18.5).

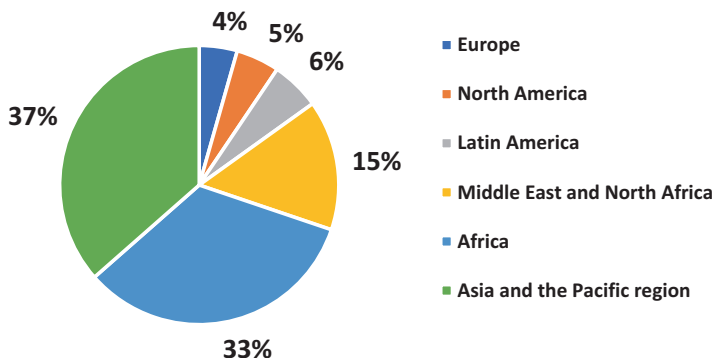


Fig. 18.3 The difficult nation in aviation communication from the participants' point of view

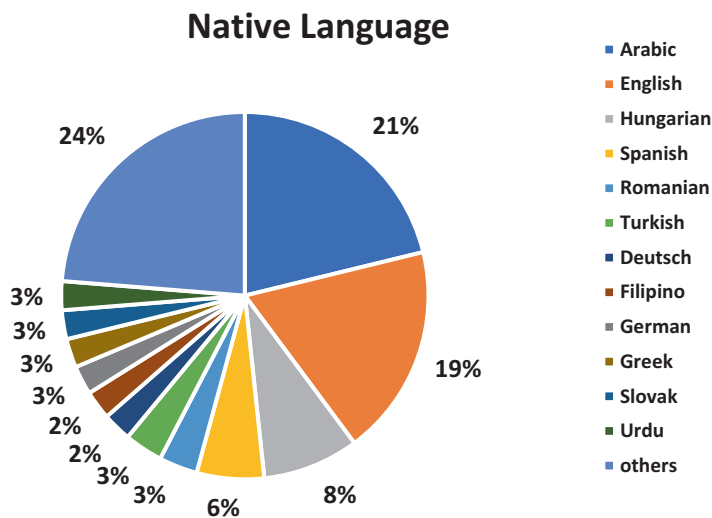


Fig. 18.4 Native language of the operators

The findings reveal that a full focus on radiotelephony communication should be established throughout operator training (pilots and ATCOs). Although the participants agreed that operators do not speak at the ICAO recommended rate, they also agreed that the ICAO standard phraseology should be more adaptable around the world, with more outreach to operators to familiarize them with their background and the applicability of ICAO phraseology.

Another important component is the operators' level of experience, and switching from active control to passive monitoring could help reduce communication demands.

The participants' opinion on whether they are satisfied with ICAO phraseology applicability is shown in Fig. 18.6.

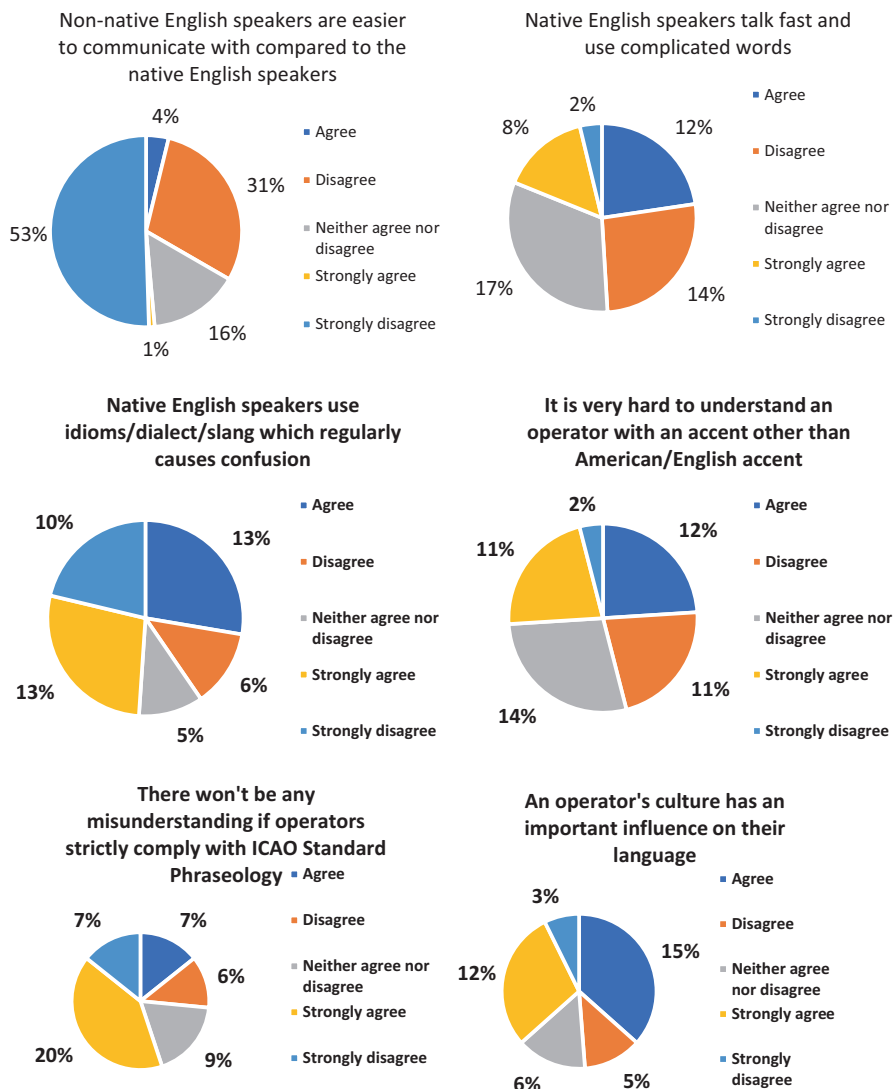
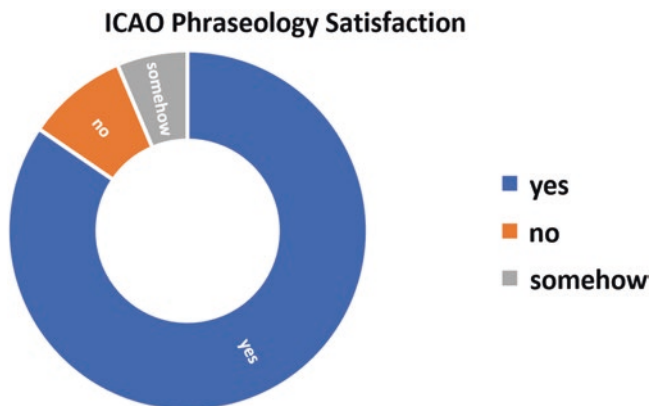


Fig. 18.5 Examples of language and culture-related questions and rate of response

An important factor in investigating the crucial issue in miscommunication between operators is to scale whether the language barrier or the operators' total load is the critical issue in miscommunication, participant opinions were more focused on the language barrier as the crucial factor.

Tables 18.1 and 18.2 below summarize the investigated descriptive characteristics of Likert-based questions in the questionnaire and the percentage of each statement, which provide a strong indication that language-based issues and how they



**Fig. 18.6** ICAO satisfaction rate

are critical between operator's communication in the current system are strongly related to cultural background and the lack of standard phraseology.

The participants were given the freedom to describe the most important factor affecting aviation communication in the final section of the questionnaire. The majority of the participants agreed with the factors mentioned in the questionnaire and mentioned some non-human based factors such as weather conditions. Although the participants mentioned language as a major issue affecting aviation communications, other important factors such as teamwork skills, operator's workload, and better operating ergonomics were also introduced in this section.

## 18.4 Conclusion

Based on a distributed questionnaire that gave an overview of the operators' opinions from experienced events and based on the current situation of aviation communication, the questionnaire focused on main aspects such as language-based issues which showed a crucial effect on aviation communication from the participant's point of view. The study highlighted the most critical aspects in aviation communication and reflected the real issues in communication between operators.

Another critical issue raised by the questionnaire is the ICAO standard phraseology and its adaptability and applicability around the world, and how it would be affected if the optimal rate or exact phraseology were not maintained, which would significantly increase the rate of misunderstanding – one of the leading causes of aviation accidents and incidents.

The current authors of the study are going to conduct comprehensive research on automation effects on operators' total loads including the communication load of pilots and ATCOs.

**Table 18.1** Descriptive characteristics of the first part of the survey responses

How much do you agree or disagree with the following statements regarding radio communication?	Agree	Disagree	Neither agree nor disagree	Strongly agree	Strongly disagree	Total
Non-native English speakers are easier to communicate with compared to the native English speakers	14%	36%	18%	4%	28%	100%
Native English speakers talk fast and use complicated words	42%	16%	20%	21%	1%	100%
Native English speakers use idioms/dialect/slang which regularly causes confusion	46%	7%	6%	34%	5%	100%
It is very hard to understand an operator with an accent other than American/English accent	41%	13%	16%	29%	1%	100%
There won't be any misunderstanding if operators strictly comply with ICAO standard phraseology	25%	7%	11%	53%	4%	100%
An operator's culture has an important influence on their language	52%	6%	7%	33%	2%	100%
Familiarity with the cultural background among the operators makes communication easier	29%	24%	22%	18%	7%	100%
Cultural misunderstandings in communication could lead to an accident	58%	5%	11%	23%	3%	100%
Good communication has a notable influence on teamwork effectiveness, workload, and safety	42%	3%	5%	49%	2%	100%

**Table 18.2** Descriptive characteristics of the second part of the survey responses

How much do you agree or disagree with the following statements regarding radio communication?	High	Low	Middle	Very high	Very low	Total
Poor language skills	24%	16%	30%	20%	10%	100%
Strong foreign accents	41%	5%	15%	37%	2%	100%
Failure to use ICAO standard phraseology	21%	23%	28%	25%	4%	100%
Too high or too low workload for controllers or pilots	25%	11%	29%	27%	8%	100%
Pilot performance issues (e.g., failure to notice and/or react to prolonged lack of R/T activity on the frequency selected, lack of situational awareness)	29%	16%	32%	16%	6%	100%

## References

- J. Alderson, Air safety, language assessment policy, and policy implementation: The case of aviation English. *cambridge.org*. **29**, 168–187 (2009). <https://doi.org/10.1017/S0267190509090138>
- ATAG. ‘Balancing growth in connectivity with a comprehensive global air transport response to the climate emergency.’ Waypoint 2050 ATAG, Second Edi(September), p. 108. Available at: [www.atarg.org](http://www.atarg.org) (2021)
- E. Aviation, S. Agency, Opinion No 10 / 2016 Performance-based navigation implementation in the European air traffic management network. **10**, 1–19 (2020)
- U. Kale, M. Herrera, A. Nagy, ‘Examining pragmatic failure and other language-related risks in global aviation’, aircraft engineering and aerospace technology. Emerald Group Holdings Ltd. **93**(8), 1313–1322 (2021). <https://doi.org/10.1108/AEAT-03-2021-0081>
- U. Kale, M.B. Tekbas, Operator’s subjective decisions-improving the operator’s (pilot and air traffic control) decision making. *Scient. Cooperat. Internat. J. Mechan. Aerosp. Eng.* **3**(1), 43–51 (2017)
- M. Papanikou et al., ‘Understanding aviation operators’ variability in advanced systems. *Aircr. Eng. Aerosp. Technol. ahead-of-print(ahead-of-print)* (2021). <https://doi.org/10.1108/aeat-03-2021-0065>
- R. Parasuraman, T.B. Sheridan, C.D. Wickens, A model for types and levels of human interaction with automation - systems, man and cybernetics, part a, *IEEE transactions on. IEEE Trans. Syst. Man Cybern. Syst. Hum.* **30**(3) (2000)
- O. Prinzo, T. Britton, ‘ATC/pilot voice communications: a survey of the literature’. Available at: <https://rosap.ntl.bts.gov/view/dot/21383> (Accessed on 24 October 2021) (1993)
- P.H. Ragan, *Deadly Misunderstandings: Language and Culture in the Cockpit* (Phoenix, AZ, In first annual aviation communications conference, 2002)



# Chapter 19

## Modeling of Exhaust Gases Jet from Aircraft Engine for Different Operational Conditions



Kateryna Synylo

### Abbreviation

CFD	Computational Fluid Dynamics
ICAO	International Civil Aviation Organization
LAQ	Local Air Quality
LTO-cycle	Landing-takeoff cycle
LES	Large Eddy Simulation Method
PolEmiCa	Pollution and Emission Calculation

### 19.1 Introduction

Ground-level emissions associated with airports have the biggest impact on local air quality while elevated aircraft emissions have less because they take place at increasing height. Figure 19.1 shows aircrafts produce approximately 54% of ground level emissions, while airport-related traffic is estimated to emit a further 28%. Of any airport-related emissions, these two sources have the most significant impact to local air quality. The other part of emissions is caused by operation of boiler plant and airside vehicles (approximately 9% each). These two sources have a lower impact on local air quality (Heathrow Air Quality Strategy, 2020).

Distribution of aircraft NO<sub>x</sub> emissions during ground operation demonstrated that the highest contribution (46%) is detected at takeoff roll stage. However, taxiing and use of auxiliary power unit (APUs) are almost as large when considered together (Fig. 19.2).

Since the most part of LTO-cycle, the aircraft (nearly 26 min) is maneuvering on the ground (engine run-ups, taxiing, accelerating on the runway), it is subjected to fluid flow that can create a strong vortex between the ground and engine

---

K. Synylo (✉)

National Aviation University, Kosmonavta Komarova, Kyiv, Ukraine

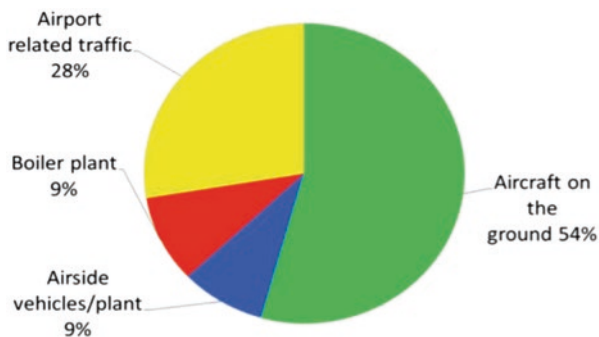


**Fig. 19.1** Estimated ground level airport-related emissions from Heathrow Airport

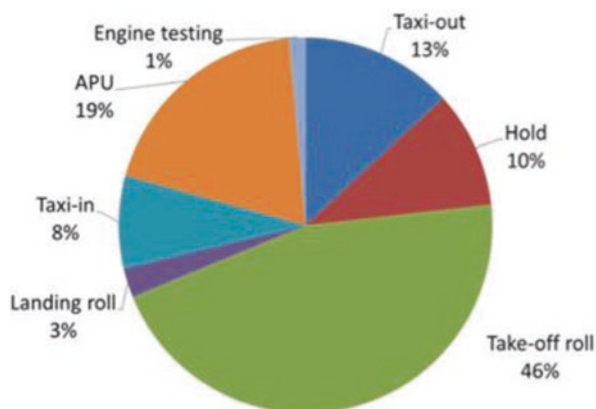


**Fig. 19.2** Estimated ground level aircraft emissions at Heathrow Airport

nozzle, which have essential influence on structure and basic mechanisms (Coanda and buoyancy effects) of exhaust gases jet from aircraft engine. The wing mounted engines are operated in the so-called “vortex region” due to proximity to the ground. Harvey & Perry conducted the tests in a wind tunnel to study the interaction of a vortex pair with a free surface (no-slip and moving floor). It was found that the primary vortices approach the ground leading to boundary layer formation (it is a subject to an adverse pressure gradient). The newly formed vorticity separates from the ground and consists a secondary vortex with opposite sign in regard to primary one. Then the second vortex wraps around the primary one and induces an upward velocity and causes primary vortices rebound from the ground. Ash et al. conducted numerical simulation of aircraft wake vortex transport near the ground by using a Reynolds turbulence model to examine crosswind and atmospheric turbulence impact on ground effects. It was reported that the ambient variables may have an essential influence on wake vortex behavior in terms of lifetime and hazard.

Over the years, many measurement campaigns of aircraft wake vortices were conducted by NASA, FAA in USA (Memphis and St. Louis Airports), and in Europe (Frankfurt and London-Heathrow Airports). Particularly, Fraport collected data of tens of thousands of wake vortex signatures and included temporal highly resolved data of three wind components, turbulence, and temperature (Ash et al. 1994; Harvery and Perry 1971). The results analysis of the experiment allowed to investigate the wake vortices transport near the ground. Thus, the ground vortices (decay rate) are insensitive to ambient turbulence. However, the crosswind causes a slight asymmetry in the decay rate and a pronounced asymmetric rebound behavior. Proctor et al. (1999) used Memphis case for the validation test of the LES model. The simulation results agreed with the measured field data. It was found that the wake vortex decay is sufficiently affected by the ambient turbulence, stratification, and wind shear.

The evaluation of emission dispersion due to the vortices circulation near the aerodrome surface is an actual task for airport air quality studies, including the ground influence on the parameters of the jet (buoyancy height, horizontal and vertical deviation) and consequently on the characteristics of air pollution provides the improvement of local air quality modeling. In the paper, an approach to the improvement of their influence assessment into local air quality in airports was underlined, first by including CFD modeling benefits. The current article is showing the results of CFD modeling and analysis for the jets close to ground surface (the solid boundaries for jet flows), simulating the aircraft engine jets' performances in airport vicinity. As it was shown, they are simulated like the wall jets and their performances may provide larger jet penetration, less jet rise, and higher vertical and horizontal jet dispersion parameters (plume deviations). The numerical simulation of wall jet by Fluent 6.3 was implemented for different combination of initial jet velocity and height of engine installation to evaluate the influence of the ground on jet's parameters (height and longitudinal coordinate of buoyancy effect, length of jet penetration). Obtained results of numerical simulations provide improvement of model PolEmiCa.

## 19.2 Numerical Simulation of Exhaust Gases Jet from Aircraft Engine by Fluent 6.3

The intensity and scale of ground vortices depend on engine power, wind velocity and wind direction, diameter, and height of engine installation. These factors have a significant impact on the mechanisms of ground vortices formation and can be represented in terms of two non-dimensional characteristics (Rehby 2007):

- The non-dimensional velocity,  $U_0/U_w$ , determined as the ratio initial velocity of the jet at engine nozzle ( $U_0$ ) to the ambient flow velocity ( $U_w$ ).
- The non-dimensional height,  $h_{EN}/D_0$ , determined as the ratio height of engine installation ( $h_{EN}$ ) to the diameter of engine nozzle ( $D_0$ ).

The work presented here was aimed to evaluate the velocity ratio and height of engine installation influence on the basic parameters of the exhaust gases jet (height and longitudinal coordinate of buoyancy effect, length of jet penetration).

With aim to evaluate the influence of non-dimensional parameters on the ground vortex formation and the jet structure the numerical simulation of wall jet by Fluent 6.3 have been implemented for different combination of initial velocity and height of engine installation.

For considered task a three-dimensional model of a jet was generated in Fluent 6.3 and Large Eddy Simulation (LES) method was used to reveal the unsteady ground vortices and their impact on jet fluid flow structure (Synylo et. al. 2017). The following boundary conditions were specified to the boundaries of the computational domain of jet flow field:

- the nozzle section of aircraft engine exhaust at which jet hot gases enter to computational domain was set as a “velocity inlet”;
- the computational surfaces adjacent to the engine section at which ambient conditions (wind velocity, wind direction and temperature) enter to computational domain was also set as “velocity inlet”;
- the external lateral surfaces of computational domain at which ambient conditions (wind velocity, wind direction and temperature) were set as “velocity inlet” also: wind direction and velocity were defined by velocity specification method, X-component of flow direction = 1;
- the ground surface, which is corresponding to the bottom of the computational domain, is set as “wall” implying a non-slip condition for velocity and with temperature 300 K. To evaluate the phenomenon of ground vortices formation between the aircraft engine exhaust and restricting surface the boundary conditions on ground surface cannot be considered anymore as a “wall”;
- the computational surface opposite to the aircraft engine exhaust nozzle, at which flow field (mixture jet and ambient air) leaves computational volume, was set as “pressure-outlet.”

All the calculations were made with a second order discretization.

Other details of the calculation schemes used for LES/Fluent 6.3 investigation are completely described.

### 19.3 Results and Discussion

Modeling results to comparison of wall jet for different initial velocity of the jet.

Modeling of exhaust gases jet from aircraft engine for different operational conditions was implemented based on the complex model PolEmiCa (free jet) and three-dimensional model (wall jet) using Fluent (version 6.3) with LES method.

For initial velocity 50 m/s the observed pattern of the jet behavior is explained by the weak impact of the ground vortices (the Coanda effect in this case is quite weak). As mentioned before, the scale and intensity of ground vortices depend on the dimensionless height and the velocity of the jet at exhaust nozzle. The combination of these dimensionless parameters, particularly low initial velocity jet, leads to the dominance of the buoyancy effect in the behavior of the jet. The comparison of the calculated parameters of the jet (height and longitudinal coordinate of jet axis arise due to buoyancy effect, length of the jet penetration) by Fluent 6.3 and semi-empirical model for aircraft engine jets implemented in complex model PolEmiCa proves the found trend of the jet behavior.

For initial velocity 50 m/s calculated by Fluent 6.3 length of jet penetration exceeds at 5% the average value from the semi-empirical model for aircraft engine jets implemented in complex model PolEmiCa of previous version (Fig. 19.3). And calculated by Fluent 6.3 longitudinal coordinate of buoyancy effect is longer at 30% (Fig. 19.4), while the height of jet rise is lower at 24% (Fig. 19.5) in comparison with the semi-empirical model for aircraft engine jets (complex model PolEmiCa) results. Obtained difference between basic jet parameters is explained by ignoring the impact of bounding processes on the surface topology and properties of the jet by the semi-empirical model implemented in complex model PolEmiCa.

For initial velocity 100 m/s the observed pattern of the jet behavior is explained by the Coanda effect and the buoyancy effect. The combination of these dimensionless parameters leads to the pushing down and clinging of the jet to the

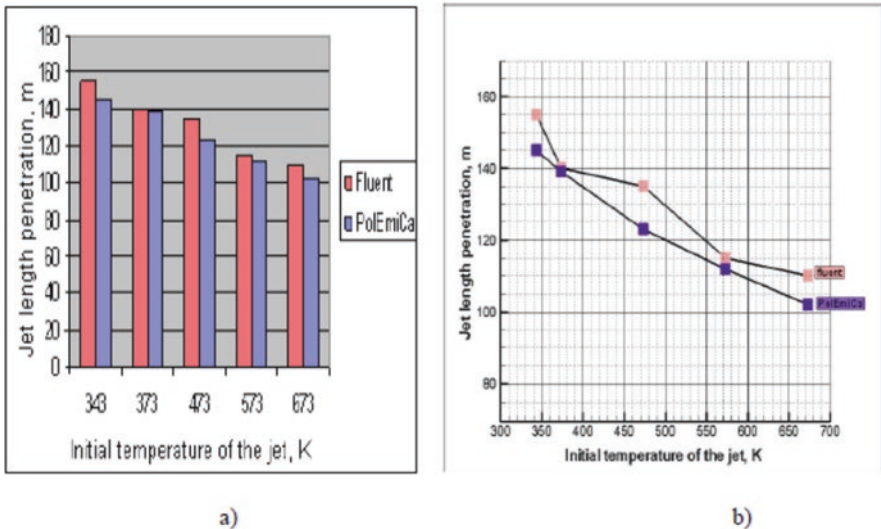


Fig. 19.3 Comparison of jet penetration length calculated by Fluent 6.3 and complex model PolEmiCa

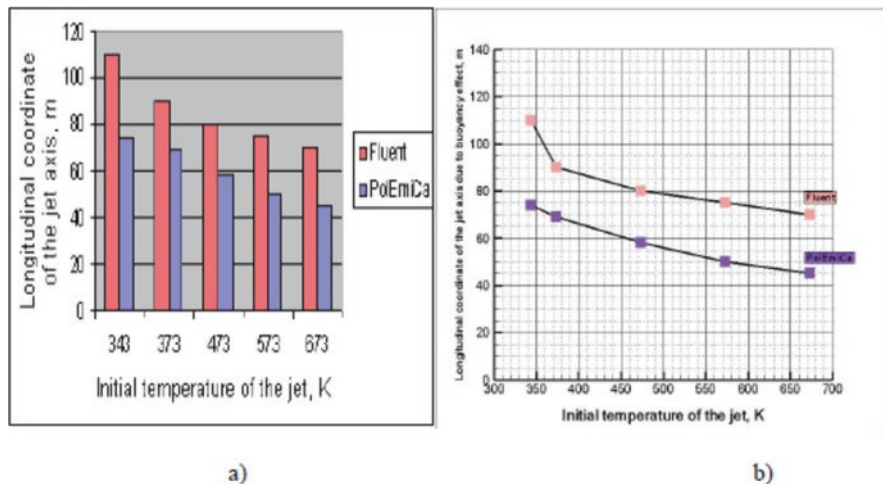


Fig. 19.4 Comparison of jet arise axis longitudinal coordinate calculated by Fluent 6.3 and complex model PoEEmiCa

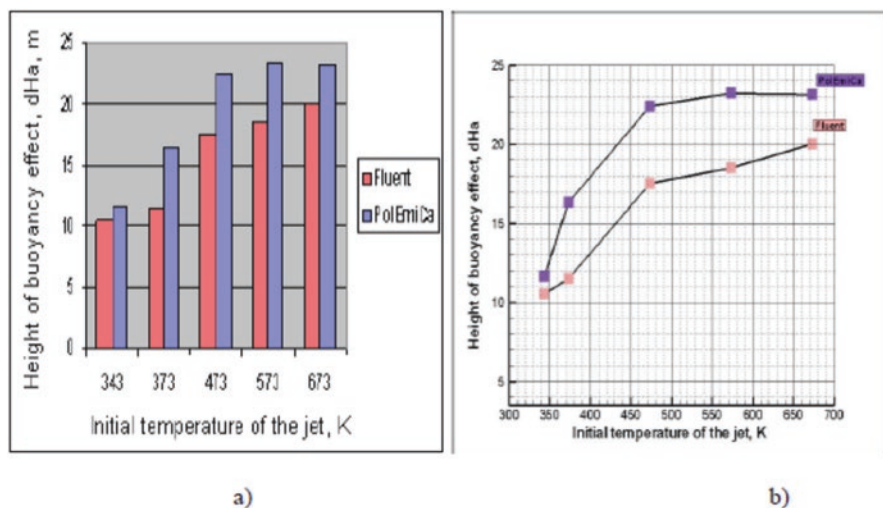


Fig. 19.5 Comparison of jet buoyancy effect height calculated by Fluent 6.3 and complex model PoEEmiCa

ground due to the Coanda effect. As the velocity further away from the jet exhaust decays, the clinging effect decreases and buoyancy takes over and rise the jet from the ground.

For initial velocity 100 m/s ground surface sufficiently impacts on jet's structure and behavior. Numerical simulations of wall jet by Fluent 6.3 defined a decrease of buoyancy effect height rise, which is 3–5 times less, and an increase of longitudinal coordinate of jet penetration at 30% (Figs. 19.6 and 19.7).

The comparison of obtained results of numerical simulations with Fluent 6.3 and semi-empirical model of jet (PolEmiCa) allow to assess an influence of initial

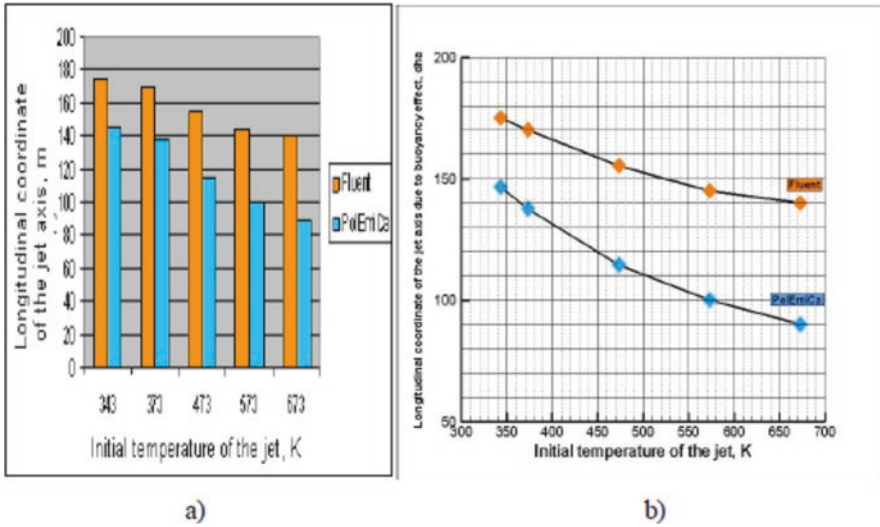


Fig. 19.6 Comparison of jet arise axis longitudinal coordinate calculated by Fluent 6.3 and complex model PolEmiCa

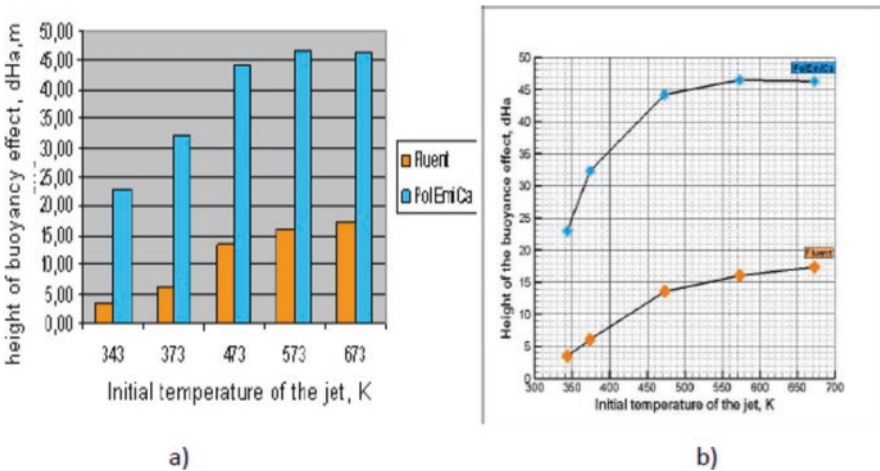
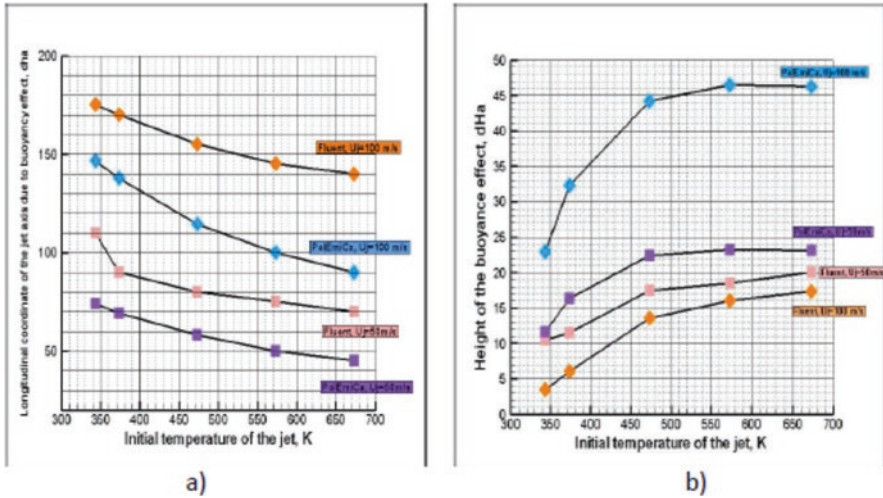


Fig. 19.7 Comparison of jet buoyancy effect height of calculated by Fluent 6.3 and complex model PolEmiCa





**Fig. 19.8** Comparison of the calculated parameters of the jet (a) height; and (b) longitudinal coordinate of buoyancy effect

conditions on jet structure and properties (Fig. 19.8). So, with increasing jet velocity, the influence of the surface on the structure and behavior of the jet increases due to ground vortices effects.

Comparison of the calculated parameters of the jet (height and longitudinal coordinate of jet axis arise due to buoyancy effect, length of the jet penetration) by Fluent 6.3 and semi-empirical model for aircraft engine jets implemented in complex model PolEmiCa proves the found trend of the jet behavior. Thus, the ground impact on the jet structure and behavior by Fluent 6.3 provides longitudinal coordinate increase and height reduction of buoyancy effect.

## References

- R. Ash, Z. Zheng, G. Greene, Cross wind effects on turbulent aircraft wake vortices near the ground, in *25th AIAA Fluid Dyn. Conf., AIAA*, (Colorado Springs, CO, 1994), p. 2381
- J. Harvey, F. Perry, Flow field produced by trailing vortices in the vicinity of the ground. *AIAA J.* **9**(8), 1659–1660 (1971)
- “Heathrow Air Quality Strategy, 2011–2020”, [https://www.heathrow.com/file\\_source/Company/Static/PDF/Communityandenvironment/air-quality-strategy\\_LHR.pdf](https://www.heathrow.com/file_source/Company/Static/PDF/Communityandenvironment/air-quality-strategy_LHR.pdf)
- F. Proctor, J. Han, Numerical study of wake vortex interaction with the ground using the terminal area simulation system, in *37th AIAA Aerosp. Sci. Meet. & Exhib.*, (AIAA, Reno, NV, 1999), pp. 99–0754



- L. Rehby, *Jet Engine Ground Vortex Studies* (Cranfield University, School of Engineering, Department of Aerospace Sciences, 2007), p. 125
- K. Synylo, O. Zaporozhets, J. Fröhlich, J. Stiller, Improvement of airport local air quality. Model. J. Aircraft **54**(5), 1750–1759 (2017)

# Chapter 20

## Automation Level Impact on the Operators' (Pilot, Air Traffic Controller) Role and Total Loads



Abeer Jazzar, Omar Alharasees, and Utku Kale

### Abbreviations

A/D/S-MAN	Arrival Manager, Departure Manager and Surface Manager
ATCOs	Air Traffic Controllers
ICAO	International Civil Aviation Organization
MCAS	Maneuvering Characteristics Augmentation System

### 20.1 Introduction

The air transport industry is on a steep uprise with the air passengers constantly growing demands. Airports and runways are busier than ever, ATCOs are under a lot of stress and pressure to manage the arriving and departing flights while maintaining safety, efficiency, and minimum delay. Numerous international airports are congested, resulting in flight delays and significant environmental consequences. As a result, ATCOs need tools to aid and guide them to deliver adequate flow management (Jung et al. 2019). Similarly, automation supports the pilots to aviate, navigate, and communicate as efficient and as safe as possible.

Automation typically refers to tools, machines, or systems under infrequent human arbitrations that can reach predetermined objectives, such as uncovering potential conflicts between aircraft through data processing, analysis, and modifying under pre-set functions (Wang et al. 2021). For ATCOs, Arrival Manager, Departure Manager, and Surface Manager (A/D/S-MAN) are sequencing tools supporting unconventional trajectory projections to optimize runway. A/D/S-MAN tools deliver automated arrangements and sequencing support for the ATCOs

---

A. Jazzar (✉) · O. Alharasees · U. Kale

Department of Aeronautics and Naval Architecture, Faculty of Transportation Engineering and Vehicle Engineering, Budapest University of Technology and Economics, Budapest, Hungary

e-mail: [abeer.jazzar@edu.bme.hu](mailto:abeer.jazzar@edu.bme.hu); [oalharseees@edu.bme.hu](mailto:oalharseees@edu.bme.hu); [kaleutku@edu.bme.hu](mailto:kaleutku@edu.bme.hu)

handling arriving/departing traffic at an airport, constantly computing arrival/departure sequences and arrangements and times for flights. It enables ATCOs to enhance their situational awareness and foresee the traffic flow. A/D/S-MAN as an intuitive decision support tool helps the ATCOs decrease their workload and mental stress (Phojanamongkolkij et al. 2014).

Likewise, automated systems liberate pilots' awareness from monotonous control tasks and allow them more time to examine, think forward, and concentrate on the big picture of the flight. Time once consumed gazing at a few tools can now be reserved to preparing for possible weather hazards, monitoring the soundness of the aeroplane's numerous systems, or pondering options should anything go wrong. Automation can lower pilots' workload and free up time, at least in some flight phases (Casner and Schooler 2014). In addition to that, Dehais et al. (2015) stated that automation allowed aviation to be safer. However, as soon as it was integrated into civil commercial aviation flights a series of accidents happened. In 1972, while the pilots were haggling with a landing gear situation the autopilot function disconnected causing an L-1011 crash into the Florida Everglades. In 2009, because of an accidental icing of the pitot tubes led to irregular speed measures and false representations in the cockpit, Air France flight AF447 crashed in international waters of the Atlantic Ocean. Mohrmann and Stoop (n.d.) discussed two fatal accidents (a Lion Air Boeing 737MAX and an Ethiopian Airlines 737MAX), which killed all passengers and crew on both flights, 346 people in total, during the end of 2018 and the beginning of 2019. Due to parallel malfunctions of the flight stabilizing program, the Maneuvering Characteristics Augmentation System (MCAS) was developed by Boeing. The MCAS system was a new advanced system modification presented into the 737MAX unaccompanied by clear training to the pilot. Dehais et al. (2015) argued that the moral of these past accidents is that the pilot, automated systems, and autopilot relationship is inclined to conflict, and there should be a predictive pilot-automation conflict tool.

The impacts of automation in aviation are twofold. Kale et al. (2020) researched the effect of automation on the operators' role and total loads to develop a monitoring and management system for the operators' load. The following loads were investigated and defined: (i) workload is the work done by an operator at a specific time as it depends on both human factors and external factors; (ii) task load is the degree of difficulty and hardness when executing a task; (iii) information load is the increasing amount of information gained from complex systems that sometimes creates confusion among operators; (iv) communication load is the level of understanding between operators; and (v) mental load is the physical and psychophysiological situation of the operators during the execution of the tasks. As the role of the operator is changing from active to passive monitoring, it is important to understand the effect and impact automation is going to reveal in the human factors. It is known that human is not good at long-duration monitoring and might lose situational awareness and with time their skills would potentially lose their efficiency. This study investigates the effects of automation, the mentioned loads, and the role of the operators.

## **20.2 Method**

This study emphasized the effect of automation on the operators' skills, operation contribution, and operators' total loads (work, task, information, communication, mental) by carrying a questionnaire. The questionnaire examines the effects of automation level and highly automated systems from the operators' perspective based on their experience and knowledge.

### **20.2.1 Participants**

This questionnaire is for operators (pilots, ATCOs). The average age for the responses was 35 years for females and 40 years for males. The collected responses included 35 pilots (five females), 16 ATCOs (six females), six ATCOs and pilots and five other professions with pilot licences. The level of experience between the responses varies. For pilots, 24 have less than 501 flight hours, ten have flight hours between 501–5000, and 12 have 5001–10,000+ flight hours. For ATCOs, four have less than five years of experience, three have between five to 11 years, and 15 have between 11–15+ years.

### **20.2.2 Design**

The questionnaire has four main parts. In part one, the participants fill their general information such as gender, age, nationality, experience level, and certification/licence types. In part two, the participants convey their degree of agreement/disagreement on statements regarding the increased use of automation. They also indicate their opinions on the effect of automation on their job security and level of contribution to operations. In part three, the operators' total loads (work, task, information, communication, mental) are explained and defined by the authors for the participant to reveal their views on the effect of automation on their total loads. Finally, the fourth part was an open-ended question. The participants report their views on reducing human factors in operations, the quality of aviation training, and the future of aviation operators, and if the industry will remain attractive for the new generations to join even if the roles of the operators change from active operating to passive monitoring.

### 20.3 Results and Discussion

The study results are represented by the following charts. The results summarize 62 responses from 27 different countries.

In Fig. 20.1, the majority disagree that automation decreases their ability to concentrate for extended periods, their problem-solving skills and decreases situational awareness and good coordination. On the other hand, the majority agrees that automation increased their decision-making skills and increased their ability to work quickly, accurately, calmly, and decisively under pressure (Fig. 20.2).

The results show that 56% of responses believe that regardless of the current technological advancements, trends and highly automated/autonomous systems, AI and advanced technologies cannot be fully trusted and will not replace humans in the system. Conversely, 43.5% of responses think that automation will eventually negatively affect their job and even eliminate their role (Fig. 20.3).

Around 53% stated that their contribution to operation is medium to very low. This indicates that most operators in this questionnaire do not consider their role to be highly influencing the operations (Fig. 20.4).

Automation and AI are introduced to aviation operations to reduce the workload and help the operators in their tasks, the results confirm that automation indeed decreased the workload. Nevertheless, highly automated systems increase the operators' information load, which is concerning as it can confuse the operator and lead to causing an accident (Fig. 20.5).

Most operators feel that the knowledge they learned while training is more than the task needs as tasks are now automated and require minimum intervention or none from the operator. However, the majority also declared that they would not prefer having manual control on the system and would prefer to rely on automation. Controversially, 44% of the responses disagree (27) to strongly disagree (16%) when asked if they can rely on automated systems to operate as planned. In contrast to 40% of responses agree/strongly agree on automation to work as designed. The rest of the participants neither agree nor disagree.

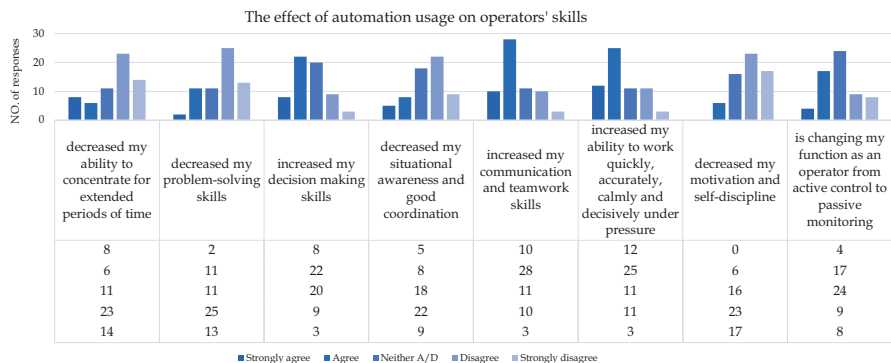


Fig. 20.1 Bar chart representing the results of statements regarding the increased use of automation

Automation effect on job security

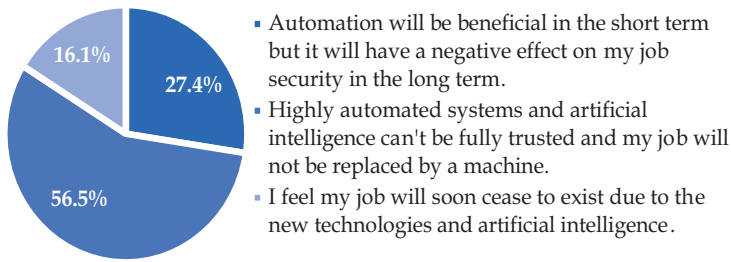


Fig. 20.2 Pie chart representing the results of job security concerns

Operators' views on their contribution to operations

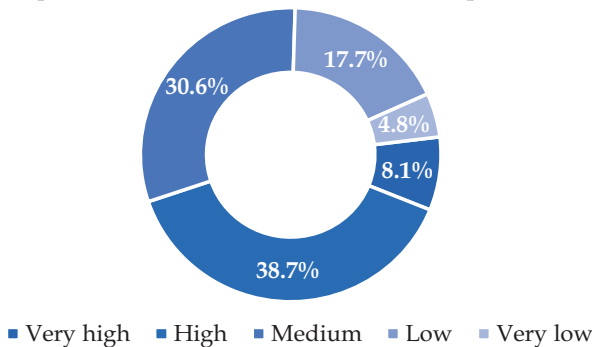


Fig. 20.3 Pie chart representing the results of operators' level of contribution to aviation operations

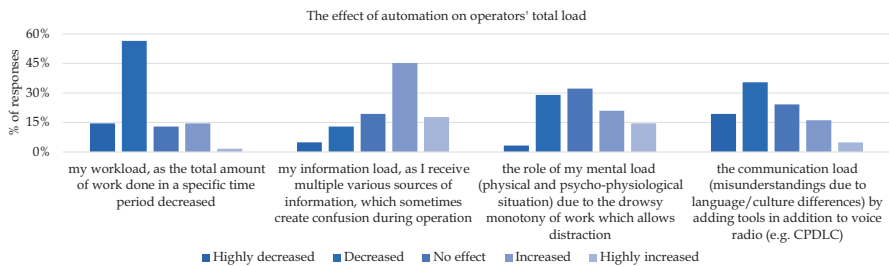
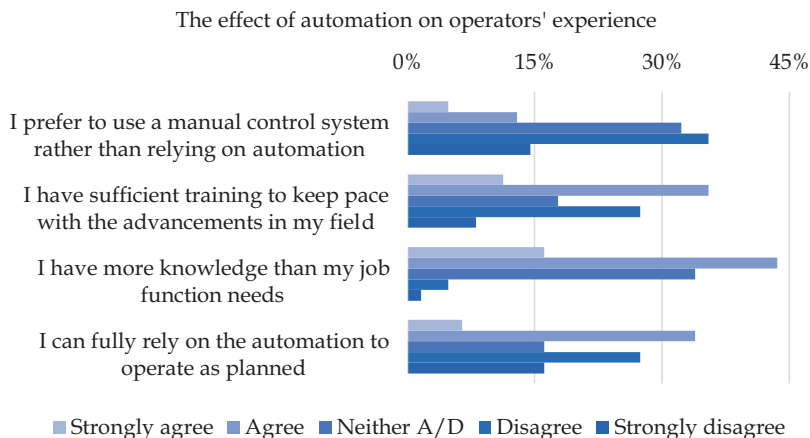


Fig. 20.4 Bar chart representing the results of the effect of the level of automation on operators' total loads

Finally, for the open-end questions, the participants are asked to mention important factors from their point of view on how to reduce the rate of mistakes from human factors in operation. The following points stood out:



**Fig. 20.5** Bar chart demonstrating the results of the effect of the level of automation on operators’ work experience

Training: many mentioned trainings and emphasized that it should be updated, more focused on automated technologies, and practical. Some said that awareness seminars would also help.

Standard operations producers (SOPs): to avoid miscommunications or loss of situational awareness, operators should always follow the SOPs no matter how simple or monotonous it is.

Human duality in operation (“two minds are better than one”): a second pilot to confirm the information and help the captain would reduce human error, in addition to reducing workload. Also, a shorter work shift reduces fatigue.

Less information: in case of an emergency only the necessary information should be shown and not overwhelm the operator and cause confusion.

Continuously checking with the reality and making sure what is outside is correctly represented by the advanced technologies.

Operators’ (“Physical and Mental and Psychological”) checks to see if the operator is suitable for the working environment.

When asked if they are satisfied with the quality of aviation training and if it prepares them for the advanced technologies in the field, almost half said no, it could be improved, and could be more adaptable.

Lastly, the participants were asked to reflect their views on whether the future aviation industry will remain attractive to the new generations. The main idea of the responses was that the new generation is accustomed and unfazed by advanced technologies and would not get the different feeling of doing the tasks differently from the old generations. This means that the aviation industry will remain attractive even if the operator role changes to passive monitoring only.

## 20.4 Conclusion

Aviation operators rapidly make decisions during operations to guarantee safe and efficient operations. The industry requires demanding skills and highly qualified individuals because their behavior has a direct impact on operations. Automation systems, tools, and technologies enhance the operations capabilities and safety by providing support to the operator and reducing the loads. Considerable attention is employed to develop and introduce advanced automation in the past recent years. However, less is known about the impact of automation on the operators' role, skills, and total load. This study investigates the effects of automation on the operators' skills, operation contribution, and operators' total loads (work, task, information, communication, mental). The results show that automation affected operators' task load by decreasing it. On the contrary, the operators believe that automation has increased the information load. Communication between operators has improved with the help of automation. The study subjects the following based on the received feedbacks on automation and operator interaction: (i) improving aviation training by constantly revising it to keep up with the advanced technologies; (ii) balancing the total loads and using human duality in operation; and (iii) adapting the new advanced technologies and always following the standard operating procedure in aviation worldwide to achieve efficient and safe operations. Further research is going on to investigate the instant and short-term effects of using highly automated systems on the operators' total loads, in addition to the long-term effects.

## References

- S.M. Casner, J.W. Schooler, Thoughts in flight: Automation use and pilots' task-related and task-unrelated thought. *Hum. Factors* **56**(3), 433–442 (2014). <https://doi.org/10.1177/0018720813501550>
- F. Dehais, V. Peysakhovich, S. Scannella, J. Fongue, T. Gateau, Automation surprise in aviation: Real-time solutions. Conference on human factors in computing systems - proceedings, 2015-April, 2525–2534 (2015). <https://doi.org/10.1145/2702123.2702521>
- Y. C. Jung, W. J. Coupe, A. Capps, S. Engelland, S. Sharma, Field Evaluation of the Baseline Integrated Arrival, Departure, and Surface Capabilities at Charlotte Douglas International Airport. Retrieved December 10, 2021, from <https://ntrs.nasa.gov/search.jsp?R=20190026511> (2019)
- U. Kale, J. Rohács, D. Rohács, Operators load monitoring and management. *Sensors (Switzerland)* **20**(17), 1–32 (2020). <https://doi.org/10.3390/s20174665>
- F. Mohrmann, J. Stoop, Airmanship 2.0. Innovating aviation human factors forensics to necessarily proactive role (n.d.)
- N. Phojanamongkolkij, N. Okuniek, G.W. Lohr, M. Schaper, L. Christoffels, K.A. Latorella, *Functional analysis for an integrated capability of arrival/departure/surface management with tactical runway management CORE view metadata, citation and similar papers at core.ac* (provided by NASA technical reports server, 2014) Retrieved December 10, 2021, from <https://ntrs.nasa.gov/search.jsp?R=20150000599>
- Y. Wang, R. Hu, S. Lin, M. Schultz, D. Delahaye, The impact of automation on air traffic Controller's Behaviors. *Aerospace* **8**(9), 260 (2021). <https://doi.org/10.3390/AEROSPACE8090260>



# Chapter 21

## Aircraft Noise Measurements in Ukrainian Airports



Oleksander Zaporozhets, Vadym Gulevets, Sergii Karpenko,  
Kateryna Kazhan, Olena Konovalova, and Vjacheslav Paraschanov

### Nomenclature

AN      Aircraft noise  
ICAO    International Civil Aviation Organization  
SAAU    State Aviation Administration of Ukraine

### 21.1 Introduction

Instrumental measurements of aircraft noise are performed in accordance with the requirements of the guidelines (SAAU Order 585 2020) to the rules (SAAU AR-381 2019), which is intended for use in determining the characteristics of aircraft noise in existing housing and residential areas planned for new construction, and/or individual structures inside the aerodrome of the airport to further establish compliance with the requirements of sanitary and construction norms and other state standards. Among them, the rules for sanitary control of noise regime (DSN 3.3.6.037 1999) and boundaries of building restriction zones (SSR-173 1996), protection of buildings from noise and even the prohibition of new construction inside existing residential territory (DSTU-N B V.1.1-31 2013), for decision-making on reconstruction

---

O. Zaporozhets (✉)

Lukasiewicz Research Network – Institute of Aviation, Warsaw, Poland  
e-mail: [Oleksandr.Zaporozhets@ilot.lukasiewicz.gov.pl](mailto:Oleksandr.Zaporozhets@ilot.lukasiewicz.gov.pl)

V. Gulevets · K. Kazhan

Department of Civil and Industrial Safety, National Aviation University, Kyiv, Ukraine

S. Karpenko · V. Paraschanov

Research Department, National Aviation University, Kyiv, Ukraine

O. Konovalova

Department of organization of aviation works and services, National Aviation University, Kyiv, Ukraine

of the airport (aerodrome), allocation of land plots for new residential or administrative construction.

The SAAU rules (SAAU AR-381 2019) does not contradict with state sanitary rules (SSR-173 1996), they only complement them with the requirements of ICAO policy (ICAO Resolution A40-17 2019) and European directive (Directive 2002/49/EC). For example, CAA rules require assessing the European noise index *LDEN*, such as in Directive 2002/49/EC, which is not required by state sanitary rules (SSR-173 1996), and to show that aircraft noise contours for *LDEN* are the same with the equivalent sound level *LAeq* at day and night time as defined by sanitary rules requirements. Also, SAAU rules require for instrumental measurements of aircraft noise, at least to prove that the calculated values are equal to measured and the contours, which must be used for noise zoning, are defined correctly.

## 21.2 Requirements for Aircraft Noise Measurements in Ukraine

Full-scale instrumental measurements of aircraft noise should be performed at the airport under investigation during the periods of maximum ground and flight intensity of the aircraft, during the flights of the noisiest aircraft types in the regulated time intervals of the day. Aircraft noise (AN) is usually created by single noise events (during which the noise may change dramatically and be absent for a significant part of the reference time interval). The duration of measurements should be chosen so that it is possible to reliably estimate the sound level *LA* for a single case. To reliably estimate the equivalent *LAeq* and/or maximum noise level *L<sub>Amax</sub>*, or the exposure level (exposure) of *LAE (SEL)*, in the interval equal to the duration of measurements, the minimum number of sound events must be set, but the time interval must be at least 2 hours at each observation point. At least five flights of the noisiest types of aircraft must be recorded at each point (SAAU Order 585 2020). Somewhere the task is not possible to be realized efficiently in one place and during a single survey because a number of airports in Ukraine still have the small air traffic and the requirements of the standards for correct and accurate sound level assessment are simply absent.

Current guidelines (SAAU Order 585 2020) determine some points of AN observation in vicinity of the airport in accordance with the requirements of international ICAO standards (ICAO Annex 16 2019) for aircraft noise, but taking in mind that standard values are normalized depending on the maximum takeoff mass of the aircraft and specific meteorological parameters. Primarily, the instrumental measurements at ICAO standard control points provide an opportunity to assess the degree of compliance of real AN levels in daily aircraft operation with the results of their official noise certification. Although the conditions of flight at the airport and during certification tests may differ significantly, thus causing a significant difference in the results of AN measurements. The basic principles for the selection of

other instrumentation sites (or the location of AN monitoring points near airports) in the three case of a specific task are given in the annex to the guidelines (SAAU Order 585,2020, paragraph 8 of Cchapter VIII). For example, the location of measuring points in the vicinity of Kyiv/ Gostomel Airport is presented in Fig. 21.1. They were chosen along flight axis from both sides of the runway, except two points N2 and N3, which are located at the front border of residential area close to aerodrome. Background noise levels at the measurement points were recorded usually lower by an average of 20–25 dBA from the sound levels of the AN events (at departures and arrivals of the aircraft), which fully meets the requirements of the standards on environmental noise measurements (SAAU Order 585 2020, ICAO Annex 16 2019).

### 21.2.1 Results of Measurements

For each of the measurement sets – departure and arrival noise – sound levels were determined at ICAO AN control points 2 and 3 (shown in Fig. 21.1, for example the points TB2S and TB2N are correspondent to arrival noise point No. 3 in both directions of landing at this airport). In dependence to their values the relationships of sound levels from distance to the point of AN observation may also be determined (shown in Figs. 21.2, 21.3, 21.4, and 21.5, respectively, for LAE and LAm<sub>ax</sub> during departure and arrival of the aircraft) by the method of least squares.



**Fig. 21.1** Location of AN measurement points in the vicinity of Kyiv/Gostomel Airport (yellow points – for departures; pink points – for arrivals)

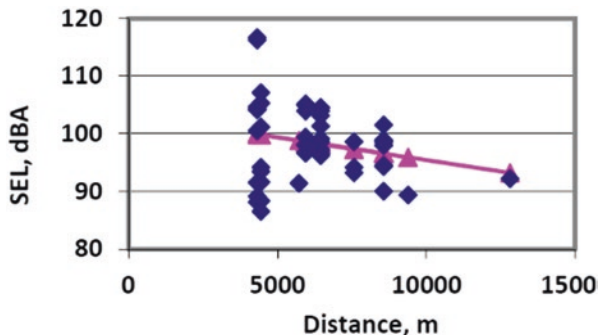


**Fig. 21.2** Dependence of sound exposure levels  $LAE$  from the distance to the point of aircraft start on runway during the aircraft departure. blue rhombus - measured values; pink triangle - linear approximation for the set

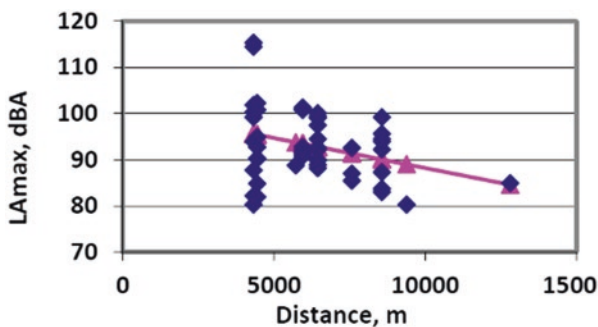


**Fig. 21.3** Dependence of the maximum sound levels  $LA_{max}$  from the distance to the point of aircraft start on runway during the aircraft departure. blue rhombus - measured values; pink triangle - linear approximation for the set

### 21.2.2 Comparison of AN Measurement Results with Calculated and Certification Noise Levels

The results of noise measurement in the vicinity of aerodrome are usually analyzed from several points of view:

- Comparison with normative values of environmental noise in accordance with the requirements of national norms and rules;
- Comparison with the results of noise certification of types of aircraft operated at the aerodrome;
- Comparison with the results of the calculation of the sound levels of the AN, performed to justify the boundaries of the zones of residential building restriction from noise conditions.

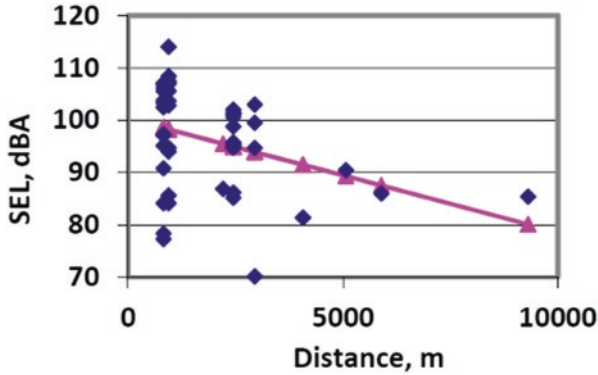


Fig. 21.4 Dependence of sound exposure levels *LAE* from the distance to the runway end during the aircraft arrival. blue rhombus - measured values; pink triangle - linear approximation for the set

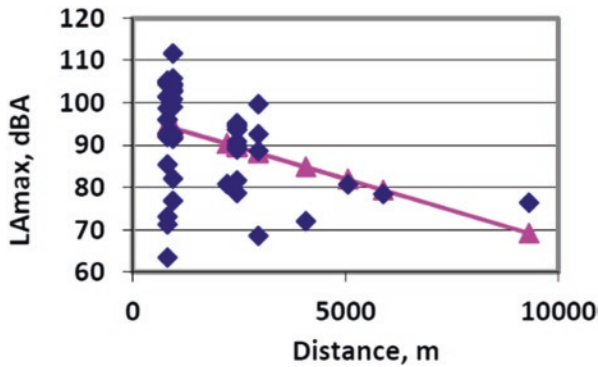
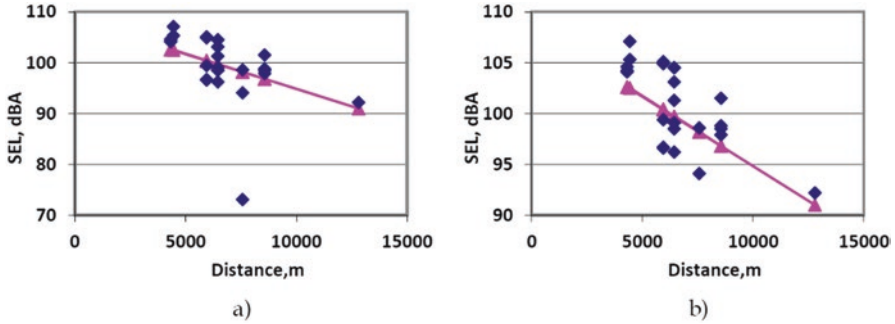


Fig. 21.5 Dependence of the maximum sound levels *LA max* from the distance to the runway end during the aircraft arrival. blue rhombus - measured values; pink triangle - linear approximation for the set

The results for the sound levels in Figs. 21.2 and 21.3 (departure) and 4 and 5 (arrival) indicate a wide range of deviations of the measured values from the averages, which necessitates the analysis of samples for each type of the aircraft and the flight stage separately. Sound levels, particularly maximum sound levels *LAmax*, at a distance of 6–8 km along the takeoff axis from the starting point on the runway essentially dominate over the regulatory values of the rules (SSR-173 1996) as for night (*LAmax* = 75 dBA) and day (*LAmax* = 85 dBA) time.

The largest data set at Kyiv/Gostomel studies was obtained for AN events for the An-124 aircraft (sound levels for the departure in Fig. 21.6 and for the arrival in Fig. 21.7). The approximation for a complete data set indicates unsatisfactory statistical values (for arrivals the correlation coefficient =  $-0.330$  and coefficients of linear approximation  $B_0 = 99.4$ ,  $B_1 = -0.00155$ , etc.), so in each of the sets, particularly for arrivals (Fig. 21.7), the measured data with significant deviations from



**Fig. 21.6** Dependence of sound exposure levels LAE for An-124 departure from the distance to the point of aircraft start on runway: (a) full set data; (b) a set with excluded highly deviated data; blue rhombus - measured data, pink triangle - linear approximation for the set

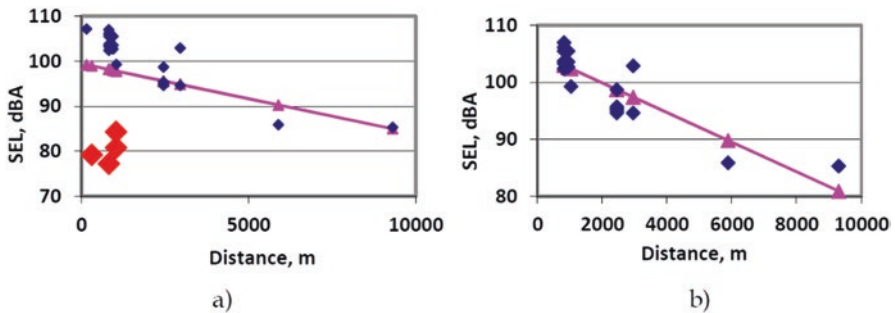


**Fig. 21.7** Dependence of sound exposure levels LAE for An-124 arrival from the distance to the runway end: (a) full set data; (b) a set with excluded highly deviated data; blue rhombus - measured data, pink triangle - linear approximation for the set; red rhombus - data with significant deviations from the approximation

the approximation line (marked in red rhombus in the corresponding figures) were excluded from further statistical analysis. The results for observation sets with the removed highly deviated data are much more correlated between themselves (standard deviations for a limited sample are 2–3 times smaller than the deviations for the full data set, correlation coefficient =  $-0.873$  and coefficients of linear approximation  $B_0 = 105.1$ ,  $B_1 = -0.0026$ , etc). These highly deviated data were excluded from comparison with the noise certification data for the aircraft also (Tables 21.1 and 21.2). Comparison between measured and calculated sound levels (Figs. 21.2, 21.3, 21.4, 21.5, 21.6, and 21.7) indicate minor differences (1–2 dBA), especially with excluded highly deviated data, the assessment of which leads to the conclusion of sufficient accuracy of the calculations, particularly for aircraft An-124 (Figs. 21.6 and 21.7), which provides the main noise load on the environment in Kyiv/Gostomel Airport.

**Table 21.1** Comparison of noise measurement with aircraft noise certification data at departure

Aircraft type	An-26	An-225	An-124	An-22	An-74
Certification EPNL, EPNdB	91.1	103.4	106.2	absent	87.8
ICAO requirements for EPNL, EPNdB	93.0	106.0	106.0	102.5	89
Recalculated L <sub>Amax</sub> from EPNL, dBA	87.4	89.1	91.9	92.2	76.9
Measured L <sub>Amax</sub> , dBA	88.6	91.5	94.4	89.0	77.0

**Table 21.2** Comparison of noise measurement with aircraft noise certification data at arrival

Aircraft type	An-26	An-225	An-124	An-22	An-74
ICAO requirements for EPNL, EPNdB	102.0	105.0	105.0	103.9	98.2
Recalculated L <sub>Amax</sub> from EPNL, dBA	90.4	95.6	94.7	94.4	86.2
Measured L <sub>Amax</sub> , dBA	84.7	97.9	95.9	97.6	83.0

### 21.3 Method of Aircraft Noise Exposure Comparison with Certification Data

A comparison of the results of measuring sound levels, including during certification tests of the aircraft for compliance with international standard requirements, with the results of calculations indicate minor differences between them (1–2 dBA). Their evaluation leads to the conclusion of sufficient accuracy of the performed calculations according to modern recommendations, particularly for the Boeing-737-800 type aircraft, which causes the main acoustic load on the environment in the vicinity of the Khmelnytski International Airport (due to the noise created by a separate event noise, and the number of operations of this type of aircraft at the airport). The measured data for such a comparison should be prepared in a specific database with results from a number of surveys at different airports and locations because it is not usually possible to provide the certification requirements in one place. Fig. 21.8 shows how the measured *SEL* for Boeing-737-800 at various surveys were accumulated for departures and approaches with their normalization to AN certification conditions for points #2 and #3 of the ICAO standard (Appendix 16, Volume 1 Aviation Noise). The calculated data are much closer to averaged data of the measured results, correspondent with the linear approximation for the sets in Figs. 21.2, 21.3, 21.4, 21.5, 21.6, and 21.7.

For the certification noise EPNL of the Boeing-737-800 aircraft, the discrepancies with the calculated results are 0.1–0.6 EPNdB at points #2 and #3 of the ICAO standard (Appendix 16, Volume 1 Aviation Noise) (Fig. 21.9). They indicate fairly accurate coefficient values of the acoustic model and of takeoff/climb and descent before landing profiles’ modeling in the international ANP database, which are used for calculations.



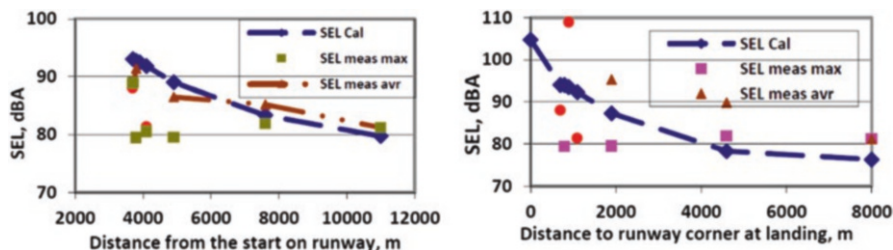


Fig. 21.8 Sound exposure levels *LAE* for noise events by Boeing-737-800 at departure and approach – measured and calculated for comparison between themselves

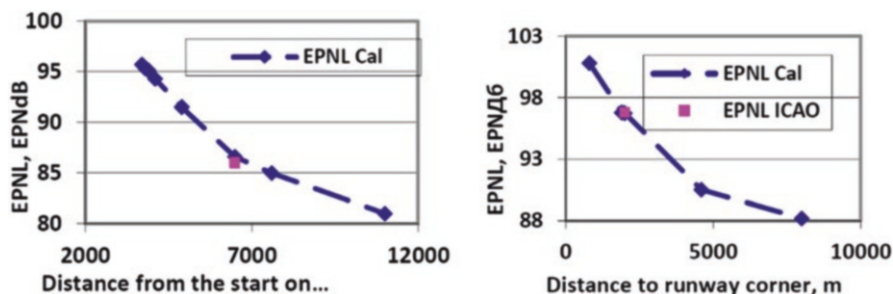


Fig. 21.9 Effective perceived noise levels *EPNL* for noise events by Boeing-737-800 at departure and approach – certified (pink) and calculated for comparison between themselves

### 21.4 Method of Noise Exposure Transfer Between the Similar AN Measurement Scenario at the Airports

In Fig. 21.10, the calculated contours of aviation noise are presented for the Khmelnytskyi Airport according to the criterion of maximum sound levels *L<sub>Amax</sub>* in the daytime. The shown points 1 and 2 are closest to the *L<sub>Amax</sub>* contours and can be both used to prove their compliance with established noise limits (SSR-173 1996) by measurements and to compare with calculated results (the contour values).

Because the airfield reconstruction and stopped air traffic at the airport, the AN measurements were carried out in the vicinity of Kyiv-Zhuliany Airport for aircraft Boeing-737 (–700 and – 800) and Airbus-320 (–321) that are planned for operation at the Khmelnytskyi Airport in the near future (after the reconstruction of the airfield). The points in the vicinity of Kyiv/Zhuliany are chosen similar to points 1 and 2 at Khmelnytskyi Airport (Fig. 21.10). The results of measurement and calculation are presented in Table 21.3.

The measured values of *L<sub>Amax</sub>* during takeoff coincide with those calculated for the aircraft B-737-700 *L<sub>Amax</sub> meas* = 78 dBA, *L<sub>Amax</sub> calc* = 78,2 dBA and higher on 3–4 dBA for the aircraft A-320 *L<sub>Amax</sub> meas* = 77,9 dBA, *L<sub>Amax</sub> calc* = 82,0 dBA. Measured *L<sub>Amax</sub>* during approach are higher of calculated on 4–6 dBA, but they are not determinative for noise contours, which are taken as a basis for establishing noise zone boundaries.



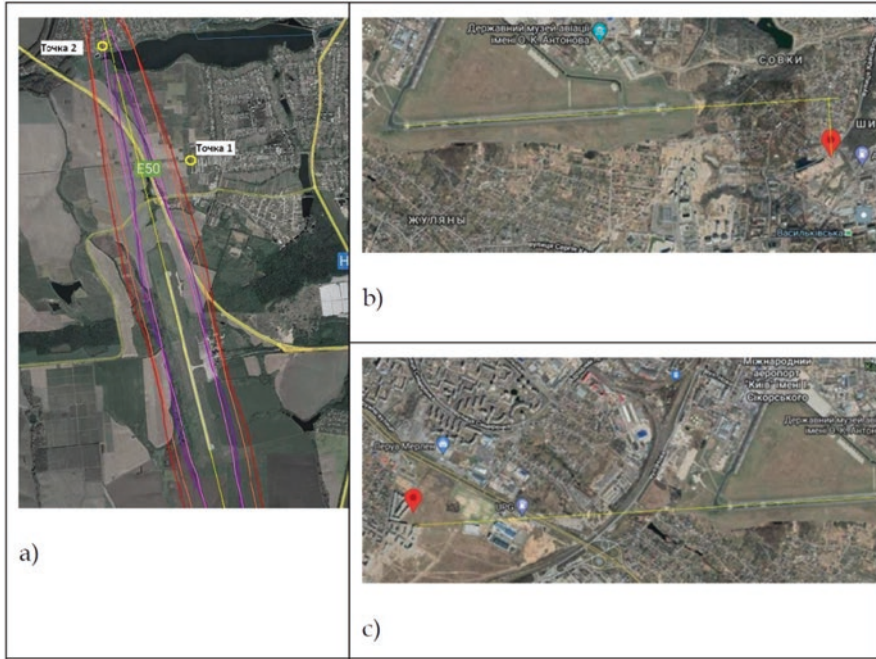


**Fig. 21.10** Sound levels  $L_{Amax}$  at Khmelnytskyi Airport: (a) calculated noise contours for noise limits during the daytime: 80 (red, orange) and 85 (magenta, pink) dBA; (b) analogue of the point 1 for Khmelnytskyi Airport at Kyiv/Zhuliany Airport; (c) analogue of the point 2 for Khmelnytskyi Airport at Kyiv/Zhuliany Airport

**Table 21.3** Comparison between measured and calculated sound levels

Aircraft type	Flight stage	Calculated $L_{Amax}$ , dBA	Measured $L_{Amax}$ , dBA		
			avr	min	max
A-320	Arrival	66.7	71	70	74
B-737-700		68.1	75	73	77
A-320	Departure	77 ... 83	77.9	77	81
B-737-700		76.1 ... 82.7	78	72	84

### 21.5 ADS-B Usage for Aircraft Location to Point of Noise Measurements

An aircraft’s spatial location during the measurements was determined using the ADS-B receiver, combined with FR24 ([www.flightradar24.com](http://www.flightradar24.com)) data, and supported by the flight data obtained from the local air traffic control. Noise measurement results, aircraft tracking data, and meteorological parameters were synchronized in time and space (distance and direction from noise level measurement points). ADS-B data were recorded at 1-second intervals by the ADS-B

receiver and used from FR24 – at 15-second interval. All the flights for testing the method were performed using the Antonov aircraft types AN225, AN124, AN22, and some smaller types, even noisier than the larger Antonov types (Fig. 21.11).

The obtained results from the measurements allow to correct the modeling results for accurate development of the noise restriction zones, especially for the  $L_{Amax}$  criterion, which is still normative in Ukraine – especially important are the sensitive levels of 70–75 dBA at night. The departure distance of 19 km is maintained only in 41% of cases, so it is worth forming using the DB Scan algorithm.

The analysis of results (Table 21.4) has shown that if the measurement point was under the flight trajectory in the high field levels, the gap between the simulation results (given the classical approach to noise modeling – AIP data instead of real routes, scheduled flights instead of real ones, etc.) and the measured results is minimal, but for points of noise control that are remote from the airport a larger deviation observed for which the correction is obviously required.

## 21.6 Conclusion

According to the measurement results, the noisiest aircraft type among those planned to operate today at the Khmelnytskyi Airport is the Boeing-737-700 (or Boeing-737-800), making the maximum contribution to the value of the equivalent sound levels  $L_{Aeq}$  during the day and at night, as well as to the value of the daily

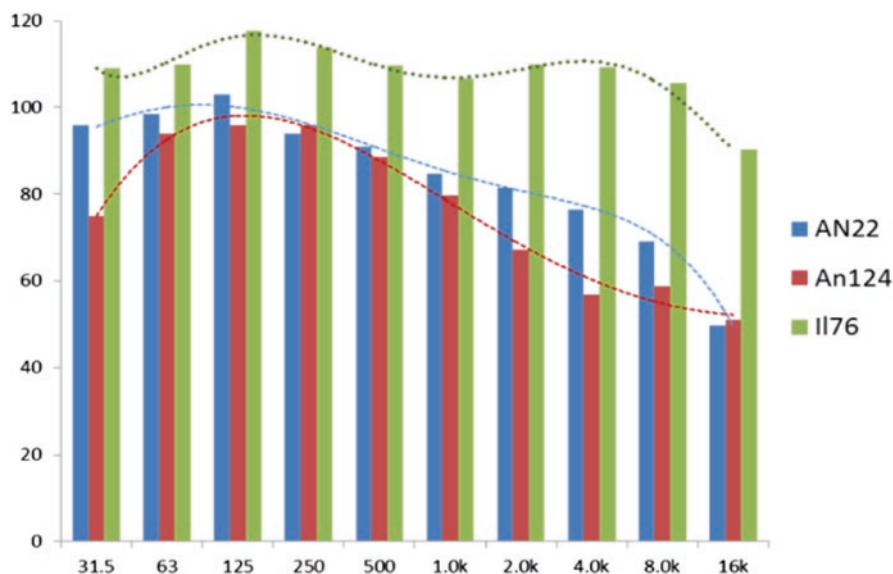


Fig. 21.11 Averaged octave spectra for aircraft types AN22, AN124, Il76 (measurement point TB1 in Fig. 21.1)

**Table 21.4** Comparison of the calculated and measured results  $L_{Amax}$  for AN124 departure operations

N	Ops. type	Latitude	Longitude	A/D	$L_{Amax}$ F, dB	$L_{Amax}$ (calc), dB	Avg.	St Dev.
1	D	50.650556	30.153639	D	85.4	92.5	–	–
2	D	50.513861	30.257694	D	84.9	80.7	–	–
3	D	50.569083	30.216028	D	92.8	95.9	99.0	3.56
4	D	50.569083	30.216028	D	100.9	95.9		
5	D	50.569083	30.216028	D	100.8	95.9		
6	D	50.569222	30.215833	D	101.3	95.9		
7	D	50.581972	30.207	D	100.8	101.9	100.9	1.10
8	D	50.582306	30.206389	D	102.3	102		
9	D	50.625056	30.175167	D	100.3	102.9		
10	D	50.625139	30.175278	D	99.2	102.5		
11	D	50.626333	30.174	D	101.8	101.7		
12	D	50.640889	30.162583	D	92.1	95.3	95.1	1.10
13	D	50.640972	30.1625	D	100.1	95.2		
14	D	50.6415	30.161278	D	99.4	94.8		
15	D	50.641611	30.158528	D	92.5	93.1		
16	D	50.64175	30.160417	D	88.9	94.4		
17	D	50.642056	30.161583	D	97.4	94.9		
21	D	50.6595	30.149917	D	87.3	91.2	93.4	3.84
22	D	50.6595	30.149917	D	94.5	91.2		
23	D	50.6595	30.149917	D	93.9	91.2		
24	D	50.659583	30.149722	D	99.2	91.2		
25	D	50.659611	30.149917	D	92.2	91.2		

noise index  $LDEN$ , which are both required today by APU-381 for the spatial zoning of the airfields from aviation noise exposure. Also, the contours of the maximum sound level  $L_{Amax}$  in the vicinity of the airport will be determined by the acoustic performances of the B-737-800. A comparison of the results of measuring sound levels, including during certification tests of the aircraft for compliance with international standard requirements, with the results of calculations indicate minor differences between them (1–2 dBA). For the certification noise  $EPNL$  of the Boeing-737-800 aircraft, the discrepancies with the calculated results are only 0.1–0.6 EPNdB at points #2 and #3 of the ICAO Standard (Appendix 16, Volume 1 Aviation Noise). The obtained data from ADS-B real flight parameters allow to correct the modelling results for the boundaries of noise restriction zones, especially defined by the  $L_{Amax}$  criterion, which is still used as a noise limit in Ukraine – especially the night noise protection limit  $L_{Amax} = 75$  dBA.

All the measured data for AN during departures and arrivals are stored in a specific database for further analysis of the accuracy of AN calculation and proving the boundaries of noise zones around the airports. The database is filled continuously with the results of AN measurements at various airports in Ukraine with some processing them for further rigorous usage. Particularly, the assessment of the accuracy of the calculation of AN contours for single flight noise events is extremely important in terms of the state regulations' requirements (SAAU AR-381, 2019).

## References

- Directive 2002/49/EC relating to the assessment and management of environmental noise. European Parliament, European Council, 25 of June 20022002. <https://eur-lex.europa.eu/>
- DSN 3.3.6.037, *Sanitary standards of industrial noise, ultrasound and infrasound* (National Sanitary Norms of Ukraine ДСН 3.3.6.037–99, in Ukrainian, 1999) 01.12.1999
- DSTU-N B V.1.1–31, *Protection of territories, buildings and structures from noise*. (National Standard of Ukraine ДСТУ-Н Б В.1.1–31:2013, in Ukrainian, 2013), 2014
- ICAO, *Annex 16 to the Convention on International Civil Aviation — Environmental Protection: Volume I — Aircraft Noise* (ICAO, Montreal, 2019)
- ICAO Resolution A40–17, *Consolidated statement of continuing ICAO policies and practices related to environmental protection – General provisions, noise and local air quality* (ICAO, Montreal, 2019), 2019. <https://www.icao.int/environmental-protection/Documents/A40-17.PDF>
- SAAU AR-381, *Requirements for operators related to noise zoning of the airport vicinity*. (Ukrainian Aviation Rules, State Aviation Service of Ukraine (SAAU), 2019), dated 26.03.2019. <https://zakon.rada.gov.ua/laws/show/z0461-19?lang=en/>
- SAAU Order 585, *Methodical instructions on airport vicinity zoning according to noise conditions*. (State Aviation Service of Ukraine, 2020), dated 23.04.2020. <https://avia.gov.ua/wp-content/uploads/2019/10/Nakaz-585-Pro-zatverdzhennya-metodichnih-rekomendatsij-2.pdf>
- SSR-173, *State Sanitary Rules for planning of inhabited localities*. (Order of Ministry of Health No 173, 1996), dated 19.06.1996. <https://zakon.rada.gov.ua/laws/show/z0379-96#Text>

# Chapter 22

## PIV Experimental Setup Integrated Wind Tunnel Initial Design: Size and Power Requirement Calculation



Murat Ayar and T. Hikmet Karakoc 

### 22.1 Introduction

Wind tunnels are structures designed and manufactured to examine, research, measure, and interpret the effects of the flow structure around it when a solid object is moving in air or when a fixed solid object is exposed to air flow (Calautit et al. 2014). These tunnels are widely used systems for aerodynamic testing of life-size objects or structures, as well as for aerodynamic testing of geometrically similar models.

Data obtained from wind tunnel tests play an important role in the design stages of an aircraft to be produced in aviation (Barlow 1999). As it is known, aircraft design and production is a very costly and time-consuming process (Cattafesta et al. 2010). While aircraft design goes through all these processes, many parameters and factors must be considered (Mehta 1979). While the aircraft is being designed, it is tested by means of these wind tunnels and its aerodynamic structure is determined, and thus its design, namely its shape, is aerodynamically improved (Noui-Mehidi et al. 2005). In this way, the most optimum aerodynamic shape and error correction

---

M. Ayar (✉)

Department of Airframe and Powerplant Maintenance, Eskisehir Technical University, Eskisehir, Turkey

Faculty of Aeronautics and Astronautics, Eskisehir Technical University, Eskisehir, Turkey

e-mail: [muratayar@eskisehir.edu.tr](mailto:muratayar@eskisehir.edu.tr)

T. H. Karakoc

Faculty of Aeronautics and Astronautics, Eskisehir Technical University, Eskisehir, Turkey

Information Technology Research and Application Center, Istanbul Ticaret University, Istanbul, Turkey

e-mail: [hkarakoc@eskisehir.edu.tr](mailto:hkarakoc@eskisehir.edu.tr)

are obtained, and high expenditures and waste of time and effort are prevented (Harvey, 2011).

Wind tunnels allow us to measure, see, and understand the effects that a real airplane will experience in the air by conducting experiments on the model. These models may also be just some parts of the aircraft, such as the wing, fuselage or tail. In addition, we can see the effects of these changes on the aircraft and whether there will be a negative or positive effect on the performance of the aircraft, thanks to the changes in the exterior design and the tests carried out in the wind tunnels.

## 22.2 Method

The starting point for calculating the dimensions of the wind tunnel is the dimensions of the test section. Therefore, the requirements for the test section were determined first. Power calculations, on the other hand, should be made over the maximum air speed that is aimed to be reached. For this reason, in line with the studies to be carried out and within the framework of the upper limits of the PIV system, the maximum air speed is 50 meters/second (Fig. 22.1).

Considering the limitations, starting from the test section dimensions, the results in the image were obtained as a result of dimensional calculations for the low-speed open-circuit wind tunnel (Morel 1975). The required length for a one meter by one meter test section was found to be two meters. The total length of the tunnel was eleven and a half meters. Thus, it will be able to settle inside the test chamber (Fig. 22.2).

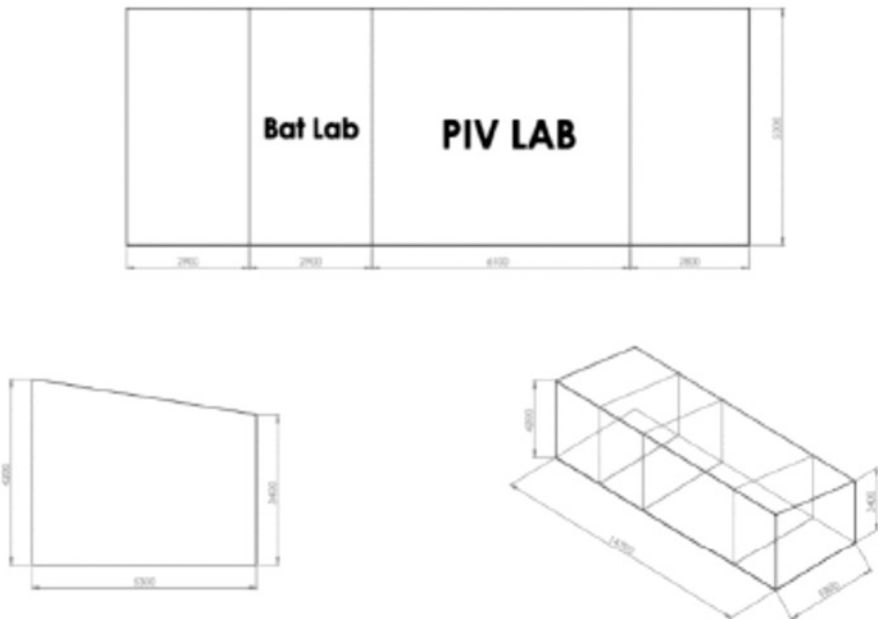


Fig. 22.1 Size constraints by laboratory

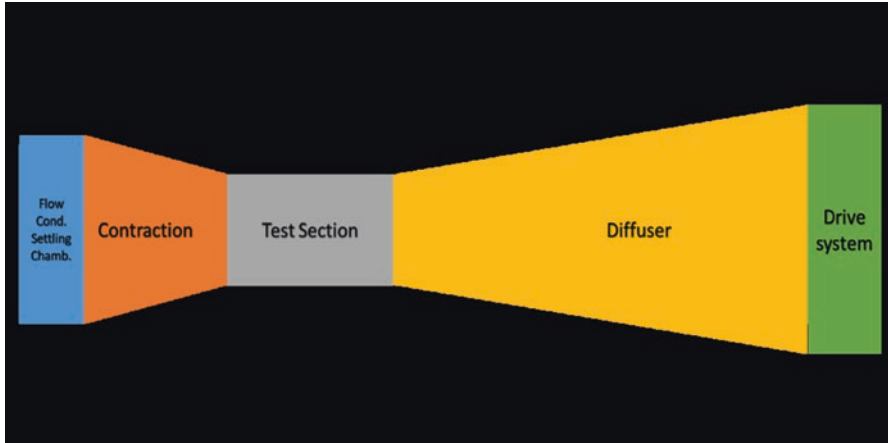


Fig. 22.2 Main dimensions

### 22.3 Results and Discussion

The power plant is essential in maintaining the flow inside the wind tunnel at a constant velocity, while compensating for all the pressure losses and dissipation. After dimensional calculations, the pressure losses were calculated for each component. Then all the losses were added up to determine the overall pressure loss of the entire circuit. This helps to determine the power needed for the wind tunnel operation. This calculation technique is compatible with both open and closed-circuit wind tunnels (Table 22.1).

From the equation, the required shaft power for the tunnel was found as 22.97 kW. In this case, it would be appropriate to choose a motor with a shaft power of more than 45 kW with a safety margin of 2.

$$E_k = \frac{1}{2} \rho V_0^3 A_0 K_t \tag{22.1}$$

$$E \sim 45 kW \tag{22.2}$$

The flow rate of the fan,  $Q_f$ , is calculated by multiplying the cross-sectional area of the test chamber with the average speed measured in the test chamber.

$$Q_f = A_0 V_0 \tag{22.3}$$

$$Q_f = 1.50 = 50 \frac{m^3}{sn} = 180\,000 \frac{m^3}{sa} \tag{22.4}$$

$$Q_f = 180\,000 \frac{m^3}{sa} \tag{22.5}$$

**Table 22.1** Losses of sections

Section	Loss
Test section (K1)	0,03255
Contraction (K2)	0,054
Mesh screens (K3)	0,0384
Honeycombs (K4)	0,032
Diffuser (K5)	0,042
Total losses (Kt)	0,19,895 $\cong$ 0,2

A sample fan that can meet the air flow requirement that can be used as a result of the calculations is in the image. Centrifugal fans will be able to provide the desired performance. It will be appropriate to choose a square section inline direct drive or belt drive fan.

## 22.4 Conclusion

Particle image velocimetry (PIV) is increasingly used for aerodynamic research and development. The PIV technique allows the recording of a complete flow velocity field in a plane of the flow within a few microseconds. Thus, it provides information about unsteady flow fields, which is difficult to obtain with other experimental techniques. The short acquisition time and fast availability of data reduce the operational time, and hence cost, in large scale test facilities. We have developed a reliable, modular PIV system for use in aerodynamic problems.

## References

- J.B. Barlow, W.H. Rae, A. Pope, *Low-speed wind tunnel testing* (John Wiley & Sons, 1999)
- J.K. Calautit, H.N. Chaudhry, B.R. Hughes, L.F. Sim, A validated design methodology for a closed-loop subsonic wind tunnel. *J. Wind Eng. Ind. Aerodyn.* **125**, 180ff194 (2014)
- L. Cattafesta, C. Bahr, J. Mathew, *Fundamentals of wind-tunnel design* (Encyclopedia of Aerospace Engineering, 2010)
- S.A. Harvey, *Low-speed wind tunnel flow quality determination*. PhD thesis, Monterey, California (Naval Postgraduate School, 2011)
- R.D. Mehta, The aerodynamic design of blower tunnels with wide-angle diffusers. *Prog. Aerosp. Sci.* **18**, 59ff120 (1979)
- T. Morel, Comprehensive design of axisymmetric wind tunnel contractions. *J. Fluids Eng.* **97**(2), 225ff233 (1975)
- M.N. Noui-Mehidi, J. Wu, I.D. Sutalo, C. Grainger Velocity distribution downstream of an asymmetric wide-angle diffuser *Exp. Therm. Fluid Sci.* **29** (2005), pp. 649–657



# Chapter 23

## Particle Image Velocimetry Measurement with Scaled-Down Aircraft Models: A Review of the Experiments and Applications



Murat Ayar, Ali Haydar Ercan , and T. Hikmet Karakoc 

### Nomenclature

CFD Computational Fluid Dynamics  
PIV Particle Image Velocimetry

### 23.1 Introduction

Aerodynamic forces and moments act on all kinds of vehicles and structures that move in the air or are under the influence of an air current. Wind tunnels are used to find these forces and determine the shape and structure of the flow. It is used to examine the aerodynamic structure, parameters such as heat, light, and smoke on the one-to-one product or scaled-down products placed in the wind tunnel under desired conditions. Therefore, the capabilities of the wind tunnel and the scale

---

M. Ayar (✉)

Department of Airframe and Powerplant Maintenance, Eskisehir Technical University, Eskişehir, Turkey

e-mail: [muratayar@eskisehir.edu.tr](mailto:muratayar@eskisehir.edu.tr)

A. H. Ercan

Department of Electronics and Automation, Porsuk Vocational School, Eskisehir Technical University, Eskişehir, Turkey

e-mail: [ahercan@eskisehir.edu.tr](mailto:ahercan@eskisehir.edu.tr)

T. H. Karakoc

Faculty of Aeronautics and Astronautics, Eskisehir Technical University, Eskisehir, Türkiye

Information Technology Research and Application Center, Istanbul Ticaret University, Istanbul, Turkey

e-mail: [hkarakoc@eskisehir.edu.tr](mailto:hkarakoc@eskisehir.edu.tr)

model used should be compatible with each other. Particle image velocimetry (PIV) is currently one of the most applied optical techniques in flow investigations, even in model basins. The PIV technique was further used already for many large-scale measurements (Dieterle et al. 1999; Gilliot et al. 2010; Grant et al. 1999; He et al. 2012). At the same time, experiments can be performed on very small-scaled models with PIV (Ergin and Alemdaroglu 2013; Jones et al. 2017; Kai et al. 2020).

Despite considerable progress in computational fluid dynamics (CFD), wind tunnels are still a prime tool to measure and predict aircraft performance for takeoff, landing, and cruise conditions (Placek et al. 2017). To make the studies more sensitive, scale models of the planes are made and the flows on them are examined. Scaled aircraft models used in PIV and wind tunnel tests consist of full models formed by modeling the whole aircraft (Reinholtz et al. 2008; Sciacchitano et al. 2018), and half models made by using the symmetrical vehicles of aircraft. In addition, it is possible to conduct tests by making only the model of the relevant region to investigate the aircraft structures where critical flow phenomena occur. As a result, it would be appropriate to divide the models used for flow analysis into three groups. In this study, only the full models used in PIV experiments were investigated and evaluated.

## 23.2 Method

The study within the scope of the study were compiled under four main groups. In the first stage, information was collected about the type and characteristics of the wind tunnel where the PIV experiments were carried out. The information obtained from here will be used for initial values to design a wind tunnel. In the second group, the type, dimensions, and physical properties of the model to be analyzed were investigated. The information here will be a reference for the studies planned to use the aircraft model. In the third group, information about the PIV experimental setup was collected. This information can be used by researchers who plan to conduct PIV experiments in their future studies. In the last group, information about the goals and objectives of the flow analysis studies was compiled.

## 23.3 Results and Discussion

The chart in Fig. 23.1 shows the wind tunnels where these experiments took place. The DNW Low speed Wind tunnel, which is part of DLR in Germany, is the tunnel where the most work is done. This wind tunnel hosted almost half of the work done with the European transonic wind tunnel.

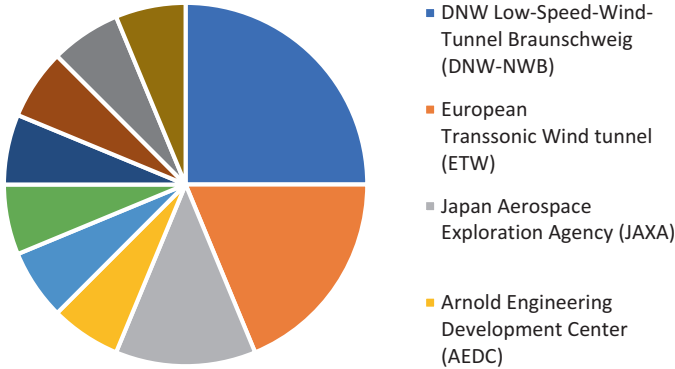


Fig. 23.1 Distribution of wind tunnels

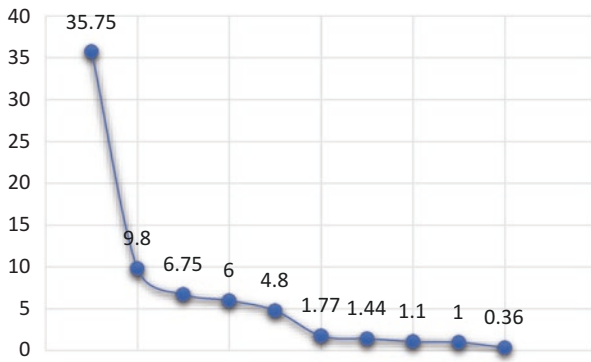


Fig. 23.2 Test section areas

In the last part about wind tunnels, the most important features of the test section area are presented in Fig. 23.2. The graph shows that the studies were carried out in a very wide range. While the wind tunnel with the largest test section is approximately thirty-five square meters, the test section of the smallest wind tunnel is only about 36 m<sup>2</sup> at the zero point. When we consider all the wind tunnels, the average test section is 6.8 m<sup>2</sup>.

The second group of the study consists of the properties of scale models. The graph on the left of Fig. 23.3 provides information about the most important feature of the models, the scales. The largest model is 17% of the original aircraft dimensions. The smallest model used is only 0.003 of the actual aircraft. This smallest scale model is actually a craft and was used for experimental purposes. As can be seen from this graph, wind tunnel scale models are preferred with an average of 10% scale. The graph on the right shows the distribution of wing span measurements to understand the actual dimensions of the models. The wing span of the largest scale model is two meters and fifteen centimeters, while in the smallest model this size is only 40 mm.

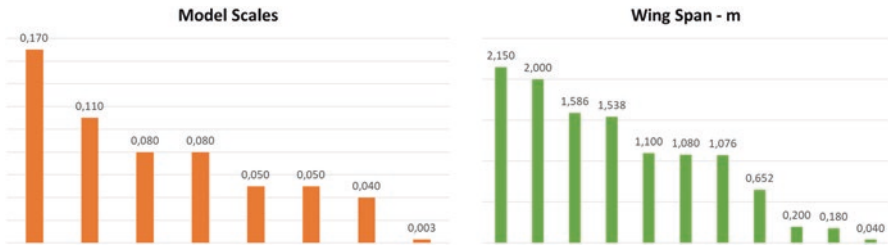


Fig. 23.3 Model dimensions

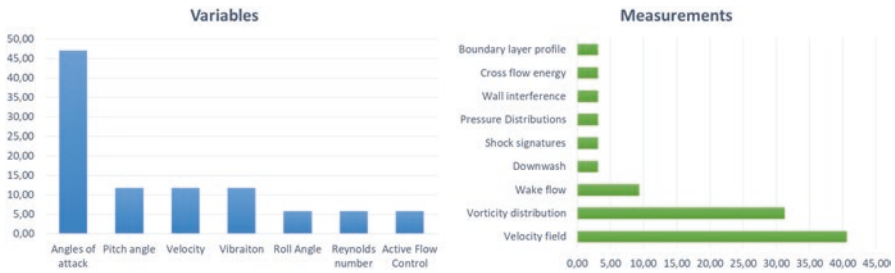


Fig. 23.4 Distribution of analyses

In the last part of the study, the analysis of the PIV test results was discussed and the variables in the experiments and the distribution of the measurements were investigated. The graph on the left of Fig. 23.4 shows that different angles of attacks are often used to investigate the behavior of the flow. It is also used in variables such as pitch angle, velocity, and vibration. The table on the right shows which outputs are used to interpret the PIV test results. This graph shows that velocity field and vorticity distribution analyses obtained by direct use of PIV experiment results are predominantly used. After these, it is seen that the inferences that occur as a result of the indirect processing of the results come.

### 23.4 Conclusion

PIV experiments undersign important studies on experimental aerodynamics, which are still used as references. Flow analysis can be done much more efficiently with the integration of wind tunnels and PIV experimental setups. The use of scale models in PIV experiments will provide a better understanding of the flow phenomena around the aircraft. It is obvious that the compatibility of the wind tunnel test section dimensions, scale model dimensions, and the capacities of the PIV setup will improve the quality of the test results. Flow fields and vorticity distributions obtained from PIV test results directly and indirectly by hand analysis can be used to determine flight characteristics.

## References

- L. Dieterle, R. Stuff, G. Schneider, J. Kompenhans, P. Coton, J.C. Monnier, *Experimental investigation of aircraft trailing vortices in a catapult facility using PIV* (EALA Conference, Rome (Italy), 1999)
- F.G. Ergin, N. Alemdaroğlu, Long-distance MicroPIV measurements of a commercial aircraft model at low Reynolds number, in *7th Ankara International Aerospace Conference*, (AIAC-2013-013, Ankara, Turkey, 2013)
- A. Gilliot, S. Morgand, J.C. Monnier, J.F. Le Roy, C. Geiler, J. Pruvost, Static and dynamic SACCON PIV tests, Part I: Forward Flowfield, in *28th AIAA Applied Aerodynamics Conference*, (2010), p. 4395
- I. Grant, M. Mo, X. Pan, P. Parkin, J. Powell, D. Hurst, A PIV and LSV Study in the wake of an aircraft model. *J. Vis.* **2**(1), 85–92 (1999)
- W. He, Z.G. Niu, B. Pan, Q. Lin, Experimental investigation on improving the aerodynamic performance of swept aircraft by DBD plasma. *Appl. Mech. Mater.* **110**, 3234–3242 (2012). Trans Tech Publications Ltd.
- A.M. Jones, K.M. Mejia, C. Ulk, Y. Murahashi, T. Nagata, A. Ochi, Comparison of PIV and CFD measurements of an advanced supersonic research concept model, in *47th AIAA Fluid Dynamics Conference*, (2017), p. 3639
- D. Kai, H. Sugiura, A. Tezuka, Dynamic wind tunnel testing of delta-wing model without support interference, in *AIAA Scitech 2020 Forum*, (2020), p. 1757
- R. Placek, P. Ruchała, W. Stryczniewicz, Ground effect influence on the aerodynamic characteristics of ultralight high-wing aircraft: wind tunnel tests. *J. KONES* **24** (2017)
- C. Reinholtz, F. Heltsley, J. Sirbaugh, J. Wehrmeyer, D. Rotach, Stereo-PIV data obtained behind an F-15 model compared to CFD results, in *26th AIAA aerodynamic measurement technology and ground testing conference*, (2008), p. 3712
- A. Sciacchitano, D. Giaquinta, J.F.G. Schneiders, F. Scarano, B.D. van Rooijen, D.E. Funes, Quantitative flow visualization of a turboprop aircraft by robotic volumetric velocimetry, in *Proceedings 18th international symposium on flow visualization*, (ETH Zurich, 2018)

# Chapter 24

## A Conceptual Use Case Evaluation of Unmanned Aerial Vehicles in the Structural Inspection of Greenhouses



Elif Koruyucu, Emre Özbek, Selcuk Ekici, and T. Hikmet Karakoc 

### Nomenclature

AI      Artificial Intelligence  
IoT     Internet of Things  
UAV:   Unmanned Aerial Vehicle

### 24.1 Introduction

The unmanned aerial aircraft sector has been growing day by day with more application areas. During the COVID-19 pandemic that started in 2019 and damaged the airliners (Nižetić 2020), the unmanned aerial vehicle sector kept increasing with the diversified application portfolio (Researchandmarkets 2021). UAVs are being replaced with manned aircraft applications due to the cost efficiency they provide in different sectors (Grenzdörffer et al. 2008).

---

E. Koruyucu (✉) · E. Özbek  
Eskişehir Technical University, UAV Technology and Operator Program, Eskişehir, Turkey  
e-mail: [elifkoruyucu@eskisehir.edu.tr](mailto:elifkoruyucu@eskisehir.edu.tr); [emreozbek@eskisehir.edu.tr](mailto:emreozbek@eskisehir.edu.tr)

S. Ekici  
Department of Aviation Iğdır University, Iğdır, Turkey

T. H. Karakoc  
Faculty of Aeronautics and Astronautics, Eskişehir Technical University, Eskişehir, Türkiye  
Information Technology Research and Application Center, Istanbul Ticaret University,  
Istanbul, Turkey  
e-mail: [hkarakoc@eskisehir.edu.tr](mailto:hkarakoc@eskisehir.edu.tr)

The cost efficiency of UAVs is mostly due to the overall system costs and pilot education processes. Also, operational advantages should be mentioned such as flying on concurrent routes throughout the waypoints autonomously and the requirement of a runway (Özbek et al. 2020). The developments in MEMs air quality and sensor types provided a wide selection of payloads and paved the way for UAVs to become the absolute dominant platforms for remote sensing operations (Yao et al. 2019).

In these days, UAV platforms are being used for a variety of applications that include 3D mapping (Nex & Remondino 2014), infrastructure (Ellenberg et al. 2015), forestry (Liang et al. 2019), and thermal imagery (Aghaei et al. 2014). Apart from this brief sort of application areas, agricultural use of UAVs is a trending field for both researchers and service providers (Norasma et al. 2019).

Agricultural UAVs are a cost-efficient service provider for agricultural services such as crop health monitoring (Devi et al. 2020); pesticide spraying (Wang et al. 2016); yield monitoring (Vega et al. 2015). These agricultural services could be summarized as pillars of precision agriculture. The term precision agriculture or smart agriculture is the phase that global agriculture sector is trying to reach with more precise decision-making tools and goal specific applications (De Clercq et al. 2018). These paradigms are shifting towards a new concept called the Agriculture 4.0. Agriculture 4.0 consists of a more data-driven agricultural management with sustainability goals (Rose & Chilvers 2018). These goals require usage of technologies such as AI, IoT, remote sensing, and neural networks to sustain a more real time data driven decision-making procedure (Zhai et al. 2020). Figure 24.1 presents the previous paradigm shifts in the agriculture sector with development of the industry and the goals of Agriculture 4.0 paradigm.

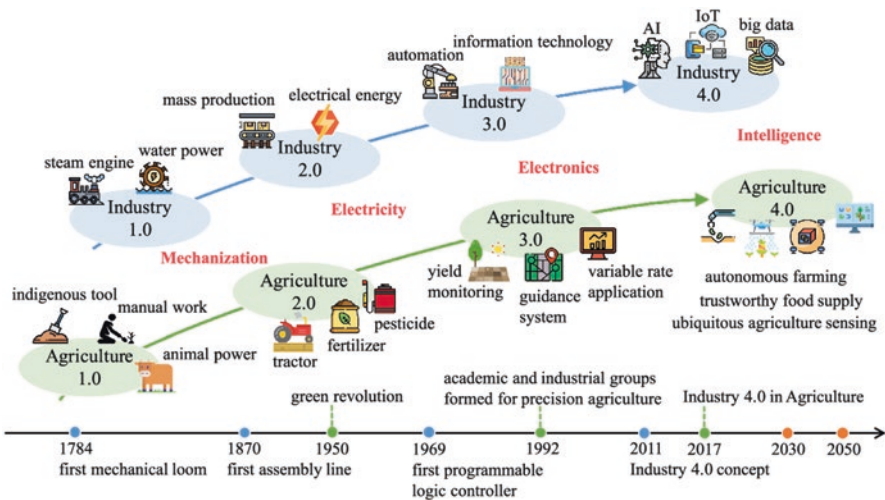


Fig. 24.1 The paradigm shifts in agriculture. (Liu et al. 2020)

## 24.2 Motivation: Food Security and the Greenhouses

The increasing world population and the requirement to increase global agricultural yield to feed them have been a severe problem for the humanity (McCarthy et al. 2018). Also, the global COVID-19 pandemic had severe disruptive effects on supply chains of food. The resilience of longer supply chains are being questioned by researchers (Chenarides et al. 2021), and relevance of shorter supply chains and local productions are being pointed out as a more sustainable food supply for cities (Cappelli & Cini 2020). Figure 24.2 presents how COVID-19 pandemic affected global supply chains.

The disruption on food supply chains resulted to a hike in food prices in 2021 as shown in Fig. 24.3 using the data from UN’s Food and Agriculture Organization’s (FAO).

Greenhouses could provide shorter and more resilient supply chains due to their advantageous non-region-dependant environment. A greenhouse use lower water, can increase crop yield, and can be delivered to consumer with a very shortened distance. Also, another paradigm that called vertical farming can be applied in greenhouses easily. The vertical farming improves crop yield without an increase in farming field area. Figure 24.4 presents lettuce production comparison of open fields, greenhouses, and vertical farms.

For a more secure food supply and higher farming yield, greenhouses offer a good solution. The energy requirement of greenhouses is also addressed with sustainable energy sources such as PV panels, wind turbines (El-Nemr et al. 2022), and geothermal energy (Al-Helal et al. 2022).

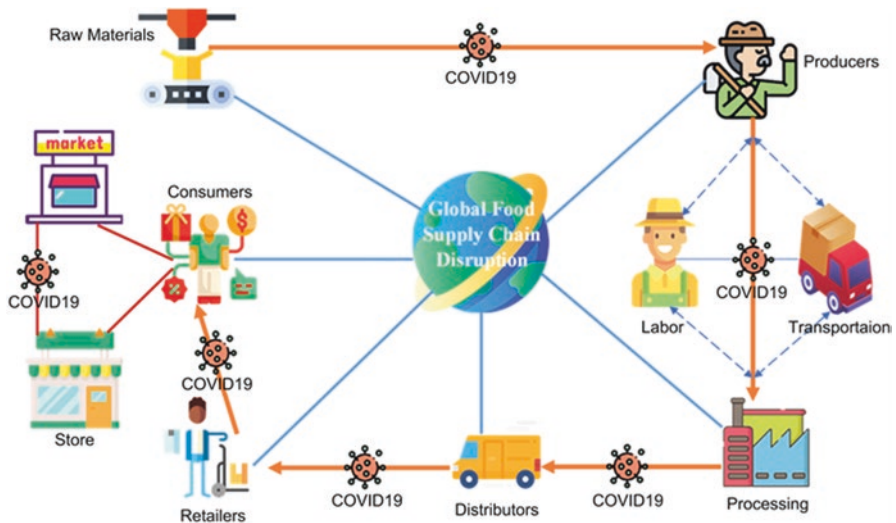


Fig. 24.2 The effect of COVID-19 pandemic on supply chains. (Nasereldin et al. 2021)



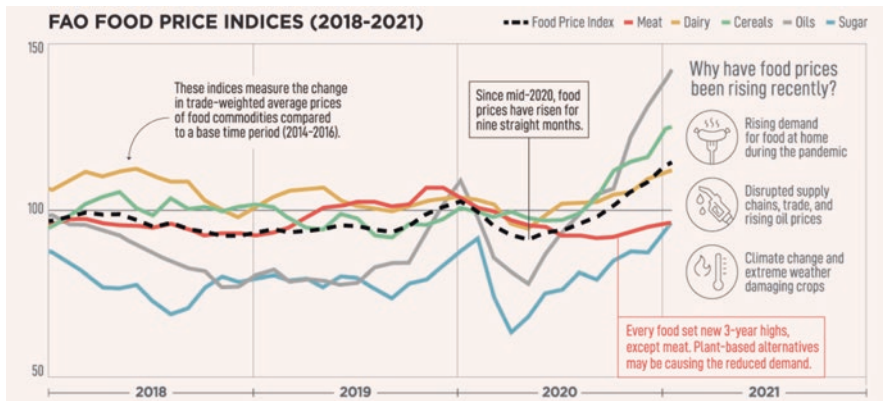


Fig. 24.3 Food prices in 2021. (Elements Report 2021)

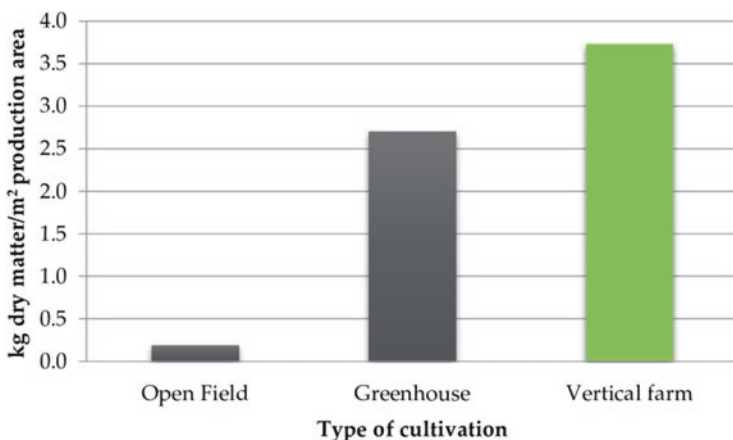
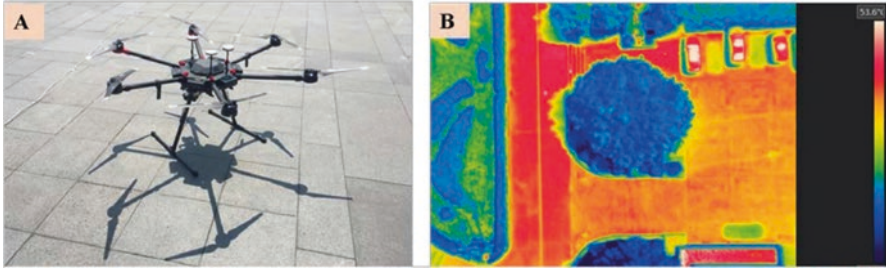


Fig. 24.4 A yield comparison of farming methods (Martin & Molin 2018)

Greenhouses are structurally covered with glass, plastic sheets, and films (Maraveas 2019). These materials are vulnerable against environmental issues such as winds, heavy rains, and hail of rain. The greenhouse structure can easily get damaged by both natural and unnatural causes, and this is a huge drawback for this farming model. The thermal management of a greenhouse is both crucial for plant health and the energy leakage. Occurrence of these problems could be inspected using remote sensing devices, which are UAVs. This paper presents a use case for a UAV with thermal imaging capability that can perform inspection over greenhouse zones at night and identify heat leakage.



**Fig. 24.5** A combination of the remote sensing platform and thermal image. (Zheng et al. 2018)

### 24.3 Greenhouse Inspection Using UAVs

There are many applications that synthesized UAV platforms with thermal imagery techniques: search and rescue operations (Rudol & Doherty 2008); agricultural uses (Messina & Modica 2020); PV panel health inspections (Quarter et al. 2014).

Figure 24.5 provides a good presentation of a thermal camera equipped hexacopter type UAV. The hexacopter UAV type is a multirotor UAV configuration that offers a good combination of both payload margin and flight time with a good gust resistance during the flight.

Multirotor UAVs configurations offer operational advantages against fixed wing UAVs such as runaway requirement and the ability to hover. Also, ease in pilotage should also be mentioned during the evaluation of two configurations. Both manually or autonomously, these inspections can be performed around the greenhouses in regular periods or after meteorological events autonomously. Figure 24.5 shows a thermal image of a greenhouse taken using infrared camera at 11:00 am.

Fig. 24.6 provides valuable information about the thermal performance of the greenhouse. Apart from leaking zone identification, the overall thermal inspections for greenhouses can be cost efficiently and autonomously performed by UAVs.

### 24.4 Conclusions

In this study, a conceptual use case and service model are presented regarding agriculture and civil UAV applications. The paper could be beneficial for entrepreneurs and farming organizations considering cost-efficient services. The paper has addressed many problems such as food security, advantages of greenhouses, UAV applications, and greenhouse structural considerations. The environmental and social requirements urge researchers and industrial stakeholders to provide solutions or control mechanisms that address previously mentioned problems. The usage of thermal imagery and UAV combination could be beneficial for both the energy management in the greenhouses and structural inspections of greenhouses after meteorological events.

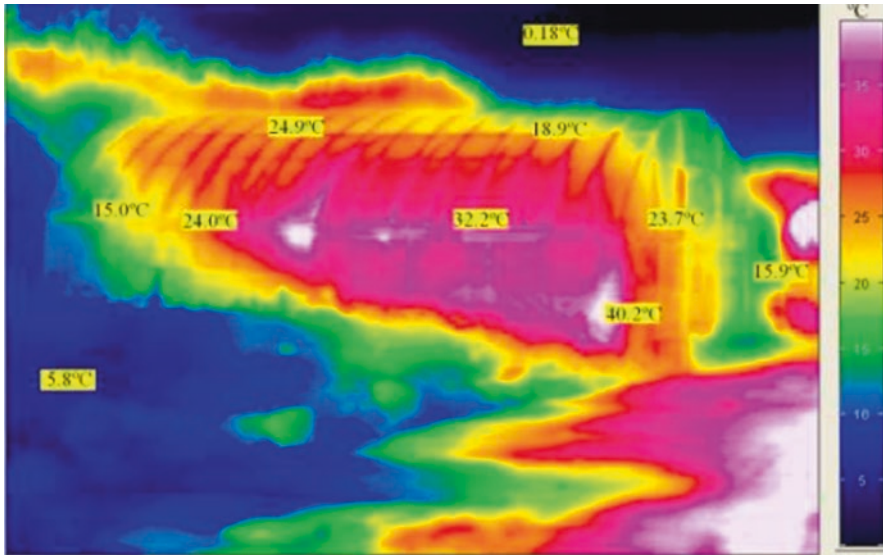


**Fig. 24.6** Thermal inspection of a greenhouse. (Lee et al. 2012)

**Acknowledgments** The research was funded by the Eskisehir Technical University with project code of 20ADP141.

## References

- M. Aghaei, P. Bellezza Quater, F. Grimaccia, S. Leva, M. Mussetta, Unmanned aerial vehicles in photovoltaic systems monitoring applications, in *European photovoltaic solar energy 29th conference and exhibition*, (2014), pp. 2734–2739
- I. Al-Helal, A. Alsadon, S. Marey, A. Ibrahim, M. Shady, A. Abdel-Ghany, Geothermal Energy Potential for Cooling/Heating Greenhouses in Hot Arid Regions. *Atmosphere* **13**(1), 105 (2022)
- A. Cappelli, E. Cini, Will the COVID-19 pandemic make us reconsider the relevance of short food supply chains and local productions? *Trends Food Sci. Technol.* **99**, 566 (2020)
- L. Chenarides, M. Manfredo, T.J. Richards, COVID-19 and food supply chains. *Appl. Econom. Perspect. Policy* **43**(1), 270–279 (2021)
- M. De Clercq, A. Vats, A. Biel, *Agriculture 4.0: The future of farming technology* (Proceedings of the World Government Summit, Dubai, UAE, 2018), pp. 11–13
- G. Devi, N. Sowmiya, K. Yasoda, K. Muthulakshmi, K. Balasubramanian, Review on application of drones for crop health monitoring and spraying pesticides and fertilizer. *J. Crit. Rev.* **7**, 667–672 (2020)
- Elements Report. <https://elements.visualcapitalist.com/shrinking-portions-visualizing-rising-food-prices/>. Accessed on 15 Oct 2021.
- A. Ellenberg, L. Branco, A. Krick, I. Bartoli, A. Kotsos, Use of unmanned aerial vehicle for quantitative infrastructure evaluation. *J. Infrastruct. Syst.* **21**(3), 04014054 (2015)
- M.K. El-Nemr, A. Elgebaly, A.I. Ghazala, Optimal Sizing of Standalone PV-Wind Hybrid Energy System in Rural Area North Egypt. *J. Eng. Res.* **5**(4), 46–56 (2022)

- G.J. Grenzdörffer, A. Engel, B. Teichert, The photogrammetric potential of low-cost UAVs in forestry and agriculture. *Int. Arch. Photogramm. Remote. Sens. Spat. Inf. Sci.* **31**(B3), 1207–1214 (2008)
- S. Lee, S.H. Kim, B.K. Woo, W.T. Son, K.S. Park, A study on the energy efficiency improvement of greenhouses—with a focus on the theoretical and experimental analyses. *J. Mech. Sci. Technol.* **26**(10), 3331–3338 (2012)
- X. Liang, Y. Wang, J. Pyörälä, M. Lehtomäki, X. Yu, H. Kaartinen, et al., Forest in situ observations using unmanned aerial vehicle as an alternative of terrestrial measurements. *Forest Ecosyst.* **6**(1), 1–16 (2019)
- Y. Liu, X. Ma, L. Shu, G.P. Hancke, A.M. Abu-Mahfouz, From Industry 4.0 to Agriculture 4.0: Current status, enabling technologies, and research challenges. *IEEE Transact. Industr. Informat.* **17**(6), 4322–4334 (2020)
- C. Maraveas, Environmental sustainability of greenhouse covering materials. *Sustain. For.* **11**(21), 6129 (2019)
- Martin, M., & Molin, E. (2018). Assessing the energy and environmental performance of vertical hydroponic farming.
- U. Mc Carthy, I. Uysal, R. Badia-Melis, S. Mercier, C. O'Donnell, A. Ktenioudaki, Global food security—Issues, challenges and technological solutions. *Trends Food Sci. Technol.* **77**, 11–20 (2018)
- G. Messina, G. Modica, Applications of UAV thermal imagery in precision agriculture: State of the art and future research outlook. *Remote Sens.* **12**(9), 1491 (2020)
- Y.A. Nasereldin, R. Brenya, A.P. Bassey, I.E. Ibrahim, F. Alnadari, M.M. Nasiru, Y. Ji, Is the global food supply chain during the COVID-19 pandemic resilient? a review paper. *Open J. Busin. Manage.* **9**(01), 184 (2021)
- F. Nex, F. Remondino, UAV for 3D mapping applications: A review. *Appl. Geomat.* **6**, 1–15 (2014)
- S. Nižetić, Impact of coronavirus (COVID-19) pandemic on air transport mobility, energy, and environment: A case study. *Int. J. Energy Res.* **44**(13), 10953–10961 (2020)
- C.Y.N. Norasma, M.A. Fadzilah, N.A. Roslin, Z.W.N. Zanariah, Z. Tarmidi, F.S. Candra, Unmanned aerial vehicle applications in agriculture, in *IOP Conference Series: Materials Science and Engineering*, vol. 506, No. 1, (IOP Publishing, 2019), p. 012063
- E. Özbek, G. Yalin, S. Ekici, T.H. Karakoc, Evaluation of design methodology, limitations, and iterations of a hydrogen fuelled hybrid fuel cell mini UAV. *Energy* **213**(118), 757 (2020)
- P.B. Quater, F. Grimaccia, S. Leva, M. Mussetta, M. Aghaei, Light Unmanned Aerial Vehicles (UAVs) for cooperative inspection of PV plants. *IEEE J. Photovolt.* **4**(4), 1107–1113 (2014)
- Researchandmarkets. <https://www.researchandmarkets.com/reports/4771948/drones-market-growth-trends-covid-19-impact#rela1-5513572>. Accessed on 27 Aug 2021.
- D.C. Rose, J. Chilvers, Agriculture 4.0: Broadening responsible innovation in an era of smart farming. *Front. Sustain. Food Syst.* **2**, 87 (2018)
- P. Rudol, P. Doherty, Human body detection and geolocalization for UAV search and rescue missions using color and thermal imagery, in *In 2008 IEEE aerospace conference*, (Ieee, 2008), pp. 1–8
- F.A. Vega, F.C. Ramirez, M.P. Saiz, F.O. Rosua, Multi-temporal imaging using an unmanned aerial vehicle for monitoring a sunflower crop. *Biosyst. Eng.* **132**, 19–27 (2015)
- C. Wang, X. He, X. Wang, Z. Wang, H. Pan, Z. He, Testing method of spatial pesticide spraying deposition quality balance for unmanned aerial vehicle. *Transact. Chinese Soc. Agric. Eng.* **32**(11), 54–61 (2016)
- H. Yao, R. Qin, X. Chen, Unmanned aerial vehicle for remote sensing applications—A review. *Remote Sens.* **11**(12), 1443 (2019)
- Z. Zhai, J.F. Martínez, V. Beltran, N.L. Martínez, Decision support systems for agriculture 4.0: Survey and challenges. *Comput. Electron. Agric.* **170**, 105,256 (2020)
- S. Zheng, J.M. Guldmann, Z. Liu, L. Zhao, Influence of trees on the outdoor thermal environment in subtropical areas: An experimental study in Guangzhou, China. *Sustain. Cities Soc.* **42**, 482–497 (2018)

# Chapter 25

## Applications of Drone Control & Management in Urban Planning



Dinh-Dung Nguyen, Utku Kale, Muhammed Safa Baş, Munevver Ugur,  
and T. Hikmet Karakoc 

### Nomenclature

ATM	Air Traffic Management
SD	Safe Distance
UAV	Unmanned Aerial Vehicle
UTM	UAV Traffic Management

### 25.1 Introduction

Recently, the world's leading scientists and high-tech pioneers have announced their intention to develop and manufacture a wide range of affordable small controlled from a distance or self-managed flying vehicles known as drones (unmanned aerial vehicles/systems—UAV, UAS, including even small pilot-less air vehicles, or air taxis). A variety of UAVs (unmanned aerial vehicles) have been widely exercised in both civil and military services, resulting in excellent utilization efficiency (Loh

---

D.-D. Nguyen (✉)

Le Quy Don Technical University, Faculty of Aerospace Engineering, Hanoi, Vietnam

e-mail: [dungnd@lqdtu.edu.vn](mailto:dungnd@lqdtu.edu.vn)

U. Kale

Budapest University of Technology and Economics, Department of Aeronautics and Naval Architecture, Budapest, Hungary

e-mail: [kale.utku@kjk.bme.hu](mailto:kale.utku@kjk.bme.hu)

M. S. Baş

University of Debrecen, Faculty of Engineering, Debrecen, Hungary

M. Ugur

Eskisehir Technical University, Department of Remote Sensing and Geographical Information Systems, Eskişehir, Turkey

T. H. Karakoc

Faculty of Aeronautics and Astronautics, Eskişehir Technical University, Eskişehir, Türkiye

et al. 2009; Greenwood et al. 2019; Ramesh and Jeyan 2020). Moreover, drones are expected to play a vital part in the smart city with a number of use cases, including transportation (Kellermann et al. 2020), medical (Rosser Jr et al. 2018), and agricultural industries (Dileep et al. 2020), in addition to military applications.

On the other hand, a serious obstacle prevents the rapid integration of drones into present city operations, particularly in smart city designs, where mobility is a key consideration (Foina et al. 2015; Dung 2020). The current air traffic management systems (ATM) are not able to control the indicated amount of drones that operate at lower altitudes in the urban region between tall and large structures and complex environmental circumstances due to limitations in system capacity, the required workforce, the expected cost, and the required duration of system development (Wilson 2018; Ramee and Mavris 2021).

The focus of this research is to propose methods for identifying parameters in a mathematical model of a drone as a control object, as well as to merge drone management and control systems. To provide a drone management system and their transportation, particularly in smart cities, operational concepts for drone operations in urban areas must be presented, including airspace design, recommended airway construction, and critical safety standards. Drone-following models, which represent the one-by-one following process of drones in traffic flow, are also required for the analysis of drone traffic safety and the development of an intelligent transportation system. The two main drone-following models discussed in this study are the SD models and the Markov drone-following model.

## 25.2 Parameters of Mathematical Model of Drones

Theoretically, identifying an unknown drone parameter may be accomplished in two ways: one, by directly calculating the drone's geometry, and the other, by analyzing the flight data. The first technique demands complex mathematical and physical computations with a high processing workload; however, the second technique just requires a simple algorithm that produces more precise results than the first technique.

The least-squares error method is an identification method utilized in this research. It is a technique that enables determining the mathematical model of an object with high efficiency, with those of the control based on data from input and output signals to the controlling object based on a recognition algorithm that is being used to determine a drone, such as precisely the following: The mathematical model simulates, then data is gathered to carry out the identification. The identification results are then assessed by comparing the pattern model to various input signals.

Additionally, drones, particularly quadrotors, were developed to be hand-operated, thus distinguishing input and output data using onboard sensors to establish the mathematical model would build a somewhat realistic, more accurate mathematical model using the modeling method. Furthermore, the least-squares

error method's approach is simple to comprehend and implement, and it allows for the computation of variables, resulting in a mathematical model of a controlled element that is generally accurate.

### 25.3 Drone Management Systems

The growing number of drones offers significant issues in aviation, particularly in air traffic control. As a result, different operational characteristics must be developed to protect daily flights in terms of safety and implementation by operators. The suggestion of UAV traffic management systems (UTM) is to assist in the successful completion of the flight and effective control of overall air traffic. A system such as this might be controlled to improve the separation between UAVs and aircraft that have been used on regular flights, as well as traffic flow order in extremely low-level airspace regions. Because of the data it receives, this system operates independently of air traffic management systems (ATM). Moreover, because drones fly in 3D space, they are affected by strong gusts of wind flow. Isolation from structures and air turbulence is a problem that is more complicated than it is for road vehicles.

Drone management is divided into six categories, each of which is based on a systematic concept:

1. Non-detected objects: those that do not occur on the surveillance screen;
2. Detected objects: those that do occur on the surveillance screen, although it is uncertain if they are passive, non-cooperating, or demonstrate non-relevant targets, such as birds;
3. Semi-active or simple cooperative objects: which give the operation center with at minimum partial relevant data;
4. Active or cooperative objects or service providers: those submit data on the objects located in the urban setting; accessible data should also include data on the vehicle type, its identification number, load, current position, intention, and the final route;
5. Connecting vehicles that cooperate and coordinate their motions passively or actively, e.g., flying in order, or utilizing conflict detection and resolution based on information being presented; and
6. Contract-based drones with certain preferences, that are contract-based and therefore must pay for the service offered.

Management and control of air traffic and the flights for drones or groups of drones are in high demand. Drones could be programmed to follow predetermined paths or corridors. Sensor fusion, fixed trajectory flowing models, centralized dynamic sectorization, active management, real-time GIS support, preset flight configurations such as flight drone following models, coordinated maneuvers, active disaster detection and resolution, and formation flights should all be used to assist and guide the drone operation. Drones flying in city areas are likely to operate at lower heights and between structures in the sky, going to create a lot of turbulence, which is



generated in effect by wind (flow) separation from buildings. Therefore, certain automation approaches, such as vehicle following models, are possibly drastically dissimilar and unlikely in vehicle and drone traffic. Thereby, flying across a tight gap is one of the most difficult autonomous drone control challenges. It necessitates the drone passing through the center with its level aligned with the gap's positioning, reducing the possibility of a crash. The one-by-one following drone method in "narrow corridors" between the residences without the need for a conventional planning and control piping system is one solution for this issue.

## 25.4 Drone Following Models

The drone following models are one of the most important elements of the drone management system. They are models that calculate the drone's acceleration based on the velocities and distances between the particular drone and the drone that is leading. Drone-following models are being designed to produce realistic speed profiles, the capacity to produce actual traffic flows, steady awareness of traffic conditions, modeling of traffic situations noticed by varying configurations of drones and control system variables, and the ability to implement them in traffic control systems.

First, the drone-following techniques are effective on the concept of maintaining a safe distance depending on the relative velocity (SD models). As a result of this technique, linear models were developed, in which the controller of the pursuing drone adjusts the accelerator to maintain relative speed with the leading drone. The SD models can be used to simulate traffic conditions in a number of different ways. They do, however, have two limitations: the constants used in the drone models are generally derived from real traffic scenarios and sustaining controller quality. Since SD models are having difficulties adjusting for advanced controllers. The Markov chain process is an advanced model which is based on an estimate of the stochastic diffusion process of speed determination. The controllers' inputs receive the appropriate adjustments in velocity from speed variations and relative distance differences between the drones. This method is more comprehensive than the SD models because the Markov chain process can work with extreme situations.

## 25.5 Results

The main findings from the simulation analysis of various drone management system applications are presented in this section.



### 25.5.1 *Experimental Result of the Difference Between Real-Desired Trajectories*

In the simulation, drones flying in an urban environment were controlled using a cloud-based method in research studies, which included the physical, cloud, and control aspects. Figure 25.1 shows the outcome of the experiment. The drone was originally put in a rest position. Once a drone receives a GCS signal, it takes off on a mission to arrive at the waypoints that have been specified. The results reveal that the desired and actual courses mostly coincide with each other. The difference between the two trajectories demonstrates the GPS location since the drone obtains the GPS location data.

### 25.5.2 *Calculation Result of Desired Orbit Landing for a Drone*

The ideal landing orbit is calculated based on the landing zones, and to provide a drone's landing precisely to the target location. Figures 25.2 and 25.3 demonstrate the simulation outcomes for a drone landing in the indicated direction.

## 25.6 Conclusion

There are three major issues that need to be solved about the management of drones:

- Design of flight networks, including a safety net of planned flight paths



Fig. 25.1 Blue line – real trajectory; purple line – requested trajectory

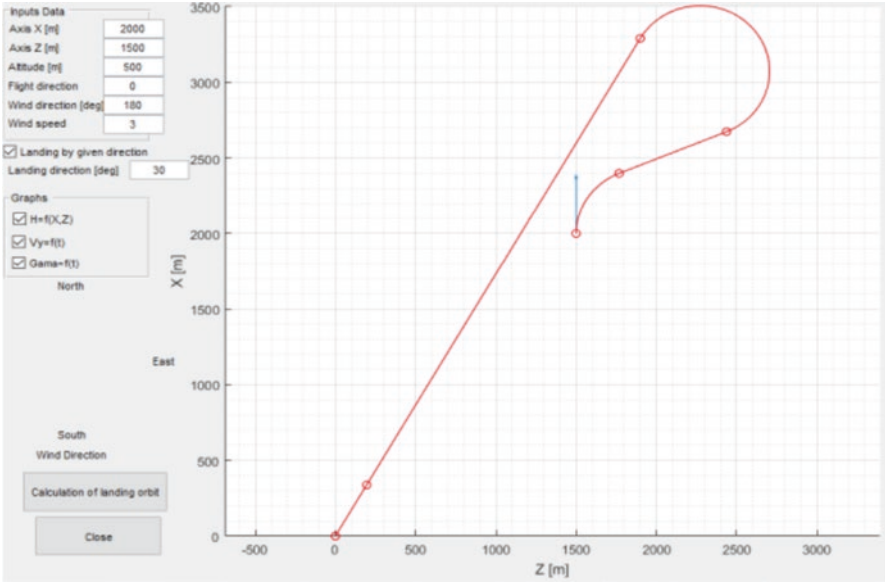


Fig. 25.2 Required landing course of a drone

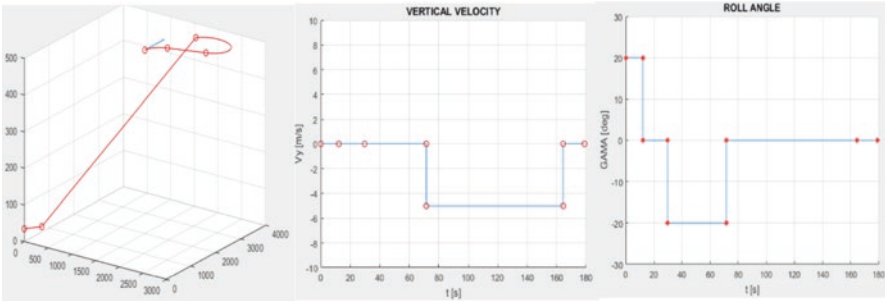


Fig. 25.3 The altitude, vertical velocity, and roll angle change when a UAV gave an instruction to land

- Defining fundamental legal requirements for traffic flow (such as separation requirements) and path of the flight (trajectory)
- Establishing a number of methods and solutions enabling secure flight conditions (such as detection and resolutions of the conflict, group flights, drone following models, etc.)

In this research paper, assembling drone management systems including the drone flow methodologies with parametric mathematic models has been suggested. To accomplish this purpose, we first offer parameters of the mathematical model of drones, particularly in quadrotors. Afterwards, we presented several methods for designing and operating drone management systems, for instance, obstacle

avoidance, the desired trajectory following management, and the required landing trajectory. Finally, we presented one of the key parts of the drone management system, drone following models with SD methods and Markov chain process to create safe flying conditions.

## References

- M.R. Dileep, A.V. Navaneeth, S. Ullagaddi, A. Danti, A study and analysis on various types of agricultural drones and its applications, in *2020 fifth international conference on research in computational intelligence and communication networks (ICRCICN)*, (2020), pp. 181–185
- N.D. Dung, Developing models for managing drones in the transportation system in smart cities. *Electr. Control. Commun. Eng.* **15**, 71–78 (2020). <https://doi.org/10.2478/ecce-2019-0010>
- A.G. Foina, R. Sengupta, P. Lerchi, Z. Liu, C. Krainer, Drones in smart cities: Overcoming barriers through air traffic control research, in *2015 workshop on research, education and development of unmanned aerial systems (RED-UAS)*, (2015), pp. 351–359
- R. Kellermann, T. Biehle, L. Fischer, Drones for parcel and passenger transportation: A literature review. *Transport. Res. Interdiscipl. Perspect.* **4**, 100088 (2020). <https://doi.org/10.1016/j.trip.2019.100088>
- R. Loh, Y. Bian, T. Roe, UAVs in civil airspace: Safety requirements. *IEEE Aerosp. Electron. Syst. Mag.* **24**, 5–17 (2009). <https://doi.org/10.1109/MAES.2009.4772749>
- C. Ramee, D.N. Mavris, Development of a framework to compare low-altitude unmanned air traffic management systems, in *AIAA Scitech 2021 Forum*, (American Institute of Aeronautics and Astronautics, 2021)
- P.S. Ramesh, J.V.M.L. Jeyan, Comparative analysis of the impact of operating parameters on military and civil applications of mini unmanned aerial vehicle (UAV). *AIP Conf. Proc.* **2311**, 30034 (2020). <https://doi.org/10.1063/5.0033989>
- J.C. Rosser Jr., V. Vignesh, B.A. Terwilliger, B.C. Parker, Surgical and medical applications of drones: A comprehensive review. *JSLs: J. Soc Laparoendosc. Surg.* **22**, e2018.00018 (2018). <https://doi.org/10.4293/JSLs.2018.00018>
- W.W. Greenwood, J.P. Lynch, Z. Dimitrios, Applications of UAVs in civil infrastructure. *J. Infrastruct. Syst.* **25**, 4019002 (2019). [https://doi.org/10.1061/\(ASCE\)IS.1943-555X.0000464](https://doi.org/10.1061/(ASCE)IS.1943-555X.0000464)
- I.A. Wilson, Integration of UAS in existing air traffic management systems connotations and consequences, in *2018 integrated communications, navigation, surveillance conference (ICNS)*, (2018), pp. 2G3-1–2G3-7

# Chapter 26

## Imaging Techniques Based on Unmanned Aerial



Alpaslan Durmuş  and Erol Duymaz 

### Nomenclature

UAV	Unmanned Aerial Vehicle
GNSS	Global Navigation Satellite System
GPS	Global Positioning System
UV	Ultraviolet
NIR	Near Infrared
SWIR	Shortwave infrared
VNIR	Visible and Near-Infrared
LiDAR	Light Detection and Ranging
UV–VIS	Visible Spectrophotometry
EMS	Electromagnetic Spectrum
HSI	Hyperspectral Imaging
RGB	Red Green Blue Visible Imaging
LiDAR	Light Detection and Ranging
SAR	Synthetic aperture radar

### 26.1 Introduction

In recent years, with the rapid development of the economy and society, great changes are constantly occurring on the world's surface. Therefore, it is in great demand to obtain remote sensing data of specific regions and update their geographic information flexibly and quickly. The UAV-based photogrammetric data acquisition system requires only a control system and a small UAV platform with a standard digital camera. Thus, the entire UAV system can be installed at a much

---

A. Durmuş (✉) · E. Duymaz  
Ostim Technical University, Ankara, Türkiye  
e-mail: [alpaslan.durmus@ostimteknik.edu.tr](mailto:alpaslan.durmus@ostimteknik.edu.tr); [abdulhamit.sevgi@ostimteknik.edu.tr](mailto:abdulhamit.sevgi@ostimteknik.edu.tr);  
[cebrail.olmez@ostimteknik.edu.tr](mailto:cebrail.olmez@ostimteknik.edu.tr)

lower price compared to digital photogrammetric systems. For these reasons, the application of UAV platforms in photogrammetric data capture can be very reasonable, especially in areas of limited scope. An example of an imaging system is given in Fig. 26.1.

UAV, colloquially known as drone, offers a new remote sensing technique that can be a viable and cost-effective alternative to traditional approaches as it reduces costs and increases the spatial resolution of aerial images. In recent years, technical development, component miniaturization, and increased sales have resulted in the rapid growth of UAV as an environmental remote sensing platform. In contrast, conventional acquisition of aerial images by aircraft is often more detailed and expensive, as it requires more operating personnel and detailed long-term planning. As a result, its use mostly covers large areas (50–100 km<sup>2</sup>), which is one of its biggest disadvantages. However, UAV technologies are much more economical, flexible, and faster, especially for environmental monitoring issues that focus on small or medium-sized areas where higher coverage rates are needed (Colomina and Molina 2014). As the technical preparation and launch of a UAV mission can usually be completed in less than 1 hour, even short periods of time are sufficient to acquire high-resolution image data to detect any object or track its actions over time. An example image obtained by UAV systems is given in Fig. 26.2.

Small model aircraft, also called fixed-wing UAV as an alternative to the widely used multi-rotor drones, have proven successful as a peripheral remote sensing platform (Laliberte et al. 2011; Colomina and Molina 2014). Thanks to the elevation created by the airflow over the wings and more efficient aerodynamics, these platforms offer the advantage of longer flight times at higher speeds and greater payloads and can thus cover larger research areas per flight compared to other multi-rotor systems. In addition, thanks to its simple structure and control electronics, it is sensitive to daily use and has low maintenance and repair costs. Several companies (e.g., SenseFly, QuestUAV, Gatewing, Trimble) offer ready-to-fly fixed-wing UAVs



**Fig. 26.1** (a) UAV platform designed for imaging; (b) multispectral; and (c) thermal camera systems

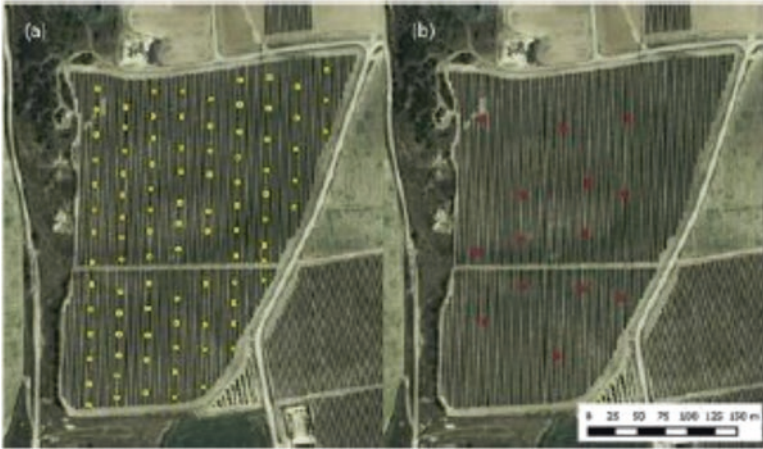


**Fig. 26.2** Example of land image acquisition and mapping



**Fig. 26.3** Fixed-wing UAV system

(including full autopilot control and camera sensors) that meet the criteria for practical applications in environmental management. However, the number of known practical applications of fixed-wing UAVs is still low. The main reasons for this may be the high costs of professional fixed-wing UAVs, technical complexities, or lack of skills in operating such systems. In addition, the required specialist knowledge in image processing and analysis is often lacking, and commercial Geographic Information Systems (GIS) and remote sensing softwares are expensive. As a result, interpretation of aerial photography is still limited to visual image interpretation, which is often time consuming. The fixed-wing UAV system is given in Fig. 26.3.

In UAV-based imaging systems, the optimum carrier and payload combination should be set after the system requirements are determined. In practice, attention should generally be paid to the specific volume, weight, and power characteristics of the UAV as well as serving specific application requirements (sensing, bandwidth, accuracy, resolution, etc.). Finding the right balance is not only difficult, but

also complex. For this reason, while making these choices, attention should be paid to the selection of the system for the task.

## **26.2 UAV Imaging Systems and Example Applications**

Various sensors and cameras are used for aerial and space image acquisition systems. This section focuses on remote sensing tools that may be suitable for micro, mini and tactical UAV payloads, especially distinguishing between visible band, near infrared, multispectral, hyperspectral, thermal, laser scanners, and synthetic aperture radar.

### ***26.2.1 Near Infrared and Multi-Spectral Cameras***

Organizations working in the photogrammetric and remote sensing field have leveraged the power of the mass market and other professional markets by leveraging them to design high-resolution remote sensing tools. Near Infrared (NIR) is a subset of the infrared band of the electromagnetic spectrum, which covers wavelengths ranging from 0.7 to 1.4 microns. This wavelength is just outside the range that humans can see and can sometimes offer clearer details than can be achieved with visible light imaging. NIR is very close to human vision but removes color wavelengths, which causes most objects to look very similar to an image converted to black and white. An exception are trees and plants that are highly reflective at the NIR wavelength and therefore appear much brighter than they are in colour. Spectral Instruments' unique pixelated multispectral filter array technology enables a single camera sensor to work like a combination of many cameras. It is available in three different types: standard snapshot cameras, dash-scan cameras, and the new mini snapshot cameras.

### ***26.2.2 Hyperspectral Cameras***

Remote sensing with hyperspectral cameras deals with imaging narrow spectral bands in a continuous spectral range, producing spectra of all pixels in the scene. In contrast, multispectral remote sensing produces discrete bands and generally has a lower spectral resolution. Therefore, hyperspectral sensors extract more detailed information than multispectral sensors, as the entire spectrum is acquired in each pixel. Unlike visible-spectrum camera developments that reach hundreds of grams of weight and tens of megapixel resolution, the miniaturization process of multi- and hyper-spectral cameras is demanding in terms of optics and sensor calibration.

Studies in agriculture and forestry involving UAVs and hyperspectral sensors are reviewed with a focus on their core objectives and general processing and analysis approaches. Although there are a significant number of applications, it is still observed to be of rare use compared to applications involving UAVs and other types of sensors, possibly due to the high-resolution spectroscopy costs that could compromise cost-effectiveness in agroforestry and related applications.

### ***26.2.3 Thermal Cameras***

The thermal camera is an imaging system that is based on invisible IR energy (heat) as an imaging method and determines the general structure of the image, colors, and shapes formed according to IR energy. It can also be used for security purposes in general, but it is also open to the use of a wide variety of sectors. Especially with the development of heat-guided missiles, night vision systems and similar military techniques, its importance has increased (Boesch 2017).

### ***26.2.4 Laser Scanners***

Light Detection and Ranging (LiDAR) is basically a remote sensing method that uses laser or light for measurement. Although it is a savior method for complex objects or regions that are impossible to measure in the map sector, it is also heavily involved in the classical construction stages. On the other hand, autonomous, that is, driverless vehicles, which is one of the trends of today's technology, can move in a controlled manner with a kind of laser eye by making instant data generation and analysis while using this method.

### ***26.2.5 Synthetic Aperture Radar***

Synthetic Aperture Radar (SAR) technology has come a long way in conventional remote sensing. However, its adaptation to the UAV is still unresolved. However, few studies have been conducted around the world on the use of this technology. The good performance of SAR despite bad weather conditions is a very useful feature not only for military groups that have traditionally supported SAR technology, but also for other civilian photometry organizations.



## 26.3 Results

Remote sensing is a well-known technique for agriculture and environmental analysis. Vegetation or biodiversity control has traditionally been accomplished using aerial and/or satellite imagery, which incurs high costs when precision resolution is required. The UAV is a smaller, cheaper to use and successful system among the remote sensing community. The range of available sensors are expanding in a natural attempt to adapt to smaller platforms where weight and size restrictions apply as opposed to manned aerial platforms, as well as to adapt to user-application needs. Aerial observation by unmanned platforms has mainly been supported in a military context. Indeed, a small, particularly handheld or hand-launched UAS can provide an army's ground troops with an "overhead" view to avoid potential unseen hazards. In larger UAS categories, large drones provide wide area surveillance, i.e., border control and restricted area surveillance. UAS have also been used as communication relays to increase battlefield awareness or as decoys to fool the enemy's radars. Near-military, search-and-rescue, or disaster management missions share many objectives with those previously mentioned (basically providing quick snapshots from an area where no supporting structures can be assumed) and thus can be somewhat classified as Intelligence, Surveillance, and Reconnaissance (ISR) missions.

## 26.4 Conclusion

Various use case examples of UAV aerial imagery studies are among the ongoing studies. As a result of such developments, UAVs have started to become standard platforms for applications aiming to capture photogrammetric data. Within the scope of this study, UAV-based photogrammetry and remote sensing systems and data collection techniques and applications are examined and the efficiency and quality of the latest technology digital aerial camera systems are examined.

## References

- R. Boesch, Thermal remote sensing with UAV-based workflows. *ISPRS Int. Arch. Photogram. Remote Sens. Spatial Inf. Sci.* **XLII-2/W6**, 41–46 (2017)
- I. Colomina, P. Molina, Unmanned aerial systems for photogrammetry and remote sensing: a review. *ISPRS J. Photogramm. Remote Sens.* **92**, 79–97 (2014). <https://doi.org/10.1016/j.isprsjprs.2014.02.013>
- A.S. Laliberte, C. Winters, A. Rango, UAS remote sensing missions for rangeland applications. *Geocarto Int.* **26**, 141–156 (2011). <https://doi.org/10.1080/10106049.2010.534557>

# Chapter 27

## Polarization Effect Between Entropy and Sustainability of Cruise Altitude for Jet-Prop Engine Performance



M. Ziya Sogut

### 27.1 Introduction

Despite the short-term contraction experienced in the aviation sector, with the shrinkage of 62% in the COVID-19 process (Hader et al. 2021), the growth trend in future scenarios provides important work areas in terms of sustainability in scientific studies. In fact, an average of 4.3% increase in the industry is expected in the next 20 years, and this effect is expected to contribute 15.5 million direct jobs and 1.5 trillion dollars to GDP in the world economy (ICAO 2021). All these expectations inevitably increase the consumption of fossil resources in the current structure of the sector and it is inevitable for the sector to develop measures for environmental sustainability in this change.

Aviation's development of environmental sustainability within the sectoral integrity is directly related to prioritizing change based on the environment. McManners (2015) showed that a fundamental change in policies should come to the fore, especially in order to improve environmental sustainability in aviation. However, ensuring sustainability, especially in fossil fuel consumption, requires the development of alternative fuels for existing conventional aircraft (Afonso et al. 2021). In this context, the priority strategies of political development in terms of sectoral targets are, together with sectoral sustainability, neutral carbon growth and reaching the 2050 targets.

Changes in engine technology have provided significant gains in energy efficiency. Although technological improvements create advantageous situations in consumption, constraints in flight processes and air traffic conditions increase consumption inefficiency. For this purpose, for environmental sustainability, reducing fossil fuel consumption and improving energy efficiency in flight processes is a multifaceted problem. The main criterion of inefficiency in engines operating on

---

M. Z. Sogut (✉)  
Maritime Faculty, Piri Reis University, İstanbul, Turkey

thermodynamic principles is irreversibility. According to the second law of thermodynamics, this condition is related to entropy. Particularly, the irreversibility of the engines caused by the power generation process – combustion – is the main source of entropy generation. This is the potential that directly affects environmental sustainability considering flight processes. This effect directly or indirectly expresses an opposite structure between the environment and entropy. In fact, this structure expresses a polarization in terms of pollution or environmental sustainability due to entropy production.

The development of operational control parameters in engines depending on flight position is important for the protection environmental sustainability (IATA,2015). However, evaluating its use in this context or determining the criteria in engines is a process related to thermodynamic parameters. In the literature, the evaluation of aviation based on environmental sustainability is an evaluation based on classical CO<sub>2</sub> emission factors, and it is seen that there are very limited studies apart from this. With the two indicators proposed and cited in this study, it is aimed at evaluating the entropy generation potential and environmental sustainability impact for engines due to inefficiency. Thus, the polarization effect and improvement potential targets between the entropy generation of the jet-prop engine and its environmental sustainability were evaluated for the defined altitude conditions of the engine's performance.

## 27.2 Entropy and Sustainable Aviation

The negative areas created by COVID-19 for all global processes can also be considered an important problem for the aviation industry. In fact, the negative impact of the number of flights has negatively affected the economic sustainability in the sectoral direction. Excluding the COVID-19 process, the energy demand of air transport has been increasing by 6% in the last decade (Sun et al. 2021).

In addition to noise pollution, resource and waste generation are other important environmental impacts from the aviation industry (Karaman et al. 2018; Grosbois 2016). The international nature of the aviation industry extends these negative effects on countries other than the main country that contribute to global climate change. Especially in the 2050 scenarios, it shows that the increase in fossil consumption will continue. Even this can be seen as a problem area for global climate change. In this context, the main question is to see what kind of impact negatively affects this sustainability. In this conceptual approach, it is a result of disorder expressed as entropy. Especially for fossil fuel-based engine technologies, this effect is a result of irreversibility that occurs at every stage for engines operating on a cycle basis. In fact, this analytical approach, based on the improvement of engine efficiency, has a key role, especially for the improvement of environmental sustainability. Especially from design to operational processes, it is shaped as maximizing engine efficiency while minimizing fossil fuel consumption. Before the design of these direct aircraft

systems, it has multi-purpose functions such as optimizing these systems, minimizing fuel consumption, or maximizing energy efficiency (Dong et al. 2018).

### 27.3 Entropy Management for Fly Process

The impact of global warming has caused the temperature to rise as a fundamental factor that negatively affects the manageability of environmental sustainability. While this situation causes an increase in global entropy, the effect of fossil fuel consumption stands out as the main input. Controlling fossil fuel management and the manageability of entropy are essential as key tools. Entropy is a quantitative tool used to describe disorder in system structures. It is a qualitative tool that develops due to structural deformation, especially in flow processes. This value also defines the size of the uncertainty that occurs in the systems. In this context, the main factors affecting the administrative processes of entropy such as system complexity, structure of the elements and irreversibility between them, and flow management, are important factors.

Entropy is the management of all processes based on the fundamentals of performance optimization, especially process usage. These are all elements based on the reduction of exergy destruction for processes (Jing 2012; Markina and Dyachkov 2014). In the aviation industry, the follow-up of emission certificates has become an important issue. Emission evaluation has been an important criterion for this document, which is especially required for aircraft with a thrust power of above 26.7 kN. In this document, which is expressed as a civil aviation contract, the fuselage and engine are direct impact points, together with the engine emissions. In Fig. 27.1, flight processes are followed in terms of and test evaluations are made according to these (Gawron and Bialecki 2016).

For conventional engines with thermal processes, temperature is a key parameter to be monitored. This is not only an environmental criterion, but also one that should

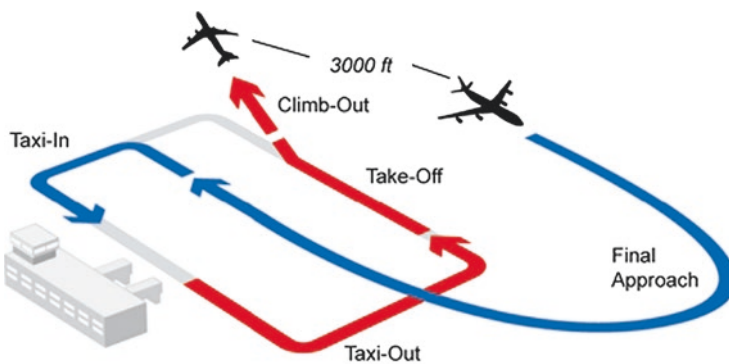


Fig. 27.1 ICAO reference LTO cycle. (Fleuti and Maraini 2012)

be evaluated for the combustion process as well as for the exhaust. It is also an important cause of deformations, especially on the engine. For example, high thrust conditions increase operating temperatures along with fuel consumption. Its continuity is an important criterion for deterioration or deformation. Whereas, thrust management directly affects fuel consumption as power management, together with optimization. Temperature and density should be monitored as inputs for flow processes. Especially at high temperatures, engine operation requires a continuous follow-up and this process should be followed in pilot management. The manageability of engine performance in engine management, especially in flight processes, is a process related to heat or temperature management.

## 27.4 Methodology

Classical engine technologies have a thermodynamically closed system, associated with the combustion process, but an open system with a continuous flow feature. For analyses based on thermodynamic principles, it is necessary to define basic thermodynamic and environmental parameters such as mass, temperature, and pressure. Particularly, establishing the fundamental energy balance depends on the definition of an adiabatically process, as given below.

$$\dot{Q} - \dot{W} + \sum \dot{E}_{in} - \sum \dot{E}_{out} = 0, \quad \text{or} \quad \dot{Q}_{net} + \sum \dot{m}_{in} h_{in} = \dot{W}_{net} + \sum \dot{m}_{out} h_{out} \quad (27.1)$$

In this equation,  $\sum \dot{E}_{in}$  is the total input energy,  $\sum \dot{E}_{out}$  is the total output energy,  $\dot{Q}$  is the total net heat transfer, and  $\dot{W}$  is the net output work. Besides, “h” is the enthalpy of input and output mass (Dincer and Rosen 2012). Based on these concepts of reversibility and absolute temperature, entropy generation is a measure of system disorder due to the exergy destruction produced from the system. For this approach, the second law of thermodynamics and relations criteria such as improvement potential and exergy losses must be prioritized. The basic equations to be used, exergy, for thermodynamic processes, defines the maximum ability to do work that can be provided in a system. In this context, the general exergy balance:

$$\sum \dot{E}_x = \dot{E}_{x,ph} + \dot{E}_{x,ch} + \dot{E}_{x,kin} + \dot{E}_{x,pot} \quad (27.2)$$

Where, “ph, ch, kin, and pot” state physical, chemical, kinetic, and potential exergies. Basic exergy balance for open systems as a thermodynamic process:

$$\sum \dot{E}_{x,in} - \sum \dot{E}_{x,out} = \sum \dot{i} \quad (27.3)$$

For this purpose,  $\sum \dot{E}_{x,in}$  is the total input exergy,  $\sum \dot{E}_{x,out}$  is the total output exergy, and,  $\sum \dot{i}$  is the total exergy destruction. In this structure, the condition in which the kinetic, potential and chemical exergies are neglected refers to the flow exergy. Flow exergy is:

$$\Sigma \left( 1 - \frac{T_0}{T_1} \right) \dot{Q}_c - \dot{W} + \sum \dot{m}_{in} \psi_{in} - \sum \dot{m}_{out} \psi_{out} = \Sigma \dot{i} \quad (27.4)$$

Where,  $\dot{Q}_c$  is the heat transfer rate for passing from system boundary,  $\dot{W}$  is the total net work,  $\psi$  is the flow exergy, and 0 is the dead state of surrounding ( $P_0$  and  $T_0$ ). Flow exergy shows as a form of enthalpy and entropy. The flow exergy is:

$$\psi = (h - h_0) - T_0 (s - s_0) \quad (27.5)$$

For all energy systems, the energy is examined with a balance and the performance impact depends on the efficiency. Efficiency is the direct relationship between output and input energies.

$$\eta = \frac{\Sigma \dot{E}_{out}}{\Sigma \dot{E}_{in}} \quad (27.6)$$

In this equation,  $\dot{E}_{in}$  is the input energy for the engine, and  $\dot{E}_{out}$  is the output energy of the engines. Accordingly, exergy efficiency of the engine is (Cornelissen 1997; Moran et al. 2011):

$$\eta_{11} = \frac{\Sigma \dot{E}_{x,out}}{\Sigma \dot{E}_{x,in}} \quad (27.7)$$

Where,  $\dot{E}_{x,in}$ ,  $\dot{E}_{x,out}$  are total exergy of input and output exergy of the engine, respectively (Moran et al. 2011). Engines, like thermal processes, contain improvement opportunities based on structural features or operational management parameters. This process, defined as the improvement potential (IP) (Van Gool 1997), is expressed by a relationship between the engine's exergy and efficiency:

$$IP = (1 - \eta) (\Sigma \dot{E}_{x,in} - \dot{E}_{x,out}) \quad (27.8)$$

In this study, the environmental performance index that can be used for engines is discussed. This index is a measure of entropy production, which is an important input into environmental pollution. This criterion has a feature that shows the change depending on the ambient temperature for the engines and expresses the size of the entropy production.

$$EPI = \left( \frac{\Sigma S_{gen}}{\Sigma \dot{E}_{x,in}} \right) * T_0 \quad (27.9)$$

EPI has a value less than one as a measure of performance. In terms of the environmental sustainability, it is important that the value approaches zero. However, zero

criterion is unrealistic, and it is necessary to have a reference limit value. For thermodynamic processes, this value is expressed by Carnot efficiency and is a value directly related to exergy efficiency. In this context, it was necessary to re-evaluate the improvement potential, especially depending on the results given below:

$$IP = (\eta_{Carnot} - \eta_{11}) \cdot (\dot{E}x_{in} - \dot{E}x_{out}) \tag{27.10}$$

The sustainable index (SI) identifies process-induced boundary conditions as a direct measure of reversibility. It is used to describe change and performance, especially in association with EPI. SI is:

$$SI = \left( \frac{\sum S_{gen,c}}{\sum \dot{E}x_{in}} \right) * T_0 \tag{27.11}$$

The total entropy production in the system is related to the IP ratio of the engine depending on the Carnot efficiency (Sogut 2021).

### 27.5 Results and Discussion

The jet-prop engine referenced in this study is a modified PA-46-310/350P from the turboprop engine. The performance evaluation is based on the consumption of the engine in two extreme conditions, especially 6000 ft. and 24,000 ft. depending on altitude. Entropy production due to exergy consumption and the environmental impact caused by this, including poles depending on altitude, were investigated. In the study, engine thrust values were taken as constant for both altitude points. Accordingly, the thermal efficiency and exergy efficiency of the engine are given in Fig. 27.2.

In the analysis, a 10.26% change in energy is observed for motor performance between 6000 ft. and 24,000 ft., while a 11.59% change in exergy is observed. This shows that the engines have better performance especially at low cruise

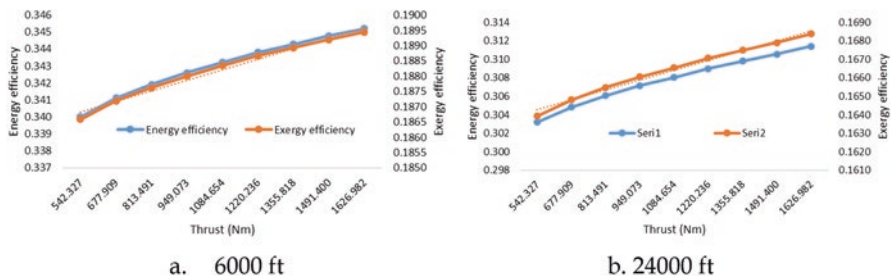


Fig. 27.2 Energy and exergy analysis of flight process

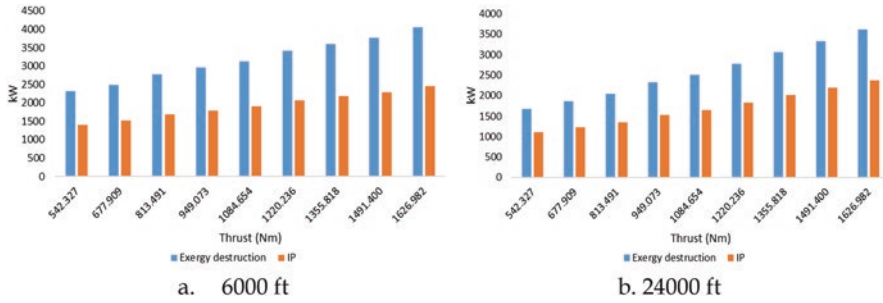


Fig. 27.3 Exergy destruction and IP performance for flight process

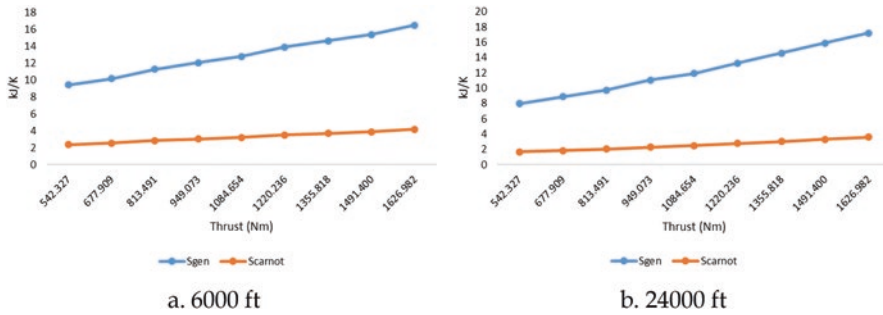


Fig. 27.4 Entropy generation performance for flight process

performance. However, for the performance management of engines, the exergy consumption and the associated improvement potentials are especially valuable due to entropy management. In this context, these values of the engine are given in Fig. 27.3.

Compared to 6000 ft., it is seen that the exergy consumption is on average 18.62% lower at 24,000 ft. The irreversibility effect of the engine shows more effective results for entropy management. The entropy production of the engine based on these data has been examined and the results are given in Fig. 27.4.

Although a similar relationship is seen in entropy production, the controllability of the change for 24 ft. is more effective than the Carnot reference conditions for a sustainable performance evaluation in terms of management. The key point in the carbon management approach is the definition of boundary conditions. In this respect, the improvement point defined for engine consumption primarily depends on environmental conditions. In this respect, it is related to natural control optimization. The relationship of this change with thrust is examined and the results are given in Fig. 27.5.

It has been observed that the IP ratio of the engines has a positive effect at high altitude, especially in terms of entropy. The analysis has shown that this effect, up to 21%, occurs at low thrust for both cruise conditions. In fact, while this effect is 21.18% for 542 nm, it shows a change of 3.38% for 1626 nm. Therefore, starting the



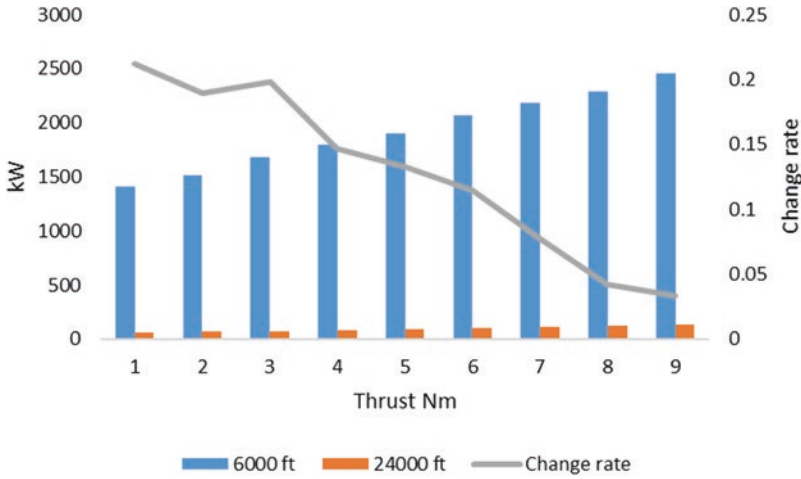


Fig. 27.5 IP effect on thrust and altitude

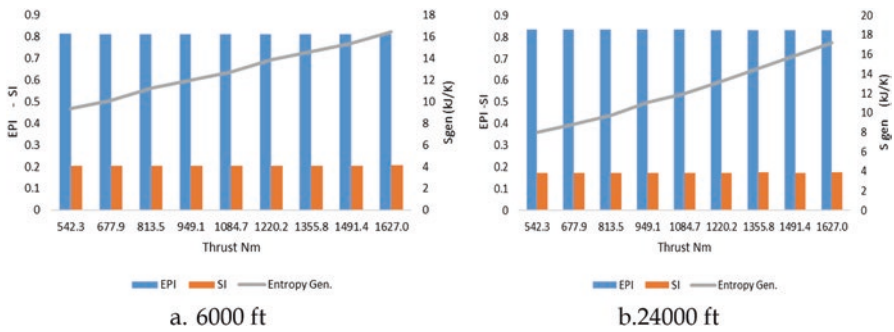


Fig. 27.6 EPI and SI distributions considering entropy generation

engines under high thrust indicates that they have altitude independence, or rather low irreversibility. The effects of the two parameters proposed as environmental indicators in the entropy management of engines for both boundary conditions depending on the cruise condition are handled separately and the results are given in Fig. 27.6.

EPI values for 6000 ft. vary between 0.811 and 0.813, while for 24,000 ft., these values vary between 0.832 and 0.836. The relationship of these distributions with thrust shows opposite properties for each altitude. Accordingly, while at 6000 ft., there is a partially decreasing effect due to thrust, this distribution has an increasing effect at 24,000 ft. The relationship between this situation and the sustainable index and its distributions is also examined together with the entropy production and is examined in Fig. 27.7 for both altitude conditions.

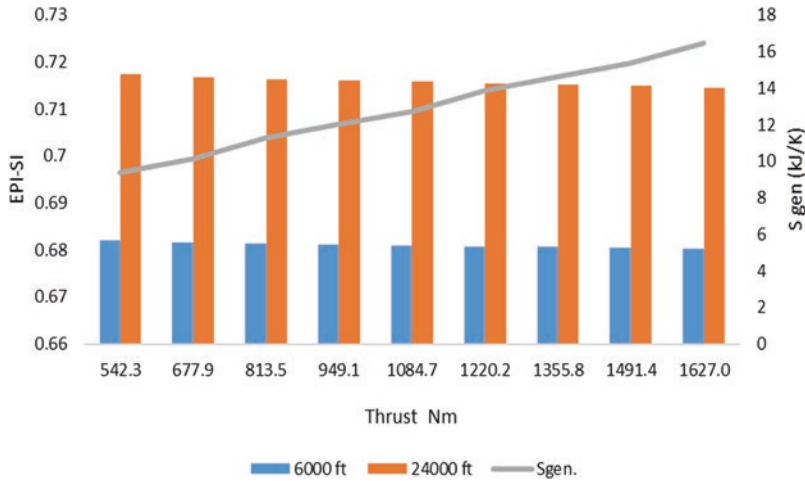


Fig. 27.7 EPI and SI distributions considering entropy generation

For 6000 ft., the potential for environmental impact due to the sustainable index was found to be 68.1%, while for the 24,000 ft. altitude condition, this potential was 71.58%. In this respect, the potential for inefficiency due to high altitude has a higher value. Considering the high entropy generation potential for the investigated engine performance, the target potential of the engine over the improvement limit was found to be 20.47% for 6000 ft., while this potential was 17.45% for 24,000 ft. In this respect, it is predicted that the target boundary conditions for the environmental impact improvement of the engine will be EPI 0.6071 for 6000 ft. This value will be 0.6591 for 24,000 ft.

## 27.6 Conclusion

In this study, with reference to an aircraft engine, the entropy generation due to the irreversibility of the engine in cruise boundary conditions related to the flight process is primarily investigated. The negative effect of atmospheric conditions and especially temperature on entropy production in the cruise conditions of the aircraft is remarkable. In this respect:

- Especially in route management, it is seen that the energy efficiency changes by 10.26% and the exergy efficiency by 11.59%, depending on the process analysis.
- While the energy efficiency of the engine, depending on altitude, was 18.87% at 6000 ft., this value was found to be 16.64% at 24,000 ft.
- At 6000 ft. and 24,000 ft., entropy production averaged 12.87 kJ/K and 12.28 kJ/K, respectively.

- Its EPI was 0.812 for 6000 ft., while its SI was 0.834. The SI values were found to be 0.205 and 0.175 in both conditions, respectively. In the study, the target improvement potential for the engine, which has a very high environmental pollution effect, was found to be 20.47% for 6000 ft. and 17.45% for 24,000 ft.

Two parameters developed in this respect, especially for the manageability of entropy, have been shown to be an effective tool in defining the improvement performances based on irreversibility. Defining targets for environmental improvement potentials of the engine stands out as another advantage. These parametric conditions developed for the engine should also be considered in terms of cost in order to evaluate their sustainability effects.

## References

- Afonso F., Ana F., Inês R., Fernando L., Afzal S. (2021) On the design of environmentally sustainable aircraft for urban air mobility, *Transp. Res. Part D: Transp. Environ.*, **91**, 102688. <https://doi.org/10.1016/j.trd.2020.102688>. ISSN 1361-9209
- R.L. Cornelissen, *Thermodynamics and Sustainable Development: The Use of Exergy Analysis and the Reduction of Irreversibility*, PhD thesis (University of Twente, 1997)
- I. Dincer, M.A. Rosen, *Exergy: Energy, Environment and Sustainable Development* (Elsevier, 2012)
- Z. Dong, D. Li, Z. Wang, M. Sun, A review on exergy analysis of aerospace power systems, *Acta Astronaut.*, **152**, 486–495 (2018). ISSN 0094-5765. <https://doi.org/10.1016/j.actaastro.2018.09.003>
- E. Fleuti, S. Maraini, *Air Quality Assessment Sensitivities (Zurich Airport Case Study, 2012)*
- B. Gawron, T. Białecki, Measurement of exhaust gas emissions from a miniature turbojet engine. *Combust. Engines* **167**(4), 58–63 (2016). <https://doi.org/10.19206/CE-2016-406>
- D. Grosbois, Corporate social responsibility reporting in the cruise tourism industry: A performance evaluation using a new institutional theory based model. *J. Sustain. Tour.* **24**(2), 245–269 (2016)
- M. Hader, R. Thomson, N. de Silva, *Likely Recovery Scenarios, the Latest Industry Thinking and the Key Emerging Trends*. Roland Berger, Visited 11.09.2021, A year on from Covid-19 in the aviation and aerospace industries (Roland Berger, 2021)
- IATA, *IATA 2015 Report on Alternative Fuels*, 10th edn (International Air Transport Association, Montreal—Geneva, 2015). <https://www.iata.org/contentassets/462587e388e749eeb040df4dfd02cb1/2015-report-alternative-fuels.pdf>
- ICAO, *Future of Aviation*, Visited 11.09.2021, Future of Aviation (icao.int) (2021)
- D. Jing, The study on business growth process management entropy model. *Phys. Procedia* **24**, 2105–2110 (2012)
- A.S. Karaman, M. Kilic, A. Uyar, Sustainability reporting in the aviation industry: Worldwide evidence. *Sustain. Account. Manage. Policy J.* **9**(4), 362–391 (2018). <https://doi.org/10.1108/SAMPJ-12-2017-0150>
- I. Markina, D. Dyachkov, Entropy model management of organization. *World Appl. Sci. J.* **30** (Management, Economics, Technology & Tourism), 159–164 (2014). ISSN 1818-4952. <https://doi.org/10.5829/idosi.wasj.2014.30.mett.66>
- P.J. McManners, The action research case study approach: A methodology for complex challenges such as sustainability in aviation. *Action Research* (2015). [OnlineFirst: August 4, 2015 as <https://doi.org/10.1177/1476750315597979>]
- M.J. Moran, H.N. Shapiro, D.D. Boettner, M.B. Bailey, *Fundamentals of Engineering Thermodynamics* (Wiley, Hoboken, 2011)

- M. Z. Sogut, New approach for assessment of environmental effects based on entropy optimization of jet engine. *Energy*, **234**, 121250 (2021). ISSN 0360-5442
- Sun X., Wandelt S., Zheng C., Zhang A., COVID-19 pandemic and air transportation: Successfully navigating the paper hurricane. *J. Air Transp. Manag.*, **94**, 102062 (2021). ISSN 0969-6997
- W. Van Gool, Energy policy: Fairy tales and factualities, in *Innovation and Technology Strategies and Policies*, (Springer, Dordrecht, 1997), pp. 93–105

# Chapter 28

## Latest Developments on Electrical Air Vehicles Powered by Electric and Hybrid Propulsion Systems



Ozgur Balli, Alper Dalkiran , and T. Hikmet Karakoc 

### Nomenclature

ICAO	International Civil Aviation Organization
CORSIA	Carbon Offsetting and Reduction Scheme for International Aviation
CO <sub>2</sub>	Carbon dioxide
IATA	International Air Transportation Association
VTOL	Vertical Takeoff Landing
MTOW	Maximum takeoff weight

### 28.1 Introduction

The International Civil Aviation Organization (ICAO) has agreed to implement a novel mechanism to reduce and control CO<sub>2</sub> emissions under the Carbon Offsetting and Reduction Scheme for International Aviation (CORSIA), which measures 2.5%

---

O. Balli

1<sup>st</sup> Air Maintenance Factory Directorate (1.HBFM), General Directorate of Military Factories (AFGM), Ministry of National Defence (MND), Eskisehir, Turkey

Aviation Science and Technology, Graduate School of Natural and Applied Sciences, Eskisehir Osmangazi University, Eskisehir, Turkey

A. Dalkiran (✉)

Suleyman Demirel University, School of Aviation, Isparta, Turkey

Projects and Publications Department, International SARES Society, Eskisehir, Turkey  
e-mail: [alperdalkiran@sdu.edu.tr](mailto:alperdalkiran@sdu.edu.tr)

T. H. Karakoc

Faculty of Aeronautics and Astronautics, Eskisehir Technical University, Eskisehir, Turkiye

Information Technology Research and Application Center, Istanbul Ticaret University, Istanbul, Turkey

e-mail: [hkarakoc@eskisehir.edu.tr](mailto:hkarakoc@eskisehir.edu.tr)

© The Author(s), under exclusive license to Springer Nature Switzerland AG 2023

T. H. Karakoc et al. (eds.), *Advances in Electric Aviation*, Sustainable Aviation,

[https://doi.org/10.1007/978-3-031-32639-4\\_28](https://doi.org/10.1007/978-3-031-32639-4_28)

of total carbon emissions in 2019. Also, it is expected to increase CO<sub>2</sub> emissions by 300% in the next 30 years (IATA 2021). Although some air travel routes and airlines have already equalized their CO<sub>2</sub> emissions, some imminent aircraft technologies may lessen 15% of total emissions; the global offsetting needs a significant change (Abrantes et al. 2021). Electric air vehicles are at the edge of delivering the necessary transformation, and many companies have started to compete for leadership. Electric propulsion systems are expected to reduce aircraft noise by 70%, emissions by 90%, and maintenance costs by 50% (Katherine Hamilton 2020).

The first electric flight was conducted at the end of 2010 and yet resulted in the research and development projects for the electric air vehicle development trend has been soared over 200 and counting worldwide reported in 2019. The research and development projects proceed as 70% of full-electric and 30% of hybrid systems (Smith 2019). This study investigates the recent developments and projects on electrical air vehicles powered by electric and hybrid propulsion systems.

## 28.2 Electrical Air Vehicles Projects

The main advantages of electric propulsion systems are (i) zero emissions, zero noise, (ii) technology ready and improving quickly, (iii) the first plane certified, while the disadvantages are (i) heavy (reduce payload), (ii) short autonomy, (iii) charging time, and (iv) high cost. Electric propulsion systems have been developed due to their environmental advantages.

Electric aircraft research and development programs have become one of the most focused subjects by the European Union's seventh Environmental Action Program for 2020. This program also made the public focus on cleaner and environmentally friendly travel, which shows a parallel growth with ICAO assumptions of 2% improvement between 2021 and 2050 (Lai et al. 2022). The recent developments will lead the urban air-taxi companies to be new unicorns shortly by at least half of all development projects. European research and development projects have taken attention by holding 72 of the total projects. The CityAirbus electric vertical takeoff and landing (VTOL) aircraft is pioneering. The North American Continent is the following region to the electric air vehicles development race by 67 projects (Dan Thisdell 2019).

On the other hand, the current projects can be categorized under single-seat or two-seat air vehicles developed by the local initiatives, university projects, or potential operators to boost urban air transportation. The mobility by the air named as air-taxi will be possible by electric propulsion systems; however, shorter distances have been achieved with the limited power supply of current batteries. However, some studies have revealed that the endurance of the air vehicle improved by dumping the batteries by 17.6% (Chang and Yu 2015). There will be more technologies available in the market to improve the endurance of the air vehicle to compete with the current energy use of commercial air vehicles. Therefore, today's regional and

large commercial electrical aircraft concepts tend to employ turbo-electric hybrid systems at present. Some project numbers are illustrated in Fig. 28.1.

Stable development efforts are ongoing for electric air vehicle design, research, and propulsion. Moreover, more initiatives are investing in the air vehicle industry. This study considers those studies as a list that has been found as remarkable globally, tries to sort out in General Aviation, Large Commercial Aircraft, Business Aircraft, and Regional Aircraft. Also, considering a relatively novel approach for VTOL air vehicles in this study, maybe called electric urban air taxis. All-electric air vehicles have been the most advantageous and cost-effective system (Alrashed et al. 2021).

Most of the above projects started to enter service starting with 2020 and are expected to be operational until 2030, yet some have already become operational. Four of the examples, such as Lilium, City Airbus, Boeing Aurora eVTOL, and Bye Aerospace Sun Flyer 2, had their first flights in 2019. Those projects have been assessed based on the below parameters, as shown in Table 28.1.

- Maximum takeoff weight (MTOW).
- Range.
- Seat Capacity.
- Payload.
- Cruise Altitude.
- Speed.

ICAO Annex 16 is required for CO<sub>2</sub> certification of air vehicles, and it is not any specific document for all-electric air vehicles (ICAO 2017). ICAO is still monitoring the all-electric aircraft development efforts to build necessary standards and recommended practices (ICAO 2020).

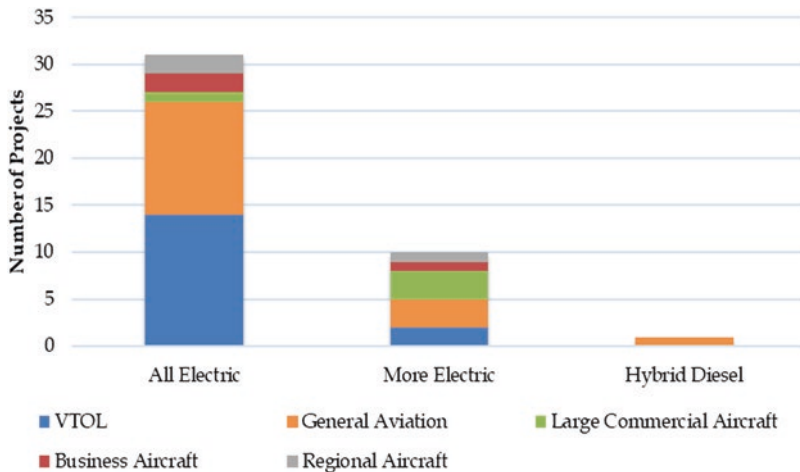


Fig. 28.1 Number of projects distributed on the electric aircraft categories (ICAO 2020)

**Table 28.1** Details on the important electric and hybrid aircraft projects

No	Project	Cruise speed (kt)	Cruise altitude (Feet)	Propulsion power (kW)	MTOW (kg)	Pax	Payload (kg)	Range (km)	Target entry service	Propulsion type	Stat.	References
1	Pipistrel Velis Electro	90	12,000	58	600	2	172	1230	2020	Electric	Und. Dev.	Pipistrel (2021)
2	Yuneec International E430	52	9840	40	470	2	220	227	UNK	Electric	Und. Dev.	Dean Sigler (2016)
3	Volta Volare DaVinci	160	12,500	220	1700	4	544	1852	2017	Hybrid elec.	Und. Dev.	Volta Volaré (2017)
4	Solar Impulse 2	38	27,887	50	1600	1	UNK	UNK	2016	Electric	Und. Dev.	La Souris Verte (2015)
5	Pipistrel Alpha Electro	85	12,000	60	550	2	200	600	2018	Electric	Und. Dev.	Pipistrel (2019)
6	PC Aero Elektra Two Solar	38	65,616	23	450	2	200	UNK	2017	Electric	Und. Dev.	Elektra Solar (2017)
7	PC Aero Elektra Solar Trainer	77	UNK	32	600	2	260	400	UNK	Electric	Und. Dev.	Elektra Solar (2020b)
8	PC Aero Elektra One Solar	76	19,600	32	300	1	100	600	UNK	Electric	Und. Dev.	Elektra Solar (2020a)
9	NASA X-57 Maxwell	149	9000	70	UNK	2	UNK	160	2020	Electric	Und. Dev.	Conner (2019)
10	Magnus Aircraft/Siemens	120	UNK	60	600	2	UNK	1100	2018	Hybrid elec.	Und. Dev.	Magnus (2021)
11	Hamilton aEro	92	UNK	80	420	1	UNK	160	2017	Electric	Und. Dev.	Jewellers (2016)
12	Siemens Extra aircraft	184	9843	260	1000	2	100	100	2016	Electric	Und. Dev.	Aerospace (2016)
13	DigiSky SkySpark	130	10,000	65	530	2	UNK	500	2009	Electric	Und. Dev.	SkySpark (2009)



No	Project	Cruise speed (kt)	Cruise altitude (Feet)	Propulsion power (kW)	MTOW (kg)	Pax	Payload (kg)	Range (km)	Target entry service	Propulsion type	Stat.	References
14	Bye Aerospace EFlyer 2	95	10,000	90	862	2	363	600	2020	Electric	Und. Dev.	Bye Aerospace (2011)
15	Airflow Model 200	UNK	UNK	UNK	UNK	9	907	805	2025	Hybrid elec.	Und. Dev.	Airflow (2020)

Those can be categorized under four main dimensions: general aviation/recreational aircraft group, business or regional aircraft, large commercial aircraft, and VTOL category. MTOW of the general aviation category points between 300 kg and 1000 kg weight. These air vehicles have generally been certified for two-seat configuration and are mostly built as all-electric air vehicles. The business or regional air vehicles are considerably more extensive than general aviation air vehicles aiming to be fly at around 1000 km with a ten-seat capacity.

The large commercial air vehicles category generally looks after a hybrid-electric single-aisle design reaching close-over hundred-seat configuration. Mostly those air vehicles are in the design stage and are expected to be in real life at around 2030. However, the VTOL category is produced more practical designs and reached up to 300 km with 450–2200 kg MTOW weights by all-electric approach.

### 28.3 Conclusion

In this study, the last situations of 16 important electric/hybrid powered air vehicle projects are analyzed. Most of the projects are not realized up to now because of technological inadequacies (suitable battery and electrical motors), economical reasons, and aviation authority restrictions. Additionally, the battery technology needed to enable regional and commercial aircraft to compete with today's propulsion systems is not expected before 2030.

### References

- I. Abrantes et al., Sustainable aviation fuels and imminent technologies – CO2 emissions evolution towards 2050. *J. Clean. Prod.* **313**, 127937 (2021). <https://doi.org/10.1016/j.jclepro.2021.127937>
- Aerospace, Extra 330LE Electric Aircraft – Aerospace Technology (2016). Available at: <https://www.aerospace-technology.com/projects/extra-330le-electric-aircraft/>. Accessed 1 Dec 2021
- Airflow, Model 200 (2020). Available at: <https://www.airflow.aero/>. Accessed 1 Dec 2021
- M. Alrashed et al., Utilisation of turboelectric distribution propulsion in commercial aviation: A review on NASA's TeDP concept. *Chin. J. Aeronaut.* **34**(11), 48–65 (2021). <https://doi.org/10.1016/j.cja.2021.03.014>
- Bye Aerospace, Electric Aircraft – all-electric eFlyer – Bye Aerospace (2011). Available at: <https://bye-aerospace.com/>. Accessed 0111T12:44:44.131Z
- T. Chang, H. Yu, Improving electric powered UAVs' endurance by incorporating battery dumping concept. *Procedia Eng.* **99**, 168–179 (2015). <https://doi.org/10.1016/j.proeng.2014.12.522>
- M. Conner, NASA Armstrong Fact Sheet: NASA X-57 Maxwell. NASA, 28 October (2019). Available at: <https://www.nasa.gov/centers/armstrong/news/FactSheets/FS-109.html>. Accessed 1 Dec 2021
- Dan Thisdell, Power up the battery. *Flight International*, 21 May (2019), pp. 30–31. Available at: [flightglobal.com](http://flightglobal.com)

- Dean Sigler, China's First Certified Electric Airplane Ready for Mass Production | Sustainable Skies (2016). Available at: <http://sustainableskies.org/chinas-first-certified-electric-airplane-ready-for-mass-production/>. Accessed 1 Dec 2021
- Elektra Solar, Elektra Two Solar – Elektra Solar (2017). Available at: <https://www.elektra-solar.com/products/elektra-two-solar/>. Accessed 1 Dec 2021
- Elektra Solar, Elektra One Solar – Elektra Solar (2020a). Available at: <https://www.elektra-solar.com/products/elektra-one-solar/>. Accessed 1 Dec 2021
- Elektra Solar, Elektra Trainer – Elektra Solar (2020b). Available at: <https://www.elektra-solar.com/products/elektra-trainer-solar/>. Accessed 1 Dec 2021
- IATA, CORSIA Fact Sheet, 1.10.21 (1.10.2021). Available at: <https://www.iata.org/en/iata-repository/pressroom/fact-sheets/fact-sheet%2D%2D-corsia/>. Accessed 1.12.21
- ICAO, Annex 16 Environmental Protection: Volume III CO2 Certification Requirement (2017)
- ICAO, Electric and Hybrid Aircraft Platform for Innovation (E-HAPI) (2020). Available at: <https://www.icao.int/environmental-protection/Pages/electric-aircraft.aspx>. Accessed 1 Dec 2021
- L. Jewellers, Electric Plane: Successful launch of the Hamilton aEro electric aircraft, Lugaro (27 Sept 2016). Available at: <https://www.lugaro.com/successful-launch-hamilton-aero-electric-aircraft-made-aerobatics/>. Accessed 1 Dec 2021
- T.M. Katherine Hamilton, Electric Aviation Could Be Closer Than You Think (10 Oct 2020). Accessed 1 Dec 2021
- La Souris Verte, Solar Impulse – Around the world to promote clean technologies (2015). Available at: <https://aroundtheworld.solarimpulse.com/>. Accessed 1 Dec 2021
- Y.Y. Lai et al., Analysing the opportunities and challenges for mitigating the climate impact of aviation: A narrative review. *Renew. Sust. Energ. Rev.* **156**, 111972 (2022). <https://doi.org/10.1016/j.rser.2021.111972>
- Magnus, FUSION BUSINESS – Magnus Aircraft Zrt (2021). Available at: [https://magnusaircraft.com/fusion\\_business/index.php](https://magnusaircraft.com/fusion_business/index.php). Accessed 1 Dec 2021
- Pipistrel, Alpha Electro – Pipistrel Aircraft (2019). Available at: <https://www.pipistrel-aircraft.com/aircraft/electric-flight/alpha-electro/>. Accessed 1 Dec 2021
- Pipistrel, Velis Electro EASA TC – Pipistrel Aircraft (2021). Available at: <https://www.pipistrel-aircraft.com/aircraft/electric-flight/velis-electro-easa-tc/>. Accessed 1 Dec 2021
- SkySpark, SkySpark (2009). Available at: <http://www.skyspark.eu/web/eng/velivolo.php>. Accessed 1 Dec 2021
- P. Smith, *Electric Aircraft Development Rising Fast* (Aerospace Testing International, 15 July 2019). Available at: <https://www.aerospacetestinginternational.com/news/electric-aircraft-development-rising-fast.html>. Accessed 10 Dec 2021.469Z
- Volta Volaré, *Performance* (Volta Volaré, 2017). Available at: <http://www.voltavolare.com/performance/>. Accessed 1 Dec 2021

# Chapter 29

## Conceptual Application of Hybrid-Electric Propulsion System Configurations on Cessna 172S



Burak Akgul and Ismail Ata

### Nomenclature

nm	Nautical mile
PMAD	Power management and distribution
CO <sub>2</sub>	Carbondioxide
CH <sub>4</sub>	Methane
CO	Carbonmonoxide
NO <sub>x</sub>	Nitrogen oxides

### 29.1 Introduction

Due to the low efficiency of conventional drivetrains and high greenhouse gas emissions because of fossil fuels' usage, there has been a rapid electrification in the world, especially in the automotive sector in recent years. Electrification steps have also been taken in aviation and many theoretical and practical studies and works have been carried out.

Pornet developed conceptual design methods for hybrid-electric aircrafts and found fuel reduction values according to battery specific energy at cell-level (Pornet 2018). Voskuijl et al. chose ATR 72-600 as a reference aircraft, designed hybrid-electric propulsion system on the aircraft, and achieved 28% reduction in emissions (Voskuijl et al. 2018). Hepperle presents electric propulsion configurations and presented a conceptual application on Dornier Do 328 aircraft (Hepperle 2012). Wall presented a model predictive power management for hybrid-electric propulsion

---

B. Akgul (✉) · I. Ata  
Graduate School of Natural and Applied Sciences, Erciyes University, Kayseri, Turkey  
Faculty of Aeronautics and Astronautics, Department of Astronautical Engineering, Erciyes University, Kayseri, Turkey  
e-mail: [burak.16.akgul@gmail.com](mailto:burak.16.akgul@gmail.com)

aircrafts and achieved conventional aircraft's performance in hybrid-electric aircraft with fuel savings (Wall 2017). Glasscock developed hybrid powerplant for UAVs and achieved 17% improvement in overall propulsive efficiency compared to a non-hybrid powerplant (Glasscock 2012). Sziroczak et al. evaluate problems for design of hybrid-electric aircraft and presented a conceptual design methodology for small hybrid-electric aircraft (Sziroczak et al. 2020). Traub developed an estimation for battery powered aircraft's range and endurance and found that increasing battery capacity reduces performance for a constrained geometry (Traub 2011). Hoelzen et al. found that hybrid-electric regional aircraft of 350 nm can be cost competitive, and other important result of their study shows that low hybridization degree brings around 8% emission reduction for similar costs, while higher hybridization degree 22% emission reduction is possible but it brings 24% direct operational cost increase (Hoelzen et al. 2018).

## 29.2 Method

In this paper, a conceptual design for electrification has been applied to reduce fuel consumption, greenhouse gas emissions, and flight costs in aircrafts using fossil-based fuels, which are the vast majority of today's aircrafts. For this purpose, Cessna 172S, one of the most common aircrafts in the world, was chosen and two different hybrid-electric configurations were conceptually applied.

The Lycoming IO-360 L2A engine of Cessna 172S is an engine that generates 119 kW power at 2400 rpm (EASA 2012), and the total fuel capacity of the aircraft is 56 gallons (Cessna Aircraft, 2007). Specifications of the configurations' elements are presented in Table 29.1. These elements will be placed on the aircraft by removing the seats other than the pilot seat, so only the pilot flies on-board.

A two-hour flight consisting of three basic phases was taken as a reference for the conceptual applications. The electric motor with a power of 15 kW provides

**Table 29.1** Elements used in the hybrid-electric configurations

Element	Model	Specifications
Aircraft	Cessna 172S	Maximum useful load 405.96 kg (Cessna Aircraft 2007)
Electric motor	Mgm Compro REX 30	5.2 kg, 15 kW max. Continuous power (Mgm Compro electric motor n.d.)
Motor controller	Mgm Compro HBC 280120-3	1.18 kg, 33 kW max. Continuous power (Mgm Compro motor controller n.d.)
Battery pack	Northvolt Voltblock C12/90	54 kg, 11.7 kWh (Northvolt n.d.)
Fuel cell module	Ballard Fcvelocity	125 kg, 30 kw (Ballard n.d.)
Hydrogen tank	Luxfer G-Stor H2 L034H35	19.82 kg with 0.82 kg hydrogen (Luxfer n.d.)

uninterrupted power for 2 h with the electrical energy from the battery or fuel cell, while the internal combustion engine in the conventional system works to generate 15 kW less power than the power required by the relevant flight stage. For this reason, total flight time will be important for the remaining capacity of battery and hydrogen amount, while the power required by the flight phase and flight phase time are important for Avgas 100LL consumption. The conceptual configurations were as follows:

In the first configuration, there were three battery packs, PMAD (power management and distribution), electric motor, and a transmission for work adjustment between propeller and hybrid-electric system. The weight of the electrical system is 168.38 kg, which is the combined weight of the batteries, electric motor, and motor controller (neglecting PMAD, wiring, and other system weights). The total capacity of three battery packs is 35.1 kWh and provide 30 kWh to the electric motor during the 2-h flight (Fig. 29.1).

In the second configuration, in addition to the conventional propulsion system, there is a hydrogen tank, fuel cell module, PMAD, electric motor, and transmission. The weight of the electrical system is 151.2 kg, excluding PMAD, cabling, and other system weights. It is assumed that the fuel cell module generates 15 kW to make a better comparison with batteries (Figs. 29.2 and 29.3).

The phases of the 2-h flight are:

- Takeoff and Climb.
- Cruise.
- Descent and Landing.

In the flight phases; the aircraft does not taxi and it is ready to takeoff on the runway during the takeoff and climb phase; at this stage, the aircraft climbs to 6000 ft. in 10 min. Cruise is carried out at 6000 ft. altitude and its duration is 100 min. Descent and landing phase is to be done under normal conditions in 10 min.

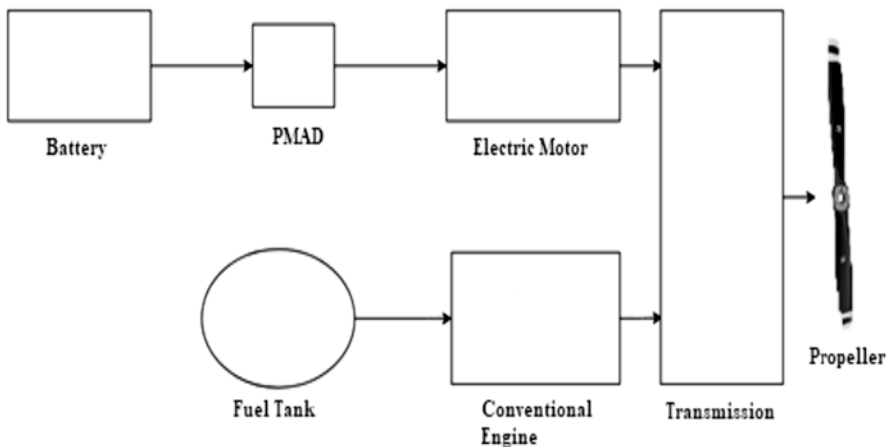


Fig. 29.1 Configuration 1, battery hybrid-electric propulsion system configuration

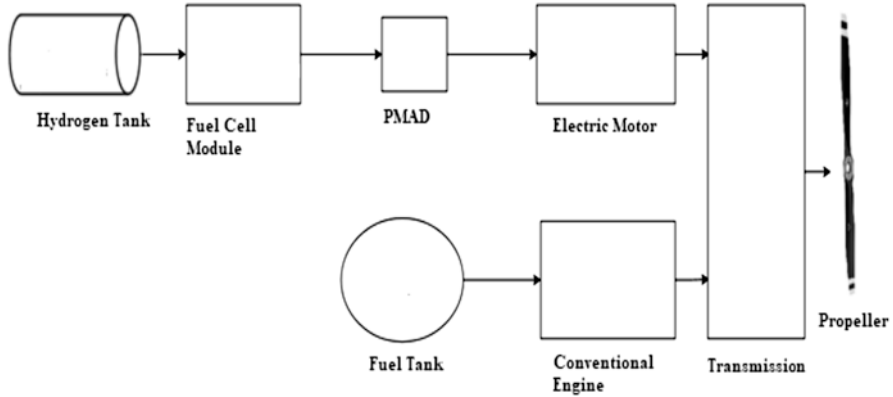


Fig. 29.2 Configuration 2, fuel cell hybrid-electric propulsion system configuration

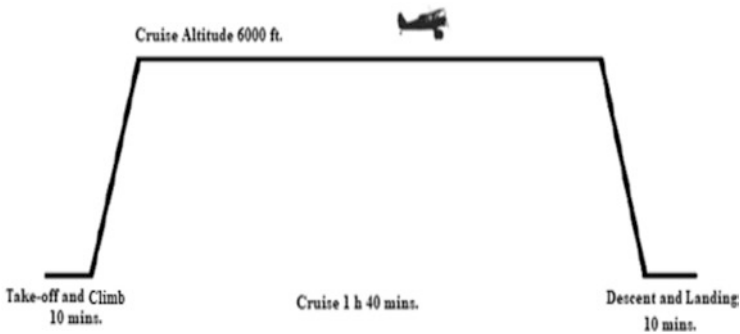


Fig. 29.3 Flight phases

The power required by the flight phases:

For takeoff and climb phase, full power (119 kW) at 2400 rpm is required, 15 kW of this power is provided by the electric motor and 104 kW power is generated by the conventional engine. The power required for cruise phase is 57% MCP (maximum continuous power) at 6000 ft. altitude at 2400 rpm in standard temperature conditions, so the power required is 67.83 kW, 15 kW is provided by electric motor and 52.83 kW is provided by conventional engine. In the descent and landing phase, the flight is carried out at 1800 rpm and the required power is 60 kW; 15 kW and 45 kW of required power is provided by electric motor and conventional engine, respectively.

The power-fuel consumption graph of the Lycoming IO-360 L2A engine in Fig. 29.4 was linearized, and the fuel consumption was found according to the power requirement for flight phases. Hourly fuel consumption values according to flight phases are shown in the table below for purely conventional flight and hybrid-electric configurations. Avgas 100LL consumption is same for two hybrid-electric configurations as 15 kW power is provided by electric motor in both configurations.

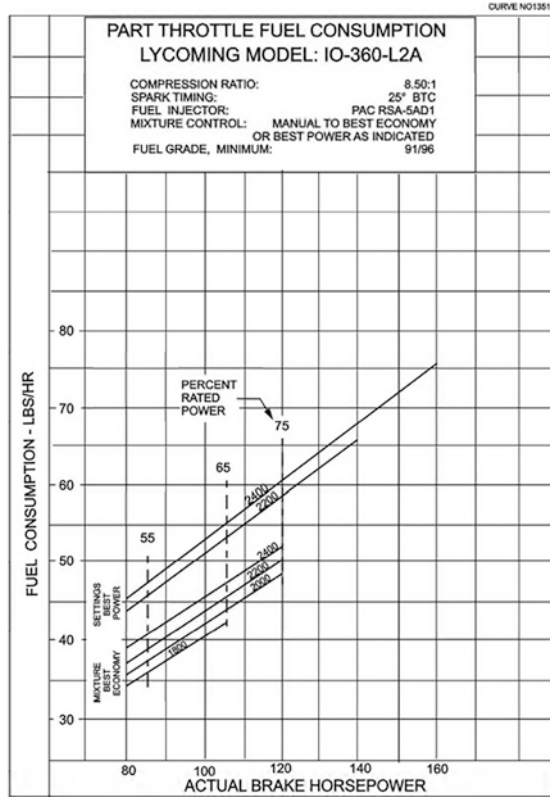


Fig. 29.4 Lycoming IO-360 L2A engine power-fuel consumption graph. (Lycoming 2005)

While the Avgas 100LL is used in conventional flight, mains electricity is used for battery charging and hydrogen is used as fuel in the fuel cell. Therefore, it is necessary to know the prices to make cost comparisons.

Prices of the conventional aviation fuel Avgas 100LL, the electricity required for battery charging, and hydrogen used in fuel cell are used. Avgas 100LL liter price in Turkey is three euros. For charging batteries, 0.8 Turkish lira per kWh is taken as average price according to the electricity billing tariff. In the light of information provided by US Department of Energy (US DoE n.d.), \$2.15 is taken as hydrogen kg price.

In this paper, greenhouse gas emissions is also compared. Therefore, the values of Avgas 100LL emissions per kg in Hospodka et al. is used. Greenhouse gas emissions per kg of Avgas 100LL are 2 kg CO<sub>2</sub>, 1.2 kg water vapor, 1 kg CO, 15 g HC, 5 g NO<sub>x</sub>, and 0.8 g lead (Hospodka et al. 2020). In addition, the electric system does not cause greenhouse gas emissions during the flight. Due to the equation  $H_2 + 1/2O_2 \rightarrow H_2O$  hydrogen fuel cell, only water vapor is produced as emission (Abdul Sathar Eqbal et al. 2018).



On the other hand, during the electric generation greenhouse gas emissions occur, too. According to the data of Turkish Electricity Transmission Corporation (TEİAŞ [n.d.](#)) and Turkish National Greenhouse Gas Inventory (Tüik [2021](#)), per 1 kWh electricity, 0.455 kg CO<sub>2</sub>,  $5.594 \times 10^{-6}$  kg CH<sub>4</sub>,  $8.884 \times 10^{-6}$  kg N<sub>2</sub>O are the emissions. In addition, these emissions also effect the hydrogen production via electrolysis; hydrogen has a value of 39.4 kWh/kg (Bossel and Eliasson [2003](#)) and in the current technology level 43 kWh (US DoE [n.d.](#)) is required for 1 kg hydrogen production in electrolysis on stack level, so hydrogen of 30 kWh needed for flight from electrolysis emissions is calculated, too.

### 29.3 Results and Discussions

The fuel consumption values obtained by linearizing the power-fuel consumption graphs of the Lycoming IO-360 L2A engine and the required power according to the flight stages obtained from the Cessna 172S flight guide are shown in Table [29.2](#). If Table [29.2](#) is examined, 16.8 gallons of Avgas 100LL is needed for 120 min flight of conventional propulsion system; on the other hand, fuel consumption decreased to 14.3 gallons in hybrid-electric configurations. So, hybrid-electric configurations provide an advantage of 14.8% for fuel consumption.

The emissions and costs of flight according to propulsion system is given in Table [29.3](#). The costs are calculated according to the 19 November 2021 exchange rates (Xe [2021](#)). When Table [29.3](#) is examined, 91.56 kg CO<sub>2</sub> gas is emitted when 120 min flight is carried out by conventional propulsion system using 45.78 kg Avgas 100LL. As a result of using the hybrid-electric configurations for the same flight, 77.94 kg of CO<sub>2</sub> is released to the atmosphere. It is seen that the 14.8% reduction in fuel consumption also reduces the greenhouse gas emission values. At the same time, because of the hydrogen usage in the fuel cell, more water vapor is released in the fuel cell hybrid-electric configuration than in the configuration with battery.

When the results shown in Table [29.3](#) are examined in terms of cost: while the conventional propulsion system costs 215.9 dollars for 120 min flight, hybrid-electric configurations cost about 185 dollars for same flight. So, it is seen that the cost advantage of around 14% is achieved by the hybrid-electric configurations.

On the other hand, indirect flight emissions arising from the electric generation which is used for battery charging and hydrogen electrolysis are shown in Table [29.4](#).

**Table 29.2** Fuel consumption according to propulsion systems and flight phases

Flight phase	Conventional propulsion system	Hybrid-electric configurations
Takeoff and climb (10 min)	2.09 gallons	1.88 gallons
Cruise (1 h 40 mins)	13.74 gallons	11.62 gallons
Descent and landing (10 min)	0.95 gallons	0.79 gallons
Total (2 h)	16.8 gallons	14.3 gallons

**Table 29.3** Emissions and costs according to the flight propulsion type

	Conventional	Battery hybrid- electric	Fuel cell hybrid-electric
Consumed avgas 100LL	16.8 gallons – 45.78 kg	14.3 gallons – 38.97 kg	14.3 gallons – 38.97 kg
CO <sub>2</sub>	91.56 kg	77.94 kg	77.94 kg
Water vapor	54.94 kg	46.76 kg	53.61 kg
CO	45.78 kg	38.97 kg	38.97 kg
HC	686.7 g	584.5 g	584.5 g
NO <sub>x</sub>	228.9 g	194.8 g	194.8 g
Lead	36.6 g	31.18 g	31.18 g
Cost	215.9 dollars	185.9 dollars	185.4 dollars

**Table 29.4** Indirect emissions from battery charging and hydrogen production for 30 kWh

Emissions	Battery hybrid-electric	Fuel cell hybrid-electric
CO <sub>2</sub>	13.65 kg	14.89 kg
CH <sub>4</sub>	1.68 × 10 <sup>-4</sup> kg	1.83 × 10 <sup>-4</sup> kg
NO	2.66 × 10 <sup>-4</sup> kg	2.9 × 10 <sup>-4</sup> kg

## 29.4 Conclusion

By using the hybrid-electric configurations, 14.8% fuel savings and decrease in greenhouse gas emissions during flight are achieved, and about 14% reduction in cost is reached. These values prove that electrification of aircrafts brings important advantages.

On the other hand, very limited payload of existing aircrafts and relatively heavy parts of the hybrid-electric configurations cause some usable payload problems. In addition, indirect flight emissions are higher than expected, so by using electricity from renewable sources decrease in indirect emissions will be achieved, too.

## References

M. Abdul Sathar Eqbal, N. Fernando, M. Marino, G. Wild, Hybrid propulsion systems for remotely piloted aircraft systems. *Aerospace* **5**(2), 34 (2018)

Ballard, (n.d.), [https://www.ballard.com/docs/default-source/spec-sheets/fcvelocitymd.pdf?sfvrsn=ebc380\\_2](https://www.ballard.com/docs/default-source/spec-sheets/fcvelocitymd.pdf?sfvrsn=ebc380_2). Retrieved Sept 2021

U. Bossel, B. Eliasson, *Energy and the Hydrogen Economy* (Methanol Institute, Arlington, 2003)

EASA, Type-Certificate Data Sheet, Number: IM.E.032, Issue: 01, 27 Sept 2012, Type: Lycoming Engines IO-360 Series Engines (2012)

R.R. Glasscock, Design, modelling and measurement of hybrid powerplant for unmanned aerial vehicles (UAVs) (Doctoral dissertation, Queensland University of Technology) (2012)

M. Hepperle, Electric flight – potential and limitations (2012)

J. Hoelzen, Y. Liu, B. Bensmann, C. Winnefeld, A. Elham, J. Friedrichs, R. Hanke-Rauschenbach, Conceptual design of operation strategies for hybrid electric aircraft. *Energies* **11**(1), 217 (2018)

- J. Hospodka, H. Bínová, S. Pleninger, Assessment of all-electric general aviation aircraft. *Energies* **13**(23), 6206 (2020)
- Information Manual Skyhawk SP, Cessna Aircraft Company Model 172S NAV III Avionics Option- GFC 700 AFCS, 20 Dec 2007 (Cessna Aircraft Company, Wichita, 2007)
- Luxfer, (n.d.), <https://www.luxfercylinders.com/products/alternative-fuel/g-stor-h2-hydrogen-cylinders>. Retrieved Sept 2021
- Lycoming, Operator's Manual Lycoming O-360, HO-360, IO-360, AIO-360, HIO-360 & TIO-360 Series, 8th Edition, Part No. 60297-12, October 2005 (2005)
- Mgm Compro, electric motor, (n.d.), <https://www.mgm-compro.com/electric-motor/25-kw-electric-motor/>. Retrieved Sept 2021
- Mgm Compro, motor controller, (n.d.), <https://www.mgm-compro.com/brushless-motor-controllers/33-kw-motor-controllers/>. Retrieved Sept 2021
- Northvolt, (n.d.), <https://northvolt.com/products/systems/voltblocks/>. Retrieved Sept 2021
- C. Pomet, Conceptual design methods for sizing and performance of hybrid-electric transport aircraft (Doctoral dissertation, Technische Universität München) (2018)
- D. Szirczak, I. Jankovics, I. Gal, D. Rohacs, Conceptual design of small aircraft with hybrid-electric propulsion systems. *Energy* **204**, 117937 (2020)
- TEİAŞ, Türkiye Elektrik Üretim-İletim 2019 Yılı İstatistikleri, 38-Grafik III.I – 2019 Yılı Türkiye Elektrik Enerjisi Üretimini Kaynaklara Göre Dağılımı (n.d.), <https://www.teias.gov.tr/tr-TR/turkiye-elektrik-uretim-iletim-istatistikleri>. Retrieved Sept 2021
- L.W. Traub, Range and endurance estimates for battery-powered aircraft. *J. Aircr.* **48**(2), 703–707 (2011)
- Tüik, Turkish Greenhouse Gas Inventory 1990–2019, National Inventory Report for Submission Under the United Nations Framework Convention on Climate Change, Tüik, Nisan 2021, <https://enerji.gov.tr/Media/Dizin/EVCED/tr/%C3%87evreVe%C4%B0klim/%C4%B0klimDe%C4%9Fi%C5%9Fikli%C4%9Fi/UlusalSeraGaz%C4%B1EmisyonEnvanteri/Belgeler/Ek-1.pdf> (2021, April)
- US DoE, (n.d.), <https://www.energy.gov/eere/fuelcells/doe-technical-targets-hydrogen-production-electrolysis>. Retrieved Sept 2021
- M. Voskuil, J. van Bogaert, A.G. Rao, Analysis and design of hybrid electric regional turboprop aircraft. *CEAS Aeronaut. J.* **9**(1), 15–25 (2018)
- T.J. Wall, Model predictive power management of a hybrid electric propulsion system for aircraft (Doctoral dissertation, Western Michigan University) (2017)
- Xe, <https://www.xe.com/currencytables/> (19 Nov 2021)

# Chapter 30

## The Effects of Total Initial Concentration in a Vanadium Redox Flow Battery



Ilker Kayali

### 30.1 Introduction

The VRFBs are of great importance in terms of high storage capacity, power capacity, medium and large-scale energy storage systems. The high-power density batteries are indispensable to satisfy the total power requirement of unmanned aerial vehicles (UAVs) (Tao et al. 2019).

One of the important parameters for VRFB is the initial concentrations. An increase of the initial concentration has seen significant improvements in both the negative and positive electrodes (Yang et al. 2015). Another important parameter for VRFB is temperature distribution which is very important for the effective and safe operation of VRFB design and control (Zheng et al. 2014).

The purpose of this study is to investigate the cell voltage, overpotential, and temperature distribution in VRFB of different initial concentrations. The initial concentrations used are  $1040 \text{ mol/m}^3$ ,  $1500 \text{ mol/m}^3$  (Lu et al. 2021), and  $1700 \text{ mol/m}^3$  (Tsushima and Suzuki 2020), respectively. To perform this work, the two-dimensional steady state is obtained using COMSOL Multiphysics 5.5.

---

I. Kayali (✉)

Department of Energy Systems Engineering, Erciyes University, Kayseri, Turkey

Kapadokya University, Kapadokya Vocational School, Nevşehir, Turkey

e-mail: [ilker.kayali@kapadokya.edu.tr](mailto:ilker.kayali@kapadokya.edu.tr)

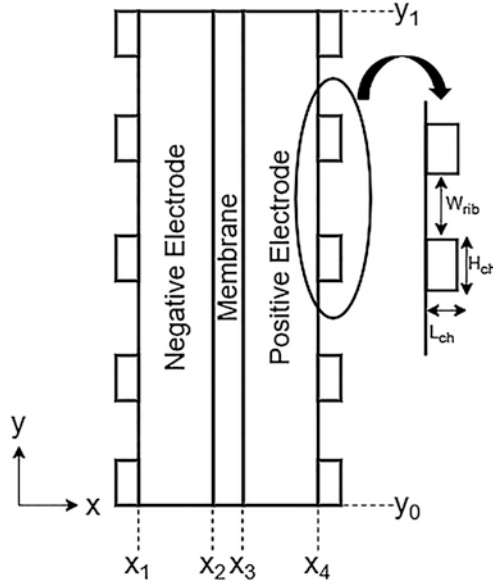


**Fig. 30.1** A two-dimensional VRFB system

## 30.2 Method

The schematic diagram and boundaries of the two-dimensional model are shown in Fig. 30.1. The model equations are solved under the specific boundary conditions according to the following assumptions:

- The process is steady state.
- The fluid flow is an incompressible flow.
- The electrodes and the membrane are isotropic and homogenous.
- Hydrogen and oxygen evolutions are ignored.
- There is no convective heat transfer between the battery and the environment.

The VRFB model consists of three layers which are positive/negative electrode and membrane. The geometric properties of the two-dimensional model are given in Table 30.1.

### 30.2.1 Model Equations

The model consists of the continuity equation, conservation of momentum, conservation of species, conservation of charges (Al-Yasiri and Park 2017), and conservation of energy (Zheng et al. 2014). The parameter values for numerical study are

**Table 30.1** The dimension of component used for the model

Symbols	Definition	Value
$L_e$	Electrode thickness	6 (mm)
$L_m$	Membrane thickness	183 ( $\mu\text{m}$ )
$H_{ch}$	Channel height	4 (mm)
$L_{ch}$	Channel thickness	1.59 (mm)
$W_{rib}$	Rib thickness	7.50 (mm)
$W_{cell}$	Electrode width	50 (mm)

shown in Table 30.2. The numerical parameters and source terms for the energy conversion equations are given in Tables 30.3 and 30.4, respectively.

### 30.2.2 Boundary Conditions

The model equations include the continuity equation, conservation of momentum, conservation of species, conservation of charges (Al-Yasiri and Park 2017), and conservation of energy (Zheng et al. 2014).

## 30.3 Results and Discussion

The numerical solution is validated using experimental data in the literature (Al-Yasiri and Park 2017) as shown in Fig. 30.2. It is observed that the average relative error is less than 1% of the discharge process.

The effect of total initial concentration on cell voltage is shown in Fig. 30.3. As the total initial concentration raise, the cell voltage is increased. Figure 30.4a, b show the overpotentials of both electrodes during discharge (from 15% to 95% SOC).

The overpotentials of both electrodes showed the smallest values at 50% SOC. As the SOC approaches 95% and 15%, both electrodes overpotentials are changed dramatically. Therefore, when SOC approaches 95% and 15%, it can cause more side reactions in the flow battery (Ma et al. 2020).

Figures 30.5a, b show the temperature distributions occurring in both electrodes for different initial concentrations at 50% SOC. As the total initial concentration raise, the temperature distribution is increased. In addition, the positive electrode has revealed higher temperature distribution than the negative electrode.

**Table 30.2** Numerical parameter

Symbol	Definition	Value
$a$	Specific surface area	$3.5 \times 10^4 \text{ m}^{-1}$
$T$	Operating temperature	298.15 K
$P_{\text{out}}$	Outlet pressure	0 (kPa)
$V_B^0$	Volumetric flow rate	75 mL/min
$I$	Applied current density	40 mA/cm <sup>2</sup>
$k_{\text{neg}}$	Negative electrode reaction rate constant	$7 \times 10^{-8} \text{ m/s}$
$k_{\text{pos}}$	Positive electrode reaction rate constant	$2.5 \times 10^{-8} \text{ m/s}$
$\alpha_{\text{neg}}$	Negative charge transfer coefficient	0.45
$\alpha_{\text{pos}}$	Positive charge transfer coefficient	0.55
$E_{0,\text{neg}}$	Standard potential for negative	-0.255 V
$E_{0,\text{pos}}$	Standard potential for positive	1.004 V
$\beta$	$\text{HSO}_4^-$ dissociation degree	0.25
$K_d$	$\text{HSO}_4^-$ dissociation rate	$10^4 \text{ S}^{-1}$
$\mu_{\text{neg}}$	Negative electrolyte viscosity	0.0025 Pa.s
$\mu_{\text{pos}}$	Positive electrolyte viscosity	0.050 Pa.s
$\rho_{\text{neg}}$	Negative electrolyte density	1300 kg/m <sup>3</sup>
$\rho_{\text{pos}}$	Positive electrolyte density	1350 kg/m <sup>3</sup>
$D_{V2}$	$V^{2+}$ diffusion coefficient	$2.4 \times 10^{-10} \text{ m}^2/\text{s}$
$D_{V3}$	$V^{3+}$ diffusion coefficient	$2.4 \times 10^{-10} \text{ m}^2/\text{s}$
$D_{V4}$	$V^{4+}$ diffusion coefficient	$3.9 \times 10^{-10} \text{ m}^2/\text{s}$
$D_{V5}$	$V^{5+}$ diffusion coefficient	$3.9 \times 10^{-10} \text{ m}^2/\text{s}$
$D_{\text{H}^+}$	Proton diffusion coefficient	$9.312 \times 10^{-9} \text{ m}^2/\text{s}$
$D_{\text{HSO}_4^-}$	$\text{HSO}_4^-$ diffusion coefficient	$1.33 \times 10^{-9} \text{ m}^2/\text{s}$
$D_{\text{SO}_4^-}$	$\text{SO}_4^-$ diffusion coefficient	$1.065 \times 10^{-9} \text{ m}^2/\text{s}$
$\epsilon$	Electrode porosity	0.929
$d_f$	Fiber diameter	50.3 $\mu\text{m}$
$C_k$	Kozeny-Carmen coefficient	180
$\sigma_s^{\text{eff}}$	Electronic conductivity of electrode	66.7 S/m
$\sigma_m$	Electronic conductivity of membrane	24.88 S/m
$Z_f$	Fixed acid concentration	-1
$C_f$	Fixed acid charge	1990 mol/m <sup>3</sup>
$D_{\text{H}^+}^m$	Membrane proton diffusion coefficient	$3.35 \times 10^{-9} \text{ m}^2/\text{s}$
$C_{V^{2+}}^0$	Initial concentration of V(II)	156 mol/m <sup>3</sup>
$C_{V^{3+}}^0$	Initial concentration of V(III)	884 mol/m <sup>3</sup>
$C_{V^{4+}}^0$	Initial concentration of V(IV)	884 mol/m <sup>3</sup>

(continued)

**Table 30.2** (continued)

Symbol	Definition	Value
$C_{V^{5+}}^0$	Initial concentration of V(V)	156 mol/m <sup>3</sup>
$C_{H_{neg}}^0$	Initial concentration of H <sup>+</sup> in negative	4447.5 mol/m <sup>3</sup>
$C_{H_{pos}}^0$	Initial concentration of H <sup>+</sup> in positive	5097.5 mol/m <sup>3</sup>
$C_{HSO_4_{neg}}^0$	Initial concentration of $HSO_4^-$ in negative	2668.5 mol/m <sup>3</sup>
$C_{HSO_4_{pos}}^0$	Initial concentration of $HSO_4^+$ in positive	3058.5 mol/m <sup>3</sup>

**Table 30.3** Numerical parameters for the energy conservation equation

Symbol	Definition	Value
$\lambda_l$	Electrolyte thermal conductivity	0.67 W/mK
$\lambda_{elec}$	Electrode thermal conductivity	0.15 W/mK
$\lambda_{mem}$	Membrane thermal conductivity	0.67 W/mK
$\rho_l C_l$	Liquid thermal capacitance(water)	4.18 x 106 J/m <sup>3</sup> K
$-\Delta S1$	Entropy associated with reaction (1)	-100 J/molK
$-\Delta S2$	Entropy associated with reaction (2)	-21.7 J/molK

**Table 30.4** Source terms in the energy conservation equation

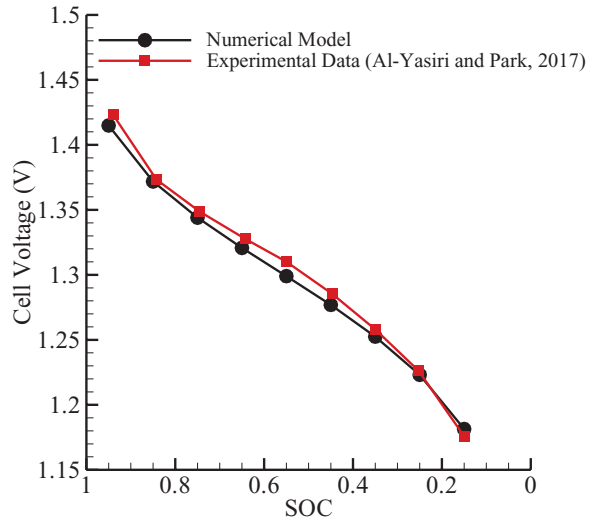
Source	Membrane	Negative Electrode	Positive Electrode
$Q_{act}$	0	$\eta_1 \nabla \cdot iloc_{neg}$	$\eta_2 \nabla \cdot iloc_{pos}$
$Q_{rev}$	0	$-\Delta S_1 T V \cdot iloc_{neg} / F$	$\Delta S_2 T V \cdot iloc_{pos} / F$
$Q_{ohm}$	$\sigma_{mem}^{eff}  \nabla \phi $	$\sigma_s^{eff}  \nabla \phi_s ^2 + K_l^{eff}  \nabla \phi ^2$	$\sigma_s^{eff}  \nabla \phi_s ^2 + K_l^{eff}  \nabla \phi ^2$

## 30.4 Conclusion

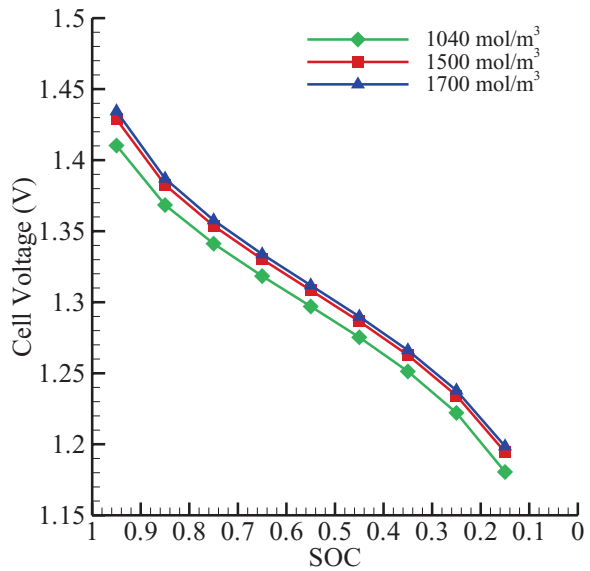
In this study, the effects of different initial concentrations of VRFB on the negative and positive electrode on cell voltage, overpotential, and temperature distributions are presented. According to the results obtained, as the total initial concentration raise, the cell voltage is increased. The overpotentials are decreased dramatically with the rise of the total initial concentration. Furthermore, the overpotential is sharply increased at 15% and 95% SOC at the negative and positive electrode, while reaching a minimum value when SOC is 50%. As the total initial concentration raise, the temperature distribution is increased. Moreover, the positive electrode has revealed higher temperature distribution than the negative electrode.



**Fig. 30.2** Comparison of experimental results and simulation data



**Fig. 30.3** The cell voltages of different initial concentrations



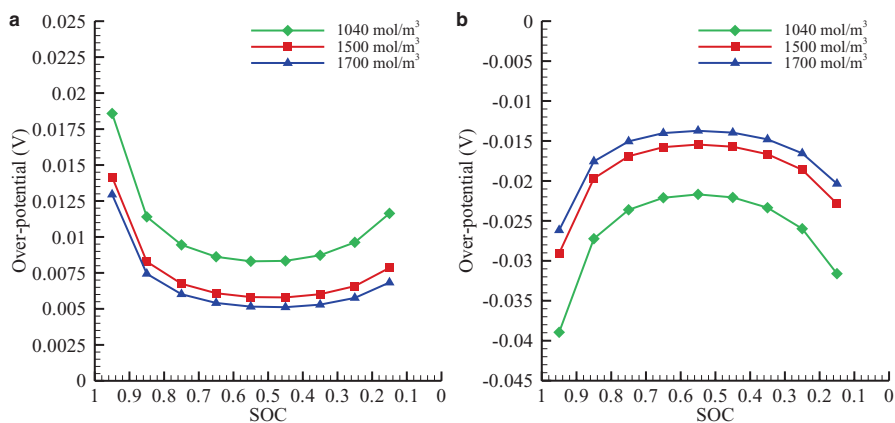


**Fig. 30.4** (a) The overpotential of the total initial concentration for the negative electrode. (b) The overpotential of the total initial concentration for the positive electrode

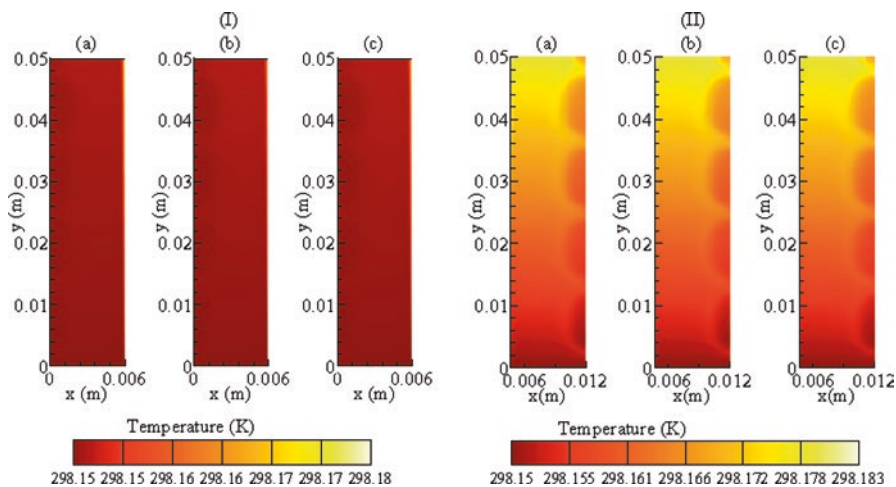


**Fig. 30.5** (a) The cell temperature distribution of the total initial concentration for the negative electrode: (a) 1040 mol/m<sup>3</sup>; (b) 1500 mol/m<sup>3</sup>; (c) 1700 mol/m<sup>3</sup>. (b) The cell temperature distribution of the total initial concentration for the positive electrode: (a) 1040 mol/m<sup>3</sup>; (b) 1500 mol/m<sup>3</sup>; (c) 1700 mol/m<sup>3</sup>

**Acknowledgement** The authors would like to thank the Scientific Research Projects Unit of Erciyes University for funding under the contract no: FYL-2020-10397.

## References

- M. Al-Yasiri, J. Park, Study on channel geometry of all-vanadium redox flow batteries. *J. Electrochem. Soc.* (2017)
- M.Y. Lu, Y.H. Jiao, X.Y. Tang, W.W. Yang, M. Ye, Q. Xu, Blocked serpentine flow field with enhanced species transport and improved flow distribution for vanadium redox flow battery. *J. Energy Storage* **35**, 102284 (2021)
- Q. Ma, L. Xing, H. Su, W. Zhang, W. Yang, Q. Xu, Numerical investigation on the dispersion effect in vanadium redox flow battery. *Chem. Eng. J.* **393**, 124753 (2020)
- L.E.I. Tao, Y.A.N.G. Zhou, L.I.N. Zicun, X. Zhang, State of art on energy management strategy for hybrid-powered unmanned aerial vehicle. *Chin. J. Aeronaut.* **32**(6), 1488–1503 (2019)
- S. Tsushima, T. Suzuki, Modeling and simulation of vanadium redox flow battery with interdigitated flow field for optimizing electrode architecture. *J. Electrochem. Soc.* **167**(2), 020553 (2020)
- W.W. Yang, Y.L. He, Y.S. Li, Performance modeling of a vanadium redox flow battery during discharging. *Electrochim. Acta* **155**, 279–287 (2015)
- Q. Zheng, H. Zhang, F. Xing, X. Ma, X. Li, G. Ning, A three-dimensional model for thermal analysis in a vanadium flow battery. *Appl. Energy* (2014)

# Chapter 31

## Effect of Phase Change Material on Thermal Behavior of a Lithium-Ion Battery



Uğur Morali

### Nomenclature

NTGK Newman, Tiedemann, Gu, and Kim

DoD Depth-of-discharge

PCM Phase change material

### 31.1 Introduction

Energy storage materials have been widely used in various applications (hybrid vehicles, hybrid electric vehicles, portable devices, and so on). This could be attributed to their high-energy density and high-power density (Zeng et al. 2021). On the other hand, thermally sensitive structures of lithium-ion batteries restrict their usage in many applications where high discharge rates are needed (Yetik and Karakoc 2020). Lithium ions move from the negative electrode to the positive electrode during the discharge operation. This operation is generally performed under a certain discharge current suggested by the battery manufacturer. Battery temperature may rise under charge and discharge conditions due to the generated heat. The battery temperature above 40 °C has negative influence on the battery performance. Therefore, this increase should be controlled to maximize the battery performance.

Simulations have been used to determine thermal behavior of batteries (Jilte et al. 2021; Kwon et al. 2006). Valuable information in analyzing battery temperature rises can be obtained by using battery thermal models. The thermal behavior of the battery can be explained by applying thermal models providing a cost-effective approach. In the literature, distinct cooling methods have been used to control battery temperature rise. Phase change materials (PCMs) have been widely used in

---

U. Morali (✉)

Department of Chemical Engineering, Eskisehir Osmangazi University, Eskisehir, Turkey

e-mail: [umorali@ogu.edu.tr](mailto:umorali@ogu.edu.tr)

battery temperature control studies owing to their absorption ability of sensible heat as well as latent heat (Choudhari et al. 2021). Therefore, the use of PCM not only absorbs heat but also may provide a discharge operation at a constant temperature (Sattari et al. 2017).

In this study, the NTGK model was implemented to obtain the battery temperatures of a lithium-ion battery. The battery temperatures are maximum battery temperature, average battery temperature, and minimum battery temperature. The battery temperatures were also obtained using PCM. The effect of using phase change material was analyzed using the numerical results.

## 31.2 Method

A lithium-ion battery was used to simulate battery thermal behavior. Maximum and minimum battery potentials are 4.20 V and 3.00 V, respectively. The lithium-ion battery was discharged from 4.20 V to 3.00 V at 3C-rate. The ambient temperature was 290 K. The battery surface temperature and phase change material temperature were assumed to be equal to the ambient temperature at the initial stage of simulation. The convective heat transfer coefficient of the battery was assumed to be 5 W/m<sup>2</sup> K. Thermal and physical properties of phase change material was obtained from (Bellia et al. 2013). Density, heat capacity, and thermal conductivity of the PCM are 750 kg/m<sup>3</sup>, 2250 J/kg K, and 0.2 W/m K, respectively. Melting heat of the PCM is 270.7 kJ/kg. Solidus and liquidus temperatures are 314.15 K and 317.15 K, respectively.

ANSYS Fluent was used to implement the NTGK model. Expressions of battery temperature are presented in Eqs. (31.1, 31.2, and 31.3):

$$\nabla(\sigma + \nabla\phi +) = -(jECh - jshort) \quad (31.1)$$

$$\nabla(\sigma - \nabla\phi -) = jECh - jshort \quad (31.2)$$

$$jECh = \alpha Y [U - (\phi + - \phi -)] \quad (31.3)$$

where  $\sigma +$  and  $\sigma -$  are electrical conductivity of positive and negative electrodes,  $\phi +$  and  $\phi -$  are phase potentials of positive and negative electrodes.  $jECh$  is produced volumetric current transfer rate.  $Jshort$  shows current transfer rate. Model parameters,  $U$  and  $Y$ , are expressed as follows (Kwon et al. 2006; Kim et al. 2009; Gu 1983):

$$3U = \alpha_0 + \alpha_1 (\text{DoD}) + \alpha_2 (\text{DoD})^2 + \alpha_3 (\text{DoD})^3 \quad (31.4)$$

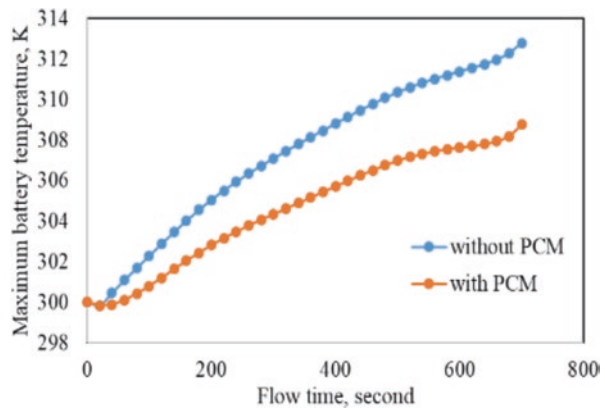
$$Y = \alpha_4 + \alpha_5 (\text{DoD}) + \alpha_6 (\text{DoD})^2 \quad (31.5)$$

where  $a_0$ - $a_6$  are the fitting parameters. In this study, the fitting parameters obtained by (Kim et al. 2011) were used to calculate U and Y model parameters.

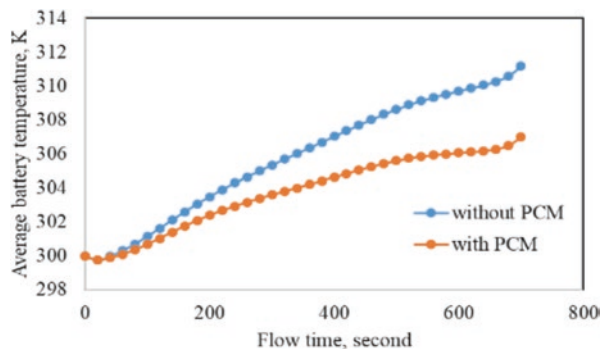
### 31.3 Results and Discussion

Figure 31.1 shows the maximum temperature of lithium-ion batteries with PCM and without PCM. The maximum battery temperature of lithium-ion battery was 312.81 K at 5C. This maximum battery temperature was within the normal range of lithium-ion battery performance (313.15 K). The maximum battery temperature was 308.75 K when the PCM was used to control the battery temperature. The average battery temperatures with PCM and without PCM are presented in Fig. 31.2. The average battery temperature at 5C was 311.16 K without PCM, while the average battery temperature with PCM was 306.98 K. Figure 31.3 shows the minimum temperature of lithium-ion batteries with PCM and without PCM. The minimum battery temperature at 5C (309.93 K) without PCM was higher than with PCM (300.96 K). Results demonstrated that the PCM showed a decrease in each battery

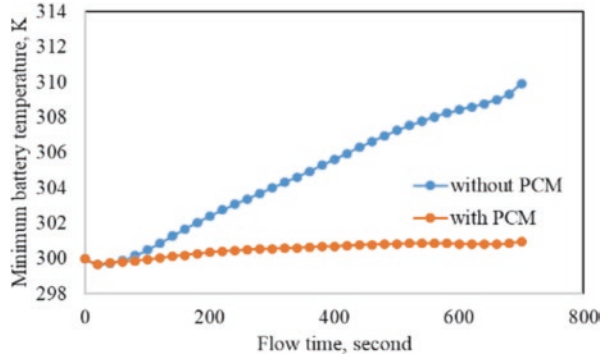
**Fig. 31.1** Maximum battery temperature at 5C-rate with and without PCM



**Fig. 31.2** Average battery temperature at 5C-rate with and without PCM



**Fig. 31.3** Minimum battery temperature at 5C-rate with and without PCM



temperature. The difference between the minimum battery temperatures with and without PCM was 8.96 K. Moreover, the difference between the average battery temperatures with and without PCM (4.19 K) was higher than the maximum battery temperatures (4.05 K).

Temperature counters for the battery static temperature are presented in Fig. 31.4. The temperature distribution shown in Fig. 31.4a was more heterogeneous than that presented in Fig. 31.4b. In other words, the lithium-ion battery using PCM exhibited a more homogeneous temperature distribution across the battery body. Temperature distribution may affect battery performance. It is anticipated that the performance of the battery using PCM will be higher than the battery without PCM, likely due to homogeneous temperature distribution and restricted temperature rise. It is important to note that the temperature counters in Fig. 31.4 showed the distribution of static temperature at the end of 5C discharge. Results also showed that such a high discharge operation increased battery temperature in a short flow time. The used PCM restricted the temperature rise and allowed heat to dissipate homogeneously across the battery surface.

## 31.4 Conclusion

The effect of phase change material on battery temperature has been investigated in this study. The battery temperature was obtained using the NTGK model. Results showed that the maximum battery temperature was 312.81 K (without PCM) and 308.75 K (with PCM). The phase change material used reduced the average battery temperature by 1.35%. PCM allowed a relatively homogeneous temperature distribution for the battery discharged at a high rate of 5C compared with the battery without PCM. It is recommended that phase change materials can be used in battery thermal management systems to obtain a homogeneous temperature distribution and to restrict the temperature rise.

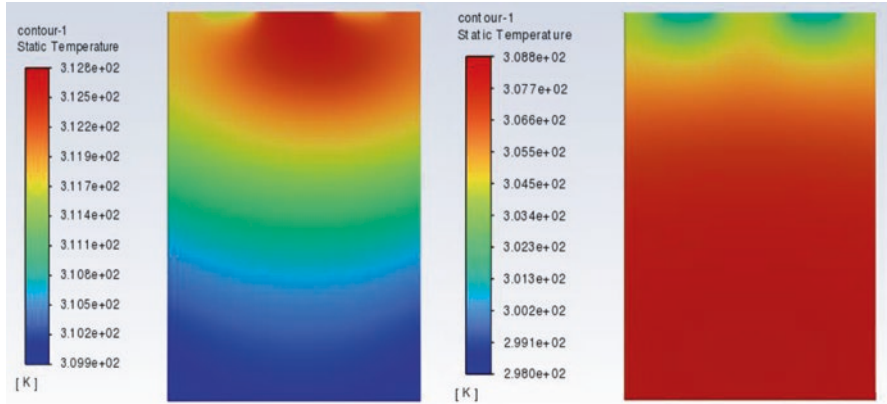


**Fig. 31.4** Distribution of static temperature at 5C-rate: (a) without PCM; (b) with PCM

## References

- L. Bellia, F. De Falco, F. Minichiello, Effects of solar shading devices on energy requirements of standalone office buildings for Italian climates. *Appl. Therm. Eng.* **54**, 190–201 (2013)
- V.G. Choudhari, A.S. Dhoble, S. Panchal, M. Fowler, R. Fraser, Numerical investigation on thermal behaviour of  $5 \times 5$  cell configured battery pack using phase change material and fin structure layout. *J. Energy Storage* **43**, 103234 (2021)
- H. Gu, Mathematical analysis of a Zn/NiOOH cell. *J. Electrochem. Soc.* **130**, 1459 (1983)
- R. Jilte, A. Afzal, S. Panchal, A novel battery thermal management system using nano-enhanced phase change materials. *Energy* **219** (2021)
- U.S. Kim, C.B. Shin, C.-S. Kim, Modeling for the scale-up of a lithium-ion polymer battery. *J. Power Sources* **189**, 841–846 (2009)
- U.S. Kim, J. Yi, C.B. Shin, T. Han, S. Park, Modeling the dependence of the discharge behavior of a lithium-ion battery on the environmental temperature. *J. Electrochem. Soc.* **158**, A611 (2011)
- K.H. Kwon, C.B. Shin, T.H. Kang, C.-S. Kim, A two-dimensional modeling of a lithium-polymer battery. *J. Power Sources* **163**, 151–157 (2006)
- H. Sattari, A. Mohebbi, M. Afsahi, A.A. Yancheshme, CFD simulation of melting process of phase change materials (PCMs) in a spherical capsule. *Int. J. Refrig.* **73**, 209–218 (2017)
- O. Yetik, T.H. Karakoc, A numerical study on the thermal performance of prismatic li-ion batteries for hybrid electric aircraft. *Energy* **195**, 117009 (2020)
- Y. Zeng, D. Chalise, S.D. Lubner, S. Kaur, R.S. Prasher, A review of thermal physics and management inside lithium-ion batteries for high energy density and fast charging. *Energy Storage Mater.* **41**, 264–288 (2021)



# Chapter 32

## Global, Regional, and Local Decision Levels to Aircraft Noise Management in Airports



Oleksandr Zaporozhets

### Nomenclature

AN	Aircraft Noise
BA	Balanced Approach
ICAO	International Civil Aviation Organization
NAP	Noise Abatement Procedures
NPZ	Noise Protection Zones
WHO	World Health Organization

### 32.1 Introduction

Aircraft noise (AN) has always been a priority subject in the framework of aviation and the environment (WHO 2018). It primarily affects residential communities close to airports, being a local stressor for the environment in nature (ICAO Resolution A40-17 2019). In a huge number of airports worldwide, this local issue is a limitation for traffic capacity in airports, reducing their operational and economic efficiencies. Combined together, these airport capacity values may produce regional and even global circumstances for the aviation sector as a whole.

Aircraft noise exposes and affects communities within an airport surrounding area, defined by the level of long-term noise exposure or for a specific noisy flyby, especially during a specific interval (during mostly sensitive to noise periods of the day) of observation, taking in mind the influence of temporal duration and number of noise events on total exposure. The AN impacts the population directly and particularly the perceived noise annoyance by communities depends upon the AN exposure, length of the noise event (especially if it is the noisiest contribution to

---

O. Zaporozhets (✉)

Lukasiewicz Research Network – Institute of Aviation, Warsaw, Poland  
e-mail: [Oleksandr.Zaporozhets@ilot.lukasiewicz.gov.pl](mailto:Oleksandr.Zaporozhets@ilot.lukasiewicz.gov.pl)

overall exposure), and the time of day, when exposure is observed, or dominant human activity performed inside the area of noise exposure (Berglund et al. 1999). Generally, AN exposure varies with the type and size of the aircraft, the power the aircraft is using at the moment, and the altitude or distance of the aircraft to the receptor. A higher distance from the source provides less noise exposure level, this is an essential condition for all noise protection programs.

Between AN exposure and its impact an essential difference exists – a number of factors, including non-acoustical factors, may influence sufficiently on impact values in the condition of the same exposure. The importance of any factor depends essentially on the object of exposure. ICAO BA guidance (ICAO Document 9829 2008) considers only the population as element-at-risk. If acoustical factors may be set into few physical values – aircraft mass and engine type installed, aircraft certificated noise performances, air traffic intensity, distribution of flights among the routes, flight procedures in use, etc., the non-acoustical factors cover a much higher number of human–social, physical, economic, cultural, and environmental issues (Zaporozhets and Blyukher 2019; Vader 2007). Most of them are the subject of human vulnerability assessment to noise exposure. If to consider the current concept for risk assessment, the complicated interdependence exists between exposure, vulnerability, and coping capacity in a noisy environment, so the effect (or damage) of AN on humans may vary considerably. Vulnerability and coping capacity of the population may change between themselves dramatically, so even for the same exposure level, for example, defined by AN exposure footprints for single flybys (Fig. 32.1), the number of the annoyed population inside the exposed area may rise or reduce essentially.

Another variable affecting the overall noise impact is a perceived increase in aircraft noise at sensitive daytime, for example at evening or night when the resting activities are dominant inside the community – when the community is most

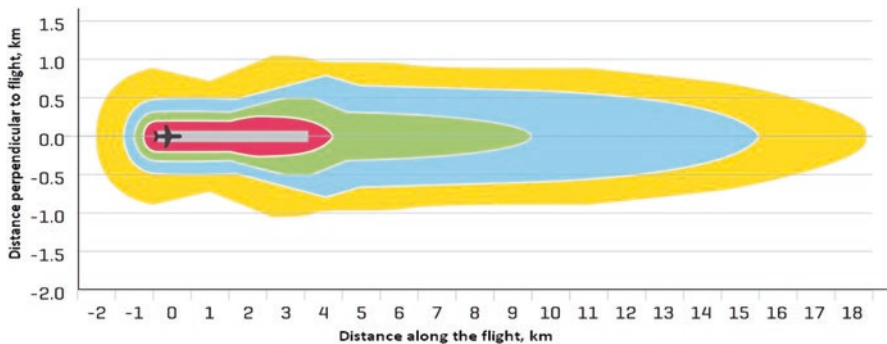


**Fig. 32.1** Noise exposure reduction of the aircraft during last 50 years from ICAO Annex 16 Chapter 2 till Chapter 14 certification norms: (a) single aircraft departure footprint for  $SEL = 80\text{dBA}$ : in yellow – Chap. 2 model of aircraft, e.g., B737–200; in blue – first-generation Chap. 3 aircraft, e.g., MD80, B737–200 Hush Kit; green – current Chap. 4 aircraft with, e.g., A320, B737–800; red – modern current Chap. 14 (aircraft with geared turbofan engines, e.g., A320neo. (European Aviation Environmental Report 2019)

vulnerable to this hazard issue. The noise limits for these sensitive periods of the day are usually 5–10 dBA stricter (less) and above all they are the limitations for the air transportation activities at airports if fulfilled whole the day. To minimize aircraft noise problems through preventive measures, ICAO policy, primarily, recommends locating the new airports at an appropriate place, such as away from noise-sensitive areas (ICAO Resolution A40-17 2019). Never mind that internationally agreed policy is recognized by the states, each airport requires its own solutions based on its specific characteristics as in noise hazard generation and propagation effects, so as in noise exposure influence on population (or other elements-at-risk) with their vulnerability and coping capacity performances. The circumstances of each airport vary significantly between themselves so an effective operational procedure or even mitigation measure at one airport may not be appropriate (or even feasible) in another.

Airports are usually located within or close to the limits of large urban areas (Fig. 32.2), in better case, a distance to existing noise-sensitive land usage (residential or recreational) may provide human protection from noise exposure and minimize the adverse impacts of their operations. The overlap of urban areas within the noise protection zones (NPZ) around aerodrome (as shown in Fig. 32.2, especially on the East from the runway) may exist and in such a case it indicates that a population inside the zones is exposed and vulnerable and even impacted (at least annoyed) by noise and needs for additional protection (due to noise insulation schemes, etc.).

## 32.2 General Considerations on Noise Management

The national legal system declares the noise limits (standard values for noise in the environment) usually in practice, which are prohibited for overloading inside the area of any human activity – especially inside residential and rehabilitation areas. The WHO (Berglund et al. 1999) recommends a value of 55 dBA  $L_{DN}$  for such a limit (long term), but practically in accordance with national approaches and possibilities (technical and economical) for noise protection, the values 65–75 dBA



**Fig. 32.2** Example of Noise Contours for NPZ at Kyiv/Zhulyany International Airport – Kyiv, Ukraine: red contour – 85 dBA  $L_{Amax}$ ; yellow contour – 80 dBA  $L_{Amax}$ ; pink boarded zones – residential areas of the Kyiv City

LDN are used to eliminate human activities with the implementation of additional protection from noise. Somewhere, particularly in Ukraine, there are few criteria used for environmental noise assessment and management (Konovalova and Zaporozhets 2021), emphasizing that noise may impact the population in a few ways including the effects during long-term and short-term exposures. Particularly for aviation noise, short-term exposure is important in case of a contribution of the noisiest flight events to overall exposure and especially in conditions of quite small flight traffic, which are observed in regional airports at the first stage of their development. For them, the noise contours for single flight event, defined for sound exposure level *SEL*, or for maximum sound level  $L_{Amax}$ , are larger in size (in area also) in comparison with equivalent sound levels  $L_{Aeq}$  (for various time intervals and day periods) or noise indices ( $L_{DN}$ ,  $L_{DEN}$ , *WECPNL*, etc.) with normative values (limits).

Of course, a scenario with small air traffic in the particular case of airport operation is not a good reason to define and implement NPZ around the aerodrome. The calculated noise contours for single flight events and for limits in  $L_{Amax}$  and/or *SEL* may restrain the inconsistency with noise development of the residential and occupational areas around the airport under consideration. That is, for airports with low air traffic, it seems appropriate to assess the boundaries of the zones based on the results of calculating the noise contour for the flight of the loudest aircraft or for the determining type of aircraft at the design stage of the aerodrome (during the design of the runway). This assumption will be valid until the growth of the traffic may reach the intensity of flights providing the more dominant equivalent sound levels  $L_{Aeq}$  over the single flight exposure *SEL* (or maximum sound level  $L_{Amax}$ ) in the definition of the noise zones' boundaries. In any case, the boundaries of the NPZ must not be assessed on the current flight traffic scenario only. It should be done with forecasted scenarios, preferably one of them with the contribution of the most possible undesirable mixture of aircraft in a fleet and their operation during the day.

From another side of the problem, the general plan of land use development around the airport should be considered and it must be consistent with the development of the airport and its noise circumstances. Community engagement in this process becomes definitive, the decision-making by airport authority alone may be mistaken (ICAO Circular 351 2016). A particular challenge was and still is the fact that successful noise impact mitigation interventions by airports often lead to noise contours shrinking size. This usually leads to new developments being approved only – resulting in no net reduction in the number of people exposed to aviation noise, sometimes even to its rise, if this development is inconsistent with shrunk noise contour.

There are few levels of decision-making that exist in a process of aircraft noise management, even in consideration of the problem at a specific airport – the global, regional, and local. The regional or state level is mostly directed on the elimination or reduction of exposed to noise population in the vicinity of the airports. A global approach to the problem solutions is concentrated on manufacturing less noisy aircraft – ICAO international standards for aircraft noise are the examples of such kind of solutions (ICAO Annex 16 2019). The total phase-out of the noisy aircraft (with noise levels under the Chap. 2 requirements) in international air transportation

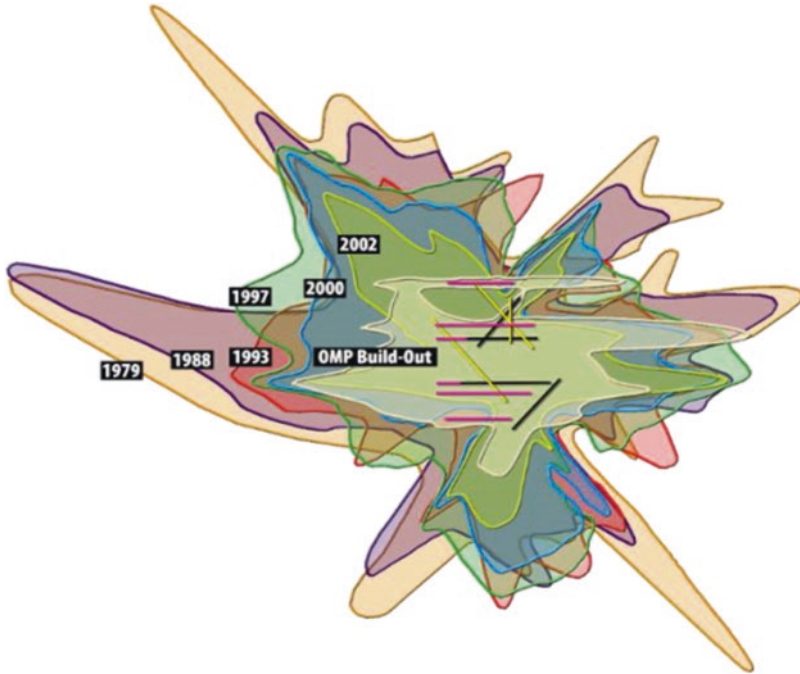


**Fig. 32.3** 65 dBA  $L_{DN}$  noise contour changes at O’Hare Airport (Chicago) due to more stringent standard requirements to aircraft noise and phasing out of noisy types from operation between 1998–2002 despite an increase in flight traffic

worldwide is also an example of a global approach, but it was a single act in aviation history at the beginning of the twenty-first century, as was agreed upon in the 28th ICAO Assembly (in Fig. 32.3 a dramatic change between the AN contours for 1998 and 2002 scenarios), which currently is not recommended by ICAO policy on environment protection. Global phase-out of the aircraft from the operation, especially those that did not reach the final operational resources, means economic damage for airlines and for total air transportation system. Nowadays, the phase-out of the noisier types of aircraft is considered as a local measure to solve the problem at any particular airport; and only in case if ICAO standards (reduction in the source), noise zoning (reduction of overall noise exposure on population), and operational low-noise procedures are not enough to balance the noise management program.

### 32.3 Balanced Approach to Aircraft Noise Management

In 2001, the 33rd Session of the ICAO Assembly adopted a new policy for aircraft noise control globally, referred to as the “balanced approach” to noise management. The ICAO BA guidance (ICAO Document 9829 2008) contains the explanation of

all elements in general details, namely: reduction of aircraft noise at source – manufacturing quieter aircraft under ICAO standard requirements; noise zoning, land-use planning, and management; noise abatement procedures for aircraft operation; and usually partial restrictions for noisy aircraft operation. The goal is to also identify the noise-related measures that achieve the maximum environmental benefit (minimum environmental risk), using objective and measurable criteria, at any specific airport most cost-effectively. If the main goal in aircraft noise control is to reduce the noise level at the source of its generation, the main goal for noise zoning and land use management is to prevent the people from the noise levels which are detrimental to their health and welfare.

The principle in ICAO BA guidance (ICAO Document 9829 2008) is that a criterion on noise exposure assessment should be day-night noise index  $L_{DN}$ , or its analogue in EU – day-evening-night noise index  $L_{DEN}$  (European Council 2002). For example, in Ukraine equivalent sound levels  $L_{Aeq}$  is used for daytime and nighttime separately, and it is not a direct analog of the day-night noise index. The second principle (not the requirement) – the overall AN exposure and the boundaries of noise zones around an airport under consideration should be defined by calculation. For that, a special method is recommended by ICAO (ICAO Document 9911 2018).

Few levels of aircraft noise assessment exist to be used for decision-making in noise abatement program compilation for the airport. The highest level of strategic solutions needs simple calculations but accurate enough for received solutions. Recommended method (ICAO Document 9911 2018) may be too complicated for that. One of the approaches for simplified calculations is based on a concept of Noise Radius which is similar to the concept of “Noise-Power-Distance” but provides a quick assessment of the exposure and its changes in accordance with considered noise abatement scenario in the airport noise management program (Zaporozhets et al. 2011; Zaporozhets and Tokarev 1998).

The area and sizes of noise zones (Figs. 32.2 and 32.3) is a subject of aircraft noise calculation (ICAO 9829 2008; ICAO 9911 2018); aircraft noise and performance data (from the international ANP database, <https://www.aircraftnoisemodel.org/>) should be used to derive the noise contours for those specified by the national rules noise levels/indices. To imagine the sizes of noise zones around the aerodrome (or separately for runway) a simple approach may be proposed (Zaporozhets et al. 2011; Zaporozhets and Levchenko 2021) – to consider the noise contours as a result of the intersection of the cylindrical surface of equal sound level (equal to the limit used for noise zoning borders) with the ground surface around the aerodrome and flight paths. It was shown that this simplified contour will be an ellipse, a small radius  $b$  which is equal to noise radius  $R_N$  (or to distance from appropriate “Noise-Power-Distance” relationship from ANP database) and big radius  $a$  – to  $R_N/\sin\gamma$  for aircraft type under consideration at this flight mode, where  $\gamma$  is an angle of climbing/descending – depending on aircraft type (number of engines in its power plant) and its flight stage (Fig. 32.4).

The main simplification in the concept of Noise Radius  $R_N$  is that it is considered as constant, at least during the definitive for noise contour assessment flight stages of the aircraft. The results of numerous researches show that  $R_N$  is varying all the



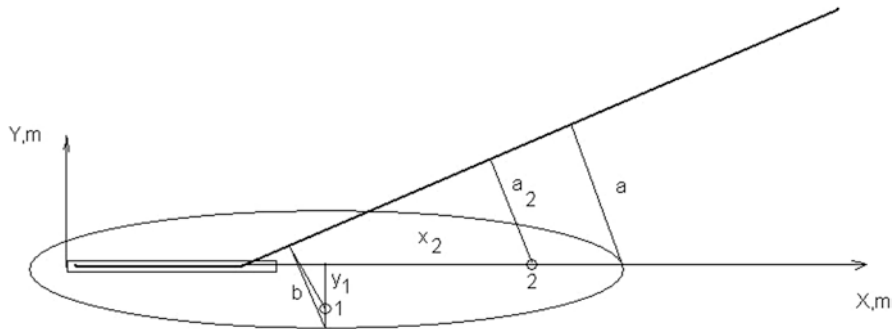


**Fig. 32.4** A simplified form of noise footprint having the shape of an ellipse under the takeoff flight path. (Zaporozhets et al. 2011).

time, it is mostly dependent on engine operation mode (engine power) and noise level (type and value) to be considered, but the altitude and speed of flight, meteorological conditions, even type of the ground covering during some specific flight stages are also influencing the value of Noise Radius and its derivatives (Zaporozhets and Levchenko 2021).

From the considerations before, the value of  $R_N$  is not the same for the definitions of semi-minor  $b$  and semi-major  $a$  axes of the equivalent ellipse for the noise contour under consideration. Because the maximum operation mode is used for engines at takeoff, the nominal – at climbing; but for quieter types of aircraft this difference is lesser (Fig. 32.1).

The most sensitive violation of the simplification of the concepts of constant noise radius and ellipse for the noise contour occurs at the point of intersection of the segments of the flight path of the altitude, which changes the mode of operation of engines (in Fig. 32.1 it corresponds to a distance of  $\sim 4$  km). But generally, the error (inaccuracy) of these changes does not seem significant in strategic assessments and decisions.

### 32.3.1 ICAO Standard Requirements to Aircraft Noise and Management of Noise Exposure around the Airports

A more significant impact on the assessment should be expected from a further reduction in noise levels at the source, when the sound levels at the control (certification) points and for the noise contours with the normative value of the sound level (e.g., 75 dBA  $L_{Amax\ night}$ ) will not be displayed on the airport noise map. As can be seen from Fig. 32.1, the noise contour for takeoff/climbing of the airplane with Chap. 14 noise performances (ICAO Annex 16 2019) is already within the runway size. Therefore, further expected more stringent requirements for aircraft noise

levels at three points of noise control (takeoff, climbing and descending before landing) will create conditions where the noise contours for single departure and arrival events will be indeterminate for exposure assessments with essential noise levels (correspondent to environmental noise limits) and decision-making in the airport noise control program.

The difference between the certified noise level at climbing flyover point ( $L_2$ ) and the level corresponding to the final point on the contour  $L$  along the departure flight (or arrival noise contour in dependence to noise level at ICAO standard point No 3) axis may be written (Powell 2003; Zaporozhets et al. 2011):

$$L_2 - L = C \lg(a / a_2), \quad (32.1)$$

where the constant  $C$  defines the attenuation rate, for cylinder spreading its value is near to 10 and for spherical spreading – near to 20,  $a$  is the minimum distance from the flight path to the final point on the contour (Fig. 32.4),  $a_2$  is the minimum distance from the taking off path to the certification point No 2 (for departure). Similar view is possible on the difference between the certified noise level at takeoff ( $L_j$ ) and the level corresponding to the final point on the contour  $L$  aside the flight – ICAO noise control point No. 1 in Fig. 32.4. The area  $S$  of noise contour at takeoff and climbing is proportional with quite high correlation to the product of  $L_2$  and  $L_j$ :

$$\lg(S) = (L_2 + L_j) / C + D, \quad (32.2)$$

which is the same as Eq. (32.1). Constants  $C$  and  $D$  are different for various types of the sound levels  $L$ ,  $L_j$ ,  $L_2$ , and for different groups of airplanes (Zaporozhets and Tokarev 1998; Powell 2003; Zaporozhets et al. 2011). Better correlation was found for sound exposure levels such as *SEL* and *EPNL*. For implementing the approach for strategic analysis of any air traffic and AN load scenario, the correlations between the exposure *SEL* and maximum  $L_{Amax}$  sound levels may be used as follows:

$$SEL = A + BL_{Amax} \quad (32.3)$$

Attention should be made in using correlations such as the above formula (if the higher accuracy of the assessment should be considered) because the constants  $A$ ,  $B$  are different not only for the types (groups) of the aircraft due to their different spectral class (explained in ANP database), but they are different in approach and departure flight stages, and are even different in their distances to flight axis (Fig. 32.5). It means that constants  $C$  and  $D$  in (2) may vary with the value of  $L$ , which is dependent to distance of noise source from the point of noise control.

Strictly speaking, not only the engine operation mode (thrust) at taking off/ climbing may influence the form of resulting contour for departure flight. Close to runway, the flight altitudes are small and distances to contour line are quite big, so lateral effect is changing the line sufficiently, mostly for the flight path segments along taking off (Fig. 32.6). If to use the concept of hypothetical contour, defined by equal noise exposure cylinder intersection with surface plane discussed above



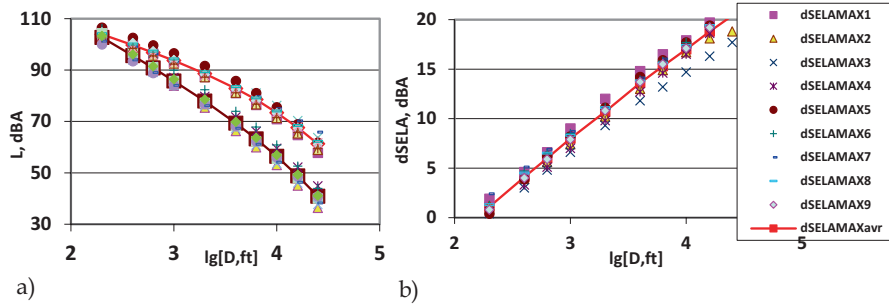


**Fig. 32.5** Dependence (a) between SEL (red rhombuses) and  $L_{Amax}$  (brown squares) and the difference (b) between them for the distance to flight axis for the airplane group A-320 and B-737

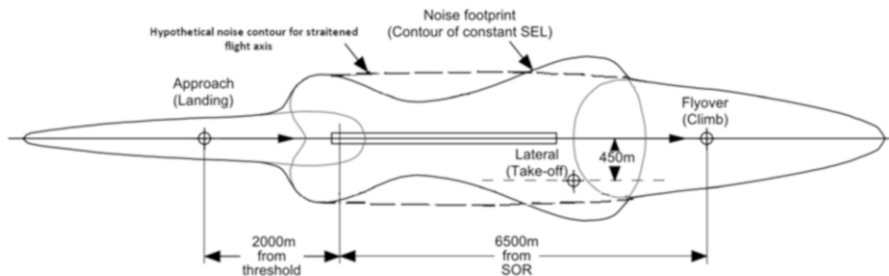


**Fig. 32.6** Hypothetical noise contour for straitened flight during departure and excluded ground effect for sound propagation close to runway

(Fig. 32.4) and the exposure level on cylinder surface is defined by character noise level for climbing flight stage (dashed line in Fig. 32.6), the changes in contour line and area are covered between themselves and the values are very close one to another for various models – simplified and in accordance with ICAO (ICAO 9911 2018) requirements (Fig. 32.7).

Particularly for airplanes with noise performances in accordance with the requirements of FAR 36 Stages 3–5, which are currently in operation, the dimensions/areas of the simplified contours for departure flight are within 10% of the accuracy of INM contour data. Bigger differences between the dimensions and areas of the simplified and INM contours for airplanes of Stage 1 and 2 performances may be described by a number of reasons – first is that the method of assessment during AN certification procedures for these stages was different from existing ones, and their data are normalized/harmonized with current method requirements not correctly always, even in ANP database (the same with INM database, which is very similar to ANP database). In fact, the results for FAR Stage 5 (equal to ICAO Chap. 14) performances are so small that the character contour for  $L_{Amax}$  night may lie closely to the runway, somewhere inside the territory of the aerodrome as shown in Fig. 32.1.

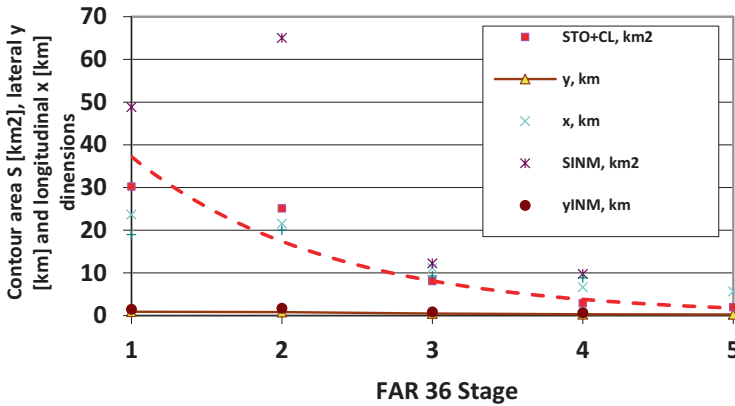


Fig. 32.7 Comparison between the dimensions and area for noise contour 75 dBA  $L_{Amax}$  defined by simplified model and INM for Boeing-737 at departure with noise performances in accordance with FAR-36 requirements (from B737-100 for Stage 1 till Boeing-737MAX for Stage 5)

Again returning to equivalent sound levels  $L_{Aeq}$  and/or noise indices  $L_{DN}$ , first because of their much higher correlation with noise impact assessment, one should consider the difference between them and single flight event value such as  $SEL$  as follows:

$$L_{Aeq} = SEL - 10 \lg T + 10 \lg n, \tag{32.4}$$

where  $T$  is a temporal interval of  $L_{Aeq}$  definition to be assessed,  $n$  – number of single events with sound exposure  $SEL$ . Here, in formula (32.4) the value of  $SEL$  is defined for determining type of the aircraft in scenario under consideration, as it was discussed before.

This simplified formula (32.4) allows to define the contour for night-time limit  $L_{Aeq} = 55$  dBA (as defined by the Ukrainian rules for noise zoning (Konovalova and Zaporozhets 2021)), the number of aircraft flight events  $n$  similar to determining type in the scenario should be  $\sim 10$  if it is equal to ICAO Chap. 2 noise performances, rising up to  $\sim 30$  if the noise performances will be equal to ICAO Chap. 14 requirements. For daytime noise limit  $L_{Aeq} = 65$  dBA, the same assessment is showing the change in a number of events  $n$  between  $\sim 140$  for ICAO Chap. 2 and  $> 500$  flybys for ICAO Chap. 14 aircraft flybys. Thus, with quieter determining aircraft in a fleet of the scenario under consideration, the dominance of the single noise exposure contour may not be diminished by noise equivalent contour. It may be a new principal condition for noise zoning determination in the future AN scenarios.

Aircraft produced today are 75% quieter than the first civilian jets that appeared in operation 50 years ago (Fig. 32.1). The newly manufactured aircraft typically produce around half the noise of the aircraft they are replacing, so with this innovation, the air traffic movements can double without increasing the total noise exposure output (ICAO Document 10127 2019). During the 50 years of aircraft noise

standardization from ICAO (first Edition of Annex 16 – Aircraft Noise was published in 1969) and continuous strengthening of the requirements from ICAO Chap. 2 up to the current Chap. 14 (ICAO Annex 16 2019), the cumulative reduction was gained up to ~35 dB, close to this value is necessary to be reached until the ACARE noise goal at 2050 (Flightpath 2050 2011). The next strengthening of noise requirements for the aircraft may provide the conditions of eliminating the single event contours sufficient for analysis and management levels ( $L_{Amax}$  75 dBA for the night and 85 dBA for the day) from consideration in population exposure tasks.

### 32.3.2 Land-Use Planning

The need for land-use planning in the vicinity of an airport was recognized in the early history of civil aviation and focused on the use and control of the land. Manual (ICAO Document 9184 2018) is focused on land use and environmental management on and around an airport. Airport operators can reduce the environmental impacts – noise, air emission/pollution, safety issues of their operations by incorporating environmental management plans and procedures with land-use compatibility planning with a broad appreciation of their relative sensitivity of the population to the aircraft operational safety, local third-party risk, and noise exposure. Among land-use planning measures, the noise zoning around airports is the primary, main, and most effective to be protected from noise exposure; they should be implemented as soon as noise problems are foreseen (Fig. 32.8). But compatible land-use planning and management should be based on appropriate forecasted aircraft noise contours, rather than current contours, which must prevent encroachment of residential development at airports where future aircraft noise levels are projected to increase.

It is still recommended that the assessment of environmental noise continue to be an integral element in identifying and solving land use planning problems and of noise management overall. Inside the zone of noise management, it is necessary to organize a set of plans (a program for noise protection) that govern urban planning and management with respect to airport activities. The principles of zoning of

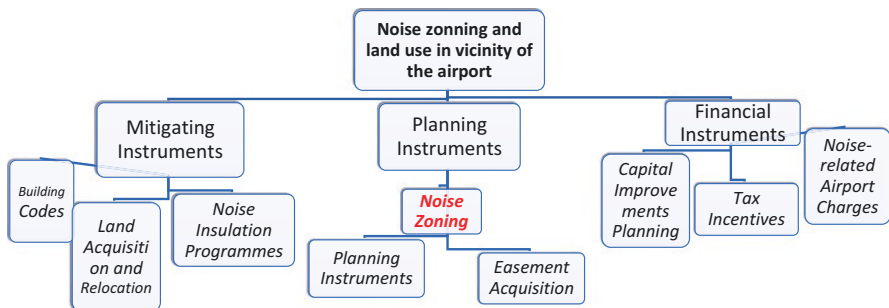


Fig. 32.8 Noise zoning and land usage instruments in airport environment

territory around the aerodrome in conjunction with the aerodrome (heliport, permanent runway) and land use are substantiated accounting on the quantity and quality of lands of any state is proved in Novakovska et al. (2020). In reality, each airport is different in its operational, social, economic and political situation, as well as in the type of land use in its vicinity. That is why the airport noise protection program should include a land-use control system to assure that all the prescribed measures not only comply with the airport development plan but also with the plan of urban development and the goals of the communities involved.

Local airport rules can include noise limits, curfews, and penalties on excessive noise levels. These measures are considered mostly as constraints, they may limit the operational capacity of airports (for example, by restrictions for flights during the night) and they may affect the economics of air transportation by limiting the takeoff weight, payload and consequently reducing the economic benefit of a specific flight.

Where the opportunity still exists to minimize aircraft noise problems through preventive measures, the main efforts should be prioritized as follows: locate new airports at an appropriate place, such as away from noise-sensitive areas; take the appropriate measures so that land-use planning is considered fully at the initial stage of any new airport or of development at an existing airport; define zones around airports associated with different noise levels considering population levels and growth as well as forecasts of traffic growth and establish criteria for the appropriate use of such land, taking account of ICAO guidance (ICAO Document 9829 2008); enact legislation, establish guidance or other appropriate means to achieve compliance with those criteria for land use; and ensure that reader-friendly information on aircraft operations and their environmental effects are available to communities near airports, etc.

Among the alternatives to regulate land developments inside the surrounding area affected by the airport, a number of modification or restriction of land uses exists to achieve greater consistency between aviation and human activities, or in other words – to reach compatibility between the airport and its environs. These control measures may be divided into three categories, as follows: Planning Instruments, Mitigating Instruments, and Financial Instruments. Some examples of these instruments are listed in Fig. 32.8.

Noise zoning is a core regulation in noise exposure/impact management on population (Fig. 32.8) realized through Planning Instruments and should specify land development depending on the level of noise exposure and use restrictions, based on certain noise levels – the limits, which are incompatible with human activities inside the zones. The limits and a list of zones around the airport are defined by the state rules, usually similar to all airports of the state. These regulations should protect both – the airport and the residents in their mutual developments. Noise exposure is not the only factor to be considered in land-use management in the vicinity of airports. It is recognized that economic factors are involved in land-use choices. Ideally, land-use decisions around airports would try to find a compatible balance between the interests in the land and the aeronautical use of the airport.

It is quite a difficult subject because the communities are striving to be closer to the airport due to the desire for better conditions in a number of businesses connected to airport activities. Land-use planning must account for existing development and ensure that future planned development is also consistent between the aviation sector and communities, and compatible with their various goals including the changes in aviation noise exposure due to changes in aircraft fleet and air traffic in airports. Easements should restrict the use of land to that which is compatible with aircraft noise levels.

Some of the airports due to their specific place in the air transportation system of the state (or inside the region) may use/implement different rules from the state rules noise limits, which may or mitigate or allow a specific land usage inside the zone. An appropriate sound insulation program should be provided to control interior noise levels inside the buildings that are impossible to be removed out of areas exposed to noise. A necessary budget for the insulation program is usually gathered by implementing the noise-related airport charges – main financial investments to any noise protection program in the airport under consideration. Noise monitoring systems – continuous or permanent – are the instrument for objective noise exposure assessment of the air traffic inside the specific zone (where a noise monitor is installed) or to be used for assessing the efficiency of any implemented noise protection measure.

The strategic routing of aircraft through navigable airspace to minimize noise impact for both sensitive land uses as well as populated areas are essential in the airport planning process. The protection of the residents is understood as a dynamic process, meaning that the evaluation criteria must be repeatedly tested and – if necessary – adapted to new scientific findings (Chyla et al. 2020). Compared with traditional ICAO balanced approach elements, which are defined by physical effects of sound generation and propagation, involving non-acoustical factors must now be included to reduce the annoyance. Up to now, annoyance was mainly explained through acoustical factors such as sound intensity, peak levels, duration of time in-between sound events, and number of events. The non-acoustical factors (“moderators” and/or “modifiers” of the effect) have still received empirical attention but without a deep theoretical approach, despite the fact that various comparative studies reveal that they play a major role in defining the impact on people.

### ***32.3.3 Noise Abatement Procedures***

Operational procedures are intended for use by aircraft of the existing fleet and have the potential to make an immediate improvement in the environmental impact of aviation, as a rule locally emphasized at airports where the noise zoning and land use procedures are realized with omissions (ICAO Document 8168 2020; ICAO Document 9888 2007). The methodology and the decision-making algorithms for environmental control needs with NAPs were given in Tokarev et al. (Tokarev and

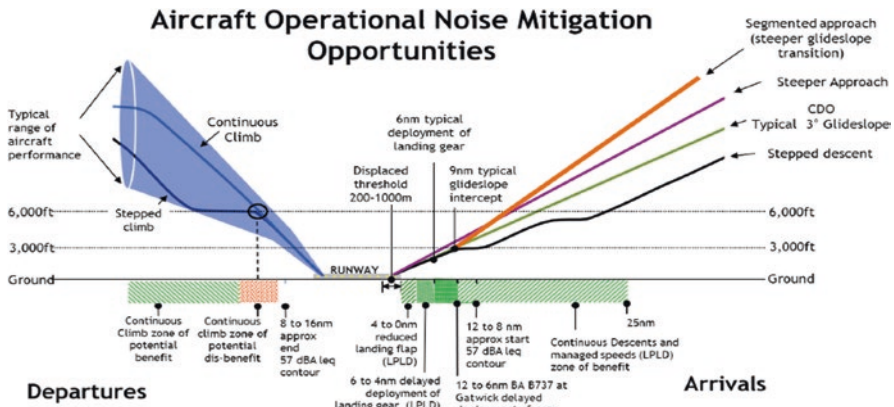


Fig. 32.9 Aircraft operational noise mitigation opportunities – illustrative, not to scale (Sustainable Aviation Noise Road-Map 2018)

Kazhan 2014), where the efficient numerical optimization was realized using the Lagrange multipliers method. Operational NAPs in use today can be categorized into three broad components: noise abatement flight procedures; spatial management; and ground movement management. Figure 32.9 schematically shows the operational opportunities of the NAPs. It also gives an indication of the areas (distances to the runway at departure and arrival) benefiting from some of any procedures outlined.

Given the above, the following guiding principles should be adopted when considering operational opportunities to reduce noise: safety must not be negatively affected; operational procedures should be developed in accordance with relevant ICAO provisions or regulatory guidance while allowing for the implementation of new procedures as that guidance evolves; changes to operational procedures must consider aircraft and operator capabilities and limitations with appropriate approval by the regulator; appropriate assessment tools and metrics to support decision-making and post-implementation review of conformance should be maintained; interdependencies should be considered between other environmental and non-environmental impacts and disproportionate trade-offs should be avoided. Of course, any progress in designing low noise aircraft would therefore lead to relaxing the stringency of the NAP to be used (Zaporozhets and Blyukher 2019).

In Fig. 32.10, it is shown that for ICAO Chap. 4 aircraft, the AN reduction ability via throttling the engines during the departure is more than twice less in comparison with Chap. 2 aircraft. Further improvements in noise generation at source (more balanced between the main acoustic sources of the aircraft) will provide much less ability for noise reduction by NAPs and the importance of the NAPs for AN management will be much limited.

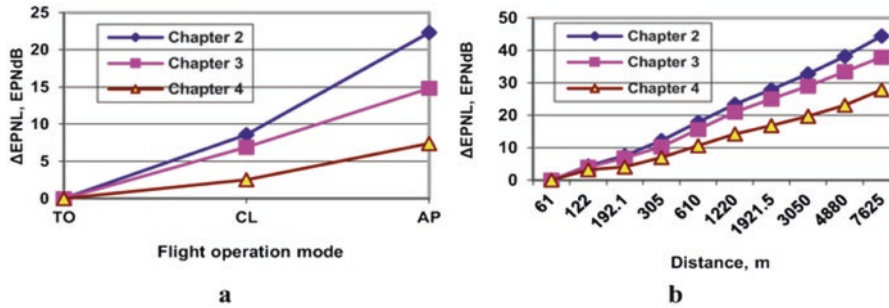


Fig. 32.10 Aircraft noise standard stringency influence on NAP ability to reduce noise level: (a) at point of noise control; (b) along with flight path distance

### 32.3.4 Aircraft Operating Restrictions to Reduce Noise Exposure

An operating restriction is defined in ICAO BA guidance (ICAO Document 9829, 2004), as “any noise-related action that limits or reduces an aircraft’s access to an airport.” The guidance recommends avoiding their application as a first measure to eliminate noise exposure in the airport vicinity, even in any specific point of noise control. Only in cases of insufficiency of the first three in reducing noise exposure levels at any location that operating restrictions may be implemented (EU Regulation 598 2014).

The decisions of the 40th Session of the ICAO Assembly on operating restrictions are contained in Assembly Resolution A40–17 (ICAO Resolution A40-17 2019), Appendix E “Local noise-related operating restrictions at airports.” As stated above, it is limiting the operational and economic efficiency of the airport work. If the benefits from the first three BA elements are limited to fulfil the environmental requirements to noise at any location, operating restrictions should be considered and implemented in the following way: be based on the acoustic performance of the aircraft, which should be determined as the noise certification results, consistent with procedures of Annex 16, Volume I (ICAO Annex 16 2019); be fitted to solving the noise problem of the airport concerned in accordance with the balanced approach principles; be mostly of a partial nature, not the complete withdrawal of operations at an airport; consider the consequences for air transport services, especially if the suitable alternatives are absent (for example, long-haul flights); conditions of competitiveness should not be violated (for example, exemptions may be granted for carriers of developing countries); be introduced stepwise, considering the possible economic burden for operators and, if reasonable, give operators advance notice and time for preparations.

Operational constraints can immediately provide a significant reduction in the impact of aircraft noise around airports, but they can increase the financial burden for both airport operators and airlines. Today, hundreds of airports worldwide are



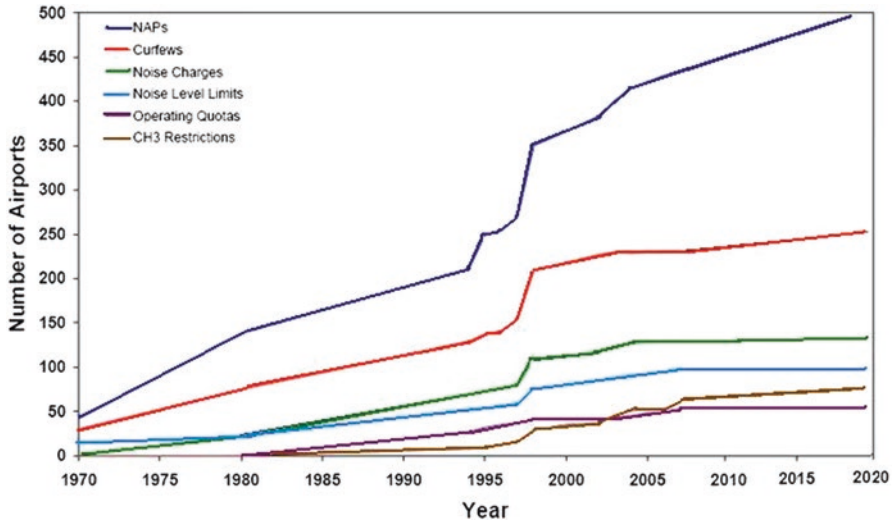


**Fig. 32.11** Growth in aircraft noise restrictions at airports worldwide; data from “Airport Noise and Emissions Regulations” (Boeing 2021)

implementing aircraft operating restrictions for noise management purposes on a case-by-case basis, whilst limiting capacity, but improving the noise climate around airports (Fig. 32.11). The figure is built on data from Boeing’s database “Airport Noise and Emissions Regulations” (Boeing 2021).

Aircraft operating restrictions for noise management may include as follows: restriction rules; noise quota or budget; non-addition rules; nature of flights; night-time restrictions; curfews; charges, etc. Any of them may fall into one or more of the four of the below-described categories, depending on how they are applied: Global (restrictions adopted worldwide – ICAO and EU decisions on Chap. 2 aircraft phase-out from the operation are the examples); Local (restrictions adopted by airport authority or by the state to eliminate the operation of noisy aircraft types, for example, Chap. 3 aircraft, another way the environmental constraints in a specific airport may reduce its efficient work); Aircraft-specific (restrictions applied to a specific type based on individual aircraft noise performance, usually at the specific route of departure or arrival at the airport); and Partial (restrictions applied for specific flight directions or/and for certain runways at the airport, during noise-sensitive time periods of the day, on specific days of the week).

## 32.4 Results and Discussion

Until now, all the existing BA elements have been assessed by changes in the noise exposure, mostly via noise contour modeling, and in some cases via monitoring. This allows for the evaluation of noise control measures to determine the most



cost-effective and beneficial for environmental protection (Zaporozhets et al. 2011). In the best cases, the process is performed with public notification and consultation procedures, supplemented with mechanisms for dealing with disputes and complaints. It requires developing noise action plans with obligatory participation of the public, especially if their residential/rehabilitation area or substantive environmental aspects are impacted by aircraft noise.

A brief analysis of all the elements of ICAO BA shows that ICAO noise standards accompanied with technological improvements of aircraft noise performances provide a reduction of aircraft noise exposure globally, at least for international air transportation. The second BA element – noise zoning and land usage – is mostly a subject of regional/national noise exposure management, predefined by regional (such as Directives inside the EU) or/and national rules.

Numerous violations of noise limits may be observed inside the zones in the vicinity of the airport, for their control a third element is included – the NAPs. Airport and airline authorities must find the best solution to what kind of the NAP will be most efficient in any specific case. This is a subject for local consideration.

Flight restrictions are mostly the subjects of local decisions and only in cases of the insufficiency of the first three BA elements. There are a number of regional and global restrictions that also exist – they are effective for all airports if implemented for the whole (national, regional, or global) system at the same time.

Besides the technical elements, which are completely based on noise intensity metrics, the noise annoyance (and other types of outcomes of aircraft noise exposure to neighbouring residents) must now be addressed. This evolution may lead to a new vision of the balanced approach to aircraft noise control in the very near future (Zaporozhets and Blyukher 2019).

Addressing such human-centric concerns, encompassing fear, negative health effects, and other environmental issues may lead to adding a fifth element to the ICAO BA to aircraft noise management around the airports. Strategies that reduce noise annoyance, as opposed to noise, may be more effective in terms of protecting public health from the adverse impacts of noise and its interdependence with other environmental, operational, economic and organizational issues of airport, and airlines operation and maintenance (Zaporozhets and Blyukher 2019).

## 32.5 Conclusion

It is important to differentiate between noise exposure and the resulting noise nuisance (primarily annoyance) in different communities and to manage each appropriately. The protection of the residents from aircraft noise exposure is understood as a dynamic process, meaning that the evaluation criteria (both for exposure and nuisance) must be repeatedly tested and – if necessary – adapted to new scientific findings (Chyla et al. 2020). Compared with the traditional ICAO BA elements, which are defined by physical phenomena of sound generation and propagation, non-acoustical factors must now be included to reduce the annoyance. Up to now,

annoyance was mainly explained through acoustical factors such as sound intensity, peak levels, duration of time in-between sound events, number of events (Janssen et al. 2011). The non-acoustical factors (“moderators” and/or “modifiers” of the effect) have still received empirical attention but without a deep theoretical approach, despite the fact that various comparative studies reveal that they play a major role in defining the impact on people (Job 1988).

ICAO BA continues to be developed in a few ways. Strategic solutions and decision-making procedures need simplified but quite accurate assessment tools of noise exposure and further – noise impact calculations. Second point – the global reduction of AN exposure at sources through technology improvements and new stringent standards implementation will continue to eliminate the NAPs and aircraft operating restrictions (as obviously shown in Fig. 32.11), at least as all of them are used today. More attention will be done to the management of non-acoustical factors, but the principles of their management are looking quite different from the current ICAO BA.

## References

- B. Berglund et al., *Guidelines for Community Noise* (World Health Organisation, 1999), revised version:141. <https://apps.who.int/iris/handle/10665/66217>
- Boeing. Airports with Noise and Emissions Restrictions. Database. (2021). <https://www.boeing.com/commercial/noise/list.page>
- A. Chyla et al., Portable and continuous aircraft noise measurements in vicinity of airports, in *Systemy i Srodki Transportu. Bezpieczenstwo i Materialy Eksploatacyjne. Red.*, ed. by K. Naukowa Leida, W.P. Monografia, vol. 20, (Wydawnictwo Politechniki Rzeszowskiej, Rzeszow, 2020), pp. 69–80
- EU Regulation 598/2014 OF THE EUROPEAN PARLIAMENT AND OF THE COUNCIL of 16 April 2014 on the establishment of rules and procedures with regard to the introduction of noise-related operating restrictions at Union airports within a Balanced Approach and repealing Directive 2002/30/EC. Available online: <https://eur-lex.europa.eu/legal-content/sv/ALL/?uri=CELEX:32014R0598>
- European Aviation Environmental Report, *European Aviation Safety Agency (EASA), European Environment Agency (EEA)* (EUROCONTROL, 2019). <https://doi.org/10.2822/309946>
- European Parliament, European Council. Directive 2002/49/EC of the European Parliament and of the Council of 25 June 2002 relating to the assessment and management of environmental noise – Declaration by the Commission in the Conciliation Committee on the Directive relating to the assessment and management of environmental noise. (2002). [https://eur-lex.europa.eu/](https://eur-lex.europa.eu/Flightpath%202050%20(2011)%20Europe's%20Vision%20for%20Aviation%20Report%20of%20the%20High%20Level%20Group.%20EU%20Directorate-General%20for%20Research%20and%20Innovation,%20Directorate%20General%20for%20Mobility%20and%20Transport%20on%20Aviation%20Research:32.%20https://op.europa.eu/en/publication-detail/-/publication/296a9bd7-fef9-4ae8-82c4-a21ff48be673)
- Flightpath 2050 (2011) Europe’s Vision for Aviation Report of the High Level Group. EU Directorate-General for Research and Innovation, Directorate General for Mobility and Transport on Aviation Research:32. <https://op.europa.eu/en/publication-detail/-/publication/296a9bd7-fef9-4ae8-82c4-a21ff48be673>
- ICAO Annex 16 (2019) to the Convention on International Civil Aviation — Environmental Protection: Volume I — Aircraft Noise; Volume II — Aircraft Engine Emissions; Volume III — Aeroplane CO2 Emissions; Volume IV — Carbon Offsetting and Reduction Scheme for International Aviation (CORSA). <https://www.icao.int/environmental-protection/CORSA/Pages/SARPs-Annex-16-Volume-IV.aspx>

- ICAO Circular 351. Community engagement for aviation environmental management. ICAO Cir. 351-AT/194:58. (2016). [https://www.icao.int/environmental-protection/Documents/COMMUNITY\\_ENGAGEMENT\\_FOR%20AVIATION%20ENVIRONMENTAL\\_%20MANAGEMENT.EN.pdf](https://www.icao.int/environmental-protection/Documents/COMMUNITY_ENGAGEMENT_FOR%20AVIATION%20ENVIRONMENTAL_%20MANAGEMENT.EN.pdf)
- ICAO Document 10127. Final Report of the Independent Expert Integrated Technology Goals Assessment and Review for Engines and Aircraft:225. (2019). <https://store.icao.int/en/independent-expert-integrated-technology-goals-assessment-and-review-for-engines-and-aircraft-english-printed>
- ICAO Document 8168. Aircraft Operations (PANS OPS) Volume I Flight Procedures. 6th Edition:279. (2020). <https://store.icao.int/en/procedures-for-air-navigation-services-pans-aircraft-operations-volume-i-flight-procedures-doc-8168>
- ICAO Document 9184. Airport Planning Manual, Part 2 — Land Use and Environmental Control. *Doc 9184 - Part 2. 4th Edition*: 218. (2018). <https://store.icao.int/en/airport-planning-manual-land-use-and-environmental-management-doc-9184-part-2>
- ICAO Document 9829. Guidance on the balanced approach to aircraft noise management. Doc 9829, AN/451:166. (2008). [https://global.ihs.com/doc\\_detail.cfm?&input\\_search\\_filter=ICAO&item\\_s\\_key=00507943&item\\_key\\_date=890221&input\\_doc\\_number=9829&input\\_doc\\_title=&org\\_code=ICAO](https://global.ihs.com/doc_detail.cfm?&input_search_filter=ICAO&item_s_key=00507943&item_key_date=890221&input_doc_number=9829&input_doc_title=&org_code=ICAO)
- ICAO Document 9888. Review of Noise Abatement Procedure Research & Development and Implementation Results:29. (2007). <https://www.icao.int/environmental-protection/Documents/ReviewNADR.D.pdf>
- ICAO Document 9911. Recommended Method for Computing Noise Contours Around Airports:210. (2018). <https://www.icao.int/isbn/Lists/Publications/DispForm.aspx?ID=1235>
- ICAO Resolution A40-17. Consolidated statement of continuing ICAO policies and practices related to environmental protection – General provisions, noise and local air quality:17. (2019). <https://www.icao.int/environmental-protection/Documents/Assembly/A40-17.pdf>
- S.A. Janssen, H. Vos, E.E. van Kempen, O.R. Breugelmans, H. Miedema, Trends in aircraft noise annoyance: The role of study and sample characteristics. *J. Acoust. Soc. Am.* **129**(4), 1953–1962 (2011). <https://doi.org/10.1121/1.3533739>
- R.F.S. Job, Community response to noise: A review of factors influencing the relationship between noise exposure and reaction. *J. Acoust. Soc. Am.* **83**(3), 991–1001 (1988). <https://doi.org/10.1121/1.396524>
- O. Konovalova, O. Zaporozhets, Noise protection zones around Ukrainian airports as an element of balanced approach to noise control. *Int. J. of Sustainable Aviation* **7**(3), 187–202 (2021). <https://doi.org/10.1504/IJSA.2021.119175>
- I. Novakovska, L. Novakovskyi, L. Skrypnyk, Peculiarities of airports development strategy in Ukraine in context of environmental friendly land management. *Int. J. of Sustainable Aviation* **6**(1), 66–86 (2020). <https://doi.org/10.1504/IJSA.2020.108095>
- Powell C.A. Noise Levels at Certification Points, NASA/TM-2003-212649:38. (2003). <https://ntrs.nasa.gov/citations/20030107607>
- Sustainable Aviation Noise Road-Map. A Blueprint for Managing Noise from Aviation Sources:112. (2018). <https://www.sustainableaviation.co.uk>
- V. Tokarev, K. Kazhan, Entropy approach for mitigation of environmental aviation impact and airport capacity increase. *Int. J. of Sustainable Aviation* **1**(2), 119–138 (2014) 10.1504/IJSA.2014.065479
- Vader R. Noise annoyance mitigation at airports by non-acoustic measure, D/R&D 07/026. (2007) WHO, *Environmental noise guidelines for European region* (World Health Organisation Regional Office for Europe, Copenhagen, Denmark, 2018), p. 160. [https://www.euro.who.int/\\_\\_data/assets/pdf\\_file/0008/383921/noise-guidelines-eng.pdf](https://www.euro.who.int/__data/assets/pdf_file/0008/383921/noise-guidelines-eng.pdf)
- O. Zaporozhets, B. Blyukher, Risk methodology to assess and control aircraft noise impact in vicinity of the airports, in *Sustainable Aviation*, ed. by H. Karakoc, C. Colpan, O. Altuntas, Y. Sohret, (Springer International Publishing, 2019), pp. 37–79. [https://doi.org/10.1007/978-3-030-14195-0\\_3](https://doi.org/10.1007/978-3-030-14195-0_3)

- O. Zaporozhets, L. Levchenko, Accuracy of noise-power-distance definition on results of single aircraft noise event calculation. *Aerospace* **8**(5), 121 (2021). <https://doi.org/10.3390/aerospace8050121>
- O. Zaporozhets, V. Tokarev, Aircraft noise modelling for environmental assessment around airport. *Appl. Acoust.* **55**(2), 99–127 (1998). [https://doi.org/10.1016/s0003-682x\(97\)00101-1](https://doi.org/10.1016/s0003-682x(97)00101-1)
- O. Zaporozhets, V. Tokarev, K. Attenborough, *Aircraft Noise: Assessment, Prediction and Control* (Glyph International, Taylor & Francis, 2011)

# Chapter 33

## Increase of Engine Characteristics Using Alcohol Conversion



Sviatoslav Kryshchtopa, Liudmyla Kryshchtopa, Ruslans Šmigins,  
Volodymyr Korohodskyi, Myroslav Panchuk, and Igor Prunko

### 33.1 Introduction

A significant part of vehicle and other types of transport use internal combustion motors with diesel systems. This requires fuel-air mixture consumption of expensive diesel fuel-air mixture with significant parameters of gas exhaust waste toxicity; thus, the feasibility of switching to more environmentally friendly and inexpensive alternating fuel-air mixtures is obvious (Panchuk et al. 2019). The diesel motor can be converted to gas-diesel or mono gas regimes (Panchuk et al. 2020). The technology of converting diesel motors to gas-diesel regime is already known and well-established at present, when both gas mixture and diesel fuel-air mixture supply are used at the same time. Diesel motor according to its construction can be converted to work with gas equipment on both methane (liquefied or compressed) and propane-butane (Boichenko et al. 2013).

Thus, the conversion of diesel engine drives of motor vehicles to mono gas motors to reduce the cost of fuel-air mixture and lubricants, and overhaul of motors is an urgent task. Diesel motor converting to mono gas one requires major changes

---

S. Kryshchtopa (✉) · L. Kryshchtopa · M. Panchuk · I. Prunko  
Ivano-Frankivsk National Technical University of Oil and Gas, Department of Automobile Transport, Ivano-Frankivsk, Ukraine  
e-mail: [sviatoslav.kryshchtopa@nung.edu.ua](mailto:sviatoslav.kryshchtopa@nung.edu.ua); [liudmyla.kryshchtopa@nung.edu.ua](mailto:liudmyla.kryshchtopa@nung.edu.ua);  
[myroslav.panchuk@nung.edu.ua](mailto:myroslav.panchuk@nung.edu.ua); [Ihor.prunko@nung.edu.ua](mailto:Ihor.prunko@nung.edu.ua)

R. Šmigins  
Latvia University of Life Sciences and Technologies, Faculty of Engineering, Jelgava, Latvia  
e-mail: [ruslans.smigins@llu.lv](mailto:ruslans.smigins@llu.lv)

V. Korohodskyi  
Kharkiv National Automobile and Highway University, Department of Internal Combustion Motors, Kharkiv, Ukraine  
e-mail: [korohodskyi@khadi.kharkov.ua](mailto:korohodskyi@khadi.kharkov.ua)

at the design of the base diesel (Gorski and Smigins 2011) contrary to the conversion of gasoline motors. The ignition of fuel-air mixture in diesel motor is carried out by warming from compressing, thus standard diesel motor cannot work on gaseous fuel-air mixture, as gas motor fuel-air mixture has a significantly higher ignition temperature compared to diesel fuel-air mixture, but it cannot be achieved with compressing ratios used at diesel motors. The creation of mono gas motors by the world's leading manufacturers of vehicle motors, which are widely used in transport, testifies to the large prospects of converting motors into gas with spark ignition (Krysh topsa et al. 2021).

From an economic point of view, it is recommendable to use methanol alcohol as an alternating fuel-air mixture for a diesel motor (Bahman et al. 2018). Methanol alcohol is a renewable natural resource, i.e., a great raw material base to increase its production and much wider used as an energy source. Methanol alcohol is widely used at chemical industry, and considerable volumes are used at production of fuel-air mixtures for vehicle motor vehicles (Havrysh et al. 2019). Using alcohol as an alternating biofuel-air mixture for vehicles is possible because of its production at affordable and inexpensive ways from food waste, agricultural, and gaseous fuel-air mixture (Krysh topsa et al. 2018).

### 33.2 Experimental Studies and Analysis of Results

The aim of experimental studies is to use methanol alcohol in converting productions by alternating fuel-air mixtures at existing diesel motors to save petroleum motor fuel-air mixture and improve their environmental characteristic. The evaluation of effectiveness of the thermochemical process of warmth utilization at the operating cycle of the diesel class D21A was performed at the laboratory on a diesel motor stand. The D21A1 diesel motor was converted to work on an alternating gases mixture. The design of the motor head is redesigned at such a way that instead of spark plugs you can light screw back the diesel fuel injector. The purpose of experimental research was to compare the main energies, fuel-air mixture-economic, and environmental characteristics of the converted diesel motor during its operation on diesel fuel-air mixture and methanol alcohol converting productions. Experimental studies were performed on the motor diesel stand of the D21A1 motor to evaluate the energy-saving effect. Experimental dependences of external speed characteristics of the diesel motor D21A1 converted for diesel fuel-air mixture and methanol alcohol converting productions are shown in Fig. 33.1. It was found that at nominal speed engine ( $n = 1800 \text{ min}^{-1}$ ), the effective energy  $N$  on diesel fuel-air mixture was 18.1 kW, but on the productions of methanol alcohol, converting it was equal to 10.1 kW. The value of the effective energy  $N$  of the motor at the entire frequency range of the crankshaft compared with diesel fuel-air mixture working on methanol alcohol converting productions decreased by 45%.

The experimental dependences of specific fuel-air mixture consumption on the crankshaft speed  $n$  of the diesel motor D21A1 worked on diesel fuel-air mixture and

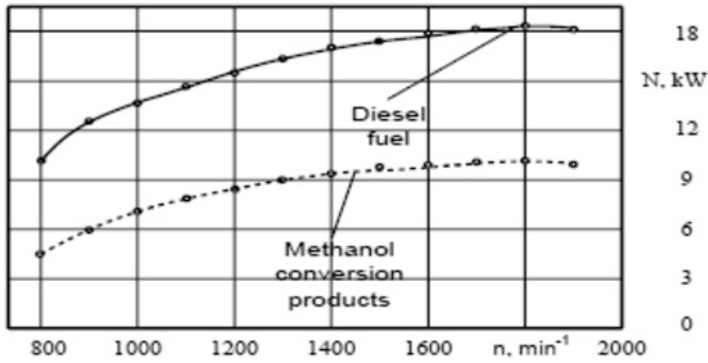


**Fig. 33.1** Experimental dependences of the effective energy  $N$  on the motor crankshaft speed  $n$  for different motor fuel-air mixtures: ----- operation of the motor on diesel fuel-air mixture; ..... motor operation on methanol alcohol converting productions

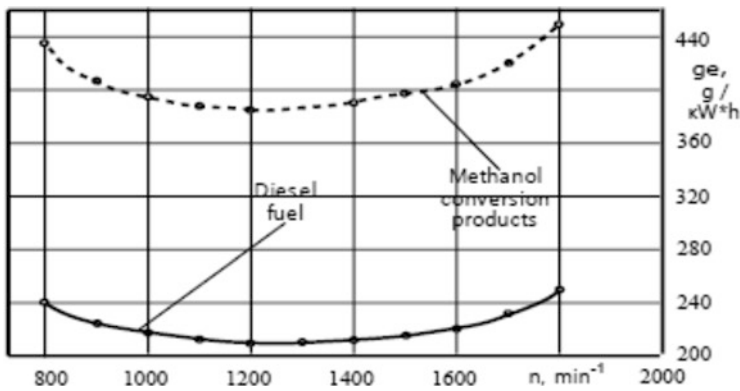


**Fig. 33.2** Experimental dependences of specific fuel-air mixture consumption on the motor crankshaft speed  $n$  for different motor fuel-air mixtures: ----- operation of the motor on diesel fuel-air mixture; ..... motor operation on methanol alcohol converting productions

methanol alcohol converting productions are shown in Fig. 33.2. It was found, analyzing the experimental energies values, that on diesel fuel-air mixture minimum specific fuel-air mixture consumption at rpm  $n = 1220\text{--}1230 \text{ min}^{-1}$  was  $211 \text{ g}/(\text{kWh})$ ; specific fuel-air mixture consumption at nominal speed engine  $n = 1800 \text{ min}^{-1}$  was  $249 \text{ g}/(\text{kWh})$ . Minimum specific fuel-air mixture consumption engine was  $387 \text{ g}/(\text{kWh})$  for productions of methanol alcohol converting; specific fuel-air mixture consumption at nominal speed was  $451 \text{ g}/(\text{kWh})$ .

Specific fuel-air mixture consumption from the motor crankshaft speed at entire range of the crankshaft speed compared with diesel fuel-air mixture working on 100% of methanol alcohol converting productions increased by 80–84%. There is a decrease at the content of nitrogen oxides at the entire frequency range of the engine

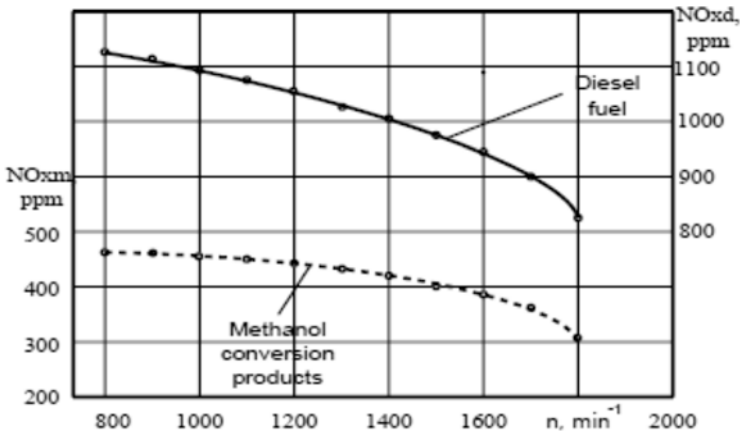


**Fig. 33.3** Experimental dependences of the content of nitrogen oxides at exhaust waste gases on the crankshaft speed of the motor  $n$  for different motor fuel-air mixtures: ----- operation of the motor on diesel fuel-air mixture; ..... motor operation on methanol alcohol converting productions

crankshaft (Fig. 33.3). The decrease at the content of nitrogen oxides engine was 59.5%.

At  $n = 1800 \text{ min}^{-1}$ , the content of nitrogen oxides engine decreased from 826 ppm when the motor is running on diesel fuel-air mixture to 305 ppm when the motor is running on the productions of methanol alcohol converting. The decrease at the content of nitrogen oxides engine during the operation of the motor on diesel fuel-air mixture compared with the operation of the motor on the productions of methanol alcohol converting is explained by lower warmth dissipation rates and less increase of burning pressure at the motor.

There is a significant decrease in the content of carbon monoxide at the entire frequency range of the crankshaft (Fig. 33.4). Thus, the content of carbon monoxide engine at  $n = 800 \text{ min}^{-1}$  decreased from 0.226% when the motor is running on diesel fuel-air mixture to 0.150% when the motor is running on the productions of methanol alcohol converting. At  $n = 1800 \text{ min}^{-1}$ , the carbon monoxide engine content decreased from 0.086% when the motor is running on diesel fuel-air mixture to 0.072% when the motor is running on methanol alcohol converting productions. That is, the decrease in carbon monoxide content occurs at the range of 62.2–52.0%.

The hydrocarbon content increases slightly at the entire range of crankshaft speed (Fig. 33.5). At  $n = 800 \text{ min}^{-1}$ , the hydrocarbon engine content varies from 0.043% when the motor is running on diesel fuel-air mixture to 0.031% when the motor is running on methanol alcohol. The decrease in hydrocarbon engine content was 26.1%. At  $n = 1800 \text{ min}^{-1}$ , the hydrocarbon engine content increases from 0.076% when the motor is running on diesel fuel-air mixture to 0.155% when the motor is running on methanol alcohol converting productions. An increase in hydrocarbons was 2.01 times higher. There was a decrease of fuel-air mixture consumption at the range of 10–14% depending on the crankshaft speed and motor loading.



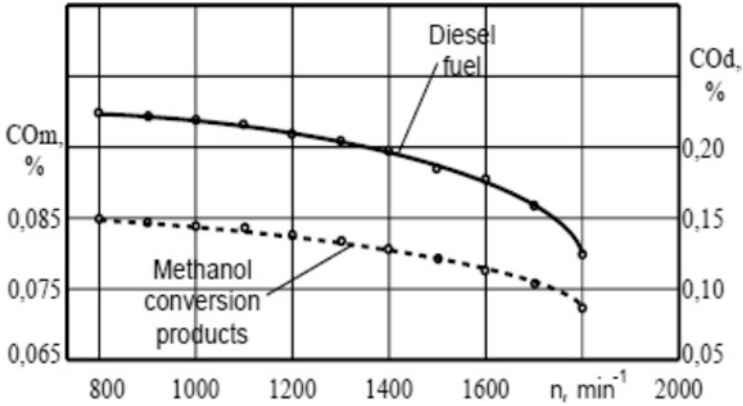


Fig. 33.4 Experimental dependences of the content of carbon monoxide at the exhaust waste gases engine on the motor crankshaft speed  $n$  for different fuel-air mixtures: - - - - - operation of the motor on diesel fuel-air mixture; ..... motor operation on methanol alcohol converting productions

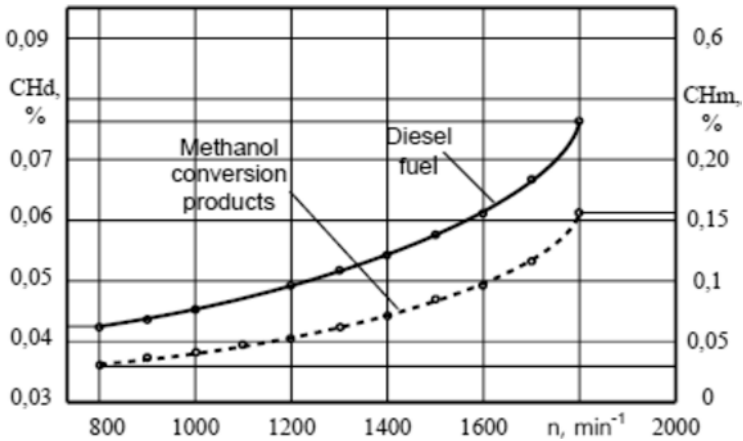


Fig. 33.5 Experimental dependences of the hydrocarbon content at the exhaust waste gases on the crankshaft speed of the motor  $n$  for different motor fuel-air mixtures: - - - - - operation of the motor on diesel fuel-air mixture; ..... motor operation on methanol alcohol converting productions

To identify the share of each factor at improving the effectiveness of the motor, it was tested using a methanol alcohol converting reactor with an autonomous electric warmer, i.e., without usage (recovery) of thermic energies of exhaust waste gases. It is established that energy saving for this diesel due to the thermochemical process of warmth utilization was 6–8%, and due to the betterment of the working process was about 4–6%.

### 33.3 Conclusion

Experimental engine studies have shown that converting diesel motors to work using methanol alcohol converting productions is quite profitable. The specific fuel-air mixture consumption from the motor crankshaft speed at the entire range of the engine crankshaft speed compared with diesel fuel-air mixture working on 100% of methanol alcohol converting productions increased by 81–83%. As the price of methanol alcohol is, on average, 15–20% of the cost of fuel diesel engine, so the conversion of diesel motors to work using methanol alcohol converting productions is very profitable. The economic characteristics of operating engine cycle at all loading regimes of the motor with thermoreactor were higher (on average by 10–15%) than on methanol alcohol without a thermoreactor. Operating engine cycle parameters almost corresponded to the basic parameters of the motor during its operation on liquefied methanol alcohol at low engine crankshaft speeds, characterized by energy grades and low temperature of engine exhaust waste gases. Reduction of fuel-air mixture consumption was accompanied by improvement of the environmental parameters of the diesel motor, which works at conjunction with a thermochemical methanol alcohol converting reactor. Depending on the engine crankshaft speed and the load on the motor formation of nitrogen oxides at the exhaust, waste gases decreased by 52–60%, carbon monoxide occurred at the range of 53–63%. Studies have shown that at loading regimes, when the temperature of the exhaust waste gases at the inlet to the thermochemical reactor exceeds 400–420 °C, the thermochemical reactor productivity including the target component reaches its highest grade, significantly increasing the effectiveness of the operating engine cycle. Its implementation does not require financial investments and radical re-equipment of existing motor production due to technical simplicity.

### References

- N. Bahman, F. Sina, S. Shahaboddin, C. Kwok-wing, R. Timon, Application of ANNs, ANFIS and RSM to estimating and optimizing the parameters that affect the yield and cost of biodiesel production. *Eng. Appl. Comput. Fluid Mech.* **12**, **1**, 611–624 (2018)
- S. Boichenko, O. Vovk, A. Iakovlieva, Overview of innovative technologies for aviation fuels production. *Chem. Chem. Technol.* **7**(3), 305–312 (2013)
- K. Gorski, R. Smigins, Impact of ether/ethanol and biodiesel blends on combustion process of compression ignition engine. 10th international scientific conference on engineering for rural development. Jelgava **260-265** (2011)
- V. Havrysh, A. Kalinichenko, O. Minkova, S. Lyashenko, Agricultural feedstock for solid and liquid biofuel production in Ukraine: Cluster analysis. *Procedia Environ. Sci. Eng. Manag.* **6**(4), 649–658 (2019)
- S. Krysh topsa, M. Panchuk, B. Dolishnii, S. Krysh topsa, M. Hnyp, O. Skalatska, Research into emissions of nitrogen oxides when converting the diesel engines to alternative fuels. *Eastern-Europ. J. Enterpr. Technol.* **1**(10–91), 16–22 (2018)

- S. Kryshchyna, L. Kryshchyna, M. Panchuk, R. Šmigins, B. Dolishnii, Composition and energy value research of pyrolysis gases. *IOP Conf. Series Earth Environ. Sci.* **628**(1), 012008 (2021)
- M. Panchuk, S. Kryshchyna, A. Śladkowski, A. Panchuk, I. Mandryk, Efficiency of production of engine biofuels for water and land transport. *Nase More* **66**(3), 6–12 (2019)
- M. Panchuk, S. Kryshchyna, A. Śladkowski, A. Panchuk, Environmental aspects of the production and use of biofuels in transport. *Lecture Notes Netw. Syst. Book Chapter* **124**, 115–168 (2020)

# Chapter 34

## Modern Tendencies in the Improvement of Technologies for Utilization of Fulfilled Tires



Anna Yakovlieva, Sergii Boichenko, Iryna Shkilniuk, and Igor Kubersky

### 34.1 Introduction

Motor transport as well as its infrastructure rapidly grow. It has led to the accumulation of waste tires, which volumes will also increase in the near future. Consequently, this will lead to environmental pollution. Modern manufacturers produce virtually indestructible tires, which cause a significant environmental problem with an estimated 1.5 billion waste tires around the world, many of which end up in forests and streams, as well as landfill (Boichenko et al. 2019). More than three million tons of used tires are produced annually only in the United States, and up to 2.5 million tons in Europe. The disposal of scrap tires occupies large amounts of valuable landfill space, poses fire and environmental hazards (Yakovlieva et al. 2021).

Naturally, the decomposition of waste rubber exceeds 100 years accompanied by soil poisoning and chemical releasing. This environmental impact could be minimized by viable alternative for the recycling of waste tires by implementing waste tire conversion technologies.

Today in the waste management world, a broad range of technologies are recognized that could be used to divert a portion of waste rubber stream currently being landfilled as well as other hydrocarbon materials (Boichenko et al. 2019).

Thus, the aim of this study is to analyze and compare existing technologies of waste tire utilization and consider the most appropriate in terms of energy efficiency and environmental safety.

---

A. Yakovlieva (✉)

National Aviation University, Scientific-Research department, Kyiv, Ukraine  
e-mail: [anna.yakovlieva@nau.edu.ua](mailto:anna.yakovlieva@nau.edu.ua)

S. Boichenko · I. Shkilniuk · I. Kubersky

National Technical University of Ukraine “Igor Sikorsky Kyiv Polytechnic Institute,”  
Institute of Energy Safety and Energy Management, Kyiv, Ukraine

## 34.2 Review of Technologies for Waste Tire Recycling

Tire waste is a special type of waste with environmental, economic, and social issues. The problem with waste tire disposal is that tires do not decay if buried, they resurface as they are of lower density than the surrounding soil. If they are stored at landfills, they give an unstable surface to any landfill and the ground cannot be used for building. If tires are accumulated on the surface, they pose a fire danger. Apart from making an environmental problem, tire waste creates a health hazard in tropical regions as they keep water inside that provides the perfect habitat for microorganisms' development (Ucar et al. 2005). In addition, tires are a high-energy material that justifies the efforts in the advancement of technology, innovation, and research and development.

The technologies for waste tire recycling or processing are classified as follows: *physical technologies* (mechanical recycling, low temperature processing, destruction and compression recycling), *chemical technologies* (ozone recycling, pyrolysis), and *energy extraction*.

Large amount of waste tires is used in crumb rubber applications. In paving, the rubberized asphalt concrete is a viable end use for tires. In molded rubber products, millions of waste tires are used for the production of crumb rubber products. Also, a crumb rubber can be used as soil additive which can increase its permeability as well as airstream (Rouse et al. 2005).

Tire-derived fuel (TDF) can be used in cogeneration facilities or cement kilns, pulp, and paper mills or industrial boilers; carbon black can be burned on site for alternative energy recovery or be sold for the needs of various applications.

The value of the end products depends on the input materials composition type of tires used as a feedstock and the specific process requirements.

The waste tire recycling process begins with inspection, which aimed on deciding what can be reused, recovered, or transformed into a new product or energy (Boichenko et al. 2019). The general scheme of possible ways of waste tire disposal is presented in Fig. 34.1 (Phale 2005). Then, the tires are transported to recovery facilities, where they are processed by the shredder and/or grinder.

### Mechanical Recycling

Mechanical recycling is based on tires shredding, cord separation, and next rubber crumb gridding to powder. The disadvantages of this technology are high-energy consumption, rapid wearing of equipment, and low quality of final product due to contaminating impurities in crumbs.

### Low-Temperature Processing

Low-temperature (cryogenic) processing of used tires performs at temperatures from  $-60\text{ }^{\circ}\text{C}$  to  $-90\text{ }^{\circ}\text{C}$  when the rubber is in crack-sensitive state. The benefits presented by this technology are metal and textile separation improvement and the yield of rubber product. The disadvantages of this technology are high cost of coolant (liquid nitrogen), power consumption, and delivery complexity.

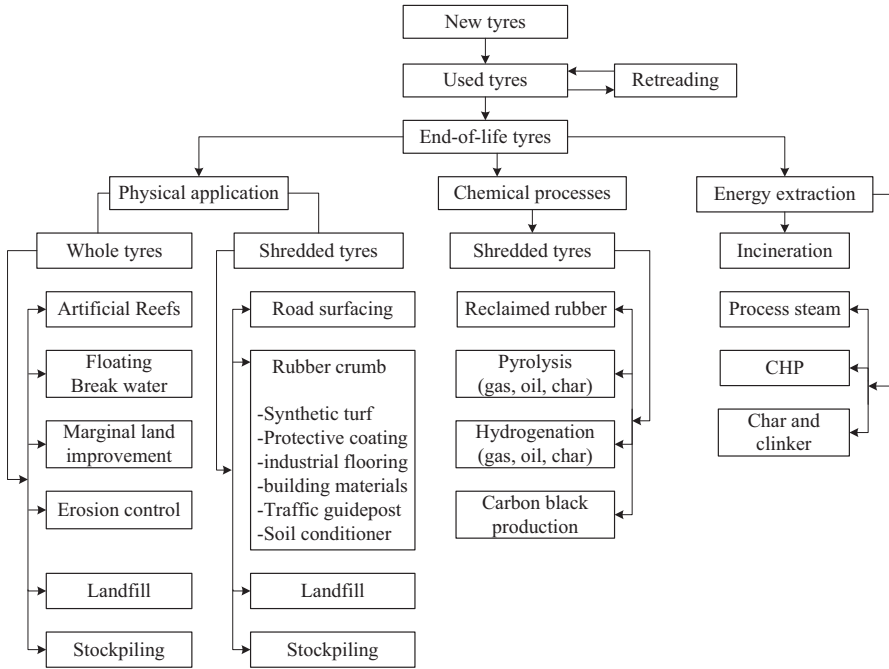


Fig. 34.1 Re-use, recycle, and disposal route for ST. (Phale 2005)

**Destruction and Compression Recycling**

The waste tires are fed through the holes to the chamber, where under the high pressure are separated on steel cord, textile, and crumb rubber. Among the disadvantages of this technology are rapid wearing of the equipment, high energy consumption, and multistage crumb rubber system.

**Ozone Recycling Technology**

The technology is based on waste tire oxidation to crumb rubber. During the ozone processing, steel and textile cords are completely separated. The high speed facilitates the gridding. This uses minimal energy involvement. The disadvantages of this technology are expensive equipment, high explosive risk, and the highest hazard class of ozone.

**Pyrolysis Technology**

As a thermal decomposition process, the pyrolysis can be used to convert scrap tires as well as other hydrocarbon materials into useable products such as oil, syngas, and carbon black. The technology is based on cracking under the high temperatures and without addition of air or oxygen. As the temperature lowers, the more pyrolysis oil is produced. As the temperature increases, the more syngas is produced (Kryshtopa et al. 2021).

The oil derived from pyrolysis process can be used as low grade fuel in boilers or separated on fractions, such as diesel, gasoline, and heavy oil. Pyrolysis gas usually satisfies systems energy needs by heating up the process.

Pyrolysis technology is one of the most environmentally friendly, energy and cost efficient solution for treating a wide variety of rubber products in the international waste management stream, implemented in the most developed countries such as the USA, Japan, Germany, Switzerland, and others (Yakovlieva et al. 2021).

### 34.3 Conclusion

The modern state of technologies for waste tire processing is shown. Due to the rapid global growth of transport sector, we may observe increasing demand in tires production. Consequently, there is an increase in the volume of waste tires. This substantiates the necessity to develop environmentally friendly and energy efficient methods for waste tire processing. Analyzing the existing and promising processing methods, we may conclude that waste tires may be efficiently use as a raw material in industries such as cement production, road construction, fuel production, and other application. Fuel production as a result of waste tire processing is a relevant direction in technologies for waste tire processing. It may have significant potential as well as energy and financial benefit. Thus, the development and implementation of system of waste tire processing may provide its long-term use as well as efficient processing and secondary use with minimal negative impact on environment.

### References

- S. Boichenko, O. Ivanchenko, K. Lejda, et al., *Ecologystyka, recyckling I utylizatsiia transport* (NAU, Kyiv, 2019), p. 266. (in Ukrainian)
- S. Kryshropa, L. Kryshropa, M. Panchuk, R. Šmigins, B. Dolishnii, Composition and energy value research of pyrolise gases. *IOP Conf. Serie: Earth Environ. Sci.* **628**(1), 012008 (2021)
- A.R. Phale. Environmental impact and waste management of used tyres in the SRA – a mini-dissertation submitted in part-fulfillment of the requirement for the degree of Magister atrium, p. 74. (2005)
- M.W. Rouse, S.K. Isayev, A.I. Khait, Manufacturing Practices for the Development of Crumb Rubber Materials from Whole Tires, in *Rubber Recycling*, (CRC Press, Taylor & Francis Group, 2005), p. 1
- S. Ucar, S. Karagoz, A.R. Ozkan, J. Yanik, Evaluation of two different scrap tires as hydrocarbon source by pyrolysis. *Fuel* **84**, 1884–1892 (2005)
- A. Yakovlieva, S. Boichenko, U. Kale, A. Nagy, Holistic approaches and advanced technologies in aviation product recycling. *Aircr. Eng. Aerosp. Technol.* **93**(8), 1302–1312 (2021)

# Chapter 35

## On the Peculiarities of Alkaline-Catalyzed Route of Synthesis of Fatty Acid Monoalkyl Esters



Serhii Konovalov, Stepan Zubenko, Lyubov Patrylak, Anjela Yakovenko, Volodymyr Povazhnyi, and Kateryna Burlachenko

### Nomenclature

DG	Diglycerides
DMFA	N, N-dimethylformamide
FAME	Fatty acid methyl esters
GL	Glycerol layer
GL1	Primary glycerol layer
GL2	Secondary glycerol layer
KOBu	Catalytic solution of butoxide
KOBu-Et	Catalytic solution of butoxide, preparing from ethoxide
KOEt	Catalytic solution of ethoxide
MG	Monoglycerides
MSTFA	N-Methyl-N-(trimethylsilyl) trifluoroacetamide
$n_{\text{cat}}$	Mass ratio of catalyst to oil, %eq KOH
$R_{\text{AO}}$	Alcohol/oil molar ratio, mol/mol
TG	Triglycerides
$t$	Reaction temperature, °C
$Y_{\text{ef}}$	Effective molar yield of esters, %
$Y_{\text{t}}$	Total molar yield of esters, %

---

S. Konovalov (✉) · S. Zubenko · L. Patrylak · A. Yakovenko · V. Povazhnyi · K. Burlachenko  
V.P. Kukhar Institute of Bioorganic Chemistry and Petrochemistry of the National Academy  
of Sciences of Ukraine, Kyiv, Ukraine



## 35.1 Introduction

The utilization of biomass-derived alternative transport fuels is able to reduce the negative impact of human activity on the environment and decrease the carbon dioxide emissions into the atmosphere. Bioethanol and biodiesel (mainly fatty acid methyl esters) are widely used as such alternative in land transport. The world production of these biofuels amounted to more than 90 million tonnes of oil in 2019 (<https://www.bp.com> 2020). As for the aviation biofuels, its production is grounded on the hydrodeoxygenation of triglycerides or fatty acids, followed by selective cracking of normal alkanes, aromatization, and isomerization of cracking products (Pearlson et al. 2013). The obtained biojet is the mixture of aromatic hydrocarbons and isoalkanes, having 7–9 carbon atoms. In other words, its chemical composition is close to the traditional petroleum jet fuels.

The utilization of fatty acid monoalkyl esters, obtained from vegetable oil, in composition of jet fuels is an object of great interest. They can be produced by simplest chemical modification of vegetable oils via transesterification with monohydric alcohols. Such products are more environmentally safe, than hydrocarbon-based biojet. One of the disadvantages of such biocomponents is the lower energy content in comparison with hydrocarbon fuels due to the presence of about 10% of oxygen in their molecules. On the other hand, the presence of oxygen may contribute to the reduction of soot formation and particulate matter emissions. But the main obstacle of the use of fatty acid esters as component of jet fuels is their dissatisfactory low-temperature properties (Lapuerta et al. 2016; Iakovlieva et al. 2016), namely, the high freezing point strongly limits the fraction of the esters in fuel mixture and flight altitude (Lapuerta et al. 2016). Primarily, this applies to the fatty acid methyl esters (FAME), which is produced at large industrial scale as biodiesel via vegetable oils' transesterification by methanol using mainly soluble base catalysts, such as hydroxides or methoxides of alkaline metals. The unsatisfactory low-temperature characteristic of esters can be improved by utilization of another longer-chain linear or branched monohydric alcohols as transesterification reagents instead of methanol. It is well-known that the increasing of the length of ester molecule alcohol moiety leads to the improving of cold flow properties (Boichenko et al. 2017; Hájek et al. 2017; Homan et al. 2017). Use of bioalcohols, such as ethanol and *n*-butanol, instead of methanol also improves the sustainability of the esters' production and utilization.

The simplest and most common for FAME production, the alkaline-catalyzed route, becomes more complex in case of longer-chain alcohols, such as ethanol and especially *n*-butanol. This is due to the decreasing of the acidity and polarity of alcohol with lengthening of its carbon chain. Lower acidity leads to the lower concentration of the alkoxide (the real catalysts in alkaline transesterification) in reaction media, which causes the decreasing of the efficiency of the synthesis, especially in presence of even a small amount of water. The low polarity of alcohols increases the miscibility of the reagents and alkali, which not only accelerates the target reaction, but also strongly increases the rate of undesirable saponification. Soaps together with unconverted monoglycerides (MG) and diglycerides (DG) strongly

contribute into the formation of stable emulsion of the ethanolysis products, making their separation difficult (Sanli et al. 2019; Cernoch et al. 2010). It should be mentioned that effective self-separation, leading to formation of so-called glycerol layer (GL), provides removal of not only by-product glycerol, but also the majority of the alkaline catalyst, soaps, and alcohol. This makes the following downstream processing of reaction products and isolation of fuel grade esters quite easier. As for the alkaline butanolysis, there is a very limited information in literature about the self-separation. Products of butanolysis tend to form homogeneous phase and additional treatment is needed to enforce their separation (Homan et al. 2017). However, earlier, our group observed the formation of high-pure glycerol layer, containing almost exclusively glycerol and alkali, when using the butoxide-containing solution to catalyze the butanolysis reaction (Patrylak et al. 2019; Konovalov et al. 2021).

This work aims to examine the early unreported peculiarities of alkaline-only ethanolysis and butanolysis of low-grade wasted frying oils, having relatively high free fatty acids content, over corresponding alkoxides, prepared in original way from hydroxide and alcohol.

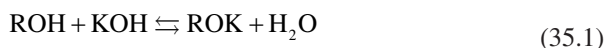
## 35.2 Methodology

The samples of wasted frying sunflower oil contained free fatty acids (FFA) in range of 0.4–2.8%, the water content was in range 0.03–0.065%. Technical grade bioethanol, containing 0.75% of organic denaturing admixtures (GC area assay), was used in ethanolysis. It was stored over synthetic zeolite KA-Y/3A (Russian Federation, dynamic water vapor capacitance – 150 mg/cm<sup>3</sup>) and the water content when using in syntheses was <0.1%. Technical grade *n*-butyl alcohol (Turkey) (GC area assay – 99.37%, water content about 0.15%) was used in butanolysis. Technical grade potassium hydroxide (China), containing 89.7% KOH was used for preparation of alkoxides' catalytic solutions. Also, reagent grade sodium hydroxide was used for the preparation of sodium butoxide for analytical purposes. Reagent grade *p*-toluenesulfonic acid and indicator bromothymol blue were used in titration of TE products. *N,N*-dimethylformamide (DMFA, 99.9%) and reagent grade *n*-hexane were used as solvents for the analytic purposes. The following reagents were used in gas chromatographic analysis: reagent grade methylpalmitate (GC area assay 98.65%), pharmaceutical grade glycerol, analytic grade ethyl alcohol, *N*-Methyl-*N*-(trimethylsilyl) trifluoroacetamide (MSTFA), pyridine solution of tricaprln, 1,2,4-butanetriol, glycerol, 1-monoolein, 1,3-diolein and triolein. High-pure helium was used as carrier gas.

Syntheses of esters were carried out in conic flasks (250). Stirring (500 rpm) and heating (if necessary) were provided with magnetic stirrer with water bath. Maintaining the lower-ambient temperature of reaction was provided by circulation of chilled water. The main technological variables in syntheses were molar ratio of alcohol to oil ( $R_{AO}$ , mol/mol), temperature ( $t$ , °C), amount of alkaline catalyst ( $n_{cat}$ , %<sub>eq</sub> KOH relative to mass of oil), and reaction time ( $\tau$ , min). Products after reaction

were immediately transferred into separation funnel, where settling and self-separation by gravity occurred. Batch distillation of esters was carried out under vacuum (about 0.3–0.4 kPa) and continuous stirring (500 rpm) in round-bottom flask (250 cm<sup>3</sup>). Heating was provided by oil bath (190–240 °C). Temperature range of ethyl esters' fraction condensation was 146–168 °C.

Alkoxides in the form of their solutions in alcohol were synthesized from the KOH by reaction (35.1), where ROH is ethanol or *n*-butanol.



To shift equilibrium (1) towards formation of alkoxide, water was selectively removed from reaction media. For butoxide, the azeotrope distillation, grounding on the property of *n*-butanol to form heterogeneous azeotrope with water, was used. Prepared in such way that butoxide catalytic solution was marked as KOBu. For ethoxide, Soxhlet-like apparatus, filled with zeolite KA-Y/3A, was used to selectively dehydrate the condensed ethanol-water azeotrope. Ethoxide catalytic solution was marked as KOEt. In more details, the alkoxides' synthesis is described in Patrylak et al. (2019) and Konovalov et al. (2021). Also, the separate portion of butoxide solution KOBu-Et was synthesized from ethoxide by means of addition of butanol to the KOEt solution, followed by removal of ethanol by distillation.

The composition of transesterification products was analyzed by gas chromatograph Agilent 7890A Series. Esters content was determined by adopted method of methyl esters analysis according to EN 14103, using J&W HP-5 capillary column. Methyl palmitate instead of methyl heptadecanoat was used as internal standard; samples were dissolved in *n*-hexane. Glycerol, monoglycerides, diglycerides, and triglycerides (TG) concentrations were determined by means of derivatization with MSTFA followed by chromatographic analyses (DB-5HT capillary column) as described in ASTM D 6584. The concentration of alcohol was determined by gas chromatographic analyses (J&W HP-5 capillary column) using calibration line method. Samples were dissolved in DMFA. Acid number was measured by means of titration by sodium butoxide solution in *n*-butanol with indicator bromothymol blue. The concentration of the potassium in composition of both alkaline catalyst and soaps was determined by titration by *p*-toluensulfonic acid with indicator bromothymol blue. FTIR-spectra were recorded by Shimadzu IRAffinity-1S infrared spectrometer, equipped with ATR accessory Specac GS 10801- B.

### 35.3 Results and Discussion

First experiments demonstrated the high efficiency of KOEt in WFO ethanolysis. Effective yield ( $Y_{\text{ef}}$ ), taking into account only esters in ester layer (EL) after phase separation, was higher than in case of KOH as catalyst. When transesterifying WFO with FFA content of 2.8%, self-separation was not observed for KOH ( $Y_{\text{ef}} = 0$ ). The conditions and results of transesterification of WFO sample (2.5% FFA) by ethanol, using KOEt catalytic solution, are given in Table 35.1.

Most syntheses were carried out at one-and-a-half excess of ethanol over stoichiometry ( $R_{AO} = 4.5$ ). The higher excess provided some higher effective yield, but self-separation in case of such high-acidic sample was not full. The total yield ( $Y_t$ ) appeared to be almost independent from another conditions (85–88%). Self-separation was not observed in synthesis E1 at highest temperature. The highest  $Y_{ef}$  (78–79%) was achieved at slightly below-ambient temperatures (10 or 18 °C) in syntheses E3 and E4. In these cases, the unreported peculiarity of alkaline ethanolysis, which is the settling of reaction glycerol directly during reaction on the bottom of the reactor in the form of dense non-fluent residue was discovered. We called it primary glycerol layer (GL1). Contrary to the secondary glycerol layer (GL2), forming during settling, it was quite pure. GL1 FTIR-spectrum (Fig. 35.1) is very close to the spectrum of pure glycerol, as well as to the spectrum of potassium glyceroxide in glycerol. It does not contain the bands of carbonyl groups of esters and soaps, which are well-expressed in the GL2 spectra.

**Table 35.1** WFO ethanolysis over ethoxide as catalyst

Characteristic	Sample					
	E1	E2	E3	E4	E5	E6
$R_{AO}$ , mol/mol	4.5	4.5	4.5	4.5	4.5	30
$n_{cat}$ , % <sub>eq</sub> KOH	1.4	2.0	1.4	1.8	1.8	2.5
$t$ , °C	60	35	10	18	52	78
$\tau$ , min	100	100	100	45	150	120
$Y_t$ , %	88	86	86	88	87	85
$Y_{ef}$ , %	0	72	79	78	68	0
GL1, % from oil	0.9	1.3	2.6	4	1.1	0.8
GL2, % from oil	0	37	25	28	40	0

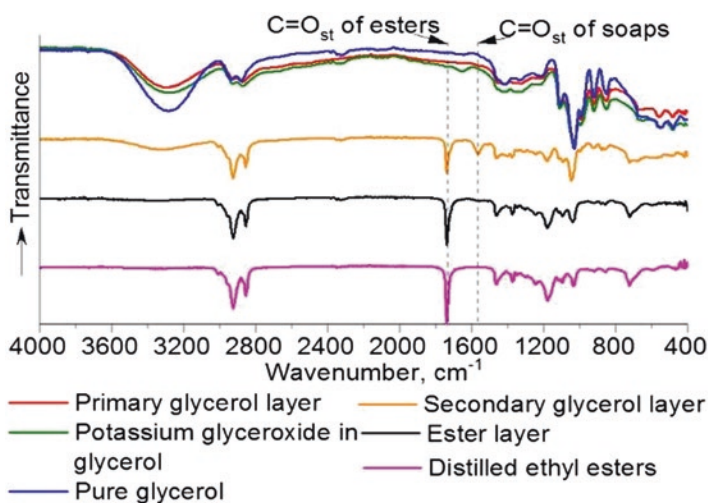


**Fig. 35.1** FTIR spectra of WFO ethanolysis products

Isolating fuel-grade esters from WFO transesterification products is not a simple task. The conventional purification methods, including washing with water and dry washing with adsorbents can provide esters' content no higher than 88–93%. These methods efficiently remove the glycerol, soaps, alcohol, and to some extent MG. But they are totally ineffective in removing oligomeric compounds, probably the dimers of ethyl esters, which is believed to be the main admixtures. Batch vacuum distillation was demonstrated to be the most efficient purification method. It can be carried out after removal of ethanol and additional phase – separation, or applied directly to ester layer. The obtained distillates are clear, colorless, or light-yellow and contain 97.5–99% of esters, <0.1% of MG, <0.05 of ethanol, and almost no DG and TG; acid value is in range of 0.1–0.4 mg KOH/g. All these quality parameters are within the requirements for biodiesel. But glycerol content may be higher than allowed by 0.02%. It seems that the additional dry-washing step is most suitable for improving this characteristic.

Butanolysis of WFO samples (Table 35.2) was carried out at one set of reaction condition, chosen on the base of previous studies (Patrylak et al. 2019; Konovalov et al. 2021):  $R_{AO} = 4.5$ ,  $n_{cat} = 1.4\%_{eq}$  KOH (plus  $0.2\%_{eq}$  KOH for neutralization of each 1% of FFA),  $t = 15$  °C,  $\tau = 20$  min. Effective yield of butyl esters was higher in case of oil with lower acidity, probably due to its lower polymerization degradation. The observed character of butanolysis products' self-separation was quite complex. The formation of GL1 during reaction was more pronounced and part of it also formed during settling. But GL2, also containing butyl esters and soaps, formed in very low amounts. As result, EL's after butanolysis had higher soaps' content. GL1's were characterized by very significant alkali content (around 10% in terms of K), most likely in the form of potassium glyceroxide. Their FTIR-spectra (not shown) contained weak bands of esters' and soaps' carbonyl group. It should be mentioned that GL1 after butanolysis of refined sunflower oil was purer and did not contain such admixtures (Patrylak et al. 2019). Such high-alkaline glycerol layer looks very promising for catalysis of transesterification reactions or another analytical purposes. Finally, let us emphasize that butoxide catalytic solution, prepared through ethoxide (KOBu-Et), appeared to be more effective from point of view of esters' yield and fullness of separation (B1 and B2 synthesis).

Developed approach for alkaline transesterification can be useful for the production of esters of another longer-chain alcohols, including even branched ones. For

**Table 35.2** WFO butanolysis over butoxide as catalyst

Characteristic	Sample		
	B1	B2	B2
FFA in oil, %	0.57	0.57	1.15
Butoxide solution	KOBu	KOBu-et	KOBu
Esters in EL, %	78.8	81.7	76.6
Yef, %	87.7	89.2	84.2
GL1, % from oil	7.4	7.8	7.1
GL2, % from oil	1.4	3.5	3.4
K in GL1, %	10.6	10.3	9.8

these purposes, the catalytic solution of corresponding alkoxide in corresponding alcohol (through the stage of ethoxide) should be prepared and the only-alkaline transesterification of oil should be carried out.

## 35.4 Conclusion

In current work, the approach was developed for carrying out effective alkaline transesterification of WFO, containing up to 2.8% of FFA, with ethanol and butanol. It includes the utilization of the corresponding alkoxides, preparing only from hydroxide and alcohols in original way, and carrying out the reaction at conditions, combining slightly decreased temperature, short synthesis duration, low excess of alcohol, and relatively high alkoxide load. Besides high esters' yield, such conditions also provide the formation of high-pure glycerol layer, containing high amount of alkali. The possibility of its reuse for alkaline catalysis of oil's transesterification for another synthetic purposes looks promising. The developed approach can also be useful for the production of esters of another longer-chain alcohols through alkaline-catalyzed route.

## References

- S. Boichenko, K. Leida, A. Yakovleva, et al., Influence of rapeseed oil Ester additives on fuel quality index for air jet engines. *Chem. Technol. Fuels Oils* **53**, 308–317 (2017)
- M. Cernoch, M. Hajek, F. Skopal, Ethanolysis of rapeseed oil - distribution of ethyl esters, glycerides and glycerol between ester and glycerol phases. *Bioresour. Technol.* **101**, 2071–2075 (2010)
- M. Hájek, F. Skopal, A. Vávra, J. Kocík, Transesterification of rapeseed oil by butanol and separation of butyl ester. *J. Clean. Prod.* **155**, 28–33 (2017)
- T. Homan, K. Shahbaz, M.M. Farid, Improving the production of propyl and butyl ester-based biodiesel by purification using deep eutectic solvents. *Sep. Purif. Technol.* **174**, 570–576 (2017) <https://www.bp.com/content/dam/bp/business-sites/en/global/corporate/pdfs/energy-economics/statistical-review/bp-stats-review-2020-full-report.pdf>. Accessed on June, 2020
- A. Iakovlieva, O. Vovk, S. Boichenko, et al., Physical-chemical properties of jet fuel blends with components derived from rape oil. *Chem. Chem. Technol.* **10**, 485–492 (2016)
- S. Konovalov, L. Patrylak, S. Zubenko, et al., Alkali synthesis of fatty acid butyl and ethyl esters and comparative bench motor testing of blended fuels on their basis. *Chem. Chem. Technol.* **15**, 105–117 (2021)
- M. Lapuerta, L. Canoira, The suitability of fatty acid methyl esters (FAME) as blending agents in jet A-1, in *Biofuels for Aviation*, ed. by C.J. Chuck, (Academic Press, Amsterdam, Mass, 2016)
- L.K. Patrylak, S.O. Zubenko, S.V. Konovalov, V.A. Povazhnyi, 2019, alkaline transesterification of sunflower oil triglycerides by butanol-1 over potassium hydroxide and alkoxides catalysts. *Voprosy Khimii i Khimicheskoi Tekhnologii* **5**, 93–103 (2019)
- M. Pearson, C. Wollersheim, J. Hileman, A techno-economic review of hydroprocessed renewable esters and fatty acids for jet fuel production. *Biofuels Bioprod. Biorefin.* **7**, 89–96 (2013)
- H. Sanli, E. Alptekin, M. Canakci, Production of fuel quality ethyl Ester biodiesel: 1. Laboratory-scale optimization of waste frying oil Ethanolysis, 2. Pilot-scale production with the optimal reaction conditions. *Waste Biomass Valor.* **10**, 1889–1898 (2019)

# Chapter 36

## Use of Polyfunctional Additives As a Part of Motor Fuels and Lubricants



Andrii Grigorov and Alexander Trotsenko

### Nomenclature

C <sub>12</sub> H <sub>11</sub> N <sub>3</sub>	1,3-diphenyltriazene
CH	Hydrocarbons
CH <sub>3</sub>	Methyl
OH	Hydroxyl
H	Hydrogen
C	Soot
ON	Octane number
CN	Cetane number

### 36.1 Introduction

Today, additives should be considered an integral part of any commercial petroleum product. This is primarily due to the difficult situation the global refining industry is on. On the one hand, there is a significant shortage of quality crude oil for the production of petroleum products; on the other – the constant increase in quality requirements. A certain compromise in this situation is the use of additives in petroleum products, which will level the quality of crude oil and obtain a product that meets all modern requirements and is competitive in the world market of petroleum products.

#### 36.1.1 Method

Current trends in the development of technology for the production of additives for fuels and lubricants are such that the additive must exhibit multifunctional properties (see Fig. 36.1).

---

A. Grigorov (✉) · A. Trotsenko  
National Technical University “Kharkiv Polytechnic Institute”, Kharkiv, Ukraine



The scheme presented in Fig. 36.1 illustrates the directions of the correction of the properties of petroleum products when a multifunctional additive is added to them. At the same time, the main prospect of using additives in the composition of petroleum products that exhibit multifunctional properties is, above all, the ability to optimize their number (package), which will simplify technology and reduce the cost of petroleum production.

Given today's realities, we can note that in addition to their influence on the properties, in our opinion, multifunctional additives should take on the function of substances – chemical markers that can be used to combat counterfeiting of petroleum products (Orzel et al. 2019; Scott 2016). Also, the use of marker substances allows to subordinate the accounting and distribution of petroleum products, and can be used to identify the source of contamination of petroleum products when calculating environmental damage (Ezeokonkwo and Okoro 2012; Rostad 2010).

It is known that in the world practice of petroleum production technology for the past 50 years, the chemicals belonging to the class of nitrogen-containing compounds (Johnson 2018; Mamytov et al. 2012) are widely used as multifunctional additives.

Based on this experience, we propose to consider the possibility of using 1,3-diphenyltriazene (gross formula  $C_{12}H_{11}N_3$ ). This substance has a number of positive properties that allow it to be considered as a multifunctional additive to motor fuels and lubricants. First, it is well soluble in petroleum products and practically insoluble in water (Scaiano et al. 1991); has a moderate cost; hazard class – irritant; and its production volumes are industrial in scale.

In addition to the above characteristics, 1,3-diphenyltriazene has the ability to give a stable (from yellow to red) color to petroleum products it dissolves in, which allows it to be considered as a marker substance.

Considering other properties of 1,3-diphenyltriazene, we note that at a temperature of about 130 °C its thermal decomposition by the following mechanism occurs.

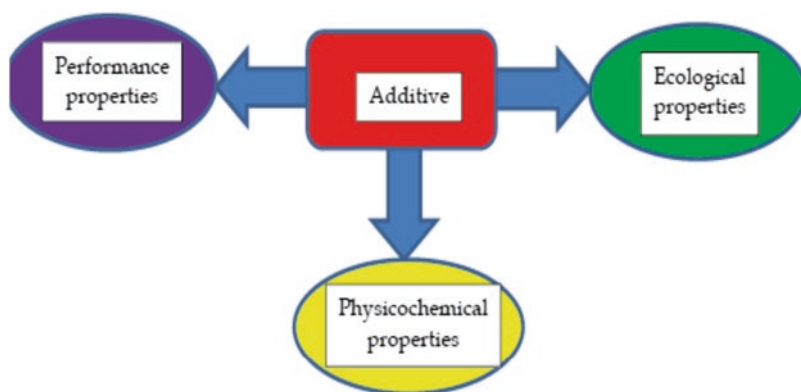
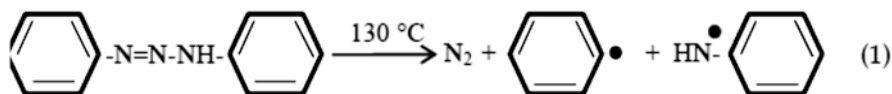


**Fig. 36.1** The scheme of influence of additives on properties of oil products





As can be seen from mechanism (1), the decomposition of 1,3-diphenyltriazene produces nitrogen and reactive radicals (Chemical Book 2017), which accelerate all fuel oxidation processes and provide a process of uniform and more complete combustion of hydrocarbon fuels.

Thus, in the case of gasoline, radicals due to their increased reactivity react instantly with atomic hydrogen, methyl, hydroxyl radicals of the fuel. In this case, stable compounds will be formed with a high probability: molecular hydrogen, toluene, and phenol. In the reaction zone with the direct participation of phenyl radicals, there is a decrease in the concentration of radicals-initiators of chain oxidative reactions, which leads to chain breakage and prevention of detonation combustion (Boichenko and Yakovlieva 2020).

When using 1,3-diphenyltriazene in diesel fuel, in our opinion, along with the completeness of fuel combustion such an indicator as flammability, expressed in units of cetane number (Sienicki et al. 1991) will increase.

The analysis of the 1,3-diphenyltriazene structure shows that in the molecule there is a weakly bound (mobile) hydrogen atom, which can easily dissociate from the N-H bond, cleave as atomic hydrogen and react instantly with oxygen-containing radicals of hydrocarbons or lubricants. In this case, the radicals are able to disproportionate or inversely convert to dimers of quinoid structure. Thus, 1,3-diphenyltriazene is able to exhibit antioxidant properties as well as industrial additives based on aromatic amines and phenols.

## 36.2 Results and Discussion

To confirm the possibility of using our proposed multifunctional additive, a study using fuel samples containing up to 1% mass. of 1,3-diphenyltriazene was conducted in the laboratory. These samples were obtained based on a straight-run gasoline (b.p.-180 °C) and diesel fractions (240–360 °C), gasoline catalytic cracking and diesel fraction obtained by thermal cracking of fuel oil.

The effect of 1,3-diphenyltriazene on the completeness of fuel combustion was studied by the content of soot (C, %) and hydrocarbons (CH, %) in the exhaust gases (see Figs. 36.2–36.3). The study was conducted on a standard 1.8 TSI engine (CJSA index) of the Skoda Octavia A7.

The study of the effect of 1,3-diphenyltriazene on such performance properties of fuels as resistance to detonation and flammability, expressed in octane (ON, unit) and cetane (CN, unit) numbers respectively, is presented in Figs. 36.4 and 36.5.

The information given in Figs. 36.2, 36.3, 36.4, and 36.5 shows the positive effect of 1,3-diphenyltriazene on the environmental and performance properties of

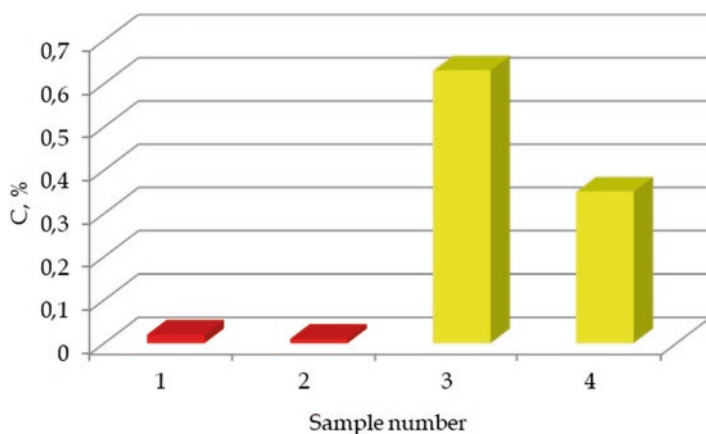


**Fig. 36.2** The content of C in the exhaust gases of the studied fuel samples: 1 - gasoline fraction; 2 - gasoline fraction + 1% additive; 3 - diesel fraction; 4 - diesel fraction + 1% additive

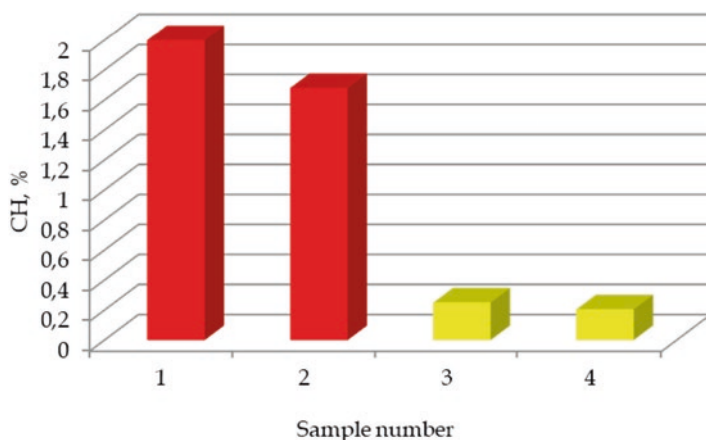


**Fig. 36.3** The content of CH in the exhaust gases of the studied fuel samples: 1 - gasoline fraction; 2 - gasoline fraction + 1% additive; 3 - diesel fraction; 4 - diesel fraction + 1% additive

motor fuels. Thus, when the content of 1% 1,3-diphenyltriazene is in the composition of motor fuels, there is an increase in the completeness of combustion of fuels (decrease in exhaust gases of soot and hydrocarbons); increase in octane number (ON) of straight-run gasoline fraction by 11 points; increase the cetane number (CN) of straight-run diesel fraction by 6 units.

Studies of the antioxidant properties of 1,3-diphenyltriazene were performed under static conditions (slow oxidation under the action of oxygen, air and light, for six months) using gasoline catalytic cracking and diesel fraction obtained by thermal cracking of fuel oil. Such objects of research were chosen by us, given the presence in their composition of olefinic hydrocarbons, which easily enter into oxidation

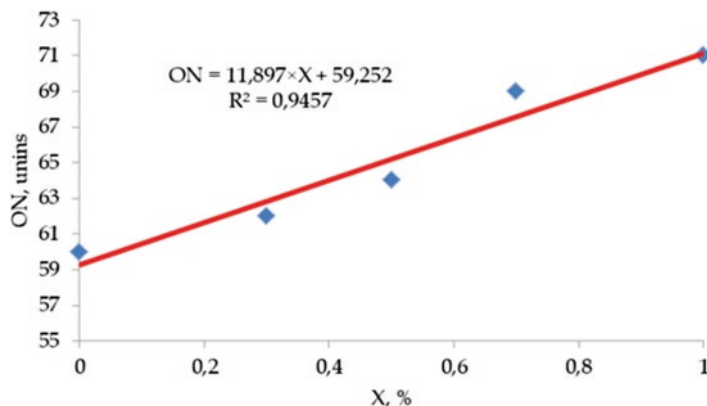


**Fig. 36.4** Dependence of ON on the content X of 1,3-diphenyltriazene in straight-run gasoline fraction

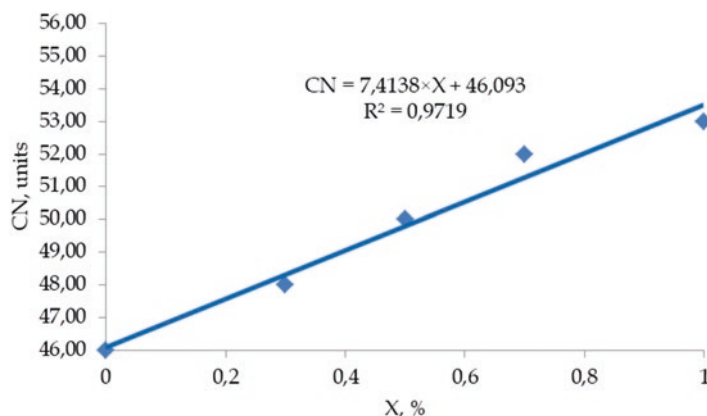


**Fig. 36.5** Dependence of CN on the content X of 1,3-diphenyltriazene in straight-run diesel fraction

reactions with oxygen in the air, resulting in relatively low chemical stability of selected fuels (Czarnocka et al. 2015).

The chemical stability of the studied fuel samples (see Fig. 36.6) was determined by the content of actual resins ( $X_r$ , mg / 100 cm<sup>3</sup> of fuel), which determines the ability of fuels to high-temperature deposits on metal surfaces of internal combustion engines (Berdnikov et al. 2019).

It was found that with increasing a duration of oxidation under static conditions in samples of fuel without additives, there is a significant (14 mg / 100 cm<sup>3</sup> of fuel for gasoline and 28 mg / 100 cm<sup>3</sup> of fuel for diesel fraction) increase of the content of actual resins indicating the oxidation processes of olefinic hydrocarbons.

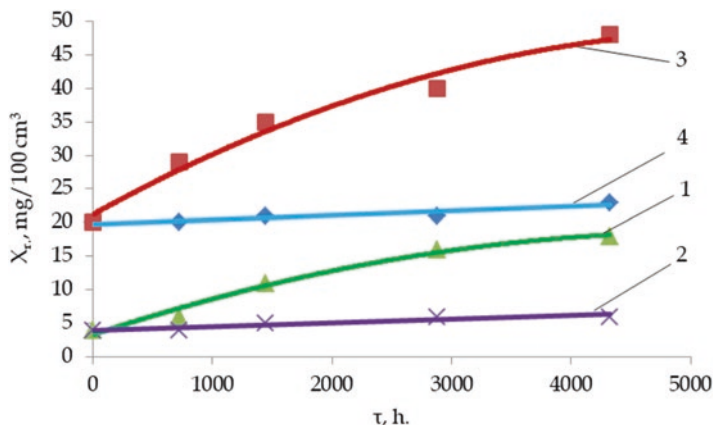


**Fig. 36.6** Dependence of  $X_r$  on the duration  $\tau$  of the study: 1 - gasoline fraction; 2 - gasoline fraction + 1% additive; 3 - diesel fraction; 4 - diesel fraction + 1% additive

Conversely, in samples containing 1% of 1,3-diphenyltriazene, the content of actual resins is characterized by a rather small increase, only 2–3 mg / 100 cm<sup>3</sup> of fuel.

### 36.3 Conclusion

The possibility and prospects of using 1,3-diphenyltriazene as a multifunctional additive for motor fuels and lubricants are theoretically substantiated. Experimental studies (on the example of motor fuels) fully confirm our theoretical justification and illustrate that the presence in fuels of 1% mass. of 1,3-diphenyltriazene can increase the completeness of fuel combustion; increase by 11 points the octane number of straight-run gasoline fraction and by 6 units cetane number of diesel fraction; and reduce during long-term storage the growth of actual resins in the fuel to a level of 2–3 mg / 100 cm<sup>3</sup> of fuel.

### References

- L.A. Berdnikov, M.E. Fedosova, M.G. Korchazhkin, A.A. Pikulkin, Problems of sediment formation in internal combustion engines. IOP Conf. Series: J. Phys. Conf. Series **1177**, 012009 (2019)
- S. Boichenko, A. Yakovlieva, Energy efficient renewable feedstock for alternative motor fuels production: solutions for Ukraine, in *Systems, Decision and Control in Energy I*, ed. by V. Babak, V. Isaienko, A. Zaporozhets, (Springer, Swizerland, 2020), pp. 247–259
- Chemical Book. (2017), Diazoaminobenzene, Access mode: [https://www.chemicalbook.com/ChemicalProductProperty\\_EN\\_CB2344713.htm](https://www.chemicalbook.com/ChemicalProductProperty_EN_CB2344713.htm)

- J. Czarnocka, A. Matuszewska, M. Odziemkowska, Autoxidation of fuels during storage, in *Storage Stability of Fuels*, ed. by K. Biernat, (InTech, In, 2015), pp. 157–188
- Ezeokonkwo, M.A., Okoro, U.C. 2012, New dyes for petroleum products. *J. Emerg. Trends Eng. Appl. Sci.*, 3 (1), pp. 8–11
- D. Johnson, *Lubrication - tribology, lubricants and additives* (IntechOpen, 2018), p. 132
- Mamytov, K. Zh., Beisenbayev, O.K., Shvets, V.F. and Syrmanova K.K. 2012, The multifunctional automobile gasoline additive on the basis of amino-aromatic hydrocarbons and oxygen-containing compounds. *Eurasian Chem. Technol. J.*, 14(3), p. 249
- Orzel, J., Krakowska, B., Stanimirova, I. and Daszykowski, M. 2019, Detecting chemical markers to uncover counterfeit rebated excise duty diesel oil. *Talanta*, 204, pp. 229–237
- Rostad, C. E. 2010, Analysis of solvent dyes in refined petroleum products by electrospray ionization mass spectrometry. *Fuel*, 89(5), pp. 997–1005
- Scaiano, J.C., Chen, C., McGarry, P.F. 1991, A flash photolysis and optoacoustic calorimetry study of the cis-trans isomerization of 1,3-diphenyltriazene. *J. Photochem. Photobiol. A. Chem.*, 62, pp. 75–81
- A. Scott, How chemistry is helping defeat fuel fraud. *Anal. Chem.* **94**(5) (2016)
- Sienicki, E., Jass, R., Slodowske, W., McCarthy, C. 1991, Diesel fuel aromatic and cetane number effects on combustion and emissions from a prototype 1991 diesel engine, SAE Technical Paper 902172

# Index

## A

Abatement, 248, 255–257  
Accident, 45, 98–101, 125, 131, 133, 136, 137, 150, 152  
Acoustic, 77–79, 82, 83, 85, 87, 126–129, 163, 167, 256, 257  
Additives, 27, 272, 283–288  
Aerodynamics, 10, 15, 91, 92, 121, 169, 172, 173, 176, 196  
Agriculture, 125, 180, 181, 183, 199, 200  
Aircraft, 1–3, 5, 9–15, 41–46, 63, 69, 70, 72–75, 80, 82–88, 94, 97–101, 104–107, 111–114, 118, 125, 126, 132, 139–146, 149, 158–167, 169, 170, 173–176, 179, 189, 196, 201–203, 209, 214–218, 221–223, 244, 246–250, 252–258, 260  
Aircraft engine emissions, 57, 63, 203  
Aircraft engine exhaust gases jet, 139–146  
Aircraft noise (AN), 83, 87, 157–164, 214, 243–260  
Air pollution, 85, 103, 141  
Airports, 3, 83–85, 87, 104, 110–115, 128, 139–141, 149, 150, 157–167, 243–260  
Air transport, 66, 70, 97–99, 103, 131, 149, 202, 257  
Alcohol converting, 264–268  
Alkoxides, 276–278, 281  
All-electric aircraft, 215  
Alternative fuels, 201  
Automation, 77, 132, 136, 149–155, 190  
Auxiliary power unit (APU), 107, 139  
Aviation emissions, 42, 103  
Aviation fuel cell, 106–107

Aviation industry, 1, 2, 41, 109, 111, 112, 114, 115, 154, 202, 203  
Aviation safety, 41, 99

## B

Barriers, 1–5, 41–46, 72, 133, 135  
Battery aging, 17–22  
Benefits, 1, 2, 15, 41, 42, 91, 92, 96, 97, 106, 111, 115, 125, 141, 248, 254, 257, 272, 274  
Big Data, 109–115  
Big Data analytics, 109–113, 115  
Butyl esters, 280

## C

Calculations, 51, 55–57, 60, 78, 87, 94, 142, 160, 162–164, 167, 169–172, 191, 248, 260  
Chemical processing, 272  
Civil Aviation, 103, 112, 114, 115, 126, 203, 213, 253  
Clean Sky, 104  
Climate change, 1, 2, 42, 117, 202  
Collision avoidance, 77–78, 82  
Communication, 101, 104, 110, 111, 121, 127, 131–137, 150, 151, 155, 200  
Cooling, 11, 63–66, 119, 122, 237

## D

Diesel engines, 263, 268  
1,3-diphenyltriazene, 284–288

Distributed propulsion (DP), 9, 10, 15, 91, 92, 96  
 Drone management, 187–193  
 Drones, 35, 91, 92, 127–129, 187–193, 196, 200

**E**

Efficiency, 1, 10, 11, 14, 52, 61, 66, 80, 82, 85, 91, 95, 105, 109, 111–113, 117, 118, 149, 150, 179, 180, 187, 188, 200–203, 205, 206, 209, 221, 222, 243, 255, 257, 271, 276, 278  
 Efficiency in the Aviation Industry, 109  
 Electric aircraft, v, vi, 1–5, 41–46, 63–66, 122, 214, 215  
 Electric aviation, 2, 3, 5, 46  
 Electric ducted fan (EDF), 91–93, 95, 96  
 Electric propulsion, 4, 17, 92, 105, 221  
 Electric propulsion systems, 10, 214  
 Electro-optic, 126, 128  
 Emission, 1–5, 25, 26, 31–33, 41, 42, 44–46, 55, 57, 58, 63, 80, 103–107, 139–141, 202, 203, 213, 214, 221, 222, 225–227, 253, 258, 276  
 Energy extraction, 272  
 Energy management, 17–22, 183  
 Entropy analysis, 207  
 Environmental impact assessment, 49–61  
 Environmental impact criteria, 60  
 Environmental sustainability, 201–203, 205  
 Ethyl esters, 278, 280  
 Exhaust gases, 139–146, 285, 286

**F**

Failure, 17, 21, 22, 99–101, 112, 113, 137  
 Flight procedures, 104, 244, 256  
 Following models, 189, 190, 192, 193  
 Fraction, 33, 274, 276, 278, 285–288  
 Fuel cells, 9–12, 14, 15, 92, 104–107, 222–227

**G**

Glitter Belt, 117, 118, 122  
 Glycerol layer (GL), 277, 279–281  
 Greenhouse, 2, 41, 54, 103, 106, 117, 179–184, 221, 222, 225–227

**H**

Heat pipe (HP), 64–66  
 High Altitude Long Endurance (HALE), 119  
 Highways, 51

Human factors, 98, 100, 150, 151, 153  
 Hybrid-electric aircraft, 222  
 Hybrid electric vehicles, 237  
 Hybrid propulsion, 213–218  
 Hydrogen combustion, 105, 106

**I**

Impact, 1, 2, 5, 22, 26–29, 42, 49–59, 61, 82, 88, 95, 96, 100, 101, 103, 106, 115, 133, 139–143, 145, 146, 149–155, 202, 203, 205, 206, 209, 243–246, 249, 252–257, 259, 260, 271, 274, 276  
 Initial concentration, 229–235

**J**

Jet-prop, 201–210

**L**

Leather industry, 25–33  
 Life cycle assessment, 25–33, 50  
 Lithium-ion battery, 237–240  
 Load management, 150  
 Local air quality (LAQ), 139, 141  
 Lubricants, 263, 283–288

**M**

Measurements, 83, 87, 93, 94, 110, 112, 141, 157–167, 173–176, 199  
 Misunderstanding, 101, 131, 133, 136, 137  
 More-electric aircraft, 9  
 Motor fuels, 283–288

**N**

Noise modeling, 83–88, 166  
 Numerical simulations of jet, 141, 142, 145  
 Numerical study, 230

**O**

Operators, 69–75, 99, 111, 115, 127, 131–137, 149–155, 189, 214, 253, 256, 257  
 Operator total load, 131, 135, 136, 149–155  
 Overpotential, 229, 231, 233, 235

**P**

Particle filter, 35–38  
 Particle image velocimetry (PIV), 170, 172–176  
 Particle sizes, 36, 38, 39

Phase change material (PCM), 237–241  
 Photogrammetry, 200  
 Physical processing, 272  
 Pilot training, 42, 75  
 Protection, 50, 84, 103, 104, 157, 167,  
 244–247, 253–255, 259  
 Pyrolysis, 272, 274

**Q**

Quadrotor, 35–38, 188, 192  
 Quantitative indicators, 50

**R**

Radars, 126, 128, 198–200  
 Radio frequency (RF), 110, 126–128  
 Radiotelephony, 134  
 Recovery, 25–33, 267, 272  
 Remote sensing, 180, 182, 183, 195–200  
 Resampling, 36, 38, 78, 79

**S**

Safe distance (SD), 188, 190, 193  
 Safety, 21, 44–46, 49–52, 54, 70, 97–101, 131,  
 137, 149, 155, 171, 188, 189, 191, 253,  
 256, 271  
 Scaled-down models, 173–176  
 Situation awareness, 69–72  
 Small unmanned aerial systems, 82, 187, 200  
 Solar, 117–120, 122, 216  
 Stakeholders, 41–46, 52, 111, 112, 115, 183  
 Structural inspections, 179–183  
 Subjective decision-making, 69–71, 73, 75  
 Sustainability, 33, 46, 50, 180, 201–210, 276  
 Sustainable aviation, 104, 106, 202–203, 256

**T**

Temperature distribution, 229, 231, 233,  
 235, 240  
 Temperature rises, 237, 240  
 Test bench, 10–12, 91, 93, 94  
 Thermal management, 64–66, 182, 240  
 Thermosyphon (TS), 64, 65  
 Transesterification, 276, 278, 280, 281  
 Transport facilities, 49–61

**U**

UAV detection and tracking systems,  
 125–128  
 Unmanned aerial vehicle (UAV), 9, 12, 14, 15,  
 125–128, 179, 180, 182, 183, 187, 189,  
 192, 195–200  
 Urban air mobility (UAM), 3, 17, 18, 77

**V**

Vanadium redox flow battery  
 (VRFB), 229–233  
 Vertical takeoff and landing (VTOL), 9, 10,  
 12–14, 214, 215, 218

**W**

Wasted frying oils, 277  
 Waste tires, 271–274  
 Wind tunnel design, 174  
 Wind tunnels, 92, 121, 140, 169–176

**Z**

Zoning, 83, 84, 158, 167, 247, 248,  
 252–255, 259